Eelgrass Stressor-Response Project 2005-2007 Report

December 2007

Nearshore Habitat Program
Aquatic Resources Division
Washington State Department of Natural Resources

PSAMP
Puget Sound Assessment
and Monitoring Program

The Eelgrass Stressor-Response Project is implemented by the
Nearshore Habitat Program. It is a component of the
Puget Sound Assessment and Monitoring Program (PSAMP).

Eelgrass Stressor-Response Project

2005-2007 Report

Acknowledgements

Contents

Kristy Kull and Sandy Wyllie-Echeverria
Friday Harbor Laboratories, University of Washington

Jill Coyle and Miles Logsdon
School of Ocean & Fisheries Sciences, University of Washington

Chuck Schietinger
Luxel Corporation

Jolene Rearick and Sandra Talbot
U.S. Geological Survey, Alaska Science Center

Sandy Wyllie-Echeverria
Friday Harbor Laboratories, University of Washington

Pete Dowty
Washington State Department of Natural Resources

APPENDICES

EXECUTIVE SUMMARY

In 2005, the Nearshore Habitat Program within the Washington State Department of Natural Resources (DNR) initiated the Eelgrass Stressor-Response Project. This decision reflected the habitat value placed on *Zostera marina* (eelgrass) – an aquatic plant that inhabits marine nearshore areas – and DNR's stewardship role with respect to state-owned aquatic lands.

The overall purpose of the Eelgrass-Stressor-Response Project is to identify and understand the nature of stressors that lead to *Z. marina* decline within greater Puget Sound. The impetus for the project was a recommendation from external reviewers that DNR's *Z. marina* monitoring project should expand its focus beyond observation of changes in *Z. marina* and include investigation into causes of change. The rationale for the program expansion is that stressors must be understood before the formulation of management actions can begin.

In its first biennium, the project initiated a series of diverse research efforts to gather information on *Z. marina* and its environment in areas of concern. Two geographic areas were identified where observed *Z. marina* declines have led to concern about further loss and a need to understand causal factors:

- Hood Canal
- San Juan Archipelago embayments, with a special focus on Westcott Bay, a site of substantial *Z. marina* losses

We developed a series of collaborative projects among independent scientists to rapidly investigate a suite of initial hypotheses concerning the causes of *Z. marina* decline. These collaborations are reflected in the contents of this report, which includes contributions from investigators at the University of Washington (Friday Harbor Laboratories and the Department of Biology) and the U.S. Geological Survey (The Alaska Science Center and the Pacific Science Center). In addition to the studies in this report, DNR initiated ongoing collaborative studies that include experimental transplants to investigate plant performance in Westcott Bay and deployment of instrumentation for continuous water quality monitoring.

A key project accomplishment was the development of a conceptual framework to structure the studies in Hood Canal and Westcott Bay. The conceptual models serve as starting points to focus initial investigations. The model for Westcott Bay focuses on low water clarity. The model for Hood Canal focuses on anthropogenic nutrient inputs and green algae blooms.

Findings
In the first biennium, the overall finding is that there is no simple and easily identified stressor that is responsible for *Z. marina* losses in Hood Canal and the San Juan Archipelago. Observed *Z. marina* losses appear to be only one manifestation of change in complex ecosystems. Key results are summarized below for each focus study area.

Key results from Hood Canal Focus Study include:

1. Stable isotope analysis was used to assess inputs of anthropogenic nitrogen to nearshore habitats, as indicated by enrichment in the ^{15}N isotope in *Z. marina* leaves. Results showed elevated *Z. marina* ^{15}N levels at southern Hood Canal sites and Dabob Bay sites, suggesting a relatively large contribution of anthropogenic nitrogen in these areas. In contrast, levels of anthropogenic nitrogen were substantially lower at sites in the northern portion of the canal. Within this broad nitrogen pattern, differences were evident in anthropogenic nitrogen level over smaller spatial scales and among seasons. This finding is supported by other research which suggests that the delivery of anthropogenic nitrogen to the nearshore through groundwater can be very localized (Chapter 3).

2. Stable isotope analysis of carbon in *Z. marina* showed an unusually high magnitude in the seasonal variation of ^{13}C. This finding may be related to strong seasonal variation in water temperature or an unusually strong variation in seasonal photosynthesis. There were no regional differences in *Z. marina* ^{13}C, which suggests that relative differences in riverine and marine influence are not significant across regions within Hood Canal (Chapter 3).

3. Hood Canal *Z. marina* populations appear to have higher genotypic richness (less clonality) and greater genetic diversity than populations in the San Juan Archipelago. Of the Hood Canal populations studied, core004 (Lynch Cove) had the lowest genetic diversity even though it has a stable *Z. marina* population. This finding argues against a key role for genetic diversity in causing *Z. marina* decline in Hood Canal (Chapter 10).

4. An analysis of impervious surface and land cover in the Hood Canal basin found that the basin has a low level of impervious surface relative to other areas within greater Puget Sound. Change analysis showed greater increases in impervious surface between 1991-1996 than between 1996-2001. The southern and northern areas of the basin have the greatest amount of impervious surface and the greatest increases (Chapter 4).

Key Results from San Juan Archipelago Focus Study include:

1. The remnant *Z. marina* population in inner Westcott Bay at Bell Point has the lowest genetic diversity of all populations analyzed in the San Juan Archipelago and Hood Canal. Genetic isolation of the inner populations in Westcott Bay could affect population viability (Chapter 10).

2. Boat-based sampling of surface waters coupled with remote sensing demonstrated that oceanic water conditions within the San Juan Archipelago vary greatly over space and time. This work provided an opportunity to assess the likelihood that Fraser River outflow stresses habitat conditions within the Westcott Bay complex. It documented complex patterns in temperature, salinity, pH, dissolved oxygen, light attenuation, and fluorescence that are linked to outflow from the Fraser River, strong currents, and basin topography. However, there was no evidence that the river plume reached the west side of San Juan Island and Westcott Bay. In addition to

providing insight into one hypothesis of *Z. marina* loss in Westcott Bay, these findings underscore the importance of intensive, local monitoring of water characteristics (Chapter 9).

3. High resolution mapping of nearshore bathymetry, substrate type, and circulation patterns was employed to characterize conditions in Westcott Bay. These results will help us to address the hypothesis that *Z. marina* loss is related to changes in turbidity associated with sedimentation or biological productivity. Nearshore mapping data can be used in future efforts to develop models of sediment transport and habitat conditions that explore environmental variability and possible thresholds of stress to *Z. marina* growth and recovery (Chapter 5).

4. A census of intertidal and subtidal *Z. marina* plant morphology at three sites characterized how plant metrics such as shoot density, shoot length, reproductive shoot density, and rhizome internode length vary with depth and with location. These results provide preliminary information on the variation of plant metrics within the San Juan Archipelago (Chapter 8).

5. A mesocosm experiment explored *Z. marina* plant growth rates and seed germination rates in sediments from sites with healthy and stressed *Z. marina* populations. Results suggest that differences in leaf elongation rates and germination rates were more closely related to shading than to sediment source (Chapter 7).

6. Physiological performance of *Z. marina* was measured at three sites by observing respiration and maximum photosynthesis rates in response to changes in applied irradiance. Results suggest that physiological performance is reduced at Bell Point, the site of a remnant *Z. marina* bed in Westcott Bay (Chapter 6).

Next Steps
The Eelgrass Stressor – Response Project is currently completing analysis of *Z. marina* transplant and water quality data collected in Westcott Bay and Hood Canal in 2007. Results of this research will be integrated with results of studies summarized in this report to refine hypotheses for *Z. marina* decline in Westcott Bay and Hood Canal and to develop field work priorities for the 2008 season.

In Hood Canal, research priorities focus on exploring plant performance and the nature of nutrient delivery to the nearshore:

- Review conceptual model of stressors in Hood Canal and consider expanding model to include potential stressors beyond anthropogenic nitrogen.
- Conduct field studies to assess plant performance in response to hypothesized stressors such as anthropogenic nitrogen, algal blooms.
- Deploy additional water monitoring systems to assess conditions in nearshore areas.
- Integrate findings from other research efforts on nutrient delivery into Hood Canal, including work by the Hood Canal Dissolved Oxygen Program and the USGS Washington Water Science Center.
- Integrate laboratory results into overall results as they become available.

1   Introduction

1.1   Origins of the Eelgrass Stressor-Response Project

In 2005, the Nearshore Habitat Program within the Washington State Department of Natural Resources (DNR) initiated the Eelgrass Stressor-Response Project. This move reflected the habitat value placed on *Zostera marina* (eelgrass) – an aquatic plant that inhabits marine nearshore areas – as well as DNR's stewardship role with respect to state-owned aquatic lands.

In greater Puget Sound, *Z. marina* provides spawning grounds for Pacific herring (*Clupea harengus pallasi*), out migrating corridors for juvenile salmon (*Oncorhynchus* spp.) (Phillips 1984; Simenstad 1994), and important feeding and foraging habitats for waterbirds such as the black brant (*Branta bernicla*) (Wilson and Atkinson 1995) and great blue heron (*Ardea herodias*) (Butler 1995). As a result, *Z. marina* receives special regulatory protections in Washington State (Washington State Department of Fish and Wildlife, WAC 220-110-250; Washington State Department of Ecology, WAC 173-26-221).

Experience in other regions has shown that losses of seagrass can be widespread and rapid (e.g. Chesapeake Bay – Orth and Moore 1983; Florida Bay – Robblee et al. 1991). Since 2000, DNR has conducted annual monitoring of *Z. marina* in greater Puget Sound to provide managers and decision makers key information on this natural resource, and to ensure early detection of *Z. marina* decline under the pressure of regional urbanization. This monitoring is conducted by DNR's Submerged Vegetation Monitoring Project (SVMP; Gaeckle et al. 2007, Dowty et al. 2005, Berry et al. 2003) and is a component of the broader Puget Sound Assessment and Monitoring Program (PSAMP; Puget Sound Action Team, 2007).

The formation of the Eelgrass Stressor-Response Project was motivated specifically by two main factors, both closely related to the SVMP. First, during a 2003 SVMP project review, external reviewers made a general recommendation that the SVMP needed to expand beyond a focus on documenting patterns of *Z. marina* distribution and change. Specifically, the reviewers recommended the initiation of process studies (field and laboratory experiments and modeling) to identify and understand the causal factors responsible for the patterns and trends detected in the monitoring project.

Second, by the time the SVMP had completed five years of monitoring, the accumulated results as well as the observations of other scientists in the region clearly identified two areas of *Z. marina* decline that were a cause for concern – Hood Canal and shallow

4

embayments within the San Juan Archipelago. The stressors causing these declines must be understood before the formulation of management actions can begin.

In response to these considerations, the Nearshore Habitat Program developed a budget proposal for the Eelgrass Stressor-Response Project that was subsequently submitted by DNR to the state legislature and ultimately approved for funding starting in the 2005-2007 biennium.

1.2   Project Purpose and Objectives

The overall purpose of this project is to identify and understand the nature of the stressors that lead to observations of *Z. marina* decline within greater Puget Sound. A key emphasis of the project is to deliver information in a form that is useful to resource managers and decision makers who play a role either directly in *Z. marina* stewardship or indirectly in the human activities that affect *Z. marina* habitat.

More specific objectives of the Eelgrass Stressor-Response Project include:

1. In coordination with the SVMP, maintain records of sites with evidence of *Z. marina* decline to serve as candidate sites for more intensive investigation. Both quantitative monitoring results and anecdotal observations are to be considered.
2. Each year, select at least two sites with *Z. marina* decline for more intensive investigation to identify causal factors.
3. Conduct a combination of continuous monitoring of environmental parameters, field and laboratory experiments, and modeling to isolate the mechanisms directly responsible for *Z. marina* decline.
4. Develop an understanding of the broader system dynamics that create these mechanisms and might be altered under alternative management scenarios.
5. Maintain a working conceptual model and a set of hypotheses to guide the investigations and tie them into a management-relevant framework.

The successful maintenance or decline of a *Z. marina* bed is the result of a complex set of hydrodynamic, geochemical and biological interactions that act at scales from the leaf to the landscape. The objectives stated above are ambitious, and a definitive understanding of the stressors and overall system dynamics at any given site is likely a long-term undertaking. The success of the project depends strongly on a combination of realistic expectations with respect to the long-term objectives and reliance on well-considered and measurable short-term benchmarks.

1.3   Project Approach in First Biennium

The immediate priorities at the outset of the project were to assemble the project team, most importantly the project lead. The emphasis was on quickly developing the capacity to initiate field work and rapidly collecting diverse sets of observations on the systems of interest. These initial observations would then form the basis for the later development of more rigorous models and hypothesis (Underwood 1997, p.9). To facilitate a quick start to

the project an existing team member (Dowty) was appointed as the lead on an interim basis during the recruitment process that ultimately identified the project lead (Schanz).

It was clear from the outset that the success of the project would rely on collaborative partnerships. The complexity and scope of the objectives call for the larger pool of expertise and capacity that only collaborative partnerships can provide. As evidenced by the content of this report, partners from the University of Washington (UW), both at Friday Harbor Laboratories (FHL) and the Department of Biology, and the U.S. Geological Survey (USGS), both at the Alaska Science Center and the Pacific Science Center (PSC), have played a major role in the work accomplished in the first biennium.

Both the FHL and the USGS PSC groups had ongoing activities in the San Juan Archipelago related to *Z. marina* when the DNR Eelgrass Stressor-Response Project was initiated. All groups have looked for opportunities to work cooperatively. A key planning meeting was held with all groups represented during the Georgia Basin Puget Sound Research Conference in Vancouver in March 2007.

Students associated with the Seagrass Lab at FHL generated five of the chapters in this report to support the development of the Eelgrass Stressor – Response Project (Chapters 6–10). While the scope and scale varies, each report discusses the application of techniques that are useful to evaluate the fitness of the *Z. marina* under site-specific and regional environmental stressors.

The initial proposal for the Eelgrass Stressor–Response Project prescribed the central role of conceptual models and explicit hypotheses in this project. These are dynamic and will be refined as the project evolves. The initial conceptual model and working hypotheses are presented in Chapter 2. The initial proposal also described two specific components of the project approach – analysis of genetic patterns in *Z. marina* in relation to observed losses and the deployment of continuous monitoring instrumentation at site selected for intensive assessment. The work accomplished in a genetics study is presented in Chapter 10. Results from the deployment of continuous monitoring instrumentation will be reported in the future.

The general approach in this first biennium was to structure the project into two elements – each associated with a geographic area where *Z. marina* loss has led to concern about further loss and a need to understand causal factors:
- Hood Canal Focus Study
- San Juan Archipelago Focus Study

Most activities have been uniquely associated with one of the focus studies with the exception of the genetic analysis (Chapter 10), which encompassed both Hood Canal and the San Juan Archipelago.

The patterns of *Z. marina* decline appear to be distinctly different in the two regions (see Figure 1-1). In the San Juan Archipelago, the most prominent losses have been in the heads of shallow embayments – first observed and most widely recognized in Westcott Bay on San Juan Island.
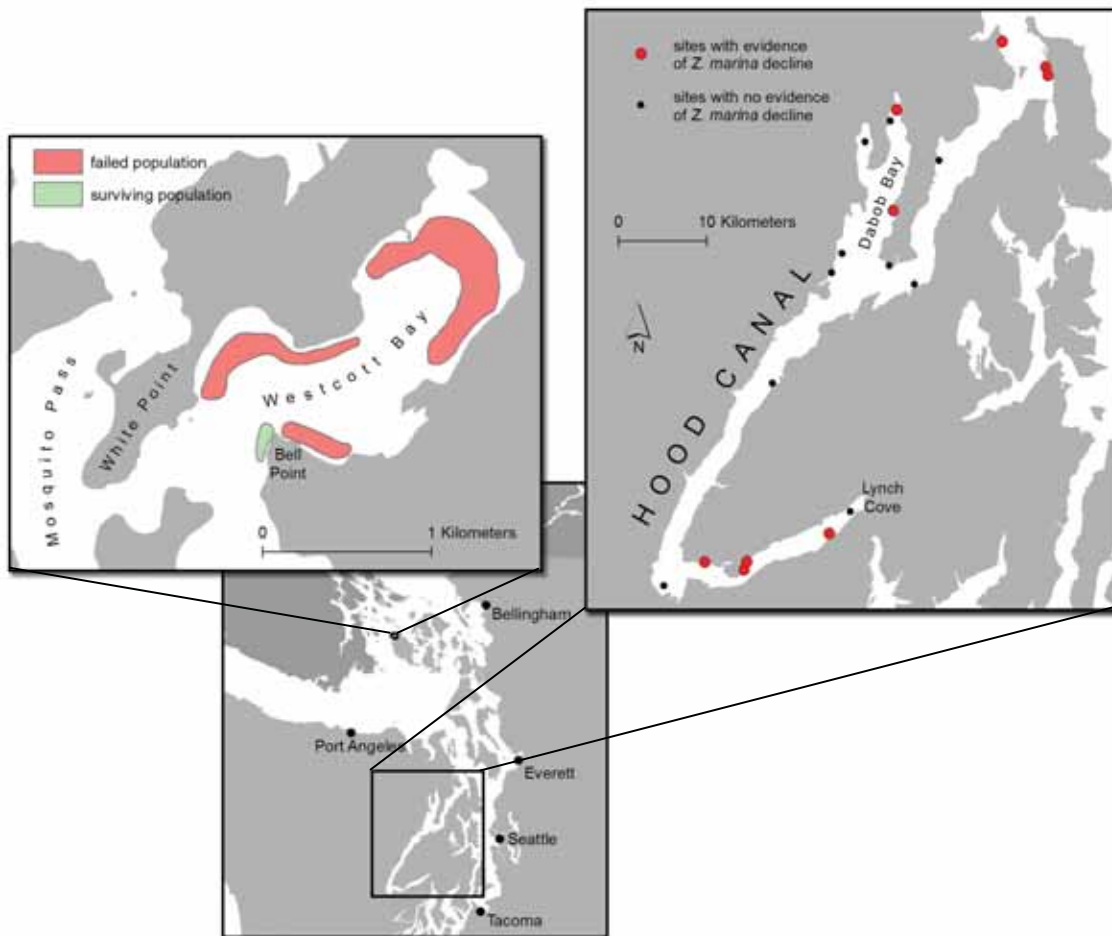
Figure 1-1. Maps of the two areas that were the focus of effort in the first biennium. Complete loss of *Z. marina* has been documented at the head of Westcott Bay (*Z. marina* populations outside of Bell Point are not shown). Several other embayments in the San Juan Archipelago appear to have similar losses. The losses in Westcott Bay occurred between 2001 and 2003. Hood Canal is the region with the greatest concentration of sites with *Z. marina* loss observed in DNR's annual monitoring results from 2000-2006 (see Appendix B for more detail).

A sharp decline in *Z. marina* in Westcott Bay was first identified in 2003. Outside of embayments like Westcott Bay, there has been no discernable pattern of change. In contrast, the losses detected by the SVMP monitoring in Hood Canal do not appear to be associated with particular geomorphological features. Interestingly, sites with apparently stable populations of *Z. marina* are intermixed with sites with declines, but overall Hood Canal contains the highest concentration of sites with observed declines within greater Puget Sound (Gaeckle et al. 2007). Once the two focus studies were initiated, summaries of the SVMP monitoring results that show sites of declining *Z. marina* were prepared to help guide site selection. These summaries appear as appendices to this report.

A major focus of DNR staff during the first biennium was the development, preparation and initiation of data collection efforts in the Westcott Bay area for the San Juan Archipelago Focus Study. The overall purpose was to begin an investigation of causes of

Z. marina decline in Westcott Bay. The DNR effort included the procurement of instruments, the design and construction of deployment apparatus and the establishment of three continuous water quality monitoring stations. DNR collaborated with the Padilla Bay National Estuarine Research Reserve on design of the deployment apparatus as well as an analysis exercise using Padilla Bay data to gain experience with the analysis of nearshore continuous monitoring data (Dowty and Bulthuis 2007).

Following the initial deployment of the DNR instruments, the maintenance of these stations has continued into the second biennium through a collaborative effort between DNR and FHL. DNR worked with Jessie Lacey and Renee Takesue of the USGS PSC, as well as FHL, to develop a program to collect and process water grab samples to support calibration of turbidity and chlorophyll probes on the instruments. A joint effort with Jessie Lacey led to the installment of two additional continuous water quality monitoring stations using USGS instruments deployed with DNR apparatus. The data collected through the fall of 2007 are currently being analyzed. Complete results will be presented in a later report.

Another major DNR initiative in Westcott Bay involved *Z. marina* transplant experiments with shading treatments at several stations in the Westcott Bay area. The purpose of these experiments was to begin to assess the current viability of habitats throughout the Westcott Bay area for supporting *Z. marina* populations. This would immediately help determine if the stressors that led to *Z. marina* decline were still acting in the head of Westcott, or if there was a discrete disturbance at the time of decline (2002-2003) and conditions have now rebounded to the point where *Z. marina* could be supported. The experiments were designed around a gradient from the mouth of the bay at Mosquito Pass, where healthy *Z. marina* beds are found, to the head of the bay where there has been a total loss of *Z. marina*. All transplants inside of Mosquito Pass were co-located with the water quality monitoring stations to allow correlation of plant performance with water quality parameters.

The experimental transplants were initiated in April 2007 and monitored by DNR and FHL staff through the spring and into the summer of 2007. At the end of the experiment, plants were harvested for laboratory analysis. Field data through the experimental growth period and laboratory results are currently being analyzed. The complete results will be presented in a future report.

1.4   References

Berry, H.D., A.T. Sewell, S. Wyllie-Echeverria, B.R. Reeves, T.F. Mumford, Jr., J.R., Skalski, R.C. Zimmerman and J. Archer, 2003, *Puget Sound Submerged Vegetation Monitoring Project: 2000-2002 Monitoring Report*, Nearshore Habitat Program, Washington State Department of Natural Resources, Olympia, Washington, 60pp. plus appendices.

Butler, R.W., 1995, The patient predator: Foraging and population ecology of the great blue heron, *Ardea herodias*, in British Columbia. *Occasional Papers for Canadian Wildlife Service* No. 86.

Dowty, P. and D. Bulthuis, 2007, Nearshore Dissolved Oxygen and Landscape-Scale Eelgrass Production, Oral Presentation at 2007 Georgia Basin Puget Sound Research Conference, Vancouver BC.

Dowty, P., B. Reeves, H. Berry, S. Wyllie-Echeverria, T. Mumford, A. Sewell, P. Milos and R. Wright, 2005, *Puget Sound Submerged Vegetation Monitoring Project: 2003-2004 Monitoring Report*, Nearshore Habitat Program, Washington State Department of Natural Resources, Olympia, 95pp.

Gaeckle, J., P. Dowty, B. Reeves, H. Berry, S. Wyllie-Echeverria, T. Mumford, 2007, *Puget Sound Submerged Vegetation Monitoring Project 2005 Monitoring Report*, Nearshore Habitat Program, Washington State Department of Natural Resources, Olympia, Washington, 93pp.

Orth, R.J. and K.A. Moore, 1983, Chesapeake Bay: An unprecedented decline in submerged aquatic vegetation, *Science*, 222:51-53.

Phillips, R.C. 1984. *The ecology of eelgrass meadows in the Pacific Northwest: a community profile*. U. S. Fish and Wildlife Service FSW/OBS-84/24. 85pp. Available online: http://www.nwrc.gov/library.html.

Puget Sound Action Team, 2007, *2007 Puget Sound Update: Ninth Report of the Puget sound Assessment and Monitoring Program*, Puget Sound Action Team, Olympia Washington, 260pp., Available online: http://www.psp.wa.gov/puget_sound/update.htm

Robblee, M.B., T.R. Barber, P.R. Carlson, M.J. Durako, J.W. Fourqurean, L.K. Muehlstein, D. Porter, L.A. Yarbro, R.T. Zieman, J.C. Zieman, 1991, Mass mortality of the tropical seagrass *Thalassia testudinum* in Florida Bay, *Marine Ecology Progress Series*, 71:297-299.

Simenstad, C.A, 1994, Faunal associations and ecological interactions in seagrass communities of the Pacific Northwest coast, pp.11-17, *In*: Wyllie-Echeverria, S., A.M. Olson and M.J. Hershman (eds), 1994, *Seagrass Science and Policy in the Pacific Northwest: Proceedings of a Seminar Series*, U.S. Environmental Protection Agency, Seattle, WA, (SMA 94-1), EPA 910/R-94 004. 63 pp.

Underwood, A.J., 1997, *Experiments in Ecology*, Cambridge University Press, Cambridge, 504pp.

Wilson, U.W. and J.B. Atkinson, 1995, Black brant winter and spring-stages use at two Washington coastal areas in relation to eelgrass abundance, *The Condor*, 97:91-98.

2   Conceptual Model

When investigating complex systems, it is important to produce and maintain a simplified version of the system – a model. This is initially a conceptual model but as an investigation develops it may or may not evolve into a numerical model. Gross (2003) gives the purposes of a conceptual model to be:

1. Formalize current understanding of system processes and dynamics
2. Identify linkages of processes across disciplinary boundaries
3. Identify the bounds and scope of the system of interest
4. Contribute to communication:
    a. Among scientists and program staff
    b. Between scientists and managers
    c. With the general public.

Conceptual models vary in complexity. The goal for the Eelgrass Stressor – Response Project is to produce simple models that are retained easily in the mind and serve to focus the diverse project activities. Rather than assemble a large number of processes that are known to operate in the nearshore, the models here are kept to as few elements as possible in order to convey the conceptual framework for the data collection and analysis efforts that are the current project focus. The intent was to develop the model only to the extent necessary to convey the hypotheses being investigated. With time, it will be necessary to add complexity to the model as our understanding expands and the focus of our work evolves. If the project grows to encompass numerical modeling, it will be necessary to more fully develop the conceptual model to explicitly support development of numerical models.

Many conceptual models of nearshore ecological functions, and seagrasses in particular, have previously been developed (Simenstad et al. 2006; Thom et al. 2005; Long Island Sound Study 2003; Cerco and Moore 2000; McFarlane 1993). These provide a broad framework for the relatively specific models that will guide the development of hypotheses and experimental designs employed in this project.

The boundaries of the modeled system can be defined in any way. To help keep the initial models as simple as possible, the boundaries are kept as close as possible to the system elements of interest – in this case, *Z. marina*. It is important to keep the boundaries broad enough so that some interaction of system elements and forcing functions is included (Odum 1994).

Throughout this report "Westcott Bay", the "Westcott Bay complex" and the "Westcott Bay system" refer to all the waters running from the mouth at Mosquito Pass, past Bell Point, to the head of Westcott Bay proper (see Figure 1-1, p.7).

The ideas presented in this chapter reflect the ideas from a number of discussions with input from a large number of people including all the contributors to this report.

2.1   Conceptual Model for Westcott Bay

Field observations of low water clarity at the head of Westcott Bay and particularly of turbidity plumes from tidal resuspension, led initial thinking about stressors in the Westcott Bay system to focus on high turbidity. This and other key biotic and abiotic observations underlying the conceptual thinking about Westcott Bay *Z. marina* are summarized below.

Biotic Observations:
- No vegetation observed at head of bay from 2003; *Z. marina* was observed by DNR in 2000, 2001, and previously in 1994.
- A gradient exists of increasing *Z. marina* toward mouth with increasing abundance with depth
- No green algae at head of bay

Abiotic Observations:
- High clay/silt fraction at head of Westcott Bay
- Frequent/persistent low water clarity observations
- High sediment organic matter content (Ginger Shoemaker and Sandy Wyllie-Echeverria, Friday Harbor Labs, unpublished data)
- Low summer water column nutrient levels (Renee Takesue, USGS, unpublished data)

In addition, an observation that other bays in the region have similar patterns of *Z. marina* distribution with evidence of decline at the head of the bay suggests that the key stressors responsible for loss at the head of Westcott operate at a regional scale rather than just locally at Westcott Bay (Wyllie-Echeverria, personal communication).

There are two general scenarios regarding the timing and nature of the stressor(s) and subsequent response:

Scenario 1
- Rare pulsed stressor in late 1990s initiates period of declining *Z. marina*.
- Initial loss triggers reinforcing feedbacks (increased resuspension) and further loss.
- Total loss by ~2002.

Scenario 2
- Rare pulsed stressor in ~2002 leads rapidly to total loss

Potential stressors that could play a role in these scenarios are given below:

Chronic Stressor(s)
1. Persistent/frequent phytoplankton blooms
2. Turbidity plumes (tidal or wind-driven resuspension, periodic Fraser River plumes)

3. Oyster farm detritus – cumulative effects

Pulsed Stressor(s)
1. Intense Fraser River outflow event (turbidity plume)
2. Coincidence of infrequent extreme low tide with infrequent extreme hot weather
3. Disease outbreak

Figure 2-1 shows a conceptual model of how either a pulsed stressor or an unusual convergence of chronic stressors could trigger a decline in *Z. marina* eventually leading to total loss (scenario 1). This model is consistent with the observations of tidal resuspension of fine sediment but it does not explain high sediment organic matter nor low water column nutrient levels at the head of Westcott Bay.

The available turbidity, chlorophyll and PAR data that has been analyzed to date is minimal so the relative importance of periodicities with a tidal period (suggesting resuspension of sediments) or longer periods (suggesting phytoplankton blooms) is not established. If the data reveal longer periods of low water clarity, this would support a conceptual model centered on phytoplankton blooms rather than the sediment resuspension shown in Figure 2-1.
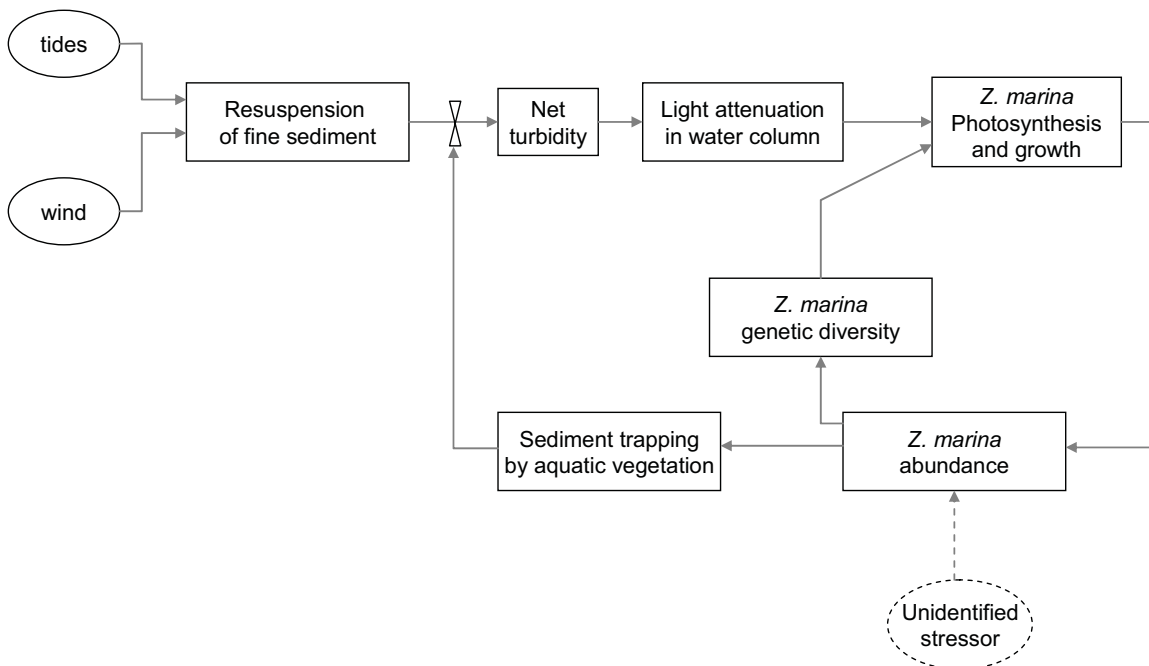
Figure 2-1. Conceptual model showing how an unidentified stressor leading to a modest decline of *Z. marina* abundance in Westcott Bay could have an amplified effect through feedback loops leading to the total loss of *Z. marina*. In one loop, the modest loss of *Z. marina* reduces the sediment trapping ability of nearshore vegetation. Turbidity then increases and reduces light availability for *Z. marina* photosynthesis leading to a further loss of abundance. In the second loop, the loss of *Z. marina* abundance leads to loss of genetic diversity and negative effects on photosynthesis and growth and further loss of abundance. The genetic feedback loop could be particularly important if the population initially had low genetic diversity.

12

There are a number of hypotheses that are being evaluated as part of the analysis of field data collected in 2007. Once these hypotheses are evaluated, the conceptual model for *Z. marina* loss in Westcott Bay will be revised.

Hypotheses to be Tested
1. *Z. marina* will not survive under the current conditions in the head of Westcott Bay in the area formerly vegetated.
2. Limited light availability at the head of Westcott Bay due to high turbidity precludes the successful growth of *Z. marina*.
3. Mean turbidity and the intensity and duration of discrete turbidity events increases from the mouth to the head of Westcott Bay.
4. Mean turbidity and the intensity and duration of discrete turbidity events increases from the subtidal to the upper intertidal for sites inside the mouth of Westcott Bay.
5. Limited nutrient supply at the head of Westcott Bay prevents the re-establishment and growth of *Z. marina* – both water column and porewater nutrients.
6. There is no transport of *Z. marina* seeds into the head of Westcott Bay.
7. There is no viable *Z. marina* seed bank in the head of Westcott Bay.

Alternate hypotheses not directly tested in 2007:
1. High water temperature events in 2002 led to direct stress on *Z. marina* in the head of Westcott Bay and promoted an outbreak of the wasting disease *Labyrinthula zosterae*. Acting together, these stressors led to *Z. marina* die-off.
2. High sediment sulfide levels resulting from high sediment organic matter and anoxic conditions led to *Z. marina* decline (Goodman et al. 1995).

The field work in 2007 was designed to take advantage of spatial gradients within the Westcott Bay complex. The rationale was that having data from stations with a range of environmental conditions would support a more powerful evaluation of the hypotheses. The key parameter along the gradient is *Z. marina* abundance (and inferred performance) as well as a hypothesized gradient in multiple interrelated environmental conditions (nutrients, salinity, temperature, turbidity, currents). Data were collected at multiple sites along this gradient in order to:

(a) develop relationships between the time series of environmental parameters and *Z. marina* performance
(b) identify thresholds in environmental parameters beyond which *Z. marina* populations in Westcott Bay are no longer viable

2.2   Conceptual Model for Hood Canal

There are three themes that underlie our approach to addressing *Z. marina* loss within Hood Canal. First, Hood Canal is currently receiving substantial attention, both scientific and political, due to the consensus that this water body suffers from problems that are

affecting its ecosystem-level functioning. In 2003, Hood Canal was listed as one of only two "dead zones" on the Pacific coast of the US – the other one was Los Angeles Harbor (Pew Oceans Commission 2003). Also, widely publicized fish kills in southern Hood Canal in recent years due to low dissolved oxygen (DO) led to the initiation of the Hood Canal Dissolved Oxygen Program (HCDOP) (Newton and Hannaflous 2007). In this context, significant effort has focused on the role of nutrients and the low flushing rate in producing hypoxic conditions. Because of this significant established effort as well as documented cases of reduced *Z. marina* performance due to low DO, nitrate toxicity and ammonium toxicity, the Eelgrass Stressor-Response Project has focused on the potential role of nutrient levels on *Z. marina* in Hood Canal.

The second theme is the multiple observations by DNR staff and others of extensive, but ephemeral green algal mats in Hood Canal – in some cases completely covering *Z. marina* beds (Figure 2-2). Algal growth has been shown to have a negative impact on seagrass (Hauxwell et al. 2003, Nelson and Lee 2001).

Figure 2-2. An extensive, dense green algae mat (*Ulva* sp.) covering *Z. marina* at Sunset Beach, near Lynch Cove, in southern Hood Canal (September 2004).

The third theme is the dispersed spatial pattern of sites with observed *Z. marina* decline in Hood Canal. Sites with observed decline are located both in southern and northern Hood Canal (see Appendix B) with stable sites in between. There are no obvious geomorphological features that distinguish declining from stable sites (e.g. located in shallow embayments as in the case of declining sites in the San Juan Archipelago).

Taken together, these themes suggest that local factors operating at very small spatial scales may be affecting both green algal blooms and *Z. marina* decline. Anthropogenic perturbations to nearshore nitrogen cycling have been shown to occur on a very localized

14

scale. Localized groundwater inputs enriched in ^{15}N from septic systems have been shown to enrich *Z. marina* and macroalgae on scales of tens of meters and produce local eutrophication effects normally associated with enclosed bays (Maier and Pregnall 1990). This is the basis for the initial working hypothesis of *Z. marina* decline within Hood Canal (Figure 2-3). Specifically, localized loadings of anthropogenic nitrogen are hypothesized to lead to localized green algal blooms that stress *Z. marina* through light limitation.
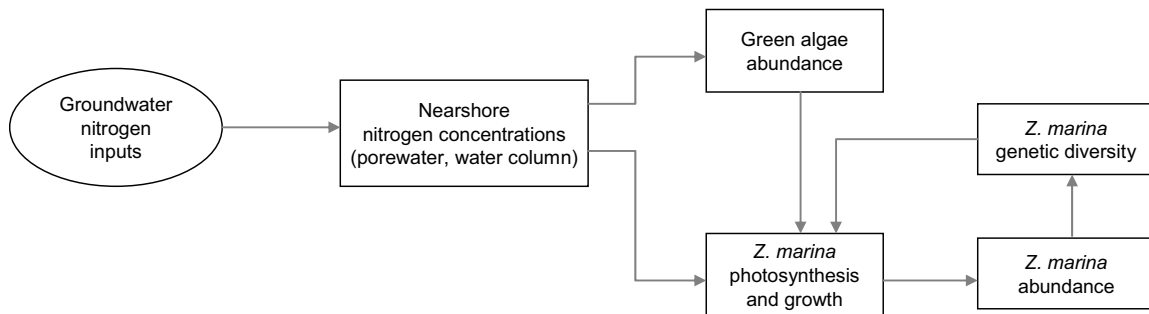
Figure 2-3. A conceptual model of *Z. marina* loss in Hood Canal resulting from increasing anthopogenic nitrogen inputs through groundwater and increasing competition with green algae mats. Initial losses could be accelerated through a feedback loop associated with loss of genetic diversity and reduced growth.

Alternate hypotheses explaining Hood Canal *Z. marina* decline include:

1. Periodic anoxia in sediments is localized in nature but directly leads to *Z. marina* decline.
2. Localized ammonium toxicity associated with groundwater nutrient inputs lead to *Z. marina* decline (Van Katwijk et al. 1997).
3. Localized nitrate toxicity associated with groundwater nutrient inputs lead to *Z. marina* decline.

2.3   References

Cerco, C.F., 2000, *System-Wide Submerged Aquatic Vegetation Model for Chesapeake Bay*, Chesapeake Bay Program Report, Available online: http://www.chesapeakebay.net/pubs/1364.pdf

Goodman, J.L., K.A. Moore and W.C. Dennison, 1995, Photosynthetic responses of eelgrass (*Zostera marina* L.) to light and sediment sulfide in a shallow barrier island lagoon, *Aquatic Botany*, 50, 37–47.

Gross, J.E., 2003, *Developing Conceptual Models for Monitoring Programs*, National Park Service Inventory and Monitoring Program, Ft Collins, Colorado. Accessed 11/5/07 at http://science.nature.nps.gov/im/monitor/ConceptualModels.cfm

Hauxwell, J., J. Cebrián and I. Valiela, 2003, Eelgrass *Zostera marina* loss in temperate estuaries: relationship to land-derived nitrogen loads and effect of light limitation imposed by algae, *Marine Ecology Progress Series*, 247:59-73.

Long Island Sound Study, 2003, *Long Island Sound Habitat Restoration Initiative: Technical Support for Coastal Habitat Restoration* (Section 3: Submerged Aquatic Vegetation), Available online: http://www.longislandsoundstudy.net/habitat/index.htm

McFarlane, R.W., 1993, *A Conceptual Model of the Galveston Bay Ecosystem*, Publication GBNEP-42, The Galveston Bay National Estuary Program, Available online: http://gbic.tamug.edu/gbeppubs/42/gbnep-42.html

Maier, C.M. and A.M. Pregnall, 1990, Increased macrophyte nitrate reductase activity as a consequence of groundwater input of nitrate through sandy beaches, *Marine Biology*, 107:263-271.

Nelson, T.A. and A. Lee, 2001, A manipulative experiment demonstrates that blooms of the macroalga *Ulvaria obscura* can reduce eelgrass shoot density, *Aquatic Botany*, 71:149-154.

Newton J. and D. Hannaflous, 1997, Hypoxia in Hood Canal: An Overview of Status and Contributing Factors, *Proceedings of the 2007 Georgia Basin Puget Sound Research Conference*, Puget Sound Action Team, Olympia WA.

Odum, H.T., 1994, *Ecological and General Systems: An Introduction to Systems Ecology*, Revised Edition, University Press of Colorado, Nitwot, Colorado, 644pp.

Pew Oceans Commission, 2003, *America's Living Oceans: Charting a Course for Sea Change*, A Report to the Nation, Available online: http://www.pewtrusts.org/uploadedFiles/wwwpewtrustsorg/Reports/Protecting_ocean_life/env_pew_oceans_final_report.pdf

Simenstad, C., M. Logsdon, K. Fresh, H. Shipman, M. Dethier and J. Newton, 2006, *Conceptual Model for Assessing Restoration of Puget Sound Nearshore Ecosystems*, Technical Report 2006-03, Puget Sound Nearshore Partnership, Available online: http://www.pugetsoundnearshore.org/technical_papers/conceptmodel_06.pdf

Thom, R.M., G.W.Williams and H.L. Diefenderfer, 2005, Balancing the Need to Develop Coastal Areas with the Desire for an Ecologically Functioning Coastal Environment: Is Net Ecosystem Improvement Possible?, *Restoration Ecology*, 13(1):193-203.

Van Katwijk, M.M., L.H.T. Vergeer, G.H.W. Schmitz and J.G.M. Roelofs, 1997, Ammonium toxicity in eelgrass *Zostera marina*, *Marine Ecology Progress Series*, 157:159-173.

3 Nearshore nitrogen sources and eelgrass decline in Hood Canal

Beth Wheat
Department of Biology
University of Washington

3.1 Summary

The objectives of this study were twofold: first, to assess eelgrass growth rates, density and reproduction at sites of eelgrass (*Zostera marina*) decline; second, to assess inputs of anthropogenic nitrogen sources to nearshore habitats, as indicated by enriched $\delta^{15}N$ isotopes. Our hypothesis was that sites of eelgrass decline would show nitrogen isotopic ratios characteristic of cultural eutrophication. We found significant enrichment in the $\delta^{15}N$ signature of oysters and eelgrass growing in the southern part of the canal. This is suggestive of anthropogenic nitrogen inputs. We have found no correlation between sites with high $\delta^{15}N$ signatures and eelgrass decline. Measurements of summertime oyster growth show significantly faster growth in south Hood Canal sites compared to north. However, there is no spatial pattern in eelgrass growth along the north–south axis of the canal.

3.2 Introduction

Eutrophication of coastal zones is a common occurrence worldwide (Pew Oceans Commission 2003) and can lead to "dead zones" caused by hypoxia. These dead zones significantly impact marine food webs and the structure of benthic communities (Turner & Rabalais 1994, Diaz & Rosenberg 1995). The proximate cause for hypoxia is heterotrophy (e.g. oxygen-consuming bacteria) outdoing autotrophy (e.g. oxygen-producing photosynthesis). However, hypoxia can have ultimate causes that are entirely natural (e.g. upwelling of low-oxygen water from the deep ocean; (Grantham et al. 2004) or that stem from cultural eutrophication (Rabalais et al. 2002). Nitrogen generally limits algal growth in marine systems, so the addition of nitrogen can cause algal blooms. The subsequent algal die-offs can lead to hypoxic conditions because the bacteria that consume the algae also consume the available oxygen in the system. The system then becomes anoxic.

Phytoplankton blooms fueled by excess nutrients can intercept light necessary for eelgrass (*Zostera marina*) production (Burkholder et al. 1992, Short & Wyllie-Echeverria 1996). Thus, eutrophication has consequences for eelgrass health. There is currently an alarming global decline of eelgrass (Lotze et al. 2006, Orth et al. 2006). Concerns arise because eelgrass is an important component of estuarine ecosystems. It provides critical habitat structure for many charismatic and commercially important species like juvenile salmonids and Dungeness crabs (Heck et al. 1995, Lazzari & Stone 2006). Eelgrass is a prodigious primary producer, and, while herbivory tends to be low on living plants, its detritus is an important base for many estuarine food webs (Simenstad & Wissmar 1985, McClelland &

Valiela 1998, Ruesink et al. 2003). Nitrogen addition can affect eelgrass in a variety of ways. Directly, excess nitrogen in the water column can reduce eelgrass growth and indirectly it can produce conditions that favor algal blooms and fouling by epibionts (Short & Wyllie-Echeverria 1996, Lotze et al. 2006).

Terrestrial land use changes can also have huge impacts on estuarine environments by altering the hydrologic regime, reducing forest cover, and adding nutrient-rich sediments and runoff. The most well-known case of hypoxia in the United States is in the Gulf of Mexico, a result of agricultural runoff into the Mississippi River (Rabalais et al. 2002). Similarly, in the Hood Canal, urban development and changes in land use may contribute to eutrophication.

The Hood Canal is a deep, narrow fjord with a sill near the mouth that prevents the circulation of water out of the Canal, especially during the summer. Temperature differences cause vertical stratification of the water column, effectively trapping water in the deep southern hook of the canal. The Hood Canal Dissolved Oxygen Program (HCDOP) has completed work on a nitrogen budget for the Hood Canal. They found that 90% of the nitrogen entering the canal is of marine origin (Roberts et al. 2005). An increase in anthropogenic inputs, by difference, must be quite small. But it is possible that these inputs occur in areas where they are particularly available to fuel production, namely in the photic zone close to shore. This increase in primary production could lead to a decrease in light available for eelgrass and ultimately cause hypoxia in the canal. Consequently, anthropogenic activities at the local scale – including land use changes, urbanization, and agricultural practices – may be accelerating the pace of ecosystem decline in Hood Canal, even though they contribute little to the overall nitrogen budget.

Long-term data sets indicate that hypoxia in the Hood Canal existed in the 1950's (HCDOP 2007). However, the affected area has been growing and the severity of fish kills has been more pronounced in recent years (HCDOP 2007). Similarly there are anecdotal reports of abundant eelgrass along the intertidal region of the Hood Canal. In the 1970s, research divers said much of the margin of the Canal was covered in eelgrass. Today, the distribution is patchy and in decline. The DNR Submerged Vegetation Monitoring Project has documented a high concentration of sites with declines in eelgrass area from 2000 to 2004 (Dowty et al. 2005). The eelgrass declines witnessed by the DNR have prompted an interest in identifying the causes of eelgrass decline in the Hood Canal.

The causal relationship between eelgrass decline and seasonal hypoxia in the Hood Canal is unclear. However, anoxic conditions impair growth and can lead to sudden eelgrass declines resulting from the build-up of toxic plant metabolites in tissues or the invasion of phytotoxins from the sediment (Larkum et al. 2006). Hypoxia in the Hood Canal is driven by a complex interaction of many factors including long residence time, changes in oceanic conditions, deforestation and eutrophication from anthropogenic nutrient sources. Hypoxia is a potentially important stressor driving eelgrass decline in the Hood Canal.

Declines of eelgrass in the Hood Canal may be a response to systemic stressors i.e.: hypoxia and eutrophication. Alternatively eelgrass may be responding to locally specific

18

stressors like nearshore bulkhead development, increased runoff, competition with non-native eelgrass, *Zostera japonica*, point source nutrient pollution (ie: leaky septics causing a problem for a particular eelgrass meadow), or damage caused by boats. That a disproportionate number of sites experiencing eelgrass decline are located in the Hood Canal is cause for concern and suggests a systemic decline.

We have developed two working hypotheses:

Hypothesis 1: Nitrogen stable isotopes in eelgrass and oysters will vary spatially through the Canal.

A) The spatial pattern for eelgrass will be more distinct than for oysters due to their method of acquiring nitrogen. By gathering stable isotope data from oysters and eelgrass we can get information about local porewater nitrogen vs. suspended phytoplankton and other particulates or nitrogen sources moving in the water column.

B) Biologically-available nitrogen in the photic zone will disproportionately derive from terrestrial sources, including surface runoff and septic leaching in the southern Hood Canal.

Hypothesis 2: We hypothesize that nitrogen loading from anthropogenic sources may be a systemic cause of eelgrass decline in the Hood Canal. Accordingly, sites of eelgrass decline will have nitrogen stable isotope signatures characteristic of cultural eutrophication. We expect these sites to show slower eelgrass growth rates and patchy eelgrass distribution. Due to eutrophication we expect oyster growth to be inversely related to eelgrass growth. Sites in decline may suffer from one or more of the following factors as a result of cultural eutrophication: light attenuation due to algal blooms and increased turbidity during critical periods of growth; fouling from epibionts responding to excess nitrogen; competition/physical damage from large floating mats of macroalgae; or dieback from the direct effects of hypoxia.

3.3   Methods

From the DNR sampling regime we selected 10 focus sites in the Hood Canal representing sites with evidence of eelgrass decline and other sites with unknown trends in eelgrass abundance (due to insufficient monitoring data) (Figure 3-1). The sites were spatially oriented so that 5 sites were in the north and 5 were in the south. In two locations, Dabob Bay and Lynch Cove, sites of eelgrass decline were located near other sites with unknown trends. In total there were 6 sites in decline and 4 sites with unknown trends split evenly between north and south Hood Canal.
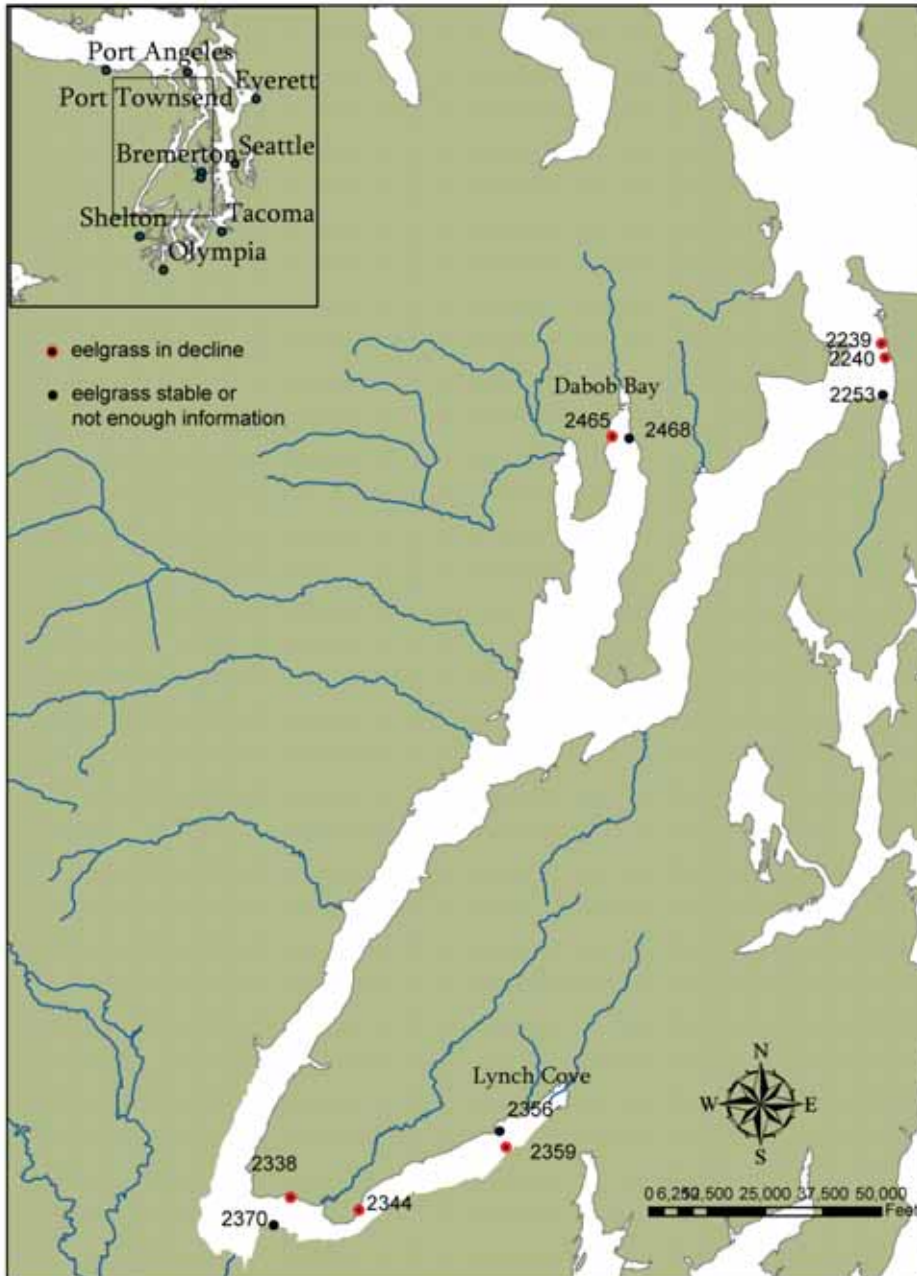
Figure 3-1. The map of sites in the Hood Canal. Red indicates sites with eelgrass in decline as determined by the WADNR's submerged aquatic vegetation surveys.

Eelgrass density was surveyed at all sites by haphazardly tossing a ¼ m^2 quadrat and counting shoots within the quadrat. The date and number of shoots/m^2 were recorded so that data can be compared in future monitoring projects. Due to time constraints counts were not performed at all sites during all of the low tides.

Eelgrass growth was measured by marking sheaths with a hypodermic needle (Zieman 1974). For statistical analyses the ratio of old growth to new growth/days of growth was used. At each site, sediment in eelgrass beds was analyzed for grain size distribution and

percent organic matter. For a comparison of all sites, including the sites where eelgrass was not found, sediment was also collected from outside the eelgrass bed. Average grain size per sample was determined using the graphic mean of the sample.

Eelgrass above- and below-ground biomass was determined by gathering all above and belowground biomass in triplicate from $1/8m^2$ samples. All samples were gathered from the upper margin of the beds, and when possible samples were gathered from the -2.5 ft equivalent tidal height [a tidal height expected to be exposed to air with similar frequency and duration as -2.5ft MLLW at Allyn]. Samples were brought to the lab and cleaned of epibionts. Stems were counted and above and below ground biomass were separated at the first rhizome node. Samples were dried at 60°C and weighed to determine biomass.

At all sites, oyster growth was measured at 0 and +2.5ft MLLW by recording the length from hinge to beak for each oyster in fall (August – November) and spring (November – April). Oysters planted in the summer were on average 3 mm. Five replicate tiles were planted at each tidal height.   Oysters planted in the fall were 6-7 mm and were planted with three replicate tiles at each tidal height. Temperature was recorded at each site using i-buttons set out April 2007 to May 2007.

For stable isotope analysis, oyster adductor muscle tissue was removed, freeze dried, and ground. Using the same method, the most recently emerged tissue from eelgrass was also prepared for isotopic analysis. Particulate organic matter (POM) samples were collected, filtered onto a quartz filter and prepared for analysis in a similar manner. All isotopic analysis was done at U.C. Davis Stable Isotope Facility in Davis, California.

Water column data were also collected at each site (as access and winter storms allowed). Monthly particulate organic matter was collected. Sample collection was done by filtering a known amount of liquid onto a pre-ashed glass fiber filter. These filters were dried for 24 hours at 60°C and weighed to determine total suspended solids (TSS). Weighed filters were then ashed in an ashing oven at 500°F for 3 hours to determine percent organic matter (POM).

Additionally, chlorophyll a samples were collected in triplicate from each site in March, April, May and June 2007. Samples were collected by filtering 125 ml of water onto a glass fiber filter. Chlorophyll was extracted in acetone following the method of (Welschmeyer 1994).

Triplicate samples of porewater from within the eelgrass meadows were collected at all sites where collection was possible. Since eelgrass meadows impact porewater nutrients, porewater was only collected from sites where eelgrass meadows were exposed at low tide (this excluded sites 2344 and 2338 from porewater testing). Porewater was collected in the field, put on ice, brought to the lab, diluted, filtered, and frozen for analysis. Porewater was analyzed for nitrates, nitrites, ammonium and phosphates by the Krogslund lab at U.W.

Statistical analysis was done in R version 2.5. Eelgrass meadow characteristics and growth data were analyzed using an ANOVA with site as a random factor. Oyster growth and stable isotope data were analyzed using a linear mixed effects model with site as a random factor.   All sites were categorized by location (North, South or Dabob Bay). Cumulative distribution graphs of sediment were prepared in Matlab and analyzed using a paired t test in R.

3.4   Results

3.4.1   Eelgrass Characteristics

Due to tidal constraints, eelgrass growth was collected only at 3 sites in summer 2006, 8 sites in April 2007, and 8 sites in May 2007 (Figure 3-2). Using a repeated measures ANOVA on the data from 8 sites in May and April 2007 there is no significant difference in eelgrass growth between sites in decline and sites with unknown trends. However, there is a significant difference in growth rates between April and May. May growth is significantly higher (p-value of 0.0018, d.f. = 1, F-value = 10.71).
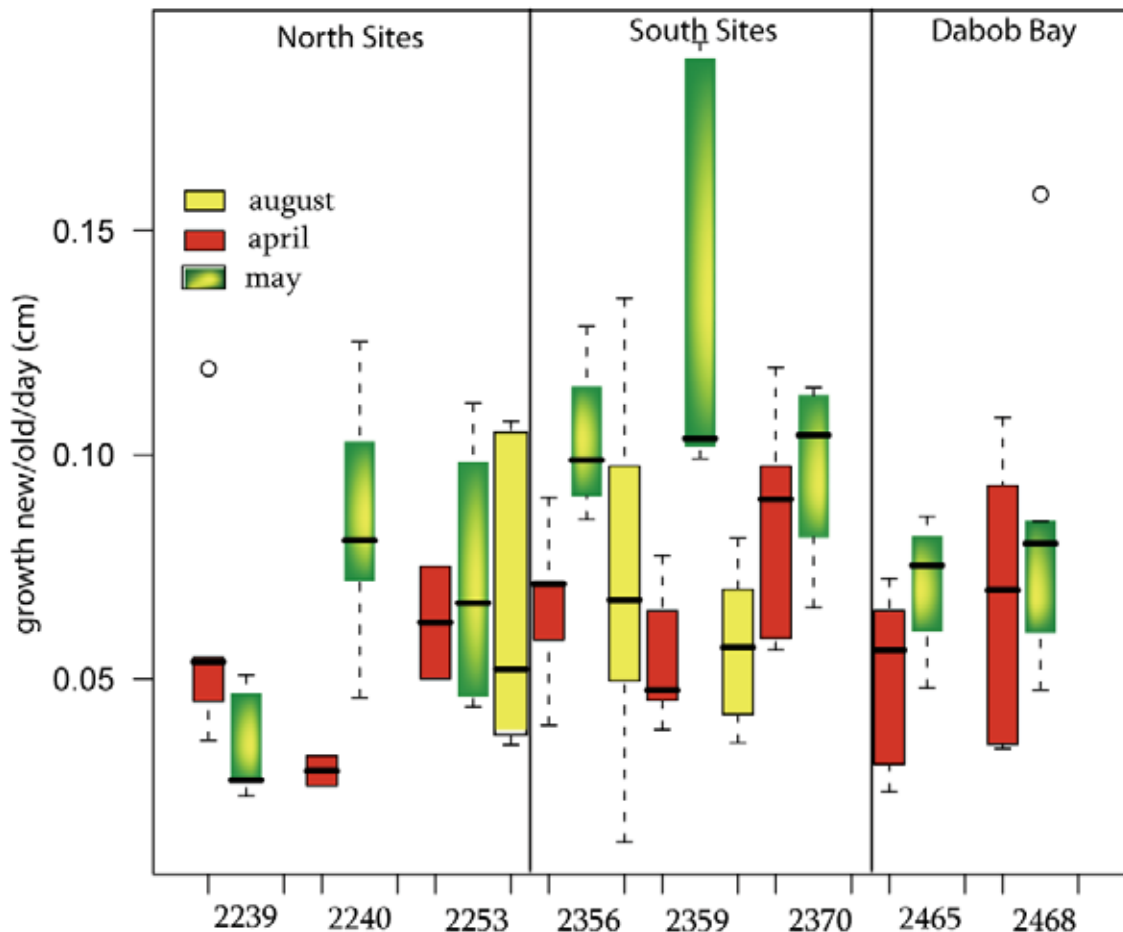
Figure 3-2. Eelgrass growth in the Hood Canal. Color distinguishes month sampled.

The biomass data show no difference between declining sites and sites with unknown trends. The ratio of above- to belowground biomass varies widely between sites. This

may in part be due to the morphological variation in the eelgrass itself. The data are in Table 3-1, averaged by site for stem density and above- and belowground biomass.

site	status	Stem Density	Aboveground Biomass (g)	Belowground Biomass (g)
2239	declining	34.67	4.02	4.60
2240	declining	55.67	7.60	10.64
2359	declining	23.50	12.30	5.38
2465	declining	22.00	0.88	2.86
2253	unknown	64.50	10.39	14.64
2356	unknown	13.33	5.26	3.62
2468	unknown	51.33	10.60	23.78

Table 3-1. Average stem density, above- and belowground biomass by site.
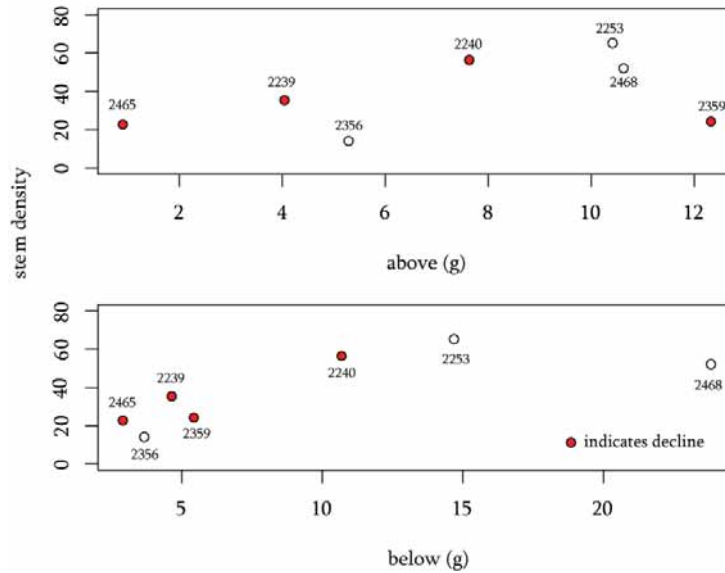
Figure 3-3. Stem density by above- and belowground biomass

Eelgrass stem density counts are highly variable and show no mean difference between meadows in decline sites versus sites with unknown trends. This may be due to the small sample size and the general inconsistency of early data collection. Stem density counts from the spring survey will be made available in the future.

3.4.2   Sediment
Sediment within eelgrass meadows has higher percent organic matter than that collected at the same site outside the meadow ($p = 0.01$, df 6, $t = 3.63$). Sites not shown to be in decline have a statistically smaller grain size ($t = -2.9922$, df = 5.363, p-value = 0.02784).
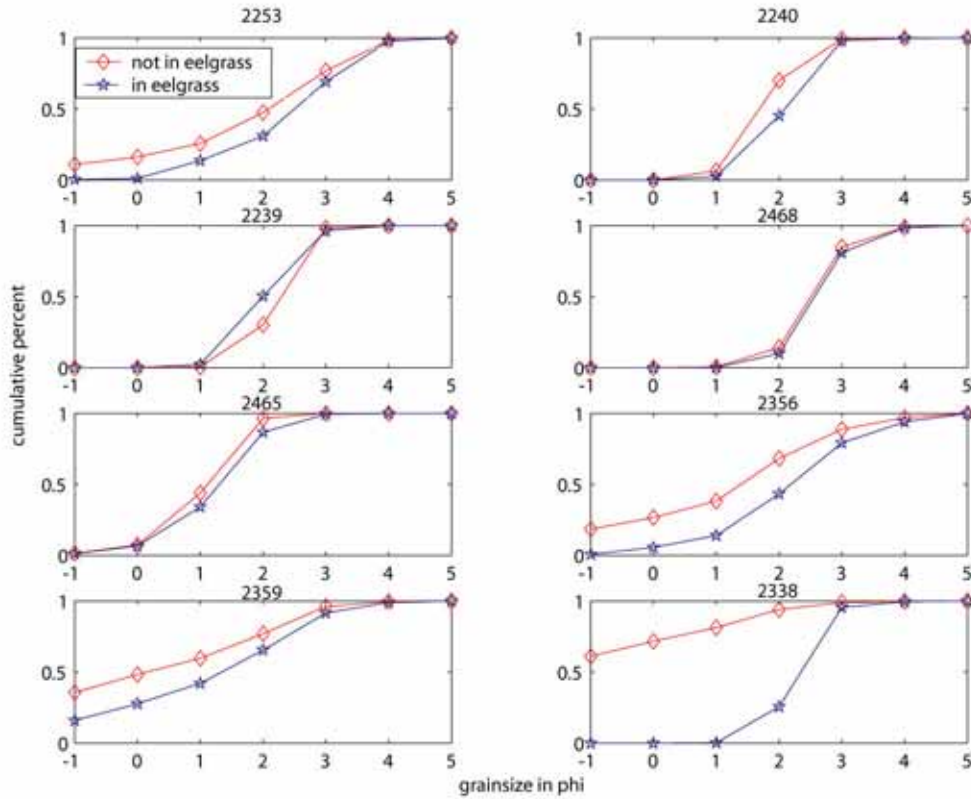
Figure 3-4. Grainsize distributions in and out of eelgrass meadows by site. The phi scale progresses from coarse (low values) to fine (high values). Phi values of -1 to 0 correspond to very coarse sand; 1-2 corresponds to medium sand; 2-3 corresponds to fine sand; 3-4 corresponds to very fine sand; 4-5 corresponds to silt.

3.4.3   Oyster Growth

At four of the five sites in the southern part of the canal, oysters showed a significantly faster growth rate compared to Dabob Bay and North Hood Canal sites. When analyzed by an ANOVA followed by a Tukey HSD post hoc test, the trend was oysters at +2.5ft MLLW grew faster than those at 0 MLLW. This trend is not significant at every site (see Figure 3-5). Winter growth patterns did not mimic summer patterns. There was no significant difference between north and south sites and no growth trend at high versus low placement within sites.
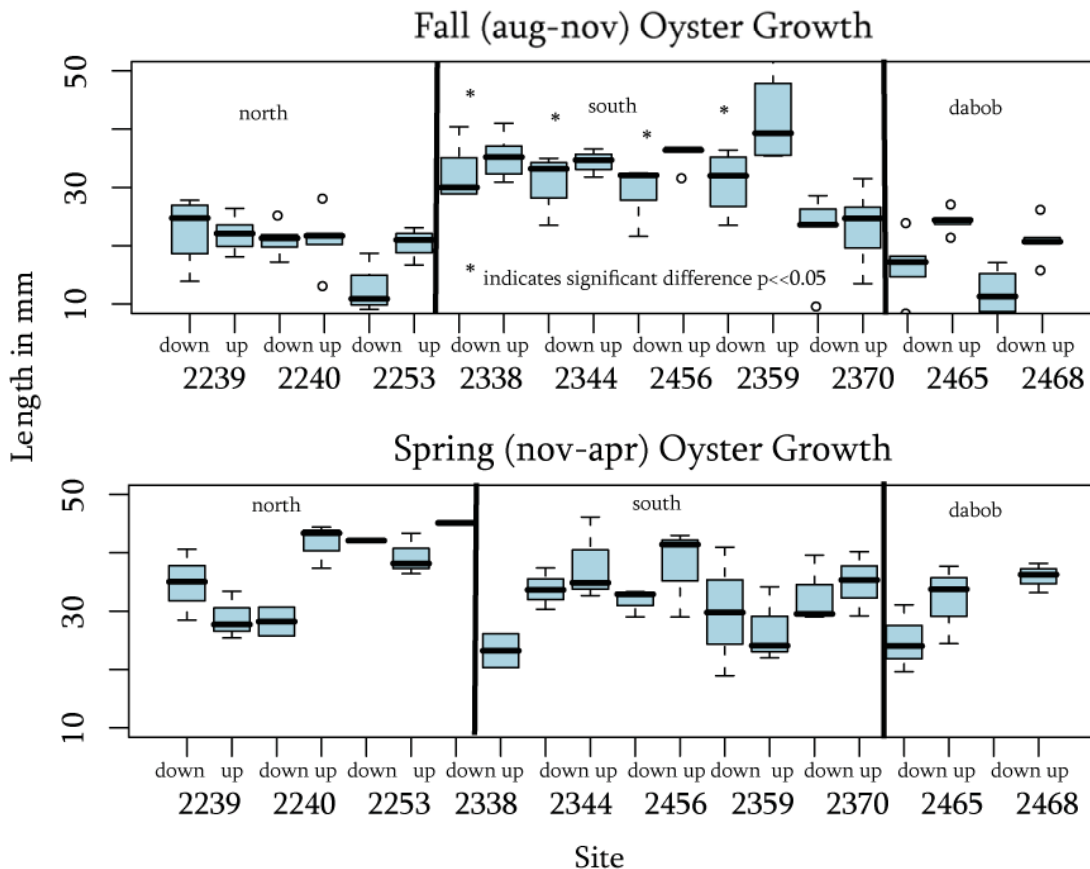
Figure 3-5. Fall and spring oyster growth. Fall oyster growth represents growth of oysters outplanted on tiles (5 replicates high and low per site) from August to November 2006. Spring growth represents growth on outplanted tiles (3 replicates high and low per site) from November 2006 to April 2007.

3.4.4   Oyster Stable Isotope Data

For carbon, both height and location were significant predictors (analyzed by a mixed effects linear model). The carbon signature for oysters at 0 MLLW is 3.5 % lower than that for oysters at 2.5ft MLLW (d.f.=83, t-value = -7.96   p-value <0.005). There was a significant difference in carbon signature for oysters grown in the south part of the canal. Those oysters had a mean carbon signature that was 11.3% lower than the mean in Dabob Bay or the North part of the Canal (d.f. = 7, t-value = -14.11, p-value< 0.005).

The nitrogen data violated assumptions of normality. After three outliers were removed, data were analyzed with a linear mixed effects model. Height and location are significant predictors of $\delta^{15}N$ values. Oysters growing higher on tiles have a 2.4% higher $\delta^{15}N$ signature than oysters growing lower (d.f. = 81, t-value = 2.31, p-value = 0.023). Oysters growing in the south part of the Hood Canal had a $\delta^{15}N$ value 19.4% higher than those growing in the North or in Dabob Bay (d.f.=7, t-value = 4.26, p-value = 0.0037).
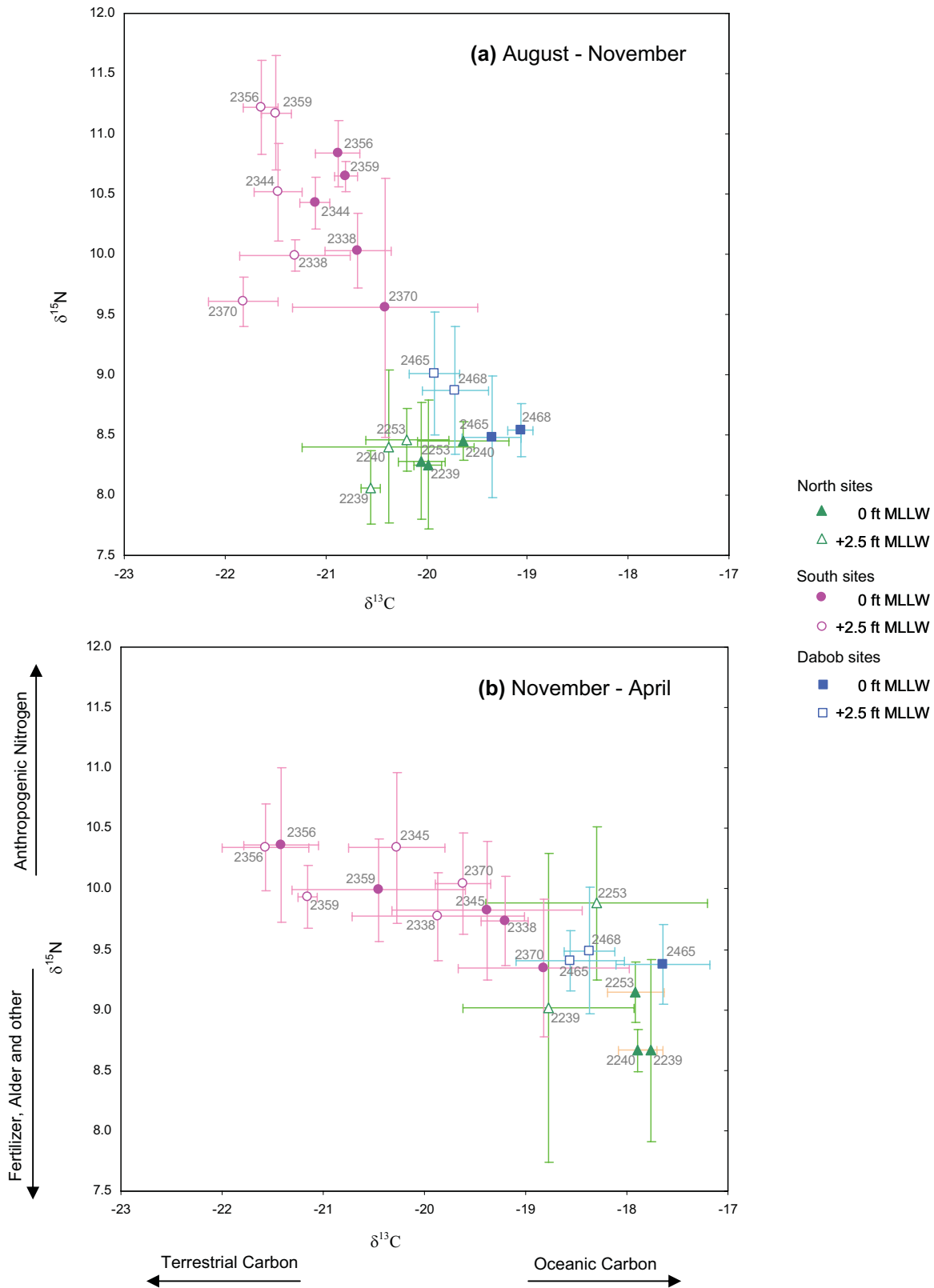
Figure 3-6. Oyster stable isotope results from the (a) August – November growth period and (b) November – April growth period. Error bars are standard deviations.
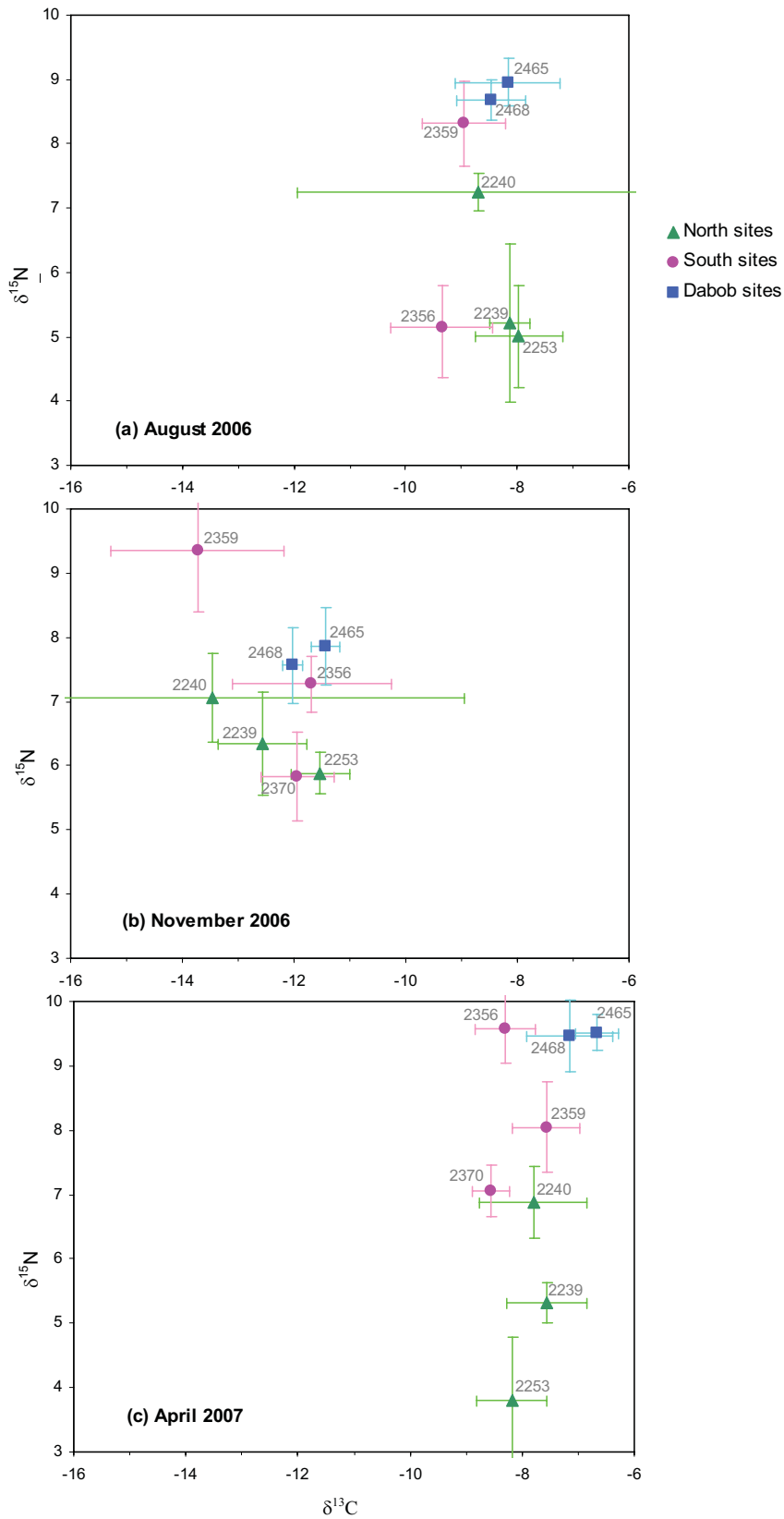
Figure 3-7. Eelgrass ^{15}N and ^{13}C results from (a) summer (August 2006), (b) fall (November 2006) and (c) spring (April 2007). Error bars are standard deviations.

3.4.5   Eelgrass Stable Isotope Data

For δ^{15}N values there are some differences by site, particularly in summer: two sites in Dabob Bay (2465, 2468), one site in Lynch Cove (2359) and one site in the North Hood Canal (2240) were enriched in nitrogen compared with sites in the north (2239, 2253) and one site in Lynch Cove (2356). There is a significant difference in δ^{13}C values between summer and winter sampling. However, there is no significant δ^{15}N change with season (paired t-test by site t = 0.5648, df = 65.182, p-value = 0.5741). Future analysis will include a repeated measures ANOVA (if the underlying assumptions of normality and balanced design are met).

3.4.6   Water Column Results

The porewater nutrient concentrations are highly variable within sites. Although they demonstrate no clear pattern by site location or eelgrass density, all of the measurements are low: eelgrass can be nitrogen limited at ammonium levels below 100µM. These measurements have been repeated in the spring 2007 tide series and future work will include analysis of these.
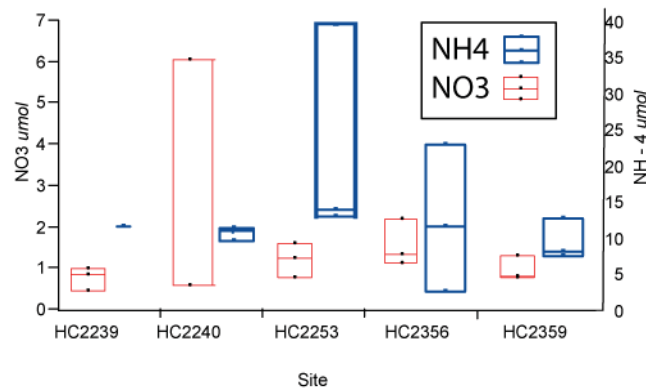
Figure 3-8. Porewater nutrients from selected sites.

TSS and chlorophyll data are still in the process of being analyzed.

3.5   Conclusions

Since nitrogen loading is fundamentally linked to eutrophication in many coastal zones, identifying nitrogen sources and their impacts on the food web is critical. Although a large proportion of the nitrogen entering the Canal is from marine sources and human inputs are relatively minor by comparison, this study suggests that anthropogenically derived nitrogen is part of the food web in the southern Hood Canal. As such nutrient loading from anthropogenic sources may contribute to the increase in both the severity and duration of hypoxic events.

A major focus of this study was to explore the potential relationship between eutrophication and eelgrass decline. Oysters were chosen as one of the target organisms because as filter feeders their stable isotope signal would reflect general spatial patterns.

In contrast, eelgrass receives much of its nitrogen through its roots, consequently it is possible that its δ^{15}N signatures reflect site specific or point-source inputs (Lepoint et al. 2004).

Hypothesis 1: Nitrogen and Carbon isotopes will vary spatially in the canal.

Carbon stable isotopes signatures of oysters vary spatially in a predictable manner within the Canal. Oysters near the mouth of the canal exhibit a marine carbon signature while oysters growing near the southern end of the canal have a predominantly terrestrial carbon source. During summer, oysters growing at 0 MLLW have a depleted carbon stable isotope source when compared to those grown at +2.5 ft. This indicates that oysters growing lower get more of their food from benthic sources within a boundary layer. The presence of a boundary layer is also suggested by the summer growth patterns on the tiles, as growth tends to be less on lower tiles than on higher ones, where food delivery is more efficient.

We found that the carbon source for eelgrass varies temporally more than spatially through the canal. This is explained by the fact that the carbon source for eelgrass is predominately the bicarbonate ion HCO_3^- (Anderson & Fourqurean 2003). Eelgrass typically exhibits seasonal patterns in carbon due to variations in productivity and boundary layer effects. Eelgrass sampled in summer was significantly enriched in its δ^{13}C signature. In times of high productivity, eelgrass discriminates less against the heavier isotope consequently incorporating more δ^{13}C into its tissues.

Summer nitrogen isotope ratios confirm that the food for oysters in the southern part of the Canal has a different nitrogen source than that in the north part of the Hood Canal, or those in Dabob Bay. This significant difference in isotope signatures lends support to the hypothesis that nitrogen from an anthropogenic source is entering the food web in the southern Hood Canal.

However, the presence of anthropogenic nitrogen sources is suggested by only one of the three sample locations for eelgrass in the southern Hood Canal. Summertime, δ^{15}N signatures for eelgrass from three locations (two in Dabob Bay and one in Lynch Cove 2359) suggest a local (point source) of anthropogenic nutrients. We were unable to collect data from sites 2344 and 2338 both of which are in the southern Hood Canal but do not have intertidal eelgrass meadows. Although summertime δ^{15}N signatures for eelgrass are enriched, oysters grown in the same locations are not particularly enriched. This contrast could indicate a very localized source of anthropogenic nutrients, the signal of which becomes diluted and does not magnify through the food web in Dabob Bay.

While the wintertime δ^{15}N signal from the two sites in Dabob Bay declines significantly, the ratio for 2359 remains high. This suggests a continuing anthropogenic nutrient source in the winter at site 2359. High concentrations of alder trees in the Dabob Bay watershed may explain seasonal shift in δ^{15}N signatures there. Alder trees have a mutualistic relationship with nitrogen-fixing bacteria. Consequently, it is possible that isotopically light nitrogen derived from alder trees can enter the food web. We expect that this nutrient

leaching will be greatest during fall and winter. In watersheds with high concentrations of alder trees, the isotopic signatures of both oysters and eelgrass might be depleted during periods of high nutrient leaching. This may explain the seasonal variation in isotopic signatures in Dabob Bay.

The significantly enriched nitrogen isotope signal in southern Hood Canal might be compounded by the presence of sulfate-reducing bacterial mats. Sulfate reducing bacteria alter the fractionation of nitrogen. They metabolize NH_4^+ and store nitrogen in their intercellular tissues. Sulfate reducing bacteria may further enrich the $\delta^{15}N$ signature of organisms in our study food web (Peterson 1999). However, the water in the Hood Canal is highly stratified so it is unclear how bacterial processes in the depths of the Canal may be affecting food web dynamics in the intertidal zone.

Hypothesis 2: Eutrophication will be linked to sites of eelgrass decline; sites of eelgrass decline will exhibit slower growth, patchier distribution and less reproduction. We hypothesized that sites with eelgrass subpopulations in decline would exhibit lower growth rates. However, when analyzed there was no consistent pattern of slower growth across sites in decline and those with unknown trends. Our spring survey did show that there is a large amount of variation in reproduction among sites. Our observations suggest that in the Hood Canal flats habitat (shallow drop in elevation and with high concentrations of fine sediment) there is more germination, whereas at sandier sites with steep banks (fringe sites) eelgrass seems to reproduce more frequently through vegetative propagation.

There are significant differences in sediment between sites. Since eelgrass is sensitive to sediment type and particularly to the amount of organic matter and silt in the sediment, it is possible that much of the eelgrass growing in the Hood Canal is growing in already suboptimal conditions. Thus, it may be less resilient to environmental stressors. However it is difficult to identify the sediment as the causal mechanism of eelgrass decline, conditions may have become suboptimal as a result of eelgrass dieback and the breakdown of a positive feedback (ie: eelgrass meadows create conditions for more eelgrass meadows). Our results did suggest that eelgrass patches have more fine-grained sediments than nearby places without eelgrass.

Analysis of carbon and nitrogen stable isotopes indicate that nitrogen from anthropogenic sources is entering the nearshore habitats of the Hood Canal. However, we cannot conclusively link sites of eelgrass decline with enriched (anthropogenically influenced) $\delta^{15}N$ signatures. Originally, we looked for a Canal-wide signal of disturbance through nutrient loading by examining nitrogen stable isotopes in oysters and eelgrass. However, it is possible that eelgrass decline in the canal may be idiosyncratic, a result of subtle differences between sites that affect their resilience in response to both anthropogenic and natural disturbance. The ultimate causes may be bulkheads increasing wave action, smothering from algal mats, desiccation stress at particularly important times (i.e., seed germination or flowering), or dieback caused by hypoxia.

Experimental manipulation of key stressors is warranted to better understand why eelgrass is declining at some sites and not at others. Particularly it may be fruitful to examine the

30

impacts of algal mats on eelgrass growth and abundance. During my site visits, I witnessed dense algal mats at many of the North Hood Canal sites. There were particularly high abundances of *Ulva* sp. during the fall tides and late summer tides (particularly at northern sites). Other studies have established a link between eelgrass decline and an increase in macroalgal canopy cover (Hauxwell et al. 2001).

There are several sites with eelgrass decline located near bulkheads. A combination of severe winter storms and inopportunely timed low tides could account for decline at these sites. Rebounding wave energy at these sites could be experimentally manipulated to determine its effects on eelgrass subpopulations. There are other potential stressors that might be experimentally manipulated, these include: competition with non-native *Z. japonica*, and direct impacts from hypoxia.

Future work for this project includes the analysis of stable isotope results from spring 2007, chlorophyll a results (from March through May), the analysis of TSS and percent organic matter data from the water column, and the porewater results from the spring survey. Thus far we have measured significant differences in oyster growth by location in the Canal, but no significant differences in eelgrass growth between sites in decline and sites with unknown trends. We found significant differences in oyster $\delta^{15}N$ by location and three sites with eelgrass that had enriched $\delta^{15}N$ values in the summertime. These results show no consistent pattern linking sites of eelgrass decline to sites with anthropogenic nutrient sources. However, the results do suggest the presence of an anthropogenic nutrient source in the southern Hood Canal nearshore food web.

Works Cited

(Pew Oceans Commission 2003) America's Living Oceans: Charting a Course for Sea Change. Pew Charitable Trust, Philadelphia, PA.

Anderson WT, Fourqurean JW (2003) Intra- and interannual variability in seagrass carbon and nitrogen stable isotopes from south Florida, a preliminary study. Organic Geochemistry 34:185-194.

Burkholder JM, Mason KM, Glasgow HB (1992) Water-Column Nitrate Enrichment Promotes Decline of Eelgrass *Zostera marina* - Evidence From Seasonal Mesocosm Experiments. Marine Ecology-Progress Series 81:163-178.

Diaz RJ, Rosenberg R (1995) Marine benthic hypoxia: A review of its ecological effects and the behavioural responses of benthic macrofauna. In: Oceanography And Marine Biology - An Annual Review, Vol 33, Vol 33, p 245-303.

Dowty P, Blain Reeves, Helen Berry, Sandy Wyllie-Echeverria, Thomas Mumford, Amy Sewell, Patricia Milos, Roselynn Wright (2005) Puget Sound Submerged Vegetation Monitoring Project 2003-04 Monitoring Report http://www.dnr.wa.gov/htdocs/aqr/nshr/pdf/2005_svmp_report.pdf.

Grantham BA, Chan F, Nielsen KJ, Fox DS, Barth JA, Huyer A, Lubchenco J, Menge BA (2004) Upwelling-driven nearshore hypoxia signals ecosystem and oceanographic changes in the northeast Pacific. Nature 429:749-754.

Hauxwell J, Cebrian J, Furlong C, Valiela I (2001) Macroalgal canopies contribute to eelgrass (*Zostera marina*) decline in temperate estuarine ecosystems. Ecology 82:1007-1022.

HCDOP (2007) Hood Canal Dissolved Oxygen Program website http://www.hoodcanal.washington.edu/observations/historicalcomparison.jsp

Heck KL, Able KW, Roman CT, Fahay MP (1995) Composition, Abundance, Biomass, And Production Of Macrofauna In A New-England Estuary - Comparisons Among Eelgrass Meadows And Other Nursery Habitats. Estuaries 18:379-389.

Larkum A, Robert Orth, Carlos Duarte (eds.) (2006) Seagrasses: Biology, Ecology and Conservation, Vol 1. Springer, Dordrecht, Netherlands.

Lazzari MA, Stone BZ (2006) Use of submerged aquatic vegetation as habitat by young-of-the-year epibenthic fishes in shallow Maine nearshore waters. Estuarine Coastal And Shelf Science 69:591-606.

Lepoint G, Dauby P, Gobert S (2004) Applications of C and N stable isotopes to ecological and environmental studies in seagrass ecosystems. Marine Pollution Bulletin 49:887-891.

Lotze HK, Lenihan HS, Bourque BJ, Bradbury RH, Cooke RG, Kay MC, Kidwell SM, Kirby MX, Peterson CH, Jackson JBC (2006) Depletion, degradation, and recovery potential of estuaries and coastal seas. Science 312:1806-1809.

McClelland JW, Valiela I (1998) Changes in food web structure under the influence of increased anthropogenic nitrogen inputs to estuaries. Marine Ecology-Progress Series 168:259-271.

Orth RJ, Carruthers TJB, Dennison WC, Duarte CM, Fourqurean JW, Heck KL, Hughes AR, Kendrick GA, Kenworthy WJ, Olyarnik S, Short FT, Waycott M, Williams SL (2006) A global crisis for seagrass ecosystems. Bioscience 56:987-996.

Peterson BJ (1999) Stable isotopes as tracers of organic matter input and transfer in benthic food webs: A review. Acta Oecologica-International Journal Of Ecology 20:479-487.

Rabalais NN, Turner RE, Wiseman WJ (2002) Gulf of Mexico hypoxia, aka "The dead zone". Annual Review Of Ecology And Systematics 33:235-263.

Roberts M, Jan Newton, and Dan Hannafious (2005) Hood Canal Dissolved Oxygen Program Integrated Assessment and Modeling Study: Year 1 Activities.

Ruesink JL, Curtis Roegner, Brett R. Dumbauld, Jan A Newton, David A Armstrong (2003) Contributions of Coastal and Wastershed Energy Sources to Secondary Production in a Northeastern Pacific Estuary. Estuaries 26:1079-1093.

Short FT, Wyllie-Echeverria S (1996) Natural and human-induced disturbance of seagrasses. Environmental Conservation 23:17-27.

Simenstad CA, Wissmar RC (1985) Delta-C-13 Evidence Of The Origins And Fates Of Organic-Carbon In Estuarine And Nearshore Food Webs. Marine Ecology-Progress Series 22:141-152.

Turner RE, Rabalais NN (1994) Coastal Eutrophication Near The Mississippi River Delta. Nature 368:619-621.

Welschmeyer NA (1994) Fluorometric Analysis of Chlorophyll-A In The Presence Of Chlorophyll-B And Pheopigments. Limnology and Oceanography 39:1985-1992.

Zieman JC (1974) Methods for Study of Growth and Production of Turtle Grass, Thalassia-Testudinum Konig. Aquaculture 4:139-143.

4   Impervious Surface and Land Cover in the Hood Canal Basin

Pete Dowty
Washington State Department of Natural Resources

4.1   Introduction

Land cover change represents a potentially important factor affecting nonpoint loadings to receiving waters. The goal of the work presented in this section was to perform a course assessment of land cover patterns in the Hood Canal basin. For the purposes of this assessment, land cover is represented by the cover of impervious surfaces and the cover of canopy with >40% canopy closure.

4.2   Methods

The land cover change analysis produced in 2005 by Sanborn for the Department of Ecology provided the source data for this assessment (Fiorella 2005). The multiple raster data layers produced as part of that project were in turn based on NOAA Coastal Change Analysis Program (C-CAP) data products with refinements based on analysis by Sanborn of additional Landsat TM imagery. Land cover data layers were produced for 1991, 1996 and 2001.

A set of sub-basins were also produced as part of the Sanborn project that were modeled after statewide watershed administrative units (WAUs). These basins were modified for the purposes of this project to fully conform to the boundaries of the Hood Canal basin.

After reviewing the intensity of impervious surface in the Hood Canal basin, an aggregation was selected that emphasized discrimination at lower intensities of impervious surface. The Spatial Modeler in Erdas Imagine 8.7 was used to aggregate the data on a pixel-by-pixel basis into the following bins and isolate each bin in a separate data layer:
   a) no impervious surface classified (none or <20%)
   b) 20 – 29% impervious surface
   c) 30 – 39% impervious surface
   d) 40 – 59% impervious surface
   e) 60 – 100% impervious surface

The Zonal Statistics function in the Spatial Analyst extension of ArcGIS 9.2 was used to summarize the data for each sub-basin for each bin of impervious surface values as well as the canopy cover data layer. The output tables were exported as dbf files and further manipulated in Microsoft Excel and ESRI ArcMap.

4.3   Results

Relative to other areas within the greater Puget Sound basin, the Hood Canal basin has low levels of impervious surface (Figure 4-1). The most obvious concentrations are in the vicinity of Lofall and the Bangor Naval Reservation; in the vicinity of Belfair and south of Lake Cushman (Figure 4-2).
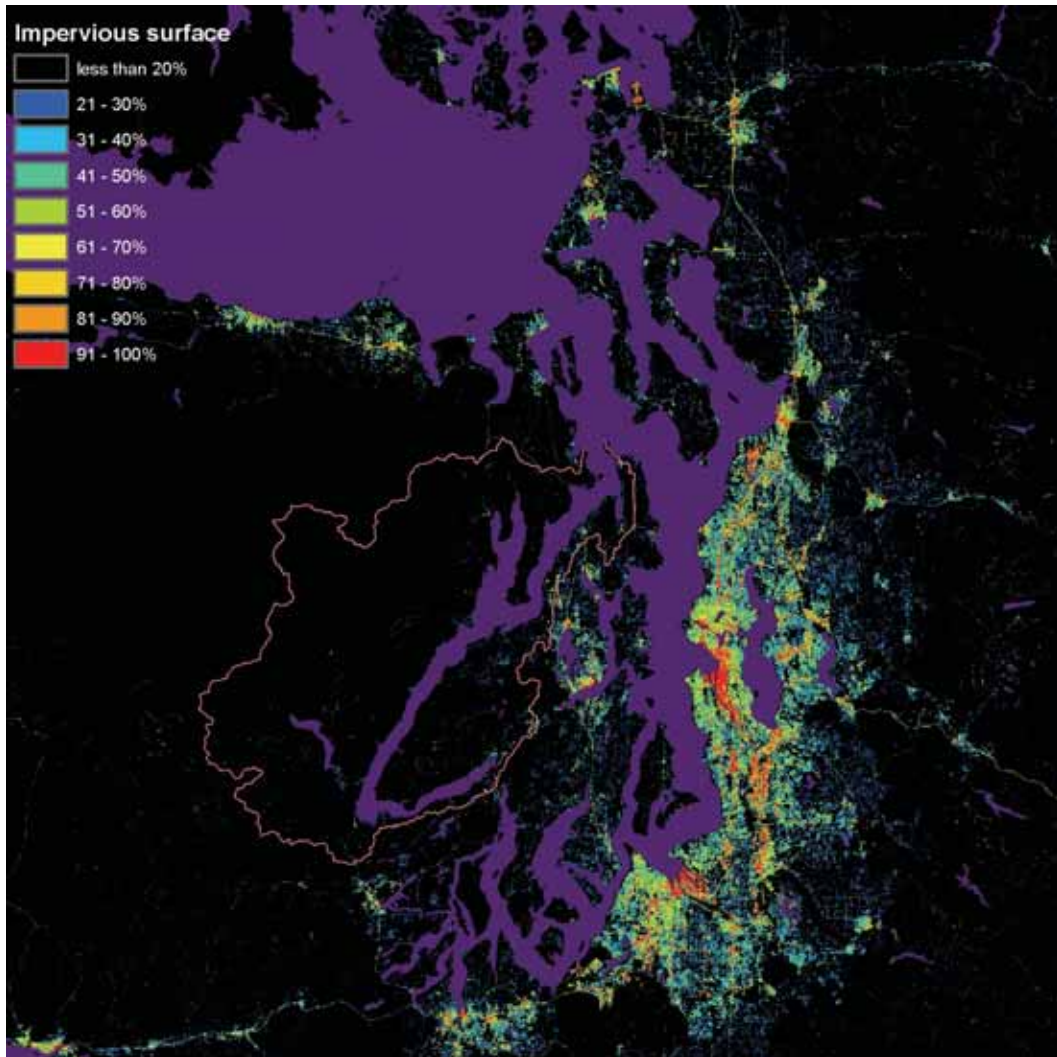
Figure 4-1. Broad pattern of 2001 impervious surface around greater Puget Sound. The Hood Canal basin, with boundary shown, has low levels of impervious surface relative to other areas. (Source data: Department of Ecology).

Figure 4-2 shows the sub-basins that were used for summarizing the canopy and impervious surface datasets and their relationship to the field sites discussed in Chapter 3 of this report. The boundaries of sub-basin 2295 were modified from the version distributed by Ecology to conform to Hood Canal drainage.
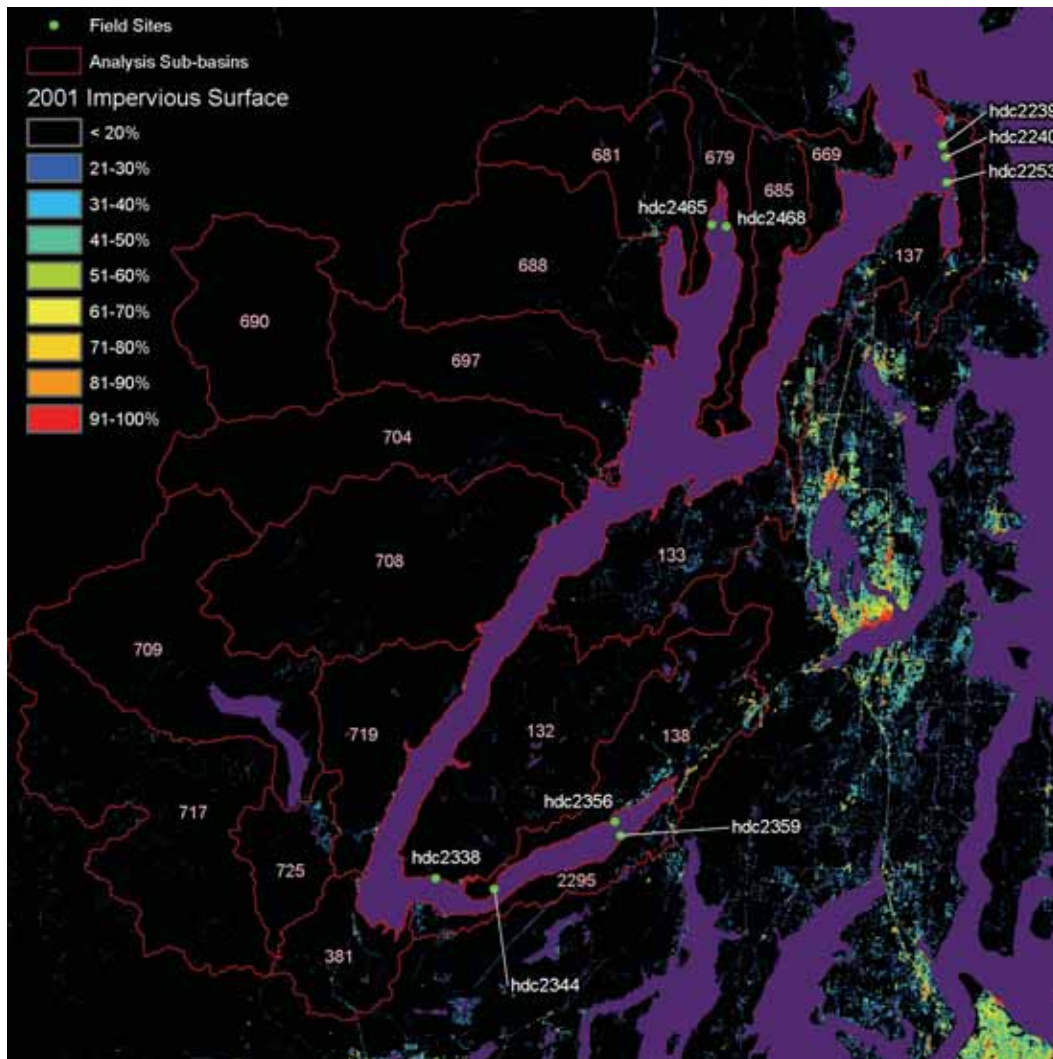
Figure 4-2. 2001 impervious surface within the Hood Canal basin. The sub-basins and their identifying numbers that were used to summarize the data are also shown. (Source data: Department of Ecology).

Given that impervious surface data are available for three time periods (1991, 1996 and 2001), it is possible to determine change over two time intervals. Figure 4-3 shows the changes in classified impervious surface in the 1991-1996 and 1996-2001 intervals for each sub-basin for each impervious surface bin.

In general, there were greater increases in impervious surface in the earlier interval. This is most dramatic in sub-basins 133, 137 (Kitsap peninsula) and 2295 (southern shore of lower Hood Canal). In the second interval (1996-2001) the sub-basins 133, 137 (Kitsap peninsula) and 138 (Belfair area, Kitsap and Mason counties) have by far the greatest increases in impervious surface area. The increases are distributed among the different bins of impervious surface intensity. This distribution varies across the sub-basins but in each case there is an increase in each bin.
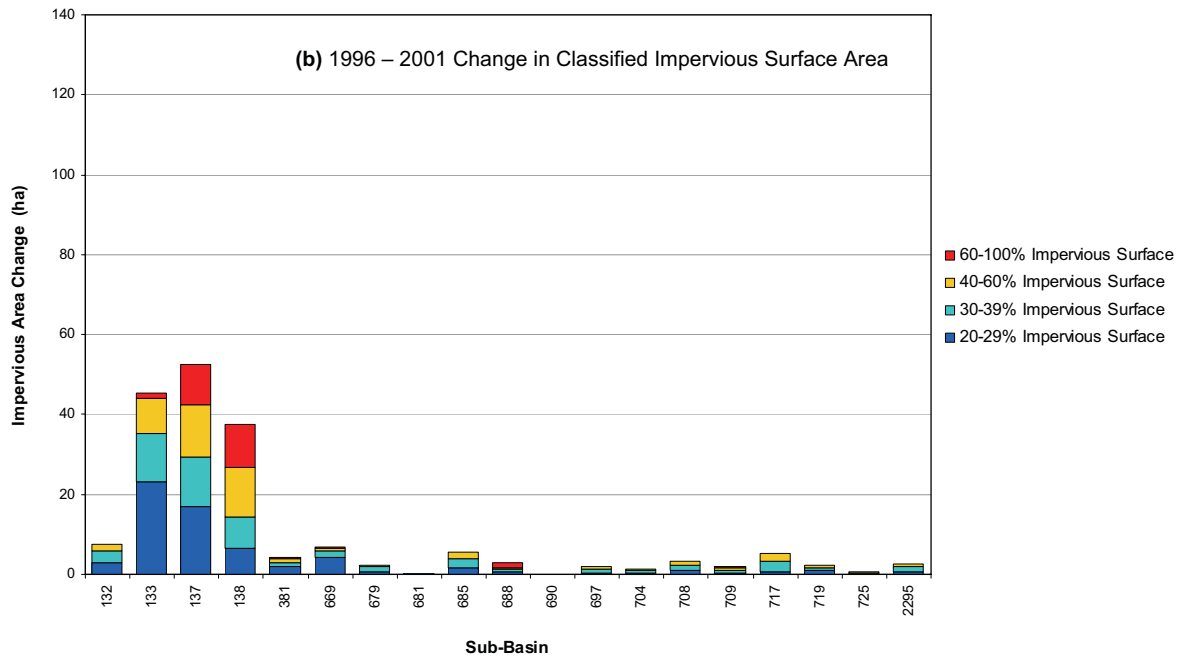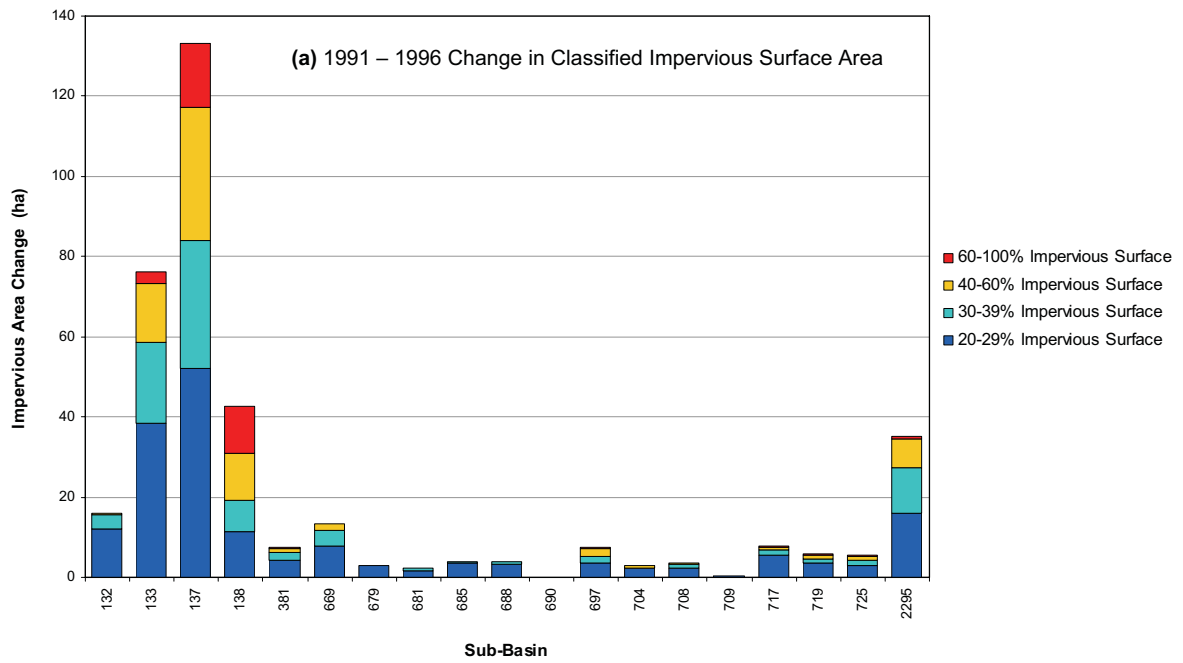
Figure 4-3. Changes in classified impervious surface within the 19 Hood Canal sub-basins for (a) 1991-1996, and (b) 1996-2001. (Source data: Department of Ecology).

Figure 4-4 summarizes the levels of canopy cover in each sub-basin for 1991, 1996 and 2001. There are strong differences among the sub-basins in level of canopy cover. Sub-basins 381 (Skokomish area) and 690 (Olympic National Park) have distinctly lower canopy cover but for very different reasons. Sub-basin 381 has large areas of floodplain and wetland and sub-basin 690 has large areas at high elevation above the tree line.

Some sub-basins are distinct in terms of their change in canopy cover over the two time intervals. Sub-basins 138, 685 and 725 had sharp decreases in canopy cover while 137 and 679 had strong increases in canopy cover.
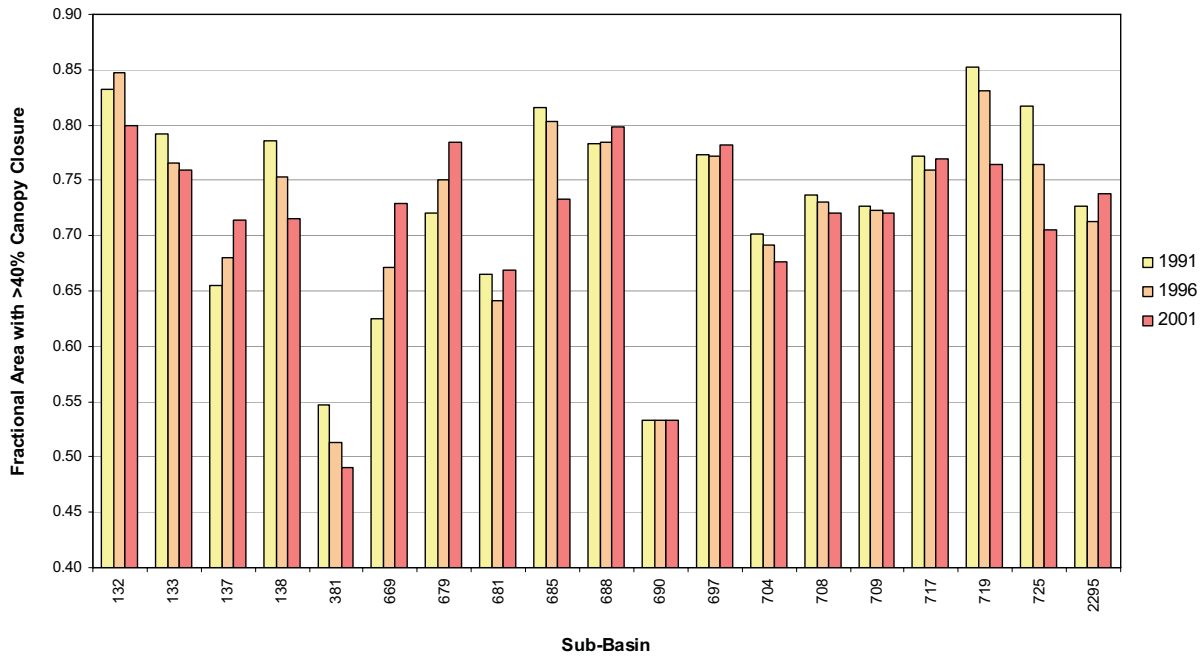
Figure 4-4. Canopy cover (areas with >40% canopy closure) as classified for 1991, 1996 and 2001 in the nineteen sub-basins shown in Figure 4-2. (Source data: Department of Ecology).

Changes in canopy cover and impervious surface can be examined together as shown in Figure 4-5. There are no clear associations between these two parameters in this representation but this does not account for spatial position of the sub-basins.
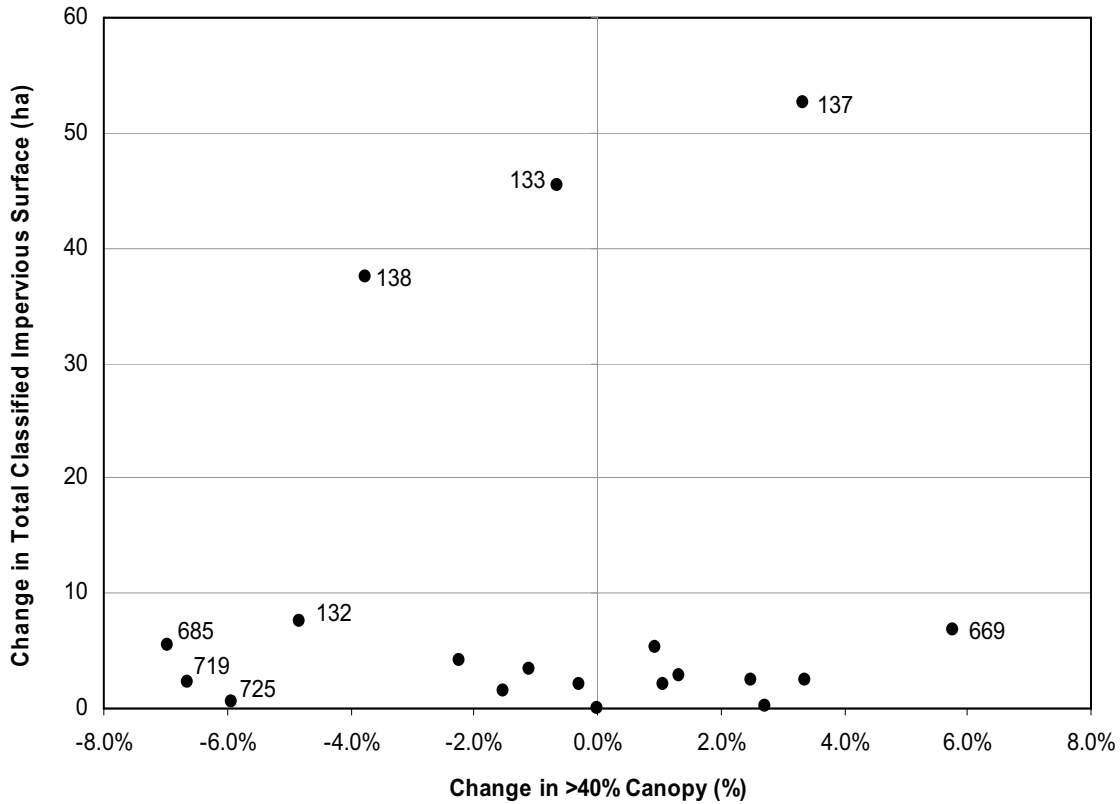
Figure 4-5. Hood Canal sub-basins plotted according to their 1996-2001 change in cover with >40% canopy closure (x-axis) and 1996-2001 change in total area classified with >20% impervious surface (y-axis). Selected data points are labeled with their sub-basin number as mapped in Figure 4-2. (Source data: Department of Ecology).

Figure 4-6 shows the same data as in Figure 4-5 but mapped onto the associated sub-basins. There is a cluster of sub-basins with high canopy loss in lower Hood Canal. There are also moderately high levels of increase in impervious surface (sub-basins 138 and 2295). The largest changes in impervious surface by far are in northern Hood Canal (133 and 137). Any changes to nonpoint loadings to the north would presumably have the benefit of greater flushing relative to lower Hood Canal.

4.4   Summary

The Hood Canal basin has distinct spatial patterns of increasing impervious surface and change to canopy cover. These can be expected to have an effect on nonpoint loadings to Hood Canal waters. The patterns presented are not consistent in a simple way with the oyster growth and nitrogen isotope results presented in Chapter 3 of this report. If other factors are considered (e.g. differential flushing rates; differential sensitivity to nonpoint loadings) then the results presented here may have more explanatory power. It is

recommended that additional analysis examine patterns at finer spatial scales with explicit consideration of upland drainage patterns and marine water circulation patterns.
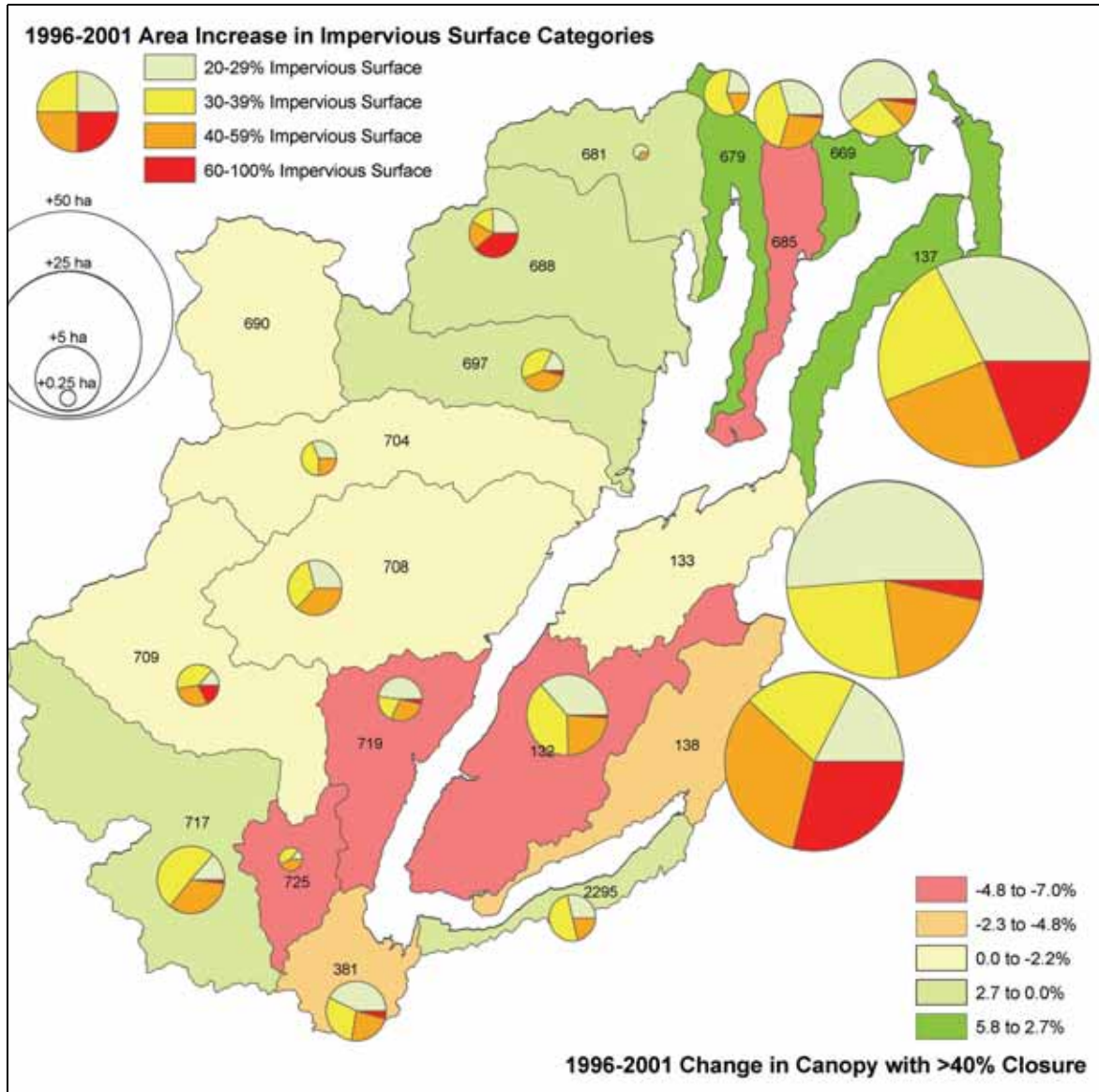
Figure 4-6. The 19 Hood Canal sub-basins classified according to 1996-2001 change in canopy cover with >40% canopy closure. The pie graphs show the total change in classified impervious surface between 1996 and 2001 (indicated by size of pie chart) and the breakdown of the total change into four categories of impervious surface density. (Source data: Department of Ecology).

4.5   References

Fiorella. M., 1995. Western Washington Land Cover Change Analysis, Final Report to the
    Washington Department of Ecology Water Quality Program, Sanborn, Portland OR.
    Data are available at http://www.ecy.wa.gov/services/gis/data/impervious/basins.htm.

5 Bathymetry, Substrate and Circulation in Westcott Bay, San Juan Islands, Washington

Eric E. Grossman
U.S. Geological Survey, Pacific Science Center

Andrew Stevens
U.S. Geological Survey, Menlo Park

Christopher Curran
U.S. Geological Survey, Washington Water Science Center

Collin Smith and Andrew Schwartz
Washington State Department of Ecology

Bathymetry, Substrate and Circulation in Westcott Bay, San Juan Islands, Washington
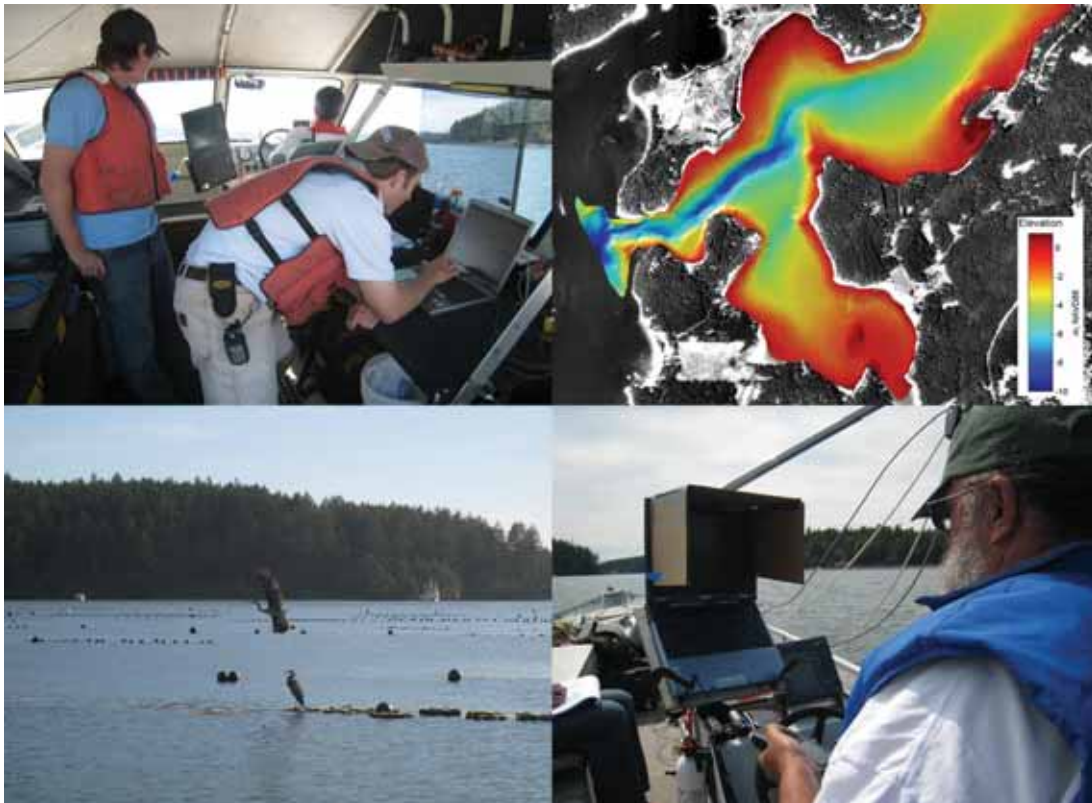
By Eric Grossman, Andrew Stevens, Chris Curran, Collin Smith, and Andrew Schwartz

Open-File Report 2007-1305

U.S. Department of the Interior
Dirk Kempthorne, Secretary

U.S. Geological Survey
Mark Myers, Director

U.S. Geological Survey, Reston, Virginia 2007

Contents

Figures

Appendixes

46

Bathymetry, Substrate, and Circulation in Westcott Bay, San Juan Islands, Washington

Eric E. Grossman[1], Andrew Stevens[2], Christopher Curran[3], Collin Smith[5], and Andrew Schwartz[5]

[1] U.S .Geological Survey, Pacific Science Center, Santa Cruz, CA
[2] U.S. Geological Survey, Menlo Park, CA
[3] U.S. Geological Survey, Washington Water Science Center, Tacoma, WA
[3] U.S. Geological Survey, Western Fisheries Research Center, Cook, WA
[3] Washington State Department of Ecology, Olympia, WA

Abstract

Nearshore bathymetry, substrate type, and circulation patterns in Westcott Bay, San Juan Islands, Washington, were mapped using two acoustic sonar systems, video and direct sampling of seafloor sediments. The goal of the project was to characterize nearshore habitat and conditions influencing eelgrass (*Z. marina*) where extensive loss has occurred since 1995. A principal hypothesis for the loss of eelgrass is a recent decrease in light availability for eelgrass growth due to increase in turbidity associated with either an increase in fine sedimentation or biological productivity within the bay. To explore sources for this fine sediment and turbidity, a dual-frequency Biosonics sonar operating at 200 and 430 kHz was used to map seafloor depth, morphology and vegetation along 69 linear kilometers of the bay. The higher frequency 430 kHz system also provided information on particulate concentrations in the water column. A boat-mounted 600 kHz RDI Acoustic Doppler Current Profiler (ADCP) was used to map current velocity and direction and water column backscatter intensity along another 29 km, with select measurements made to characterize variations in circulation with tides. An underwater video camera was deployed to ground-truth acoustic data. Seventy one sediment samples were collected to quantify sediment grain size distributions across Westcott Bay. Sediment samples were analyzed for grain size at the Western Coastal and Marine Geology Team sediment laboratory in Menlo Park, CA. These data reveal that the seafloor near the entrance to Westcott Bay is rocky with a complex morphology and covered with dense and diverse benthic vegetation. Current velocities were also measured to be highest at the entrance and along a deep channel extending 1 km into the bay. The substrate is increasingly comprised of finer sediments with distance into Westcott Bay where current velocities are lower. This report describes the data collected and preliminary findings of USGS Cruise B-6-07-PS conducted between May 31, 2007 and June 5, 2007.

Introduction

In response to recent, extensive loss of the eelgrass *Z. marina* throughout the San Juan Islands (Berry et al. 2003; Wyllie-Echeverria et al. 2003), scientists from Washington State Department of Natural Resources (WADNR) Aquatic Resources Division, University of Washington (UW), and the U.S. Geological Survey (USGS) have initiated studies of nearshore habitat structure and hydrodynamic processes to examine possible stressors. A principal hypothesis for the loss of *Z. marina* in Westcott Bay, San Juan Island, is a recent decrease in light availability for eelgrass growth due to increase in turbidity associated with either an increase in fine sedimentation or biological productivity within the bay. To examine conditions influencing possible *Z. marina* recovery in Westcott Bay *Z. marina* transplant studies were paired with time-series water column property measurements during the summer of 2007 as part of the WA DNR "Eelgrass Stressor-Response Project". To characterize sources and processes influencing sediment transport and turbidity that affect light conditions for *Z. marina*, bathymetric, substrate, and circulation mapping were conducted. This report describes the bathymetry, substrate, and circulation data collected and preliminary findings that relate to the nearshore and *Z. marina* habitat in Westcott Bay.

Study Area

Westcott Bay is located along the northwest coast of San Juan Island (Figure 1).
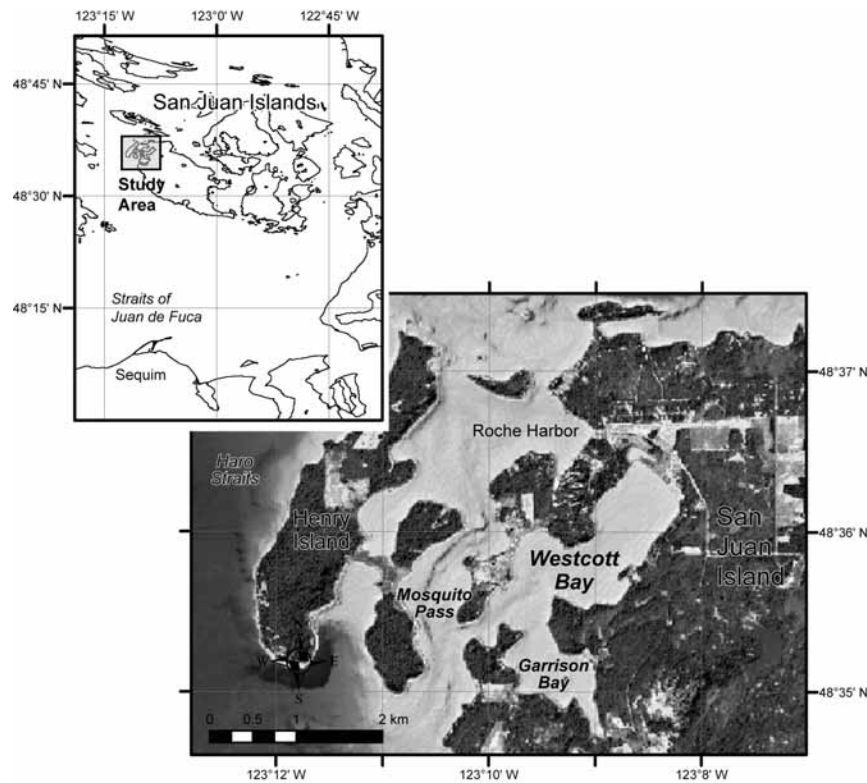
Figure 1. Location map showing Westcott Bay study area.

Westcott Bay is 3 km in length and averages 800 m in width and is connected to Garrison Bay inside of a narrow (150 m) mouth opening into Mosquito Pass. Westcott Bay is relatively shallow reaching a maximum depth of approximately -8.5 m, although 35% of the bay is less than -2 m and 48% is less than -3 m. It is bounded by a relatively low relief watershed composed of Paleozoic and Mesozoic sedimentary rocks that have been folded into a broad syncline, some of which have been metamorphosed by igneous rocks of Mesozoic age. Two small intermittent streams discharge into the head of the bay. Westcott Bay is oriented WSW-ENE and because of its narrow mouth, receives little swell in the form of wind waves originating from summertime northwest and periodic wintertime southwest fetch. This region of the San Juan Islands is characterized by a 3.5-4.0 m tide regime which generates strong observable tidal currents in Mosquito Pass. Sediment sources for Westcott Bay are likely to include fluvial-derived sediment input from the two small streams, erosion of bedrock outcrops near headlands and along the seafloor, autochthonous organic matter and calcareous shell production, and possibly import of fine materials from outside the bay through advection.

Data Acquisition

Bathymetric mapping

Sixty-nine (69) kilometers of acoustic bathymetry/substrate data were collected with a dual-frequency (200 and 430 kHz) Biosonics DT-X sonar system along 142 transects in Westcott and Garrison Bays between 5/31/07 and 6/2/07 (Fig. 2, Appendix 1).
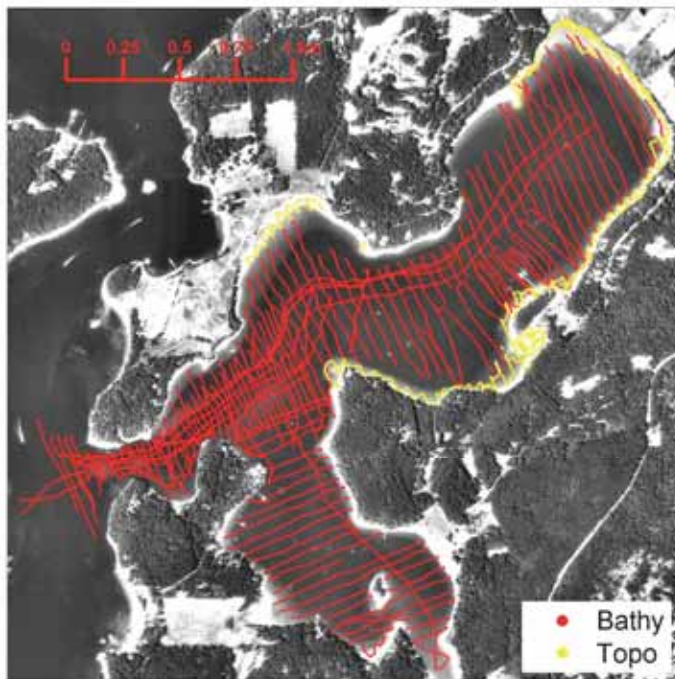
Fig. 2. Map of survey track lines where bathymetry and acoustic substrate data (red) and topographic RTK-DGPS data (yellow) were collected

The Biosonics sonar generates a 6-degree cone of sound, which translates into a footprint on the seafloor ranging 0.2 to 0.8 m for the water depths surveyed (2 - 8 m). Ship speed generally ranged 4.0-4.5 kts and data were merged with GPS positions at 1 Hz. Resulting data therefore represent 0.2-0.8 m pixels on the seafloor spaced approximately 1-2 m apart along track lines. Track lines were spaced 25 m apart. Twenty (20) km of topographic elevation data were also collected across the upper intertidal region by walking the shoreface with a portable Trimble 4700 RTK-DGPS receiver. This receiver utilized a Trimble Zepher Antenna and Pacific Crest radio receiver to obtain real time position corrections from a base station operating a Trimble 4400 receiver and L1/L2 antenna with a Pacific Crest 35 Watt radio transmitter. Elevation data over emergent beaches and tide flats collected by walking are 2-3 times denser as a result of survey speeds ranging 0.5-1.0 kts. The combined bathymetric and topographic data were merged to create a digital elevation model representing the surface topography of Westcott Bay. This surface is referenced to the WGS 84 datum in the UTM Zone 10 North projection with a horizontal accuracy of 2.3 cm. Elevations are referenced to NAVD88 with an estimated vertical accuracy ranging 2.6-9.8 cm. This includes error from the RTK-DGPS and Biosonics sonar, and errors introduced in data processing. The root mean square (RMS) error of the processed surface elevation values were derived from survey line crossings. Line crossings did not always capture the same point on the seafloor (because of GPS accuracy, navigation, currents, and timing of data recording). Therefore, variability in elevation values at crossings is likely in part derived from variability in the bathymetry of the seafloor where line crossings spanned 0.5 to 2 m apart in the horizontal.

Because there can be significant natural variability in depth/elevation across 0.5 to 2.0 m of the seafloor, the vertical error of the survey was determined from analysis of three classes of elevation values at line crossings:

1) values within 2 m of each other from all areas of Westcott Bay including vegetated, rocky and smooth areas (RMS=9.8 cm, n=66)
2) values within 2 m of each other from the smooth area between Bell Point and the head of Westcott Bay (RMS=3.6 cm, n=22)
3) values within 0.5 m of each other within the smooth area between Bell Point and the head of Westcott Bay (RMS=2.6 cm, n=6)

The overall error for the entire survey is therefore 9.8 cm, although particular areas, especially characterized by low relief likely have much smaller errors.

Sediment Samples for Grain Size Analyses

Sediment samples were collected using a van veen grab sampler at 71 stations on a 200-250 m grid (Fig. 3) to characterize grain size distribution throughout Westcott Bay and sources of fine material for suspension and transport.

50
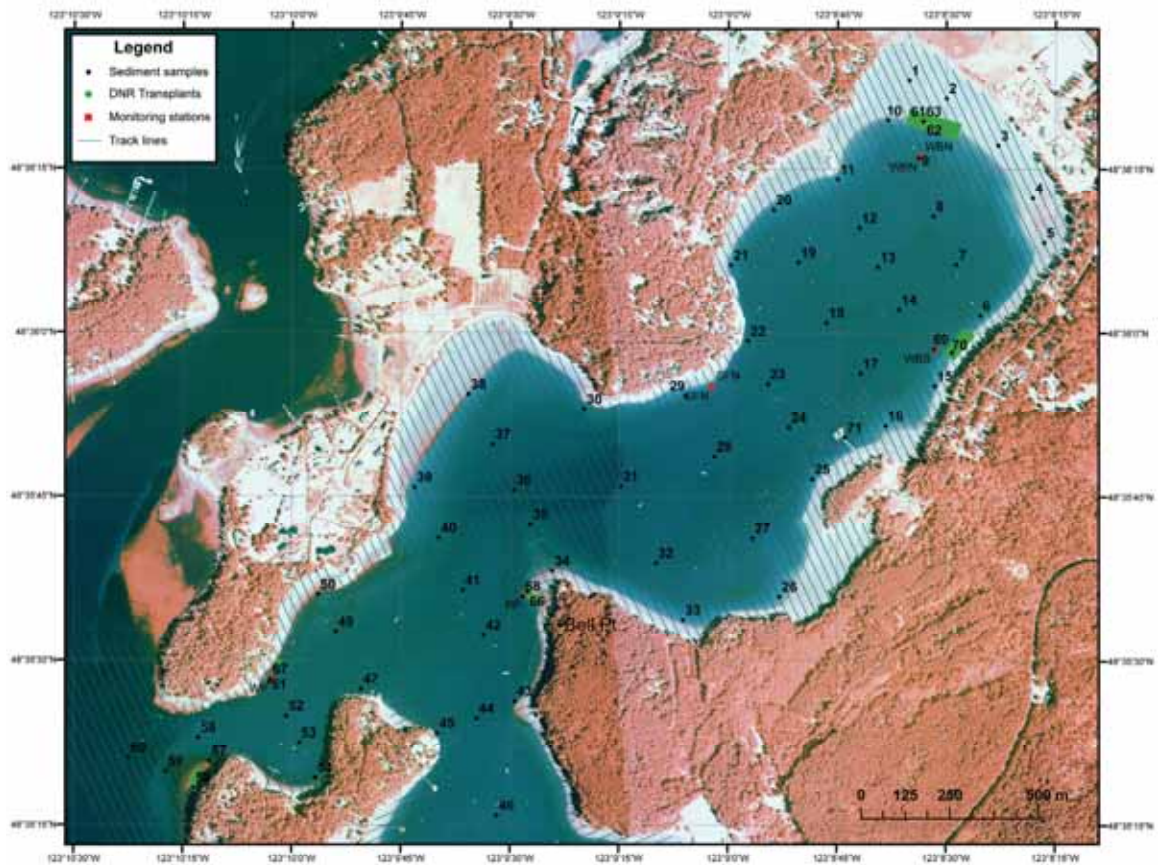
Fig. 3. Map showing sediment grab sample locations.

The shallow stratigraphy was well-preserved in the sediment grabs so that a 1-3 cm thick aerated surface layer could be observed at most stations dominated by fines (Figure 4).
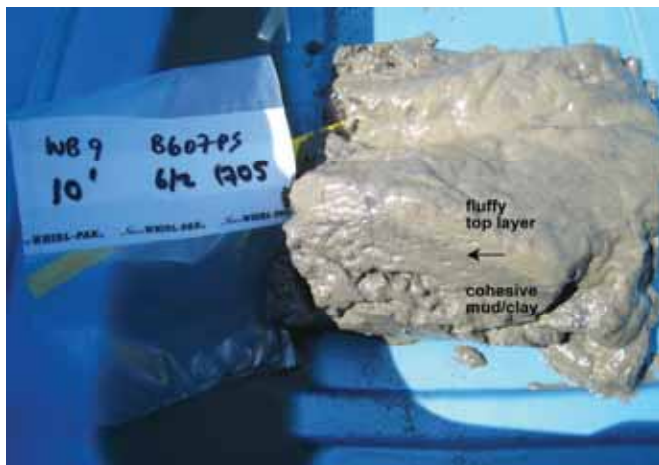
Fig. 4. Photo of sediment grab sample WB9 showing fluffy, light colored, aerated top layer overlying a sharp contact (arrow) with a denser, cohesive mud/clay below.

In the field, a sub-sample of the uppermost 1-3 cm of each grab was collected and placed into storage bags, labeled, logged, and frozen. Several 10-cm push cores were also collected. Triplicate samples were collected at sites WBN and BP for error analyses. Appendix 2 summarizes sample times and environmental conditions at collection sites.

In the laboratory, sediment samples were split for grain size and carbon analyses and later archived at the Western Coastal and Marine Geology Team sediment laboratory in Menlo Park, CA. Samples were disaggregated and sieved through 2000 and 62 micron screens to separate gravel, sands and mud after the organic component was removed by treatment with hydrogen peroxide. Sediment grain size of sands was determined using the settling methods and principles of Stokes Law (Guy 1969) on the USGS 3-m long settling tubes. The fine fraction (silts and clays) were analyzed on a Coulter 230 Laser Particle Analyzer. Three samples had less than 3% intermediate fraction and were analyzed on the Coulter. Single sample runs were made on the tubes, while results from the laser particle analyzer are averages of triplicates with standard deviations around the mean ranging 18 to 24 microns due to instrument errors. Results from the tubes and laser particle analyzer were merged using standard USGS methods found in the USGS particle analysis program pcSedSize http://water.usgs.gov/software/sedsize.html). Analyses of triplicate samples collected at stations WBN and BP show that inter-station variability around the mean grain size ranged ±0.054 mm. The complete grain size results are provided in Appendix 3. These results were then gridded across the bathymetric surface with a nearneighbor gridding algorithm averaging between the three nearest points.

Video of the seafloor was collected along several principal transects in the western and central portions of Westcott Bay to ground-truth the sonar data and provide direct observations of the complex substrate, substrate transitions, and benthic vegetation. These results will be furnished in subsequent revisions to this report.

Nearshore Currents

Current velocity, direction and backscatter amplitude were collected along 65 transects in Westcott Bay (Fig. 5) with a 600 kHz RDI ADCP (Acoustic Doppler Current Profiler) and recorded with WinRiver software following Oberg and others, (2005). Select transects at the mouth of Westcott Bay, Bell Point and immediately east of the Westcott Sea Farm were repeated ~2-3 times under flooding and ebbing tides. ADCP were recorded with GPS position at 1 hz with a ship speed of 2.0-2.5 kts, so raw ADCP data cover a lateral distance of 1.00 to 1.25 m. The raw ADCP data were vertically binned at 0.25 m and include a blanking distance of 0.25 m (no data in uppermost 0.25 m below the transducer). The RDI ADCP is accurate to within 0.25% of boat + water velocity, resulting in an error for our velocity data of 0.25 to 0.45 cm/s based on our survey speed of 2 kts and measured velocities ranging 0 to 1.5 m/s.
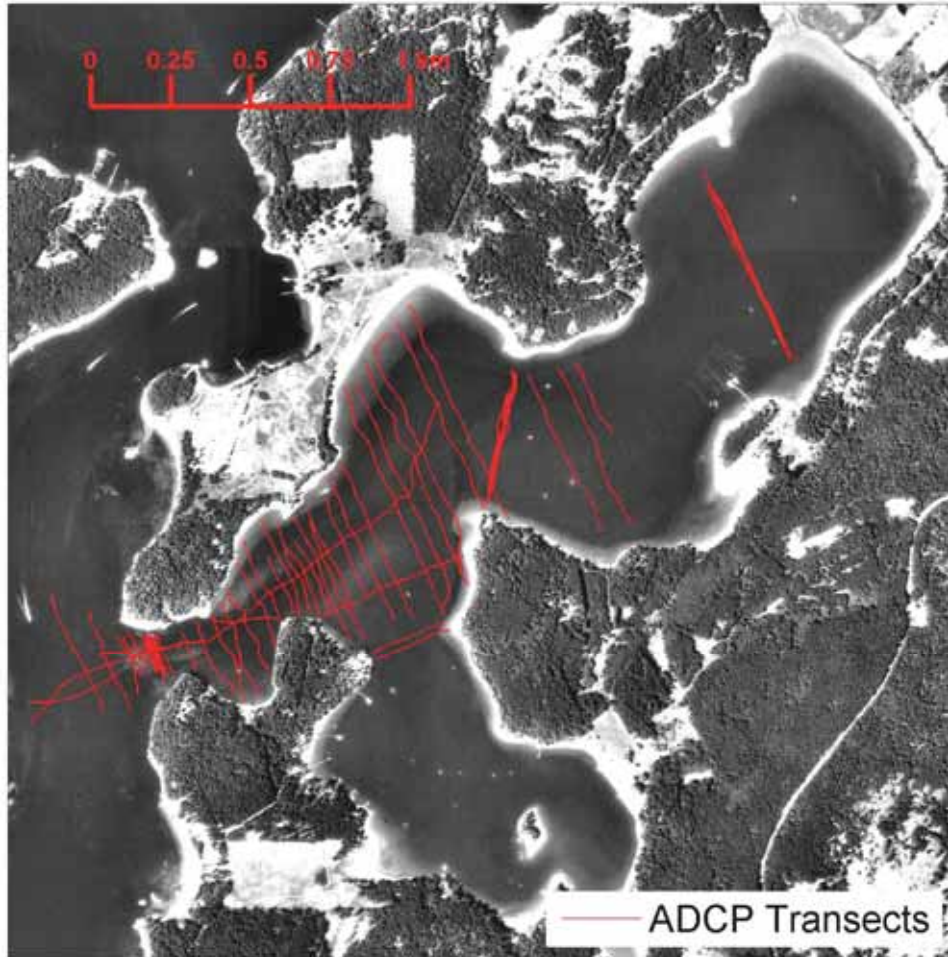
Fig. 5. Map of ADCP survey lines. Three principal lines (bold lines) at the mouth of Westcott Bay, Bell Point and just east of the sea farm were repeated multiple times to examine variability under ebb and flood tides.

Results

Bathymetry and geomorphology

The resulting bathymetric surface map derived from the combined DGPS and biosonics sonar data shows that the seafloor of Westcott Bay is complex with high relief between the entrance at Mosquito Pass and Bell Point, while the head of the bay is shallow, smooth and lacking relief (Fig. 6). A distinct narrow channel incises to -8.5 m along the central axis of the outer bay and is deeper along the north edge of the entrance to the bay. A sill 7-8 m deep separates Mosquito Pass from Westcott Bay. The channel/trough extends east to the area north of Bell Point, where it gradually shallows toward the head of the bay. The

margins of the trough are relatively steep, exceeding 35-40% slope immediately southeast of White Point (Fig. 7). These complex sill and trough features are likely a result of complex and strong currents, the presence of rocky substrate at the seafloor, and the regional glacial history. The bathymetry between Bell Point and the head of the bay is relatively smooth and featureless likely reflecting extensive sedimentation of fine material.
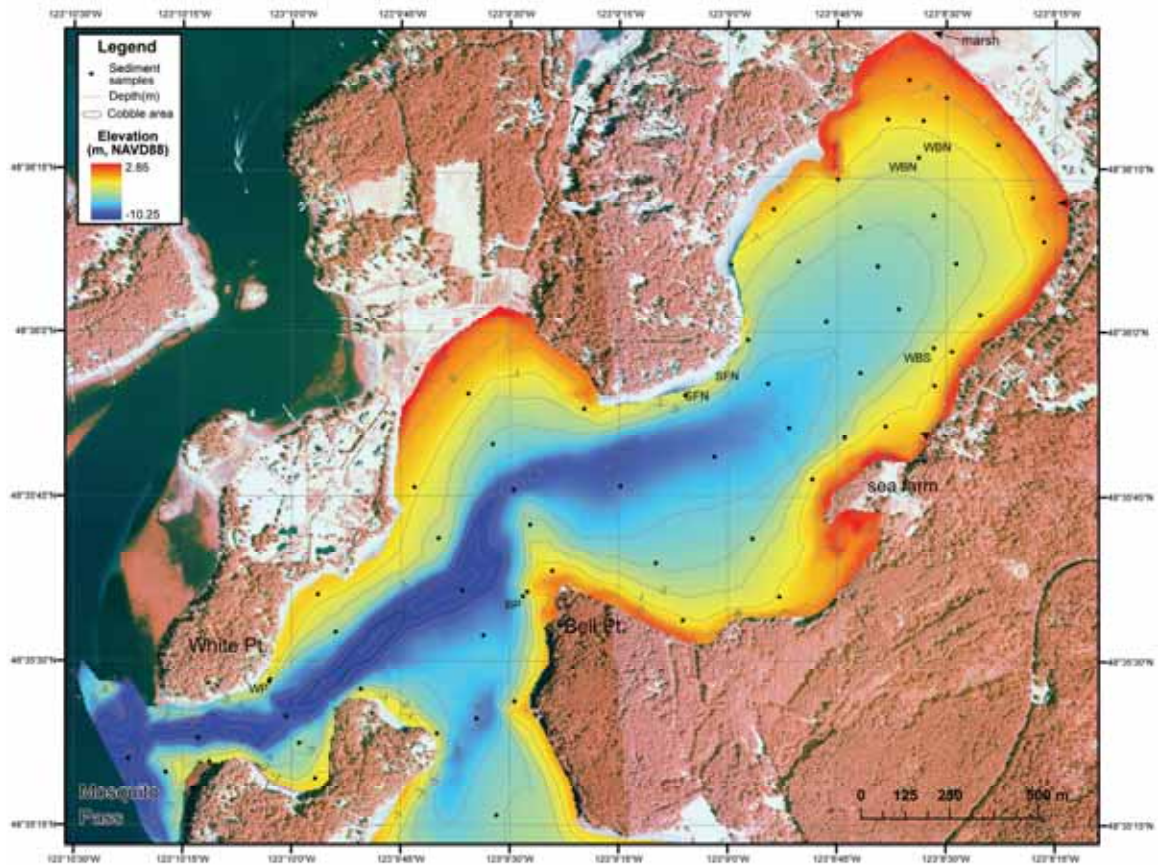
Fig. 6. Surface map of Westcott Bay based on bathymetry and topographic data collected showing narrow linear deep trough along center axis of outer Westcott Bay and shallow smooth surface of the head of the bay.
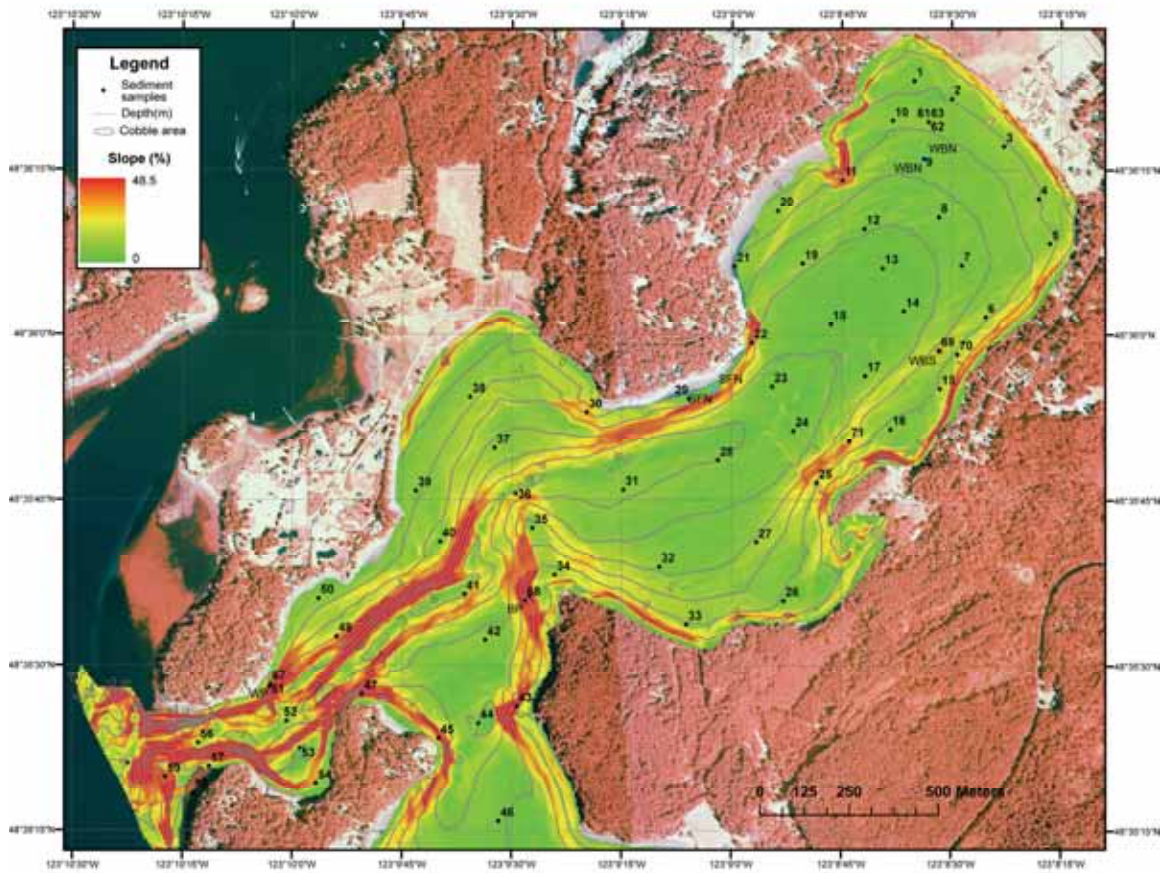
Fig. 7. Map showing seafloor slope of Westcott Bay with steep slopes characterizing the complex sill and trough region of the western half of the bay and relatively low slopes common of the broad gentle seafloor at the head of the bay.

Sediment grain size distribution

Figure 8 shows the mean grain size distribution in mm of unconsolidated sediments across Westcott Bay. Although the substrate was generally rocky in Mosquito pass and at the mouth of Westcott Bay, sand occurred within what appeared to be thin veneers of surface sediments. This region supported diverse communities of large kelp, seaweeds and algae. Along the central channel extending from Mosquito Pass to Bell Point, video observations along with grain size analyses indicated that the bottom was characterized by coarse sediments including gravel and cobbles. This region is delineated on all subsequent grain size distribution maps with a dotted polygon. Sand also dominates unconsolidated materials on the seafloor at the entrance to Garrison Bay, and near the intermittent stream mouths at the head of the bay and at the inlet to the marsh at the northeast corner of the bay. Otherwise silt predominates as the mean grain size throughout the central region and head of the bay.
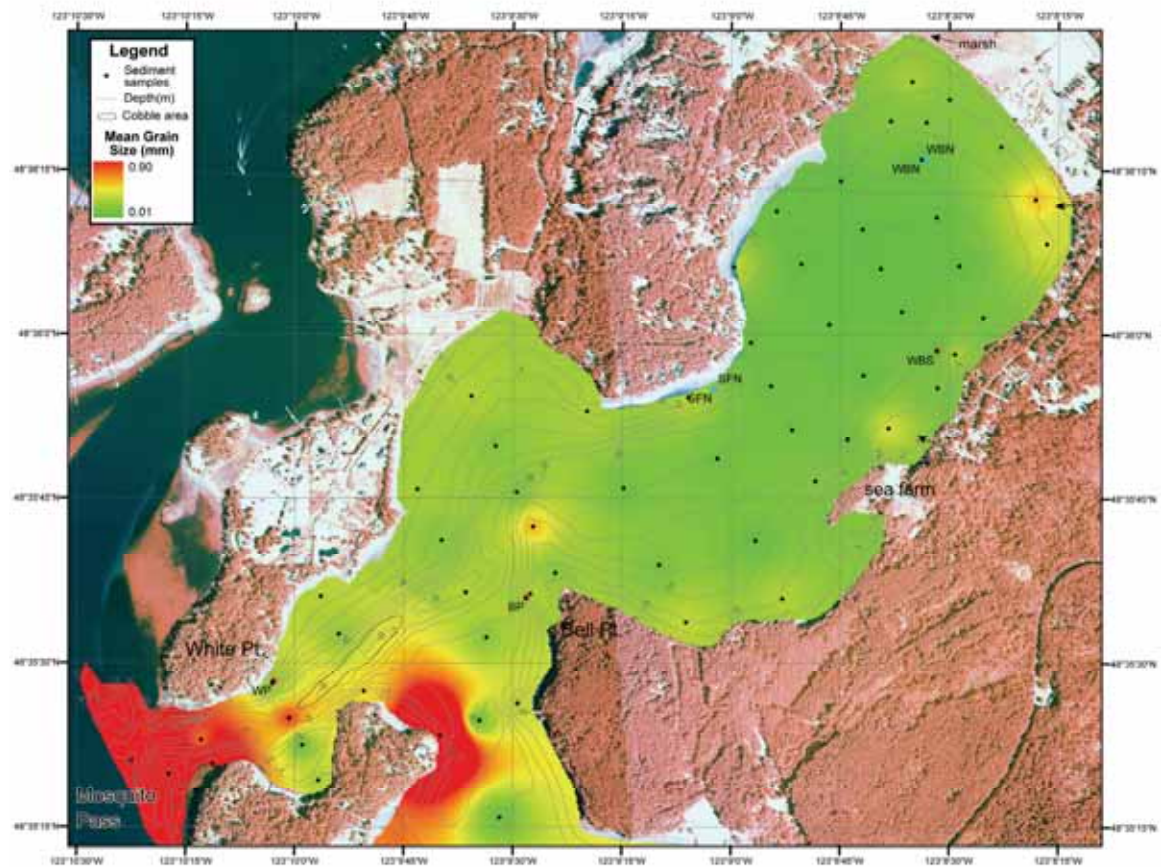
Fig. 8. Map of mean grain size in mm across the study area. Cobble- and pebble-rich channel outlined in black dotted polygon; streams shown with black arrows.

Figure 9 shows the mean grain size in mm classified by predominant grain size classes. This better shows the isolation of medium sands and coarser material near the entrance to Westcott and Garrison Bays, and fine silts in the central head of the bay. Exceptions to this include very fine to fine sand along the shoreline at the head of the bay likely associated with the two creeks and lagoon that meet the shore there.
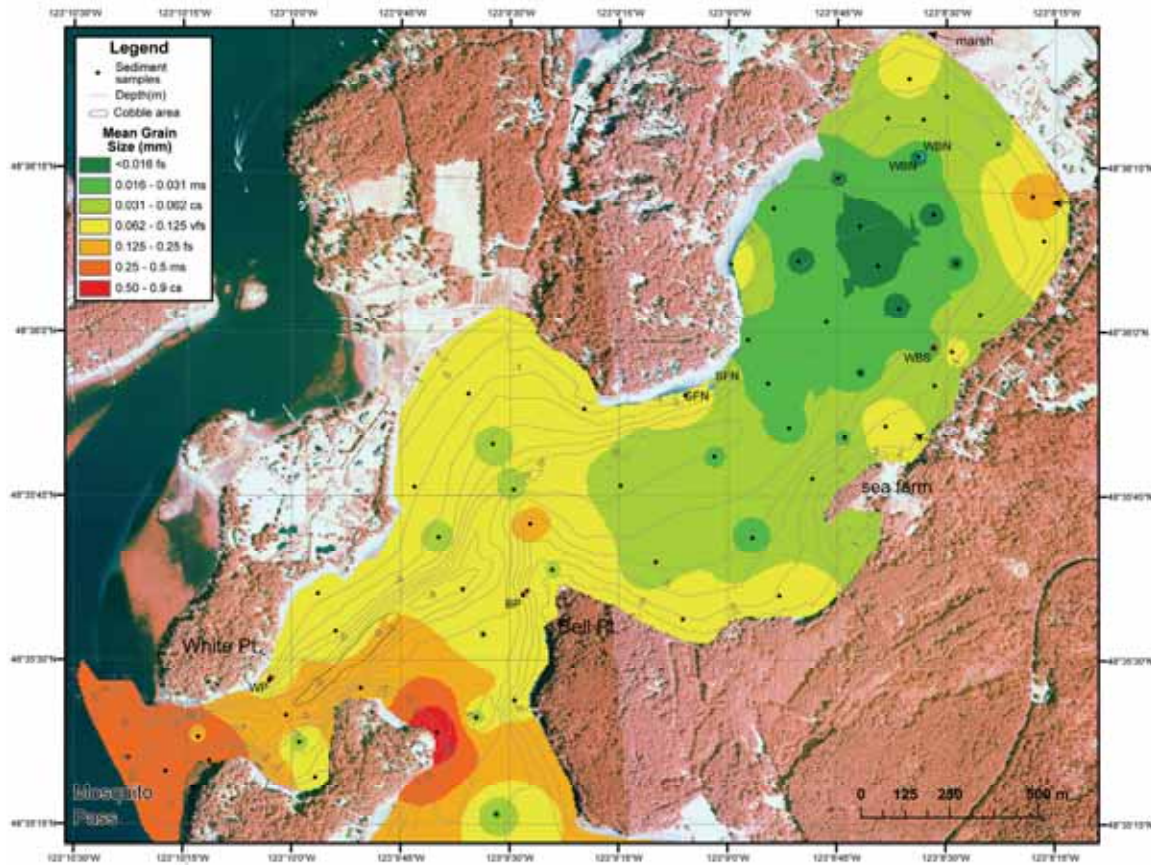
Fig. 9. Map of mean grain size classified by classes (in mm) across the study area. In order of increasing size (top to bottom) beginning with <0.016 mm, fs=fine silt, ms-medium silt, cs=coarse silt, vfs=very fine sand, fs=fine sand, ms=medium sand, 0.5-0.9 cs=coarse sand. Cobble- and pebble-rich channel outlined in black dotted polygon; streams shown with black arrows.

Figure 10 shows the mean grain size distribution in phi units, which allows for slightly greater dynamic range in display of the size gradients. Similar to figure 8, sands are restricted to the mouth and entrance to Garrison Bay, as well as, the small intermittent stream mouths at the head of the bay. Silt dominates the center and head of the bay.

Fig. 10. Map of mean grain size in phi units across the study area. Cobble- and pebble-rich channel outlined in black dotted polygon; streams shown with black arrows.

58

Figure 11 displays the mean grain size in phi units classified by dominant grain size classes. This also shows that medium and coarse sands occur near the mouth and entrance to Garrison Bay, and fine silts dominate in the central head of the bay, except along the shore at the head of the bay where fine sand is associated with the mouth of the intermittent streams.
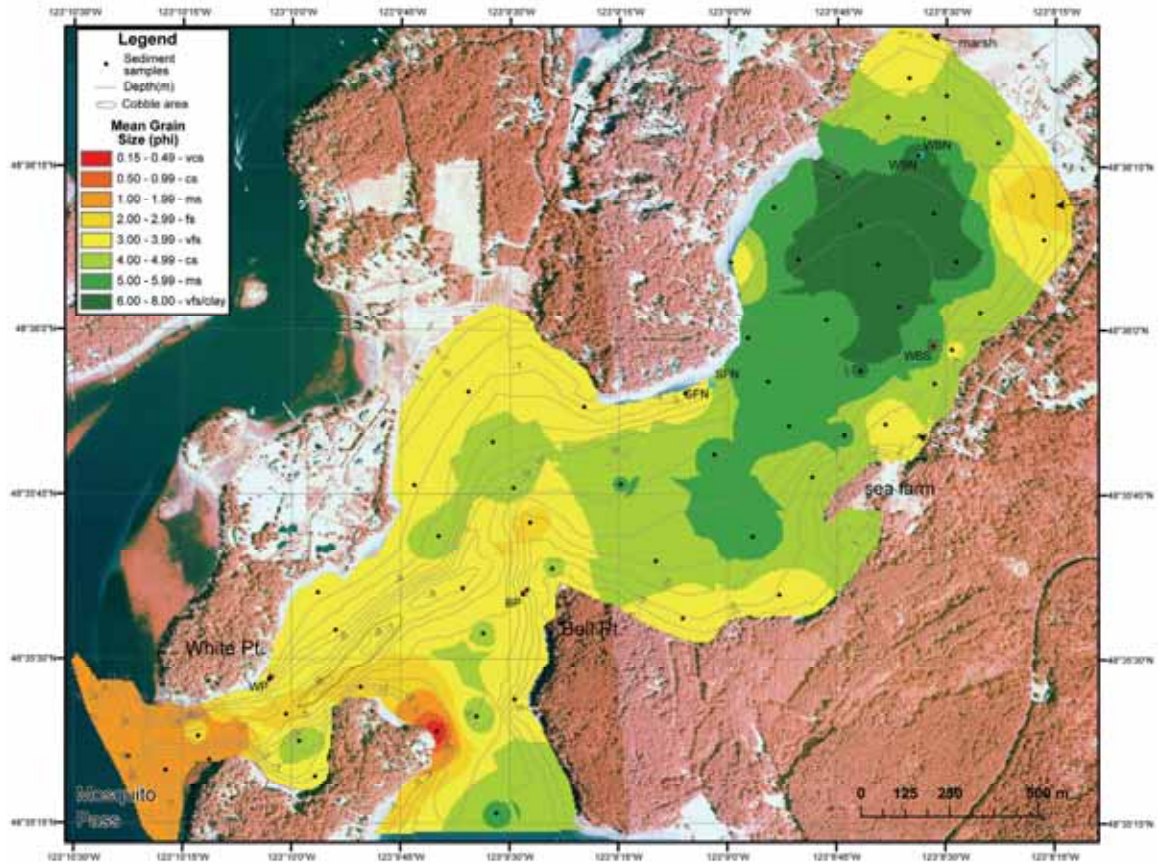
Fig. 11. Map of mean grain size classified by classes (in phi) across the study area. In order of decreasing size (top to bottom) beginning with 0.15-0.49 vcs=very coarse sand, cs=coarse sand, ms=medium sand, fs=fine sand, vfs=very fine sand, cs=coarse silt, ms=medium silt, vfs/clay=very fine silt/clay. Cobble- and pebble-rich channel outlined in black dotted polygon; streams shown with black arrows.

Figure 12 shows the degree of sorting of surface sediments across Westcott Bay. This is the calculated standard deviation around the mean grain size. Poorly sorted areas are reflected in the warm (red) colors, while well sorted areas are depicted in cool (blue) colors. Poorly sorted sediments were common immediately inside Westcott Bay across an inverted, u-shape area around the entrance to Garrison Bay. Sediments were generally poorly sorted along the eastern central bay and at the far head of the bay. Sediments were well-sorted along the central axis in the head of the bay and at the easternmost stream mouth and lagoon inlet. Sediments were generally well sorted inside the entrance to Garrison Bay. These variations in sorting are likely associated with strong circulation processes that oscillate in and out of the bay daily and sediment sources (e.g. the intermittent streams). Sediments were generally poorly sorted near the sea farm.
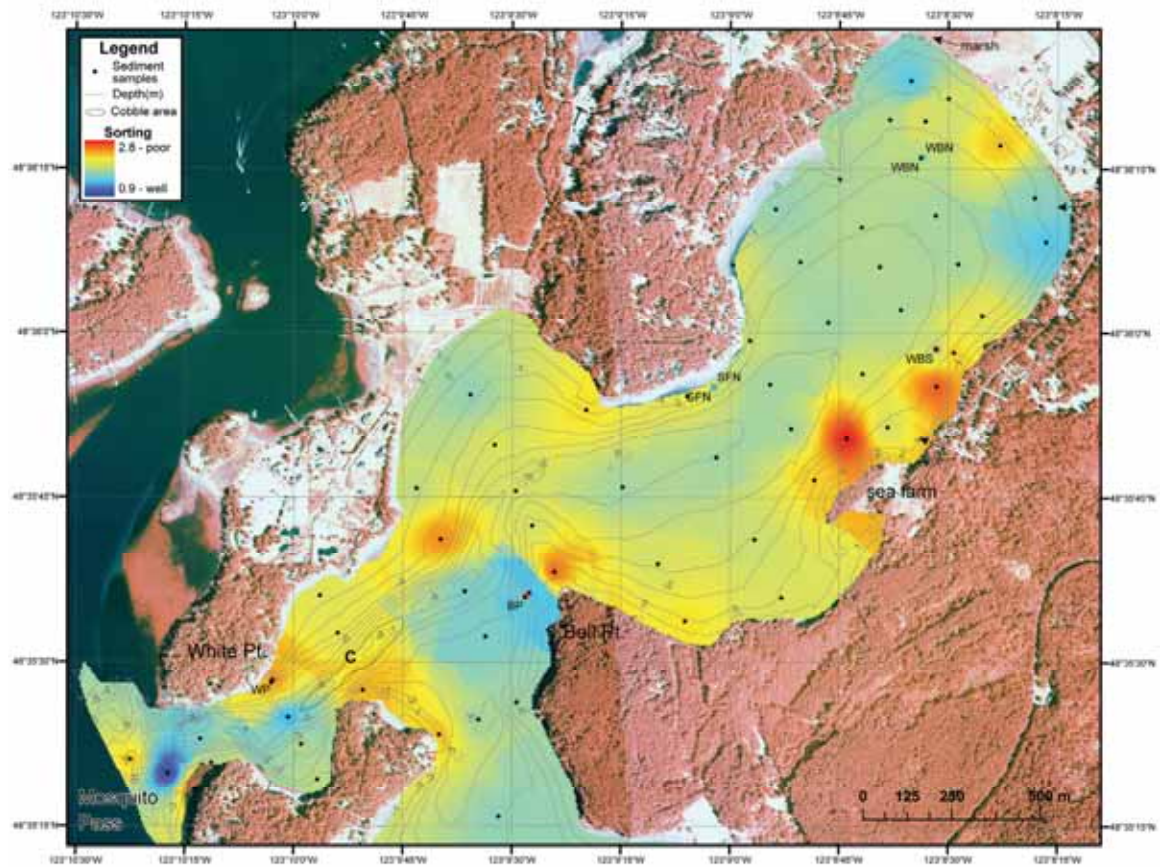
Fig. 12. Map of sediment sorting across the study area. Poorly sorted sediment are represented with warm (red) colors; well-sorted sediments with cool (blue) colors. Cobble- and pebble-rich channel outlined in black dotted polygon; streams shown with black arrows.

Figure 13 shows the fraction of sand in surface sediments across Westcott Bay in percent of total size classes. At the mouth of the bay and small intermittent stream, sand makes up >80% of seafloor sediment. In the central bay west of Bell Point, sand comprises generally >50% of all material, while to the east toward the head of the bay sand reaches a low of 5%.
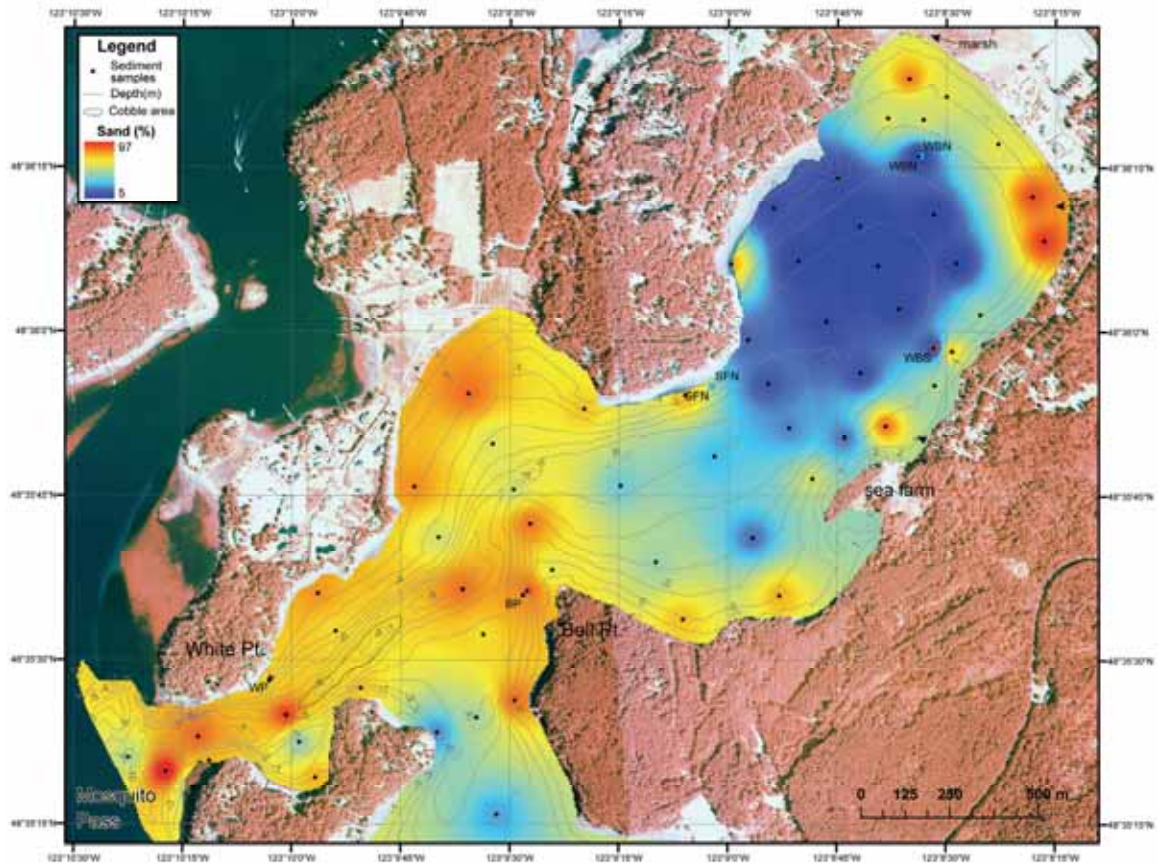
Fig. 13. Map of percent sand occurrence across the study area. Cobble- and pebble-rich channel outlined in black dotted polygon; streams shown with black arrows.

Figure 14 shows the fraction of silt in surface sediments across Westcott Bay in percent of total size classes. Silt is clearly restricted to the areas within Garrison Bay and within the head of Westcott Bay where it reaches a maximum of 76%. East of Bell Point, silt generally comprises at least 50% of the sediment.
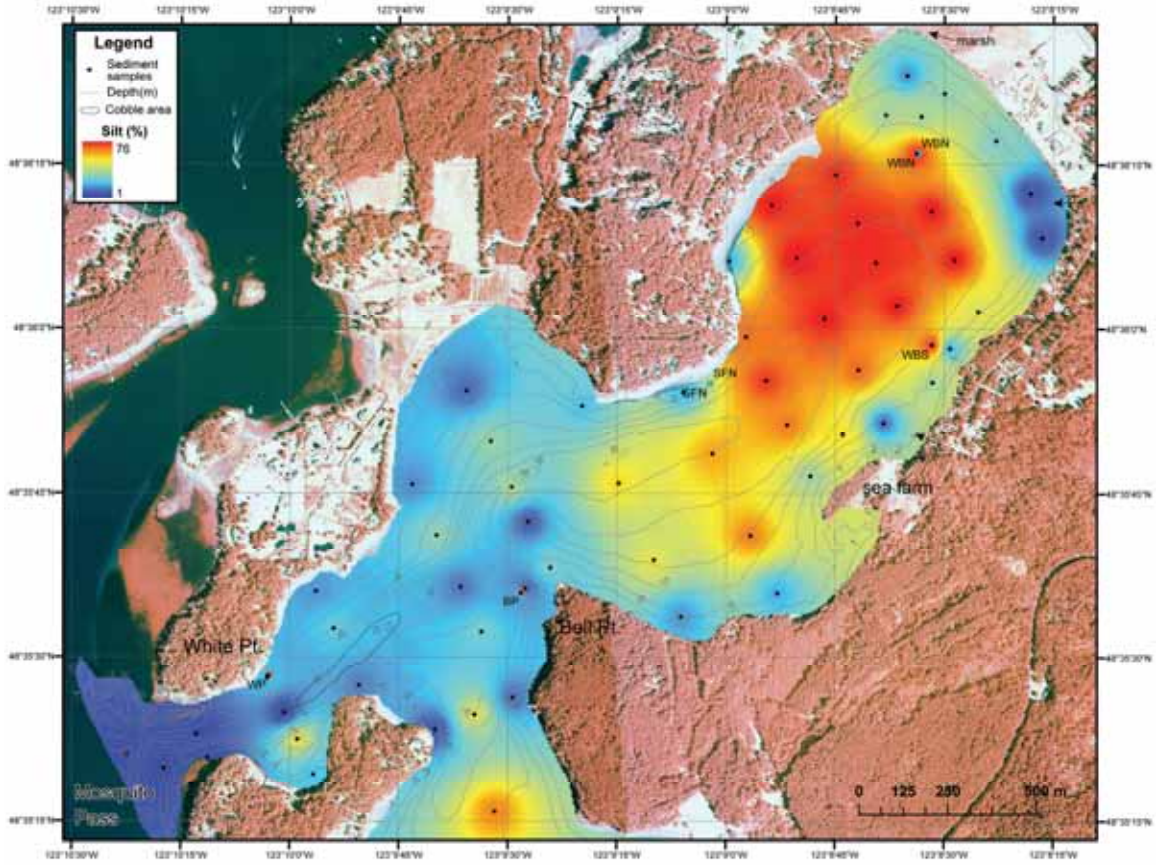
Fig. 14. Map of percent silt occurrence across the study area. Cobble- and pebble-rich channel outlined in black dotted polygon; streams shown with black arrows.

Figure 15 shows the fraction of clay in surface sediments across Westcott Bay in percent of total size classes. Clay is largely absent west of Bell Point, except for two isolated stations just northwest of Bell Point where it reaches ~10%. Within the head of the bay, clay comprises up to 21% of the sediment.
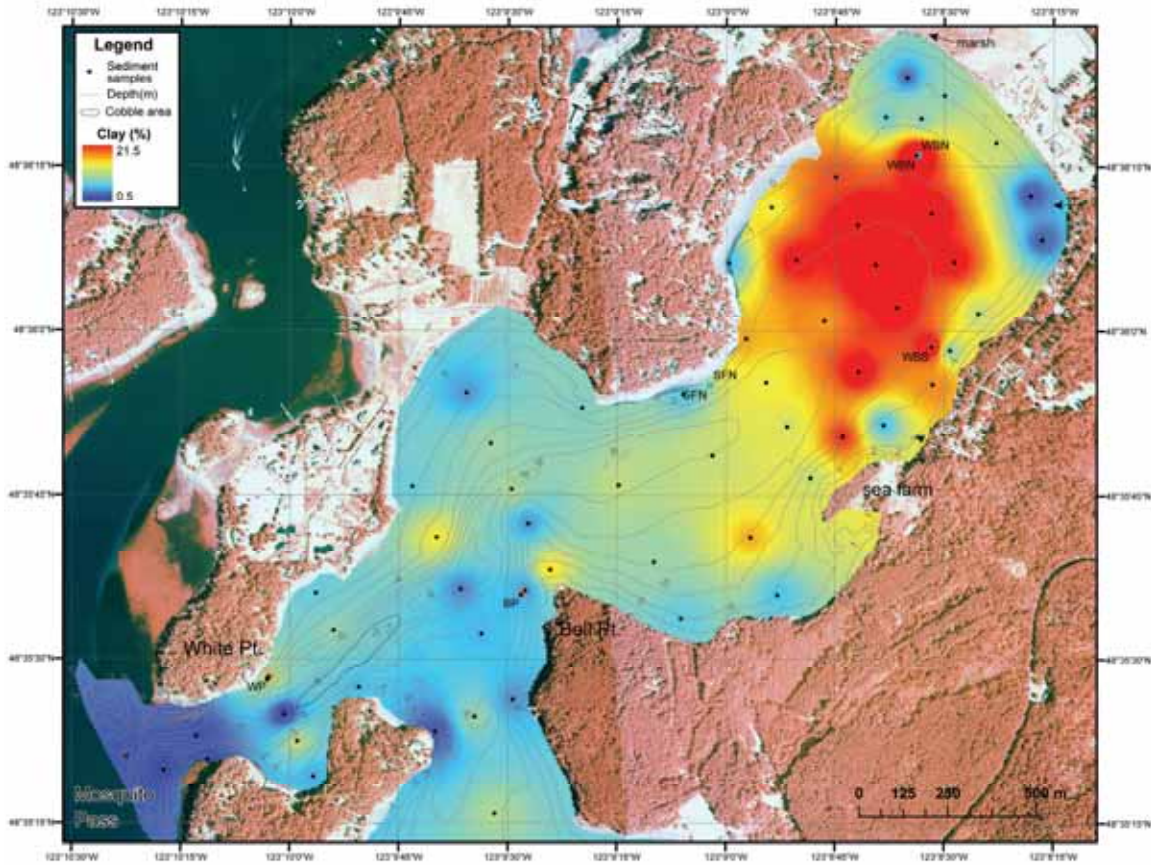
Fig. 15. Map of percent clay occurrence across the study area. Cobble- and pebble-rich channel outlined in black dotted polygon; streams shown with black arrows.

In summary, sand size sediment dominates at the mouth of Westcott and Garrison Bays and along the shoreline at the head of the bay near the small intermittent stream and lagoon inlet. Along the deep trough in the center of the bay, surficial sediments are also characterized by sand and coarse silt with outcrops of rock and cobbles. Inside Garrison Bay and the head of Westcott Bay and especially east of Bell Point, sediments are dominated by silt with a significant (15-20%) proportion of clay.

Nearshore currents and circulation

Figures 16 and 17 illustrate the boat-mounted ADCP-derived currents at the entrance to Westcott Bay under a flooding tide of May 31, 2007. The highest current velocities occur along the north edge of the entrance along the deep trough found there. Current velocities at the surface reached 0.75 to 1.00 m/s.
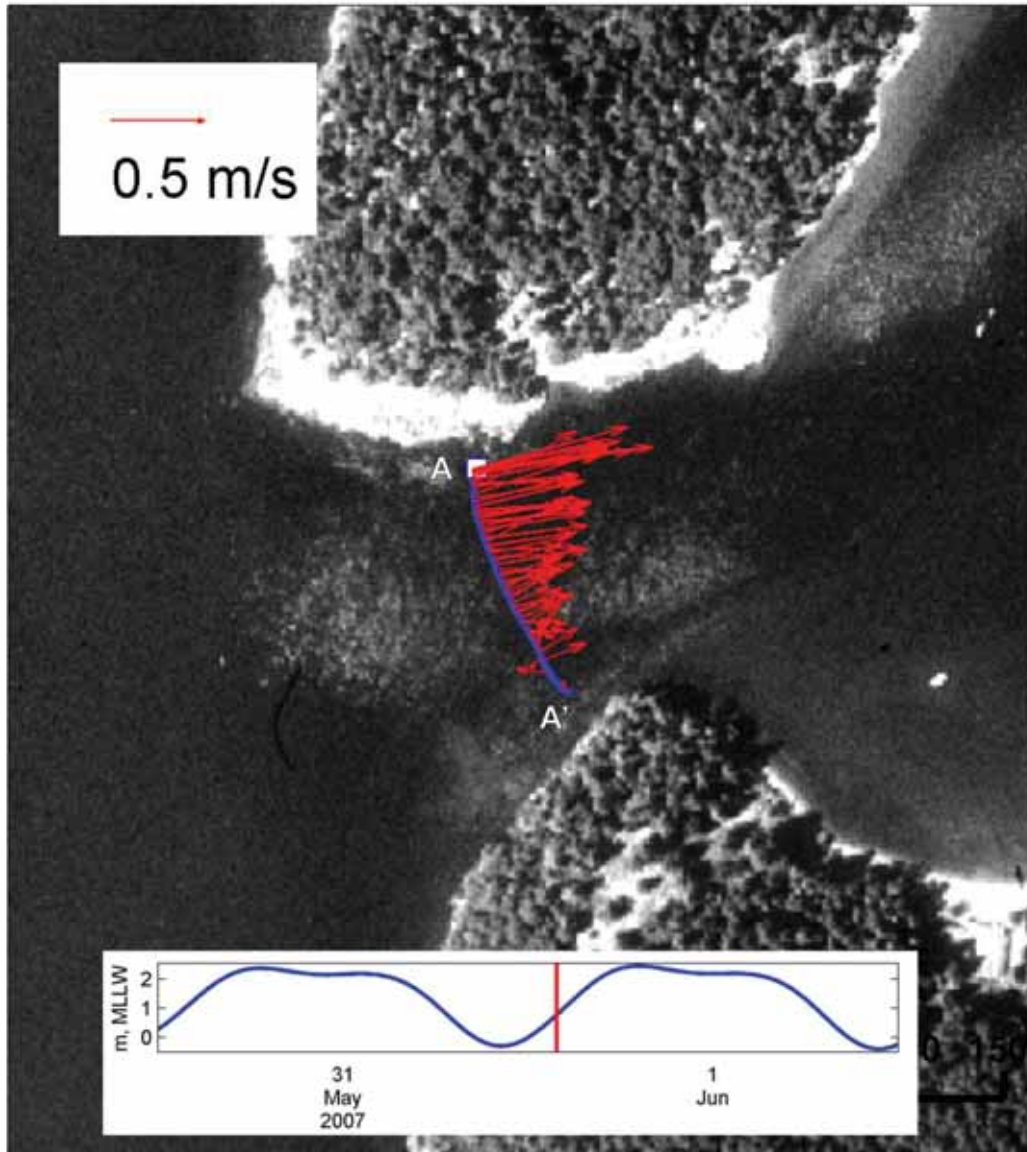
Fig. 16. Map of depth-averaged current velocity averaged across 5 ensembles (lateral distance) during flooding tide of May 31, 2007 (inset; water level from Friday Harbor tide predictions, http://tidesandcurrents.noaa.gov/data_menu.shtml?stn=9449880%20Friday%20Harbor,%20WA&type=Tide+Predictions). Current velocities were stronger along northwest edge of the entrance to Westcott Bay, likely associated with deeper trough there.
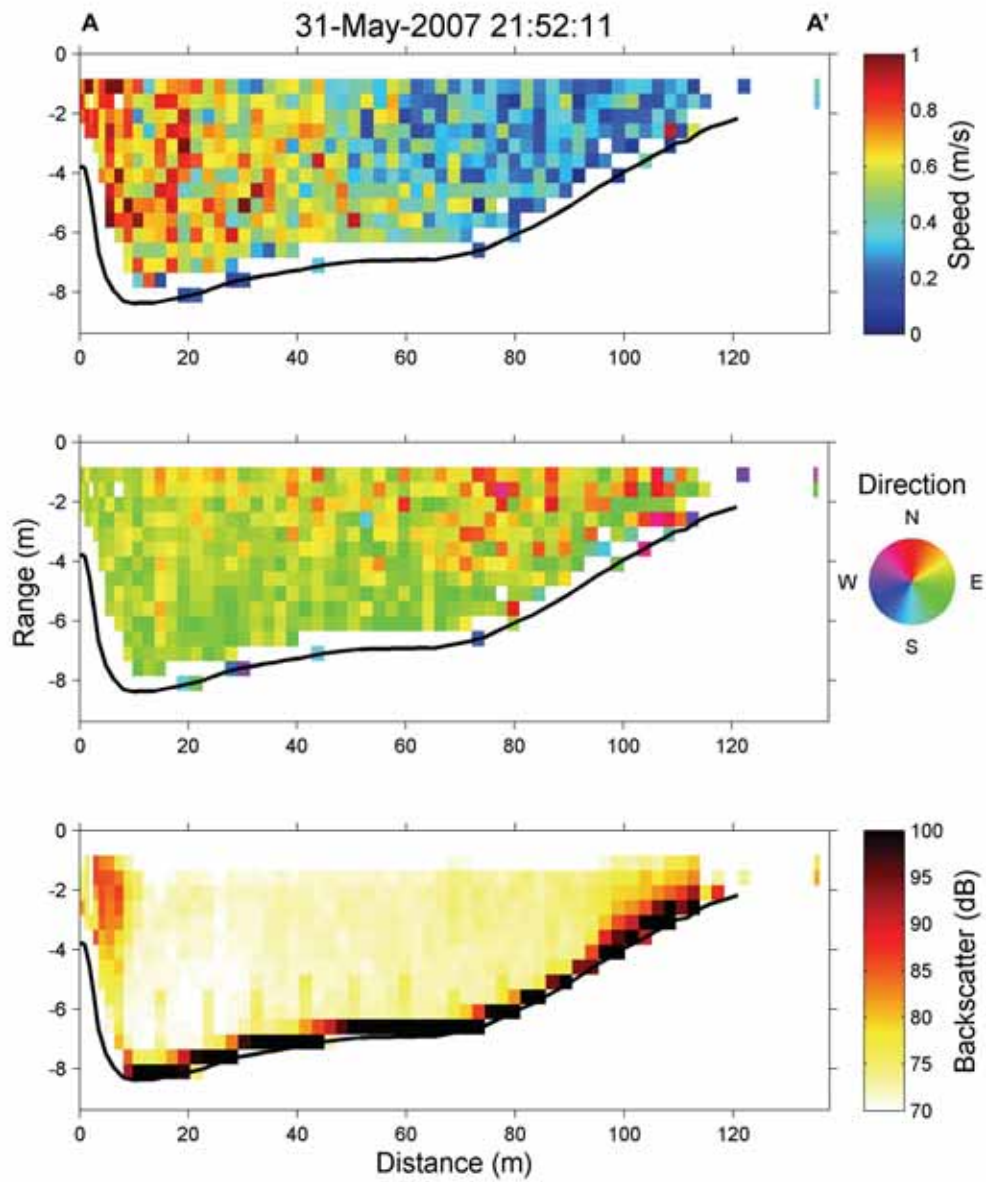
Fig. 17. Cross-sectional diagram of ADCP derived current velocity (top), current direction (middle) and measured backscatter (bottom) showing stronger current velocities along northwest edge of the entrance to Westcott Bay (left edge of top plot) Data averaged across 5 ensembles (across distance).

Figures 18 and 19 illustrate the strong currents flowing out of the entrance of Westcott Bay under an ebbing tide of June 2, 2007. Current velocities were strongest (0.5-0.6 m/s) in the middle of the Westcott Bay entrance and lacked the lateral asymmetry observed during flood tide (Fig. 16).
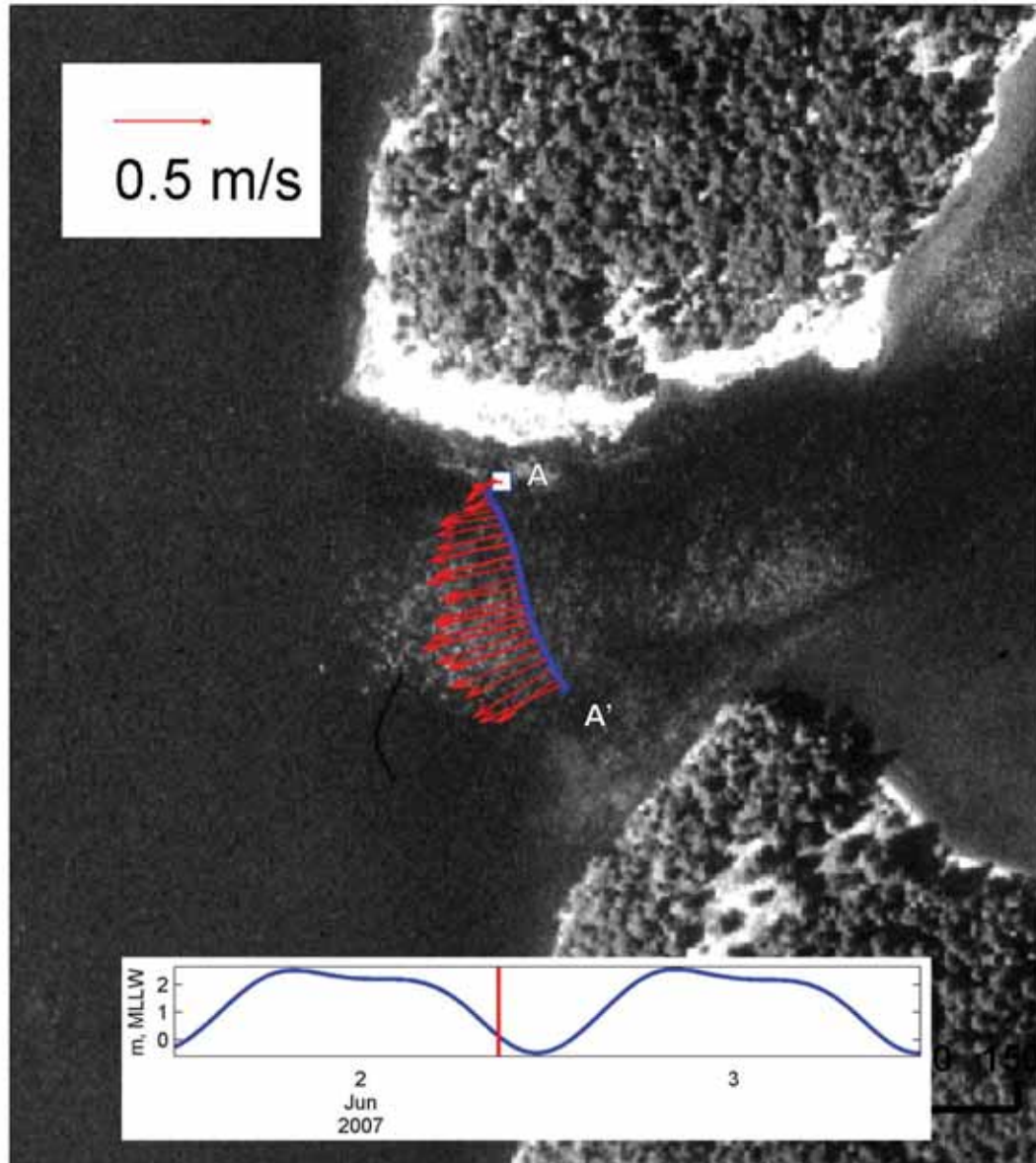
Fig. 18. Map of depth-averaged current velocity averaged across 5 ensembles (lateral distance) during ebbing tide of June 2, 2007 (inset). Current velocities were strongest in the middle of the Westcott Bay entrance and lacked the lateral asymmetry observed during flood tide.
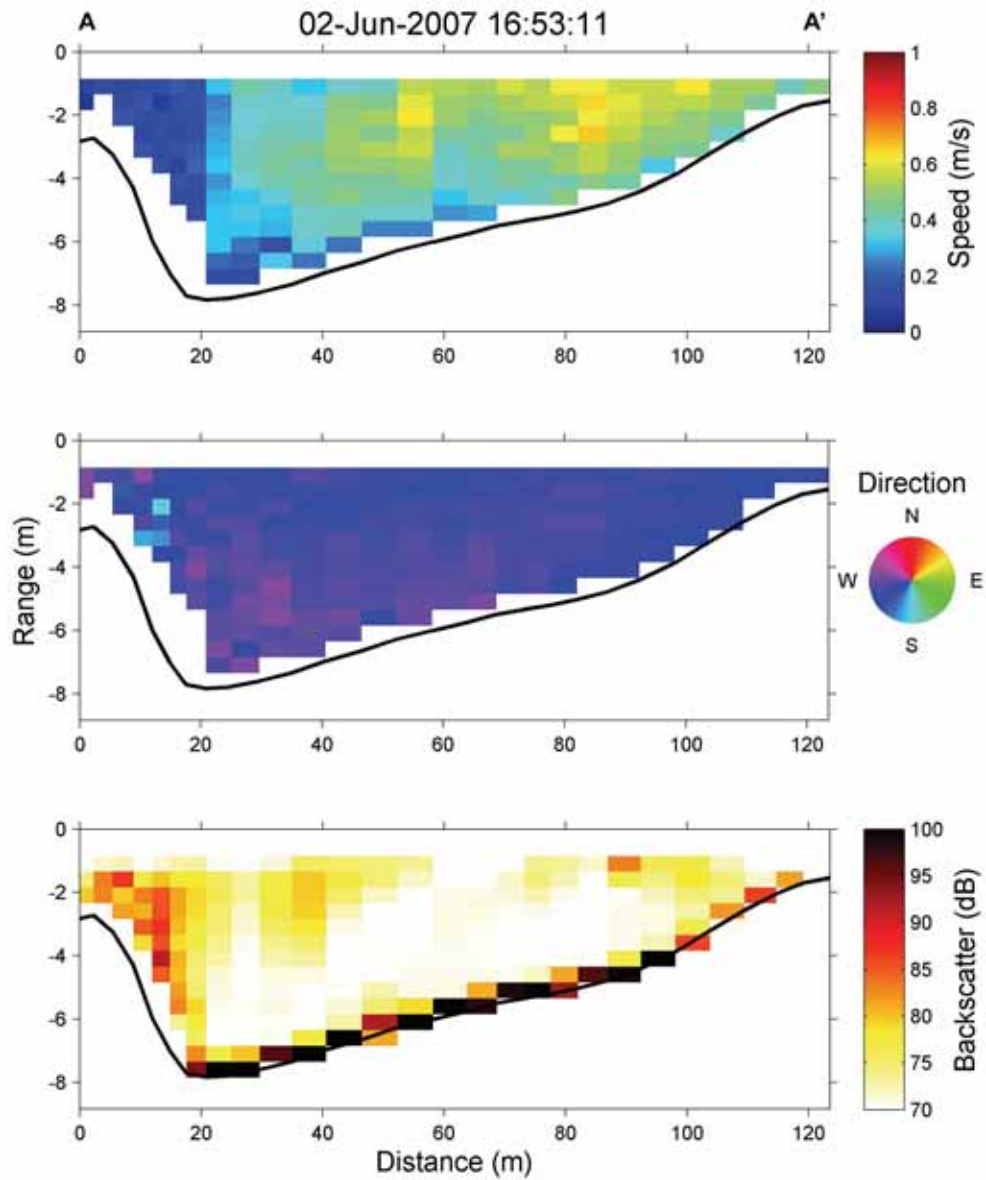
Fig. 19. Cross-sectional diagram of ADCP derived current velocity (top), current direction (middle) and measured backscatter (bottom) during an ebbing tide. Currents were stronger in the middle of the entrance to Westcott Bay and more symmetric than during flood tide. Data averaged across 5 ensembles (across distance) and are coarser than data in Figure 17 because of higher boat speed during data collection.

Figure 20 shows the ADCP data collected on all transects of May 31, 2007 (from west to east) over the period of 2 hours as the tide flooded into Westcott Bay. Generally, higher currents were found along the central axis of Westcott Bay, and especially along the northwest edge of the entrance to Westcott Bay. A slight eddy was apparent west of Bell Point in the entrance to Garrison Bay with flow directed in a clockwise gyre. The northern portion of this eddy (black arrows) correlates with a region of poor sediment sorting (Fig. 12).
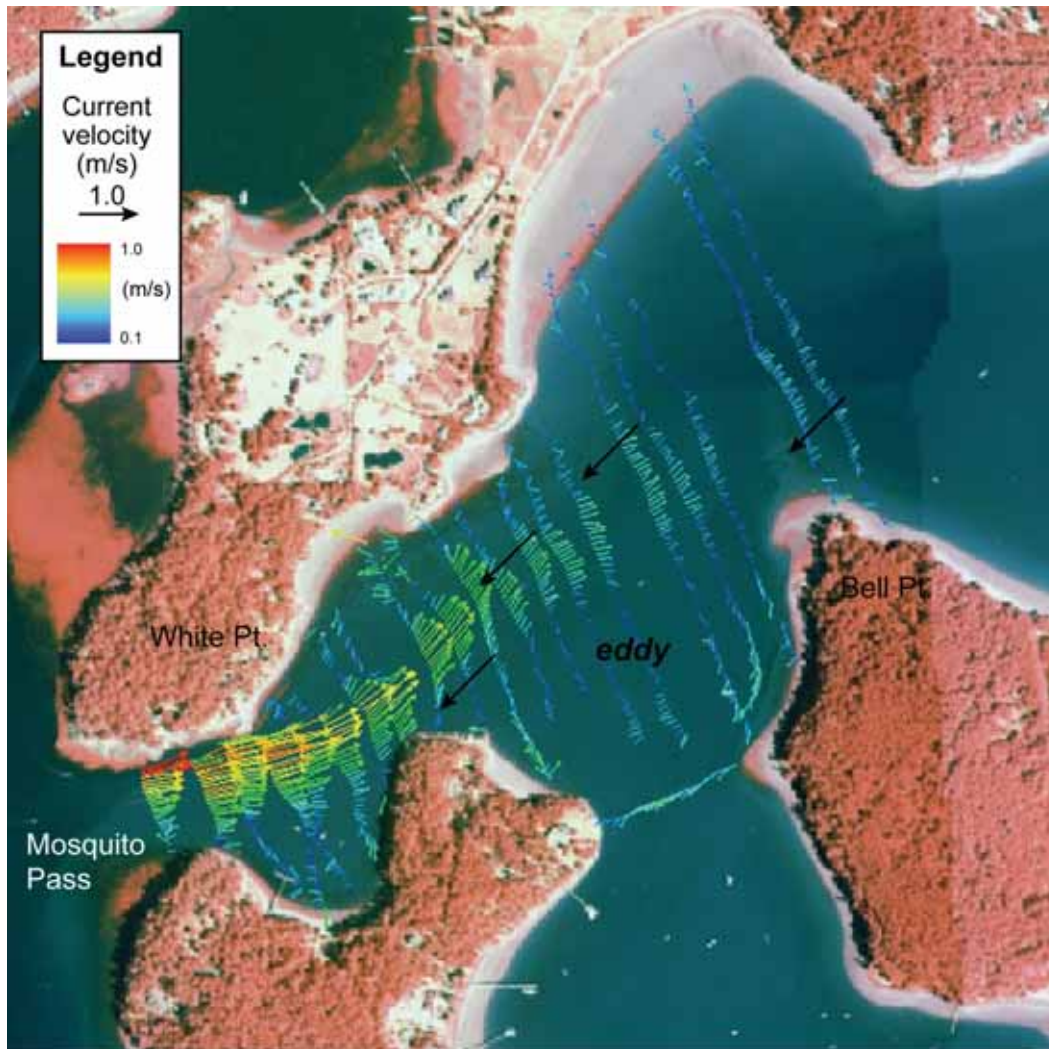
Fig. 20. Map of depth-averaged current velocities and directions over a 2- hour flood tide period on May 31, 2007 (velocities scaled to arrow in legend and color coded: red=high, blue=low). Highest velocities were observed along the northern portion of the main channel into Westcott Bay, while lower velocities occured along the edges inside the entrance and generally within the central bay. A clockwise eddy was apparent west of Bell Point within the entrance to Garrison Bay. The northern margin of the eddy (black arrows) correlates with the area of poor sorting in Figure 12.

Conclusion

Seafloor mapping using a dual-frequency Biosonics acoustic sonar along with a boat-mounted ADCP and RTK-DGPS enabled characterization of seafloor depth, morphology and nearshore circulation patterns during a range of tide regimes. Contemporaneous sampling and subsequent analysis of surface sediment grain size distributions provide quantitative data for classifying the seafloor by principal morphology and substrate types. Westcott Bay seafloor composition and morphology is complex in its western half where high-relief bedrock and extensive reaches of sand, gravel and cobble are exposed along a linear channel northeast from the entrance of Westcott Bay toward Bell Point. This complex topography and substrate is associated with strong currents that reach 1.0 m/s and scour the bottom. Stronger currents along this deep channel indicate that the circulation is also partly controlled by the geomorphology. A sill 0.5-1.0 m shallower than the channel separates Westcott Bay from Mosquito Pass. The eastern half of Westcott Bay (east of Bell Point) in contrast, is broad, gently sloping and the surface sediments are dominated by high silt and clay fractions. Current velocities decreased steadily with distance into the head of the bay. In the central portion of Westcott Bay an eddy circulating in a clockwise rotation was observed during a flood tide. A portion of this eddy coincided with a region of poor sediment sorting and complex seafloor morphology. It remains uncertain if the flux, transport, and accumulation of sediment in Westcott Bay are adversely impacting *Z. marina*. Ongoing and future efforts will synthesize the data reported here with time series measurements of water quality to develop models of sediment transport and habitat conditions to explore environmental variability and possible thresholds of stress to eelgrass growth and recovery.

Acknowledgements

References

Berry, H.D., A.T. Sewell, S. Wyllie-Echeverria, B.R. Reeves, T.F. Mumford, Jr., Skalski, R.C. Zimmerman, and J. Archer. 2003. Puget Sound Submerged Vegetation Monitoring Project: 2000-2002 Monitoring Report. Nearshore Habitat Program, Washington State Department of Resources. Olympia, WA. 60 p.

Friends of the San Juans, J. Slocomb, S. Buffum-Field, S. Wyllie-Echeverria, J. Norris, I. Fraser, and J. Cordell. 2004. San Juan County Eelgrass Survey Mapping Project Final Report, Friday Harbor, WA, 40.p.

Guy, H.P., 1969. Laboratory theory and methods for sediment analysis. In: Techniques of Water-Resources Investigations of the United States Geological Survey, United States Government Printing Office, Washington, DC, pp.iii-55.

Oberg K.A., Morlock, S.E., and Caldwell, W.S., 2005, Quality-assurance plan for discharge measurements using acoustic doppler current profilers: U.S. Geological Survey Scientific Investigations Report 2005-5183, 46 p. [http://pubs.usgs.gov/sir/2005/5183/SIR_2005-5183.pdf].

Wyllie-Echeverria, S., Mumford, T., Gaydos, J. and Buffum, S. 2003. *Z. marina* declines in San Juan County, WA. Westcott Bay Taskforce Mini-Workshop 26, July 2003. 18. p. http://mehp.vetmed.ucdavis.edu/pdfs/eelgrassrpt.pdf

Revision Information

Please refer to http:pubs.usgs.gov/of/2007/1305/ for additions and revisions to this report.

Data Catalogue

All data generated from this mapping of bathymetry, substrate type and nearshore currents are referenced to USGS Cruise ID B-6-07-PS.

Metadata

Metadata are available at URL:
http://walrus.wr.usgs.gov/infobank/b/b607ps/meta/b-6-07-ps.meta.html

Digital surface elevation data

A survey log summarizing line numbers, file names, survey information and environmental conditions are provided in Appendix 1.

Digital x,y,z (depth) data for individual survey lines are provided as text files on the data CD under B-6-07-PS/bathymetry/line#.xyz and for the entire survey under B-6-07-PS/bathymetry/westcott0507.xyz.

Digital sediment grain size data

Station information for the sediment grain size samples is provided in Appendix 2 and the summary grain size results are listed in Appendix 3.

Digital ADCP data

The ADCP data with current velocity, direction and backscatter amplitude are transferred to DNR on the attached data CD in three formats:

1) original WinRiver filename_T.OOO format, which can be opened with any text editor software
(see B-6-07-PS/ADCP/WESTCOTT_DAY#/filename)
- (3 folders, one for each day)
2) graphic JPG cross-sections of the RAW ADCP bottom tracked data by line
(see B-6-07-PS/ADCP/WESTCOTT/ADCP_jpegs/)
3) graphic JPG cross-sections and depth averaged maps of currents averaged across 5 ensembles (horizontal averaging) by line
(see B-6-07-PS/ADCP/WESTCOTT/ADCP/processedData/)

Please refer to Appendix 1 to cross reference filename with line number.

APPENDIX I. Bathymetry/ADCP Survey Log for USGS Cruise ID (B-6-07-PS)

Line	Biosonics_Filename	Date Collected	Elapsed Time (min)	Total Length (m)	ADCP_Filename	Comments
line56_1	20070531_192732.dt4	39233.47745	10.13	1385.45	-	4-m contour alongshore 215 to mouth
line56_1a	20070531_193744.dt4	39233.48455	6.76	877.4	-	Part 2 of line
line126	20070531_194740.dt4	39233.49144	3.93	499.19	-	shallow reef at start; algae
line124	20070531_195257.dt4	39233.49512	2.93	447.99	-	veg at start; kelp mid
line122	20070531_195741.dt4	39233.49839	2.09	233.43	-	reef at start
line115	20070531_200441.dt4	39233.50326	1.46	123.97	-	-
line114	20070531_200633.dt4	39233.50456	1.29	132.1	-	-
line112	20070531_200912.dt4	39233.50639	1.53	155.95	-	eelgrass at start; strong current into bay
line110	20070531_201133.dt4	39233.50802	1.87	197.82	-	end at dock
line108	20070531_201509.dt4	39233.51056	2.5	264.65	-	-
line106	20070531_201843.dt4	39233.513	2.5	316.36	-	-
line104	20070531_202313.dt4	39233.51613	1.73	230.74		end in eelgrass
line102	20070531_202613.dt4	39233.51821	2.32	184.11		steep rock at end with algae
line100	20070531_202924.dt4	39233.52042	1.56	186.36	-	-
line116	20070531_215040.dt4	39233.9102	2.29	137.74	WESC053107_000	eelgrass at end; strong current into bay
line113	20070531_215450.dt4	39233.91308	2.39	150.83	WESC053107_001	eelgrass at start
line111	20070531_215830.dt4	39233.91564	4.62	278.88	WESC053107_002	circumvent dock near end
line109	20070531_220607.dt4	39233.92093	4.7	285.15	WESC053107_003	-
line107	20070531_221224.dt4	39233.92528	3.86	335.26	WESC053107_004	DNR Sonde at start; high backscatter near mid channel
line105	20070531_221812.dt4	39233.92931	3.19	303.98	WESC053107_005	eelgrass at start/end; platform at 6m
line103	20070531_222309.dt4	39233.93274	3.22	291.39	WESC053107_006	strong currents/backscatter mid channel
line101	20070531_222923.dt4	39233.93709	2.66	275.26	WESC053107_007	-
line98	20070531_223323.dt4	39233.93985	3.43	322.16	WESC053107_008	veg/resuspension? mid channel
line96	20070531_223837.dt4	39233.94348	3	320.43	WESC053107_009	rock at start; high backscatter mid; sand/rock at end
line94	20070531_224300.dt4	39233.94652	4.06	427.19	WESC053107_010	rock at start; high backscatter mid
line145	20070531_224950.dt4	39233.95126	3.09	255.9	WESC053107_011	across Garrison Bay mouth
line92	20070531_225616.dt4	39233.95573	3.22	361.47	WESC053107_012	rock at end

Line	Biosonics_Filename	Date Collected	Elapsed Time (min)	Total Length (m)	ADCP_Filename	Comments
line90	20070531_230027.dt4	39233.95865	3.59	364.13	WESC053107_013	start just offshore of rock shoal
line88	20070531_230525.dt4	39233.96209	5.13	506.17	WESC053107_014	start mid Garrison Bay; rock at end
line86	20070531_231154.dt4	39233.96659	4.45	550.35	WESC053107_015	End mid Garrison Bay
line84	20070531_232300.dt4	39233.97431	6.73	689.43	-	start mid Garrison Bay; turbid water visible
line82	20070531_233149.dt4	39233.98042	7.33	802.11	WESC053107_016	turbid at start
line80	20070531_234002.dt4	39233.98613	6.42	773.01	WESC053107_017	eelgrass at start; strong current
line78	20070531_234719.dt4	39233.99119	6.69	790.38	WESC053107_018	-
line76	20070531_235515.dt4	39233.99669	6.79	764.38	WESC053107_019	-
line74	20070601_000446.dt4	39234.00331	4.79	609.06	-	-
line72	20070601_001128.dt4	39234.00796	10.09	663.51	WESC053107_020	Bell Pt.; ADCP at 2kts
line70	20070601_002231.dt4	39234.01563	6.92	748.56	WESC053107_021	-
line35	20070601_011712.dt4	39234.05362	9.76	1102.25	-	start E side of dock; through oyster beds
line30	20070601_012702.dt4	39234.06047	9.83	1095.63	-	2nd half of oysters E side
line38	20070601_013911.dt4	39234.06889	8.23	783.01	-	Oyster beds W side of dock
line42	20070601_014748.dt4	39234.07487	8.85	1053.39	-	2nd section of oysters W side
line4	20070601_030128.dt4	39234.12602	2.97	184.64	-	-
line6	20070601_030543.dt4	39234.12898	3.79	420.21	-	-
line8	20070601_031111.dt4	39234.13278	4.56	591.91	-	-
line10	20070601_031654.dt4	39234.13675	6.16	713.08	-	poor water quality NW head of bay
line12	20070601_032411.dt4	39234.14179	0.77	54.84	-	-
line14	20070601_033317.dt4	39234.14811	5.73	775.76	-	-
line16	20070601_033954.dt4	39234.15271	5.99	787.77	-	rough microtopography? mid; whispy blades near end
line18	20070601_034644.dt4	39234.15747	5.69	751.72	-	poor WQ; floating debris/solids
line20	20070601_035342.dt4	39234.1623	5.8	750.28	-	-
line22	20070601_040033.dt4	39234.16706	5.89	747.84	-	start near DNR station; poor WQ
line24	20070601_040724.dt4	39234.17181	7.5	805.2	-	avoid rock at start; revetment at end
line26_1	20070601_041630.dt4	39234.17814	6.76	780.2	-	revetment
line28b	20070601_042418.dt4	39234.18354	6.3	819.6	-	microtopography? 100-200 m into line?
line1	20070601_175546.dt4	39234.74706	5.62	386.02	WESC060107_000	-
line117_1	20070601_181300.dt4	39234.75921	2.23	121.99	WESC060107_001	-

Line	Biosonics_Filename	Date Collected	Elapsed Time (min)	Total Length (m)	ADCP_Filename	Comments
line68	20070601_181628.dt4	39234.76144	4.09	428.22	-	Alongshore ~2m depth
line28	20070601_182129.dt4	39234.76491	0.49	43.85	-	alongshore
line28a	20070601_182843.dt4	39234.76993	3.23	456.97	-	alongshore
line68a	20070601_183840.dt4	39234.77684	4.86	517.76	-	-
line66	20070601_184430.dt4	39234.7809	4.53	545.71	-	-
line64	20070601_185020.dt4	39234.78495	4.52	526.99	-	-
line62	20070601_185645.dt4	39234.78941	5.36	558.28	-	-
line60	20070601_190253.dt4	39234.79367	5.59	546.01	WESC060107_002	-
line58	20070601_190926.dt4	39234.79821	5.16	538.53	WESC060107_003	-
line56	20070601_191526.dt4	39234.80238	5.03	548.42	WESC060107_004	-
line54	20070601_192149.dt4	39234.80681	2.36	264.09	WESC060107_005	-
line52	20070601_194548.dt4	39234.82347	2.19	239.94	-	-
line50	20070601_194845.dt4	39234.82553	1.69	182.88	-	-
line48	20070601_195107.dt4	39234.82716	1.53	177.97	-	-
line46	20070601_195319.dt4	39234.8287	1.55	184.74	-	-
line44	20070601_195531.dt4	39234.83022	1.92	216.15	-	-
line42_1	20070601_195835.dt4	39234.83235	1.93	214.84	-	-
line40	20070601_200135.dt4	39234.83443	2.8	292.29	-	-
line38a	20070601_200607.dt4	39234.83759	2.79	333.72	-	-
line36	20070601_200924.dt4	39234.83986	2.55	327.44	-	-
line34	20070601_201255.dt4	39234.84231	2.77	362.52	-	-
line32	20070601_201618.dt4	39234.84465	2.79	329.52	-	-
line30a	20070601_202008.dt4	39234.84733	3.16	405.49	-	-
line29	-	39234.87569	-		WESC060107_006	-
line7	-	39234.84306	-		WESC060107_007	-
line117_1	-	39234.85427	-		WESC060107_008	-
line109a	20070601_213757.dt4	39234.90135	3.62	266.08	WESC060107_009	-
line120	20070601_214756.dt4	39234.90831	3.77	144.07	WESC060107_010	-
line129	20070601_215431.dt4	39234.91285	8.27	1047.41	-	alongshore deep section of channel
line129a	20070601_220256.dt4	39234.9187	8.77	1101.94	-	alongshore
line129b	20070601_221150.dt4	39234.92488	6.65	814.84	-	alongshore

Line	Biosonics_Filename	Date Collected	Elapsed Time (min)	Total Length (m)	ADCP_Filename	Comments
line127	20070601_222008.dt4	39234.93065	10.3	1111.56	-	alongshore
line127b	20070601_223034.dt4	39234.93789	8.93	938.82	-	alongshore
line117_1	-	39234.51984	-	-	WESC060107_011	-
line1	-	39234.98581	-	-	WESC060107_012	-
line137	20070601_235118.dt4	39234.99399	8.96	487.5	WESC060107_013	Garrison Bay
line1a	20070602_000201.dt4	39235.00154	4.93	314.37	-	sandlance/smelt? Eelgrass
line147	20070602_000709.dt4	39235.00497	2.93	297.05	-	-
line149	20070602_001132.dt4	39235.00802	4.13	430.32	-	-
line151	20070602_001733.dt4	39235.01219	4.03	491.6	-	-
line153	20070602_002252.dt4	39235.01588	5.33	580.7	-	-
line155	20070602_003013.dt4	39235.02098	4.56	589.98	-	-
line157	20070602_003610.dt4	39235.02513	4.8	520.42	-	-
line159	20070602_004309.dt4	39235.02997	4.07	480.18	-	-
line161	20070602_004811.dt4	39235.03346	3.89	466.29	-	-
line163	20070602_005332.dt4	39235.03718	4.25	539.41	-	-
line165	20070602_010202.dt4	39235.04309	2.52	331.02	-	-
line167	20070602_010524.dt4	39235.04542	4.99	715.89	-	-
line169	20070602_011120.dt4	39235.04955	6.13	713.93	-	-
line171	20070602_011826.dt4	39235.05447	3.06	359.12	-	-
line173	20070602_012254.dt4	39235.05757	2	236.97	-	-
line175	20070602_012602.dt4	39235.05975	2.27	237.31	-	-
line177	20070602_012857.dt4	39235.06178	1.86	216.17	-	-
line179	20070602_013136.dt4	39235.06362	1.79	212.06	-	-
line181	20070602_013347.dt4	39235.06513	3.8	264.35	-	-
line171a	20070602_024828.dt4	39235.11699	2.26	258.12	-	-
line173a	20070602_025142.dt4	39235.11922	2.26	276.34	-	-
line175a	20070602_025445.dt4	39235.12135	3.33	348.32	-	-
line177a	20070602_025834.dt4	39235.124	2.69	330.08	-	-
line179a	20070602_030156.dt4	39235.12634	2.56	304.66	-	-
line1b	20070602_030433.dt4	39235.12816	1.97	235.78	-	-
line181a	20070602_030944.dt4	39235.13176	1.73	201.16	-	-

Line	Biosonics_Filename	Date Collected	Elapsed Time (min)	Total Length (m)	ADCP_Filename	Comments
line183	20070602_031224.dt4	39235.1336	1.4	164.83	-	-
line184	20070602_031414.dt4	39235.13487	10.66	1491.02	-	alongshore
line57	20070602_032915.dt4	39235.1453	10.06	1417.65	-	oyster farm
line57a	20070602_033921.dt4	39235.15233	5.06	722.42	-	oyster farm surface map
line117_1	-	39235.59931	-	-	WESC060207_000	-
line144	-	39235.60972	-	-	WESC060207_001	Garrison Bay at mouth
line1	-	39235.61389	-	-	WESC060207_002	-
line29	-	39235.62222	-	-	WESC060207_003	-
line117_1	-	39235.63194	-	-	WESC060207_004	-
line1	-	39235.6375	-	-	WESC060207_005	-
line29	-	39235.64444	-	-	WESC060207_006	-
line117_1	-	39235.65347	-	-	WESC060207_007	-
line1	-	-	-	-	WESC060207_008	time in file
line29	-	39235.66944	-	-	WESC060207_009	-
line117_1	-	39235.67847	-	-	WESC060207_010	-
line1	-	-	-	-	WESC060207_011	time in file
line29	-	39235.69375	-	-	WESC060207_012	-
line117_1	-	39235.70347	-	-	WESC060207_013	-
line68_3	20070602_175434.dt4	39235.74623	13.69	2045.87	-	alongshore
line73	20070602_181503.dt4	39235.76045	7.16	554.73	WESC060207_014	across Mosquito Pass; boat wake; eelgrass
line73_2	20070602_193824.dt4	39235.81833	4.62	333.02	WESC060207_015	across Mosquito Pass (replicate)
line193	20070602_194305.dt4	39235.82159	10.37	1435.99	-	along main axis of Westcott Bay channel
line2	20070602_201318.dt4	39235.84257	13.86	1430.5	WESC060207_016	alongshore
line117_1	-	39235.85417	-	-	WESC060207_017	-
line126a	20070602_203845.dt4	39235.86024	4.22	455.88	WESC060207_020	-
line123	20070602_204727.dt4	39235.86628	5.27	341.79	WESC060207_021	-
line121	20070602_205353.dt4	39235.87074	2.53	207.56	WESC060207_022	boat wake
line119_1	20070602_205741.dt4	39235.87338	2.02	139.15	WESC060207_023	-
line118	20070602_210119.dt4	39235.87591	1.85	109.13	WESC060207_024	-
line117_1	-	-	-	-	WESC060207_025	-
line99	20070602_211052.dt4	39235.88257	3.49	209.19	WESC060207_026	eelgrass

Line	Biosonics_Filename	Date Collected	Elapsed Time (min)	Total Length (m)	ADCP_Filename	Comments
line97	20070602_211614.dt4	39235.88632	4.67	247.86	WESC060207_027	eelgrass
line95	20070602_212315.dt4	39235.89116	4.65	262.69	WESC060207_028	eelgrass
line93	20070602_212925.dt4	39235.89544	8	450.8	WESC060207_029	-
line117_1	-	-	-	-	WESC060207_031	-
line138	20070602_222112.dt4	39235.9314	3.49	457.26	-	-
line140	20070602_222543.dt4	39235.93454	2.99	408.46	-	-
line142	20070602_222930.dt4	39235.93716	2.5	335.21	-	-
line91	20070602_230431.dt4	39235.96148	2.46	325.6	-	-
line89	20070602_230728.dt4	39235.96353	2.66	359.33	-	-
line87	20070602_231106.dt4	39235.96605	2.59	348.12	-	-
line85	20070602_231421.dt4	39235.9683	3.75	418.67	-	-
line83	20070602_231849.dt4	39235.97141	3.43	432.02	-	-
line81	20070602_232255.dt4	39235.97425	3.79	471.36	-	-
line79	20070602_232712.dt4	39235.97723	3.46	480.54	-	-

APPENDIX II. Sediment Sampling Log (B-6-07-PS)

Station	Local_Time	UTC	Lon	Lat	Depth_m	Comment
1	6/1/07 20:44	6/2/07 3:44	-123.1430877	48.60642247	2.286	-
2	6/1/07 20:35	6/2/07 3:35	-123.1416559	48.60596625	2.1336	18.6 C
3	6/1/07 20:28	6/2/07 3:28	-123.1396819	48.60476647	2.4384	22.4 C
4	6/1/07 20:21	6/2/07 3:21	-123.1383557	48.6034425	2.4384	21 C
5	6/1/07 20:10	6/2/07 3:10	-123.1379259	48.60230609	2.1336	-
6	6/1/07 20:05	6/2/07 3:05	-123.1403608	48.60044935	3.3528	-
7	6/2/07 16:50	6/2/07 23:50	-123.1412818	48.60175168	3.6576	-
8	6/2/07 17:00	6/3/07 0:00	-123.1421506	48.60297386	3.6576	19 C
9	6/2/07 17:05	6/3/07 0:05	-123.1427175	48.6044497	3.048	WBN-SONDE
10	6/1/07 20:48	6/2/07 3:48	-123.1438967	48.60541356	3.048	-
11	6/1/07 20:54	6/2/07 3:54	-123.1458085	48.60390776	3.3528	-
12	6/2/07 16:27	6/2/07 23:27	-123.1449813	48.60267691	3.9624	-
13	6/2/07 16:35	6/2/07 23:35	-123.1442752	48.60168593	3.9624	-
14	6/2/07 16:45	6/2/07 23:45	-123.1434713	48.60059519	4.572	-
15	6/1/07 19:24	6/2/07 2:24	-123.1421019	48.59864869	2.4384	-
16	6/1/07 17:10	6/2/07 0:10	-123.1439795	48.5976315	2.1336	floc?
17	6/2/07 15:40	6/2/07 22:40	-123.1449351	48.59896955	4.2672	-
18	6/2/07 16:05	6/2/07 23:05	-123.1462388	48.60026471	4.572	-
19	6/2/07 16:09	6/2/07 23:09	-123.1473201	48.60179786	3.6576	-
20	6/2/07 16:20	6/2/07 23:20	-123.148262	48.60313373	2.1336	-
21	6/2/07 16:15	6/2/07 23:15	-123.1498974	48.60172972	1.9812	-
22	6/2/07 15:20	6/2/07 22:20	-123.1492409	48.59979738	2.4384	-
23	6/2/07 15:30	6/2/07 22:30	-123.1484785	48.59869397	5.0292	-
24	6/2/07 15:35	6/2/07 22:35	-123.1476722	48.59758652	5.1816	-
25	6/1/07 17:00	6/2/07 0:00	-123.1467698	48.59627812	2.286	-
26	6/1/07 16:45	6/1/07 23:45	-123.1480227	48.59330183	2.1336	-
27	6/1/07 16:55	6/1/07 23:55	-123.1490594	48.59477483	4.4196	-
28	6/2/07 15:05	6/2/07 22:05	-123.1505265	48.59684596	5.1816	mud
29	6/2/07 15:15	6/2/07 22:15	-123.1516348	48.59839777	1.6764	-
30	6/2/07 14:28	6/2/07 21:28	-123.1554968	48.59805066	1.0668	-
31	6/2/07 14:35	6/2/07 21:35	-123.1541046	48.59609766	5.1816	-

Station	Local_Time	UTC	Lon	Lat	Depth_m	Comment
32	6/1/07 16:40	6/1/07 23:40	-123.1527509	48.59414851	3.9624	-
33	6/1/07 16:35	6/1/07 23:35	-123.1517106	48.59270764	1.2192	-
34	6/1/07 16:27	6/1/07 23:27	-123.1567103	48.5939465	1.8288	-
35	6/1/07 16:20	6/1/07 23:20	-123.1575561	48.59512673	3.5052	-
36	6/1/07 16:14	6/1/07 23:14	-123.1581907	48.59599792	7.0104	-
37	6/1/07 15:30	6/1/07 22:30	-123.1589914	48.59715466	3.9624	-
38	6/1/07 15:18	6/1/07 22:18	-123.1599242	48.59843233	1.524	-
39	6/1/07 15:10	6/1/07 22:10	-123.1619828	48.59606753	1.2192	-
40	6/1/07 15:00	6/1/07 22:00	-123.1610457	48.59478295	5.7912	-
41	6/1/07 14:55	6/1/07 21:55	-123.1601357	48.5934547	8.5344	-
42	6/1/07 14:40	6/1/07 21:40	-123.1593413	48.59231698	5.7912	-
43	6/1/07 14:34	6/1/07 21:34	-123.1581413	48.59064567	1.8288	water temp 65 F
44	6/1/07 14:28	6/1/07 21:28	-123.1595903	48.5902156	5.1816	-
45	6/1/07 14:15	6/1/07 21:15	-123.1611018	48.5898281	2.1336	-
46	6/1/07 14:05	6/1/07 21:05	-123.1588285	48.58774659	3.048	-
47	6/1/07 13:50	6/1/07 20:50	-123.1640143	48.59094643	1.524	eelgrass dense
48	6/1/07 13:40	6/1/07 20:40	-123.1645209	48.59171271	7.62	cobble
49	6/1/07 13:35	6/1/07 20:35	-123.1649866	48.59240379	1.8288	fish
50	6/1/07 13:32	6/1/07 20:32	-123.1656586	48.59335283	0.762	patchy eelgrass
51	6/1/07 13:08	6/1/07 20:08	-123.1675292	48.591132	1.0668	eelgrass near DNR site
52	6/1/07 13:00	6/1/07 20:00	-123.1668798	48.59026557	6.096	sandy
53	6/1/07 12:57	6/1/07 19:57	-123.1663797	48.58958473	1.8288	-
54	6/1/07 12:50	6/1/07 19:50	-123.1657538	48.58869312	0.9144	-
55	6/1/07 12:40	6/1/07 19:40	-123.170589	48.59020657	5.7912	rock, no sample
56	6/1/07 12:25	6/1/07 19:25	-123.1702311	48.58971595	6.096	sand cobble
57	6/1/07 12:15	6/1/07 19:15	-123.1698061	48.58911829	0.9144	eelgrass
58	6/1/07 12:05	6/1/07 19:05	-123.1704144	48.5884425	0.4572	sand, cobble, eelgrass
59	6/1/07 23:55	6/2/07 6:55	-123.171477	48.5888478	1.9812	Rocky, eelgrass (drops=3)
60	6/1/07 11:35	6/1/07 21:35	-123.1729	48.58919782	8.5344	Mosquito Pass
61	6/2/07 13:28	6/2/07 20:28	-123.1425453	48.6053862	0.3048	WBN-1
62	6/2/07 13:28	6/2/07 20:28	-123.1425453	48.6053862	0.3048	WBN-2
63	6/2/07 13:28	6/2/07 20:28	-123.1425453	48.6053862	0.3048	WBN-3

Station	Local_Time	UTC	Lon	Lat	Depth_m	Comment
64	6/2/07 13:59	6/2/07 20:59	-123.1576585	48.5934125	0.4572	BP-1
65	6/2/07 13:59	6/2/07 20:59	-123.1576585	48.5934125	0.4572	BP-2
66	6/2/07 13:59	6/2/07 20:59	-123.1576585	48.5934125	0.4572	BP-3
67	6/2/07 14:12	6/2/07 21:12	-123.1674891	48.5911956	1.524	WP-SONDE
68	6/2/07 14:19	6/2/07 21:19	-123.1578369	48.5933055	2.5908	BP-SONDE
69	6/2/07 14:47	6/2/07 21:47	-123.1421332	48.5996015	1.3716	WBS-SONDE
70	6/2/07 14:52	6/2/07 21:52	-123.141445	48.5995073	0.9144	WBS
71	6/1/07 10:00	6/1/07 17:00	-123.145544	48.597332	2.4384	SF_Dock
72	6/2/07 13:28	6/2/07 20:28	-123.1425453	48.6053862	0.3048	WBN-PUSH
73	6/2/07 13:59	6/2/07 20:59	-123.1576585	48.5934125	0.4572	BP-PUSH

NOTES: Depth=depth in meters at time of sampling (not corrected to a datum).
Triplicates taken at WBN and BP.
PUSH=Pushcore 6 inch.

APPENDIX III. Grain size results. Size classes in percent.

Station	Boulder	Cobble	Gravel	Sand	Silt	Clay	Mud	Mean Phi	Mean mm	Std_Dev	Skewness	Kurtosis
1	0	0	0.46	80.41	15.96	3.17	19.13	3.552	0.085	1.482	2.246	10.021
2	0	0	0	61.11	31.68	7.21	38.89	4.174	0.055	2.011	1.306	4.317
3	0	0	0.6	61.16	28.84	9.4	38.25	4.102	0.058	2.354	0.975	3.356
4	0	0	3.11	87.59	6.85	2.44	9.29	2.588	0.166	1.673	1.847	9.374
5	0	0	0	90.17	7.16	2.67	9.83	3.015	0.124	1.473	2.733	11.841
6	0	0	0	45.37	45.31	9.32	54.63	4.731	0.038	2.112	0.866	3.148
7	0	0	0	7.02	75.28	17.7	92.98	6.207	0.014	1.816	0.651	2.778
8	0	0	0	5.82	75.34	18.84	94.18	6.34	0.012	1.799	0.607	2.689
9	0	0	0	6.08	72.56	21.37	93.92	6.486	0.011	1.888	0.264	2.915
10	0	0	0	59.01	34.67	6.32	40.99	4.292	0.051	1.86	1.414	4.69
11	0	0	0	10.14	74.02	15.84	89.86	6.019	0.015	1.826	0.75	2.937
12	0	0	0	5.85	73.9	20.25	94.15	6.391	0.012	1.856	0.443	2.767
13	0	0	0	8.19	73.86	17.94	91.81	6.185	0.014	1.839	0.675	2.708
14	0	0	0	6.78	75.13	18.09	93.22	6.216	0.013	1.831	0.671	2.73
15	0	0	0.94	49.29	35.59	14.18	49.77	4.644	0.04	2.672	0.487	2.26
16	0	0	0.49	81.68	12.86	4.98	17.84	3.024	0.123	2.047	1.84	6.068
17	0	0	0.39	14.25	66.93	18.42	85.36	6.053	0.015	2.025	0.328	2.946
18	0	0	0	11.37	74.86	13.77	88.63	5.832	0.018	1.774	0.953	3.269
19	0	0	0	6.29	76.13	17.59	93.71	6.226	0.013	1.807	0.596	2.945
20	0	0	0	13.6	75.04	11.37	86.4	5.637	0.02	1.728	1.048	3.733
21	0	0	0	75.91	19.13	4.96	24.09	3.307	0.101	2.043	1.624	5.127
22	0	0	0	20.47	66.11	13.42	79.53	5.627	0.02	1.965	0.632	2.963
23	0	0	0.23	16.12	72.3	11.35	83.65	5.546	0.021	1.789	0.902	3.954
24	0	0	0	25.32	64.51	10.16	74.68	5.288	0.026	1.797	1.162	3.891
25	0	0	0	56.15	34.26	9.59	43.85	4.311	0.05	2.319	0.961	2.98
26	0	0	1.86	73.81	19.21	5.12	24.33	3.44	0.092	2.065	1.343	5.08
27	0	0	0	22.68	64.09	13.23	77.32	5.556	0.021	1.977	0.7	3.052
28	0	0	0	31.3	59.35	9.35	68.7	5.129	0.029	1.788	1.258	4.16
29	0	0	0.07	73.92	20.54	5.48	26.02	3.383	0.096	2.145	1.393	4.508

Station	Boulder	Cobble	Gravel	Sand	Silt	Clay	Mud	Mean Phi	Mean mm	Std_Dev	Skewness	Kurtosis
30	0	0	0.07	70.95	22.17	6.81	28.99	3.504	0.088	2.273	1.3	4.014
31	0	0	0	37.33	53.64	9.03	62.67	5.005	0.031	1.798	1.355	4.274
32	0	0	0	45.66	46.63	7.71	54.34	4.548	0.043	2.054	0.861	3.5
33	0	0	5.83	71.86	16.62	5.69	22.31	3.235	0.106	2.264	1.069	4.732
34	0	0	0	60.23	27.5	12.27	39.77	4.142	0.057	2.65	0.856	2.554
35	0	0	4.83	81.73	9.44	3.99	13.43	2.516	0.175	2.04	1.734	6.928
36	0	0	0	56.26	35.43	8.31	43.74	4.426	0.047	2.037	1.214	3.83
37	0	0	0.09	59.17	32.8	7.93	40.73	4.27	0.052	2.069	1.241	3.997
38	0	0	0	83.21	12.6	4.19	16.79	3.415	0.094	1.724	2.154	7.729
39	0	0	0	78.16	15.93	5.91	21.84	3.599	0.083	1.937	1.866	6.029
40	0	0	0	57.11	31.54	11.35	42.89	4.23	0.053	2.532	0.85	2.695
41	0	0	0	82.7	13.58	3.72	17.3	3.393	0.095	1.63	2.318	8.568
42	0	0	0	68.39	26.83	4.78	31.61	4.047	0.06	1.615	1.989	7.181
43	0	0	0.05	83.08	12.88	3.99	16.87	3.237	0.106	1.776	1.989	7.358
44	0	0	0	48.26	44.07	7.67	51.74	4.676	0.039	1.798	1.477	4.769
45	0	0	64.34	26.01	7.59	2.07	9.66	0.153	0.9	2.357	2.247	7.7
46	0	0	0	28.4	63.26	8.34	71.6	5.085	0.029	1.701	1.405	4.733
47	0	0	10	70.51	14.45	5.04	19.49	2.732	0.151	2.404	0.978	4.434
49	0	0	0	68.63	24	7.37	31.37	3.873	0.068	2.133	1.409	4.218
50	0	0	0	77.45	16.7	5.84	22.55	3.345	0.098	2.102	1.581	5.143
51	0	0	0.51	71.69	19.64	8.17	27.8	3.601	0.082	2.334	1.315	3.996
52	0	0	5.57	90.39	2.82	1.22	4.04	2.001	0.25	1.401	1.837	13.66
53	0	0	0	43.83	47.12	9.05	56.17	4.852	0.035	1.841	1.363	4.26
54	0	0	0	73.72	21.7	4.58	26.28	3.479	0.09	1.903	1.515	5.539
56	0	0	9.46	84.86	3.95	1.73	5.67	2.129	0.229	1.619	1.382	10.384
57	0	0	21.69	73.62	3.47	1.22	4.69	1.067	0.477	1.84	1.529	7.735
58	0	0	43.39	42.38	10.05	4.17	14.23	1.407	0.377	2.846	1.113	3.762
59	0	0	0.6	97.52	1.31	0.57	1.88	1.912	0.266	0.909	4.175	35.176
60	0	0	41.8	51.4	4.69	2.11	6.8	1.104	0.465	2.329	1.164	5.014
61	0	0	0.95	56.72	35.26	7.06	42.32	4.282	0.051	2.03	1.031	4.249

Station	Boulder	Cobble	Gravel	Sand	Silt	Clay	Mud	Mean Phi	Mean mm	Std_Dev	Skewness	Kurtosis
62	0	0	0	40.16	48.98	10.86	59.84	5.019	0.031	2.06	0.924	3.142
63	0	0	0	52.8	39.54	7.66	47.2	4.489	0.045	1.977	1.167	3.915
64	0	0	0.12	86.21	9.86	3.81	13.67	3.262	0.104	1.623	2.553	9.711
65	0	0	0	90.18	7.22	2.6	9.82	3.043	0.121	1.392	3.172	13.942
66	0	0	0.88	90.82	6.06	2.24	8.3	2.984	0.126	1.356	2.796	14.549
67	0	0	1.33	66.3	22.94	9.43	32.37	3.684	0.078	2.551	1.019	3.223
68	0	0	0	75.03	20.02	4.94	24.97	3.886	0.068	1.654	2.142	7.432
69	0	0	0	9.18	71.74	19.08	90.82	6.268	0.013	1.907	0.412	2.689
70	0	0	1.07	72.42	19.21	7.3	26.51	3.523	0.087	2.339	1.203	3.975
71	0	0	7.42	23.29	52.75	16.54	69.29	5.161	0.028	2.851	-0.363	2.892

6 Physiological performance of *Zostera marina* in response to stress: Importance of analysis in assessing declining populations

Katherine Selting, Emily Carrington and Sandy Wyllie-Echeverria
Friday Harbor Laboratories
University of Washington

Physiological performance of *Zostera marina* in response to stress: Importance of analysis in assessing declining populations

Katherine Selting, Emily Carrington and Sandy Wyllie-Echeverria

Abstract

The purpose of this study was to explore the importance of analysis of variation in physiological performance of the seagrass *Zostera marina* in response to stress. Previous studies have related the decline in seagrass populations to low light conditions. After the local extinction of *Z. marina* occurred within the head of Westcott Bay, San Juan Island, investigation of causes of decline began by a team of scientists from the University of Washington, Friends of the San Juans, the United States Geological Survey and the Washington State Department of Natural Resources. In order to access the ability of analysis of physiological responses of *Z. marina* to evaluate stress in populations, we collected and examined photosynthetic responses of *Z. marina* populations both in early and late spring from three sites throughout the San Juan Archipelago, including a disturbed site (Bell Point, Westcott Bay, San Juan Island), an undisturbed site (Picnic Cove, Shaw Island), and one additional site between these two locations (Mosquito Pass, San Juan Island). Examining both seedling and adult samples, we used oxygen electrode analysis to observe the rate of change in oxygen concentrations for each sample, in response to changes in applied irradiance. Respiration and maximum photosynthesis rates were derived for each sample and averaged within each site. Both respiration and light saturated photosynthetic rate varied with site and sample date. Respiration rates were significantly higher at Bell Point, while photosynthesis rates were significantly higher at Picnic Cove. This variation between sites suggests different levels of stress among populations and as well, emphasizes the value of physiological performance analysis of *Z. marina* in accessing stress and understanding causes of decline in seagrass populations. Continued studies may assist in future identification of sites of concern for preservation and conservation.

Introduction

The primary objective of this pilot study was to explore the value of laboratory analysis of variation in the physiological performance of the seagrass *Zostera marina* (eelgrass) to augment an ongoing seagrass stressor project initiated by the Washington State Department of Natural Resources. Zimmerman et al. (1991) demonstrated the value of this technique to explain the very shallow ($\leq$ -1 m MLLW) distribution of *Z. marina* in San Francisco Bay. Results from this work revealed that while *Z. marina* had adapted to low light conditions within the bay, unless water clarity improved, the zone of growth was restricted to – 1 m MLLW. The consequence of this finding was to alert resource agencies, responsible for the protection of *Z. marina,* that further reductions in water clarity, at both local and regional scales, could result in the loss of this valuable resource.

In 2003, a local extinction of *Z. marina* occurred within the head of Westcott Bay, a small embayment on San Juan Island in the San Juan Archipelago (Wyllie-Echeverria et al. 2003a). Retrospective analysis of historical air photos determined patch fragmentation began between 1995 and 2001, after which time population stability was threatened and total loss followed (Wyllie-Echeverria in prep). This analysis also revealed that reductions in *Z. marina* cover occurred in other small embayments within the archipelago. While investigation is underway to determine cause, because the relationship between reduction in the submarine light environment and *Z. marina* persistence is well documented (Zimmerman et al. 1991; Dennison et al. 1993), research is needed to determine the photosynthetic response of *Z. marina* under varied submarine light environments.

We designed our experiment to determine if the photosynthetic performance of lower intertidal populations of *Z. marina* varied between a disturbed site (Bell Point, Westcott Bay, San Juan Island), and an undisturbed site (Picnic Cove, Shaw Island) within the San Juan Archipelago. Because these sites are separated by several kilometers (Figure 1), we included a third site (Mosquito Pass, San Juan Island; Figure 1) that was near the disturbed site but where the population compared more favorably to the undisturbed site within Picnic Cove.

Methods

Field measurements

Five non-flowering whole plant ramets (e.g. leaves, sheath and rhizome) were collected from three sites within the San Juan Island Archipelago, in early spring (March 21st-25th) and late spring (June 11th-16th) 2007. Collections occurred along a permanent transect established by the University of Washington in 2005 (Wyllie-Echeverria et al. unpublished data). Individual ramets were selected haphazardly at a distance of approximately 20 m apart along the transect. Specimens were extracted from the sediment, kept moist and cool and transported to the laboratory. Care was taken to remove a minimum of 15 cm of rhizome and several intact leaves with each individual. In the lab, samples were held in flowing seawater for up to two days until leaf segments were used for physiological analyses.

Z. marina seedlings were obtained as follows: generative shoots were collected from Picnic Cove on 5 September 2006, kept moist and cool and transported to the Friday Harbor Laboratories. Shoots were then placed in flowing seawater and from 4-6 October the bottom water was sieved and released seeds retained (Wyllie-Echeverria et al. 2003b). Some seeds were held in cold storage (approx. 5° C) in the dark and others were planted in individual sediment filled test tubes and placed in flowing seawater. Our intent was to analyze seedlings that germinated within the separate test tubes however, marine worms (Family Nereidae identified by E. Kozloff) killed several seedlings in our treatments (leaves were "glued" to the sediment surface and then covered with sediment resulting in seedling death). We were able to analyze two seedlings from these treatments. Three others that had germinated in cold storage were moved to flowing seawater tanks and allowed to develop foliage leaves

86
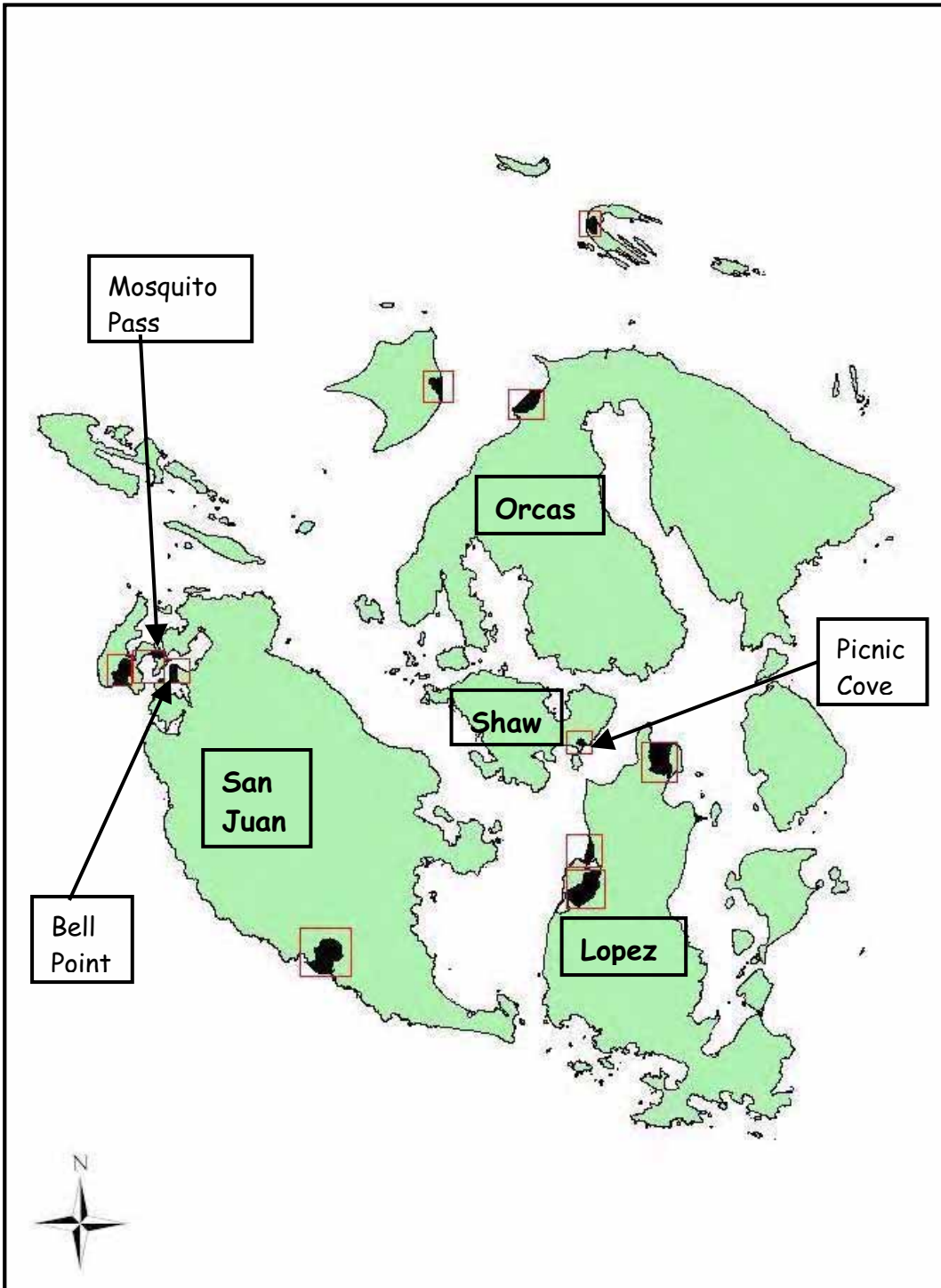
Figure 1: Field collection sites within the San Juan Archipelago; Bell Point (Westcott Bay, San Juan Island), Picnic Cove (Shaw Island) and Mosquito Pass (San Juan Island).

Laboratory Oxygen electrode measurements

We used a Clark-type oxygen electrode system (Hansatech DW3) to examine photosynthetic responses of *Z. marina* samples to varying irradiances. The electrode setup consisted of a water filled reaction chamber cooled by a temperature controlled water jacket. Seawater in the reaction chamber was filtered (1 µm) and kept at 10 degrees Celsius, similar to measured water temperatures in the field. We used a Kodak Carousel 4200 Slide Projector as the light source. A range of irradiances (0- 1600 µmol m^2 s^{-1}) were achieved with combinations of neutral density filters, determined using a light meter (Hansatech Quantitherm). An electrode at the base of the reaction chamber measured oxygen concentration, and software (Hansatech Oxygraph) was used to determine the metabolic rate (change in oxygen concentration over time) for each treatment. The baseline drift of the instrument was measured periodically and subtracted from each measurement.

Each adult sample (approximately 20mm x 10mm) was cut approximately 4 cm from the leaf sheath on the second youngest blade and placed between plastic clips within a 10 mL reaction chamber. Metabolic responses of the smaller seedlings (approximately 20 mm x 1.5 mm) were measured within a 2 mL reaction chamber. After securing the samples within the chamber, different irradiances were applied at intervals of 5 minutes. Rates of oxygen flux (nmol O_2 mL^{-1} min^{-1}) were measured over intervals of 2-5 minutes, approximately 90 seconds after each change in irradiance. All metabolic rates were normalized to the surface area of the sample, in square millimeters, yielding a rate of oxygen flux with units of nmol O_2 mm^{-2} min^{-1}. Rates normalized to sample dry weight were similar and are not presented here.

Two variables were extracted from these data for further statistical analysis: R, or dark respiration (irradiance equals 0 µmol m^{-2} s^{-1}) and $P_{max,}$, or light saturated net photosynthesis (irradiance ranging 865-1000 µmol m^{-2} s^{-1}). A Two-Way Analysis of Variance was used to evaluate the effect of sample date and collection site on the two metabolic rates. When applicable, a Student-Neuman-Kuehls procedure was used for pairwise comparisons between treatments (SigmaStat v. 2.03; SPSS Inc.).

Results

The metabolic response to light of adult *Zostera marina* samples collected from the three sites are presented in Figure 2. Each curve represents the average of five samples; occasionally a specimen was omitted due to abnormal physiological performance (low metabolic rate, limited response to light, etc.), reducing the sample size to four. Note that a higher range of irradiances (> 1000 µmol m^2 s^{-1}) were used in the June analyses. We used a hyperbolic tangent model to estimate saturating irradiance for each treatment (see Sebens et al. 2003 for details). Photosynthesis consistently saturated between 26 and 270 µmol m^2 s^{-1}, confirming the lower range of irradiances used in March were indeed sufficient for light saturation.

The dark respiration rate of adult samples varied with sample date and collection site (P < 0.05; Table 1; Figure 3). Respiration was significantly higher in March than in June, and was significantly higher for Bell Point compared to the other two sites (SNK comparisons, P < 0.05). There were no significant Date x Site interactions (P = 0.336).

Figure 2. Mean light response of adult *Z. marina* samples collected from three sites: Bell Point (circles), Mosquito Pass (triangles), and Picnic Cove (squares). Symbols are means (± SE) of 4-5 samples. A. March collection. B. June collection.
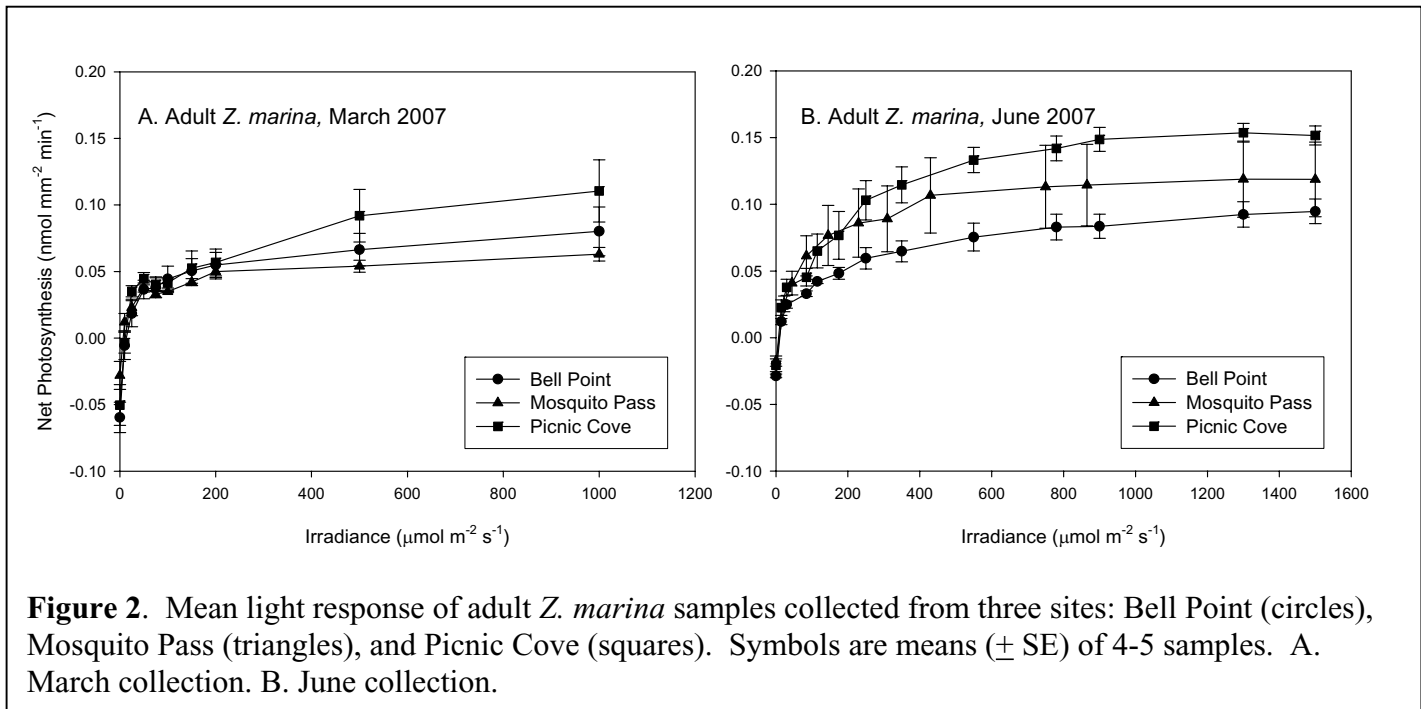
The light saturated photosynthetic rate of adult samples varied with collection site (Two-Way ANOVA, P < 0.05; Table 1). Rates were significantly higher for Picnic Cove compared to the other two sites (SNK comparisons, P < 0.05). While the effect of sample date was not significant (P = 0.052), the trend was for higher photosynthetic rates in June compared to March. (Figure 3). As with dark respiration, there were no significant Date x Site interactions (P = 0.336).

Table 1. Summary of Two-Way Analysis of Variance of dark respiration and light saturated photosynthesis of *Z. marina*. Significant treatments are indicated in bold

Source of Variation	DF	SS	MS	F	P
Dependent variable: Dark Respiration					
Date	**1**	**0.0017**	**0.0017**	**4.589**	**0.043**
Site	**2**	**0.0028**	**0.0014**	**3.867**	**0.036**
Date x Site	2	0.0008	0.0004	1.147	0.336
Residual	22	0.0080	0.0004		
Total	27	0.0134	0.0005		
Dependent variable: Light Saturated Photosynthesis					
Date	1	0.0067	0.0067	4.212	0.052
Site	**2**	**0.0114**	**0.0057**	**3.577**	**0.045**
Date x Site	2	0.0030	0.0015	0.954	0.401
Residual	22	0.0351	0.0016		
Total	27	0.0561	0.0021		
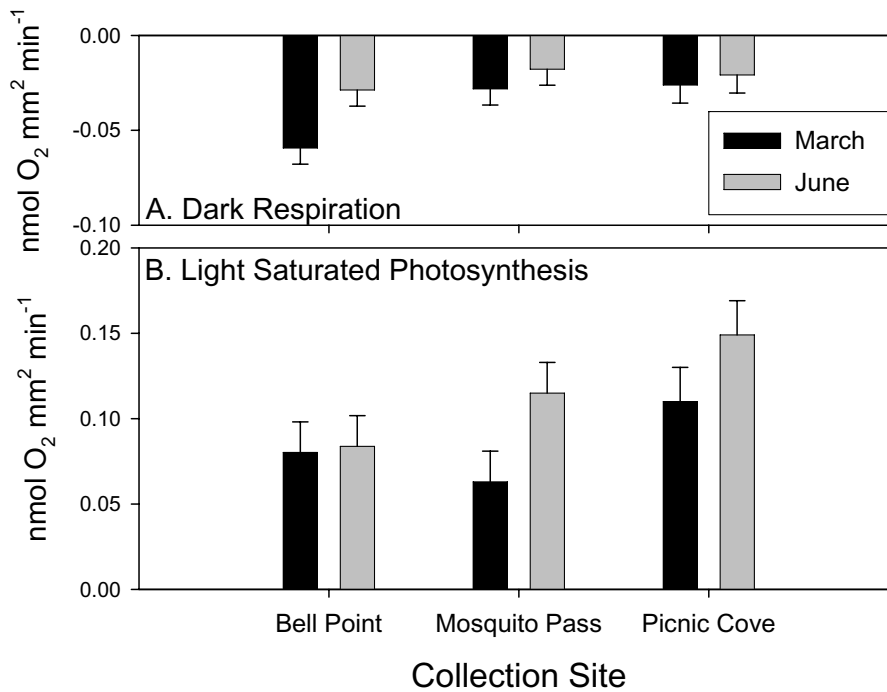
Figure 3. Dark Respiration and light saturated photosynthesis of adult *Z. marina* samples collected from three sites. Bars are least square means $\pm$ SEM.

Finally, the metabolic response of *Z. marina* seedlings to light is presented in Fig. 3. While the samples are considerably smaller than the adult samples (see Appendix), the response curve is most similar in magnitude to Bell Point; samples from Picnic Cove had considerably higher photosynthetic rates. The saturating irradiance for the seedling was estimated to be 202 μmol m^2 s^{-1}, similar to the range of values reported for adults.
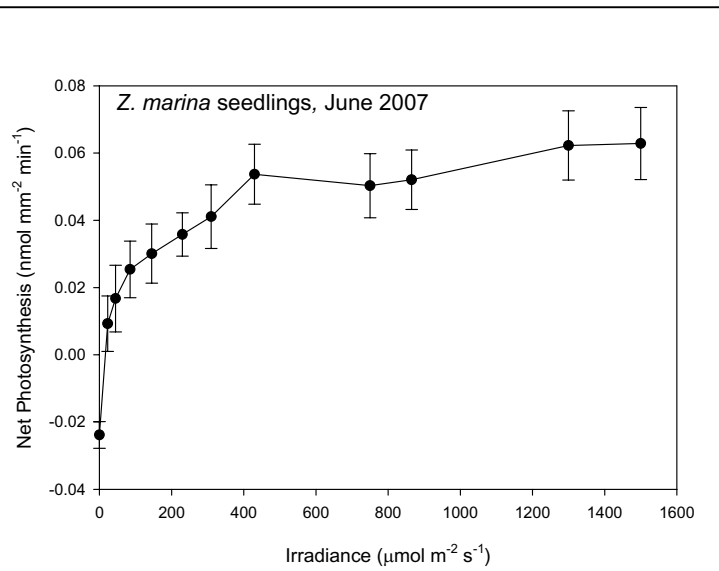
Figure 4. Mean light response of *Z. marina* seedlings.

90

Discussion

Analysis of variance in physiological performance of *Zostera marina* through oxygen electrode analysis proved beneficial in assessing stress in *Z. marina* populations. The variation by site suggests that stress is occurring in certain sites and can be observed through impacts to photosynthetic behavior in both seedling and adult seagrass samples.

Significantly higher light saturated photosynthetic rate at Picnic Cove compared to other sites suggests low stress conditions for the population. The results also show low levels of stress at Mosquito Pass. Further observations of abundant stem counts at each of these sites supports the results. Significantly higher respiration rates and lower maximum net photosynthesis values at Bell Point suggests that some higher level of stress is impacting the population. From recent stem counts (Wyllie-Echeverria et al., in prep.), decline in the population has been observed. The local extinction of *Z. marina* from the head of Westcott Bay, near to Bell Point, may have been caused by a similar stressor to that currently impacting the Bell Point site. Further studies combining this approach with field studies are crucial to the examining causes of decline and in ensuring future existence of seagrass populations throughout the San Juan Archipelago.

Although we did not examine changes in salinity or temperature within this study, the investigation of photosynthetic versus irradiance response revealed that other stressors may impact *Z. marina* photosynthesis versus irradiance behavior. Given the limitations of the study, more research must be conducted in order to access conditions of populations and causes of decline. Our pilot study was limited to laboratory analysis, and should be combined with field studies for future investigation. Other limitations include the collections of shoots restricted to the lower intertidal zone of each site, in addition, the seedlings examined were germinated in the lab and were not exposed to field conditions.

The observed variation in physiological response across site and date demonstrates the importance of oxygen electrode analysis in assessing stress in *Z. marina* populations. From these results and with this approach, we can begin to assess stressors and conditions of local *Z. marina* populations. This approach brings added value to a more comprehensive investigation of environmental stress on *Z. marina* populations, which WDNR should consider in the future in order to maintain and preserve current populations throughout the San Juan Archipelago and other regions in the greater Puget Sound.

Literature Cited

Dennison, W.C., R.J. Orth, K.A. Moore, J.C. Stevenson, V. Carter, S. Kollar, P.W. Bergstrom and R.A. Batiuk. 1993. Assessing water quality with submerged aquatic vegetation. *BioScience* **43**: 86-94.

Sebens, K.P., B. Helmuth, E. Carrington, and B. Agius. 2003. Effects of water flow on growth and energetics of the scleractinian coral *Agaricia tenuifolia* in Belize. Coral Reefs 22: 35- 47.

Wyllie-Echeverria, S, P.A. Cox, A.C. Churchill, J.D. Brotherson and T. Wyllie-Echeverria. 2003b. Seed size variation within *Zostera marina* L. (Zosteraceae). *Botanical J. Linn. Soc.* **142**: 281-288.

Wyllie-Echeverria, S., T.F. Mumford, J. Gaydos and S. Buffum. 2003a. Z. marina declines in San Juan County, WA: Westcott Bay Taskforce Mini-Workshop. 26 July 2003. SeaDocs Society.

Zimmerman, R.C., J.L. Reguzzoni, S. Wyllie-Echeverria, M. Josselyn, R.S. Alberte. 1991. Assessment of environmental suitability for growth of *Zostera marina* L. (eelgrass) in San Francisco Bay. *Aquatic Botany* **39**:353-366.

Appendix 1. Raw data collected for *Z. marina* during March and June 2007. All respiration measurements were conducted on samples from adult plants collected in the field, except for the seedlings, which were grown in the laboratory. Sites are Bell Point (BP), Mosquito Pass (MP) and Picnic Cove (PC). R is dark respiration and P_{max} is light saturated net photosynthesis (irradiance ranging 865-1000 μmol m^{-2} s^{-1}) in units of nmol O_2 mm^{-2} min^{-1}. The size (area = length x width) and dry weight of each sample was also recorded.

Date	Developmental Stage	Site	Sample	R	P_{max}	Area (mm^2)	Dry Wt. (mg)
March	Adult	BP	1	-0.079	0.067	220	6.4
			2	-0.064	0.129	191	4.8
			3	-0.020	0.117	161	5.7
			4	-0.084	0.055	199	6.8
			5	-0.050	0.033	207	9.4
		MP	1	-0.058	0.066	199	7.3
			2	-0.022	0.051	205	8.9
			3	-0.046	0.057	186	6.6
			4	-0.001	0.060	233	8.7
			5	-0.014	0.081	229	8.2
		PC	1	-0.001	0.109	161	5.1
			2	-0.041	0.061	158	3.2
			3	-0.003	0.173	127	4.2
			4	-0.060	0.099	130	3.6
June	Adult	BP	1	-0.026	0.070	219	7.9
			2	-0.028	0.080	215	9.0
			3	-0.026	0.091	235	7.3
			4	-0.033	0.063	210	9.7
			5	-0.031	0.115	198	9.9
		MP	1	-0.004	0.185	223	7.5
			2	-0.025	0.174	236	9.9
			3	-0.017	0.037	197	9.1
			4	-0.025	0.126	152	5.6
			5	-0.018	0.051	211	7.0
		PC	1	-0.021	0.161	204	7.3
			2	-0.015	0.166	201	5.3
			3	-0.034	0.128	186	6.6
			4	-0.013	0.140	190	6.9
	Seedling	Lab	1	-0.035	0.042	29	0.6
			2	-0.024	0.063	31	0.6
			3	-0.019	0.032	37	0.7
			4	-0.018	0.070	22	0.4

7 Variation in Leaf Elongation Rates and Germination: A pilot study to evaluate the influence of sediment and submarine light on *Zostera marina* fitness in the San Juan Archipelago

Zachary Hughes and Sandy Wyllie-Echeverria
Friday Harbor Laboratories
University of Washington

Variation in Leaf Elongation Rates and Germination: A pilot study to evaluate the influence of sediment and submarine light on *Zostera marina* fitness in the San Juan Archipelago.

Zachary Hughes and Sandy Wyllie-Echeverria

Introduction

Leaf elongation rate measurements can be a good indicator of overall seagrass fitness within a particular environment (Brun et al. 2006). Sub-optimal environmental conditions such as reduced submarine light conditions (Moore and Wetzel 2000) and sulfide toxicity (Holmer and Bondgarrd 2001) can negatively effect leaf elongation, and may result in a reduction of above ground biomass which can, in turn, influence the survival of individual ramets and clonal patches.

The seagrass *Zostera marina* disappeared from the head of Westcott Bay, a small embayment located on the northwest side of San Juan Island (Wyllie-Echeverria et al. 2003a). To date, the cause for this loss is unknown. The intent of this pilot study was to determine if the organic rich sediment in Westcott Bay (Figure 1, Chapter 6, p.87; Takesue & Wyllie-Echeverria, unpublished data) limits leaf elongation rates (LER) of whole plant transplants into the bay and seed germination thereby demonstrating that the site may not be optimal habitat for *Z. marina*.

Methods

To initiate our experimental design we collected 30 whole plant *Z. marina* ramets (leaves, sheath and a minimum of 15 cm rhizome and attached roots) from Picnic Cove (Figure 1; Ch. 6) on 11 July 2006. These individual ramets became our 'experimental unit' and were planted into sediments from Westcott Bay, Mosquito Pass and Picnic Cove during the week of 6 July 2006. Sediments were kept in the flowing seawater tanks before planting. Individual ramets were placed in sediment treatments in a randomized block design within two mesocosms (Ambient and Shaded (20-25% of ambient light depending on sky conditions)) on the same day of collection. Fifteen ramets were placed in each mesocosm.

The mesocosms were made from clear Plexiglas flow-through seawater tanks. Tanks were side by side with full exposure to the sun and were aerated. The ambient light tank had only a metal grating on top to keep out foraging animals (e.g., raccoons). The shaded tank was topped with a wooden frame and three layers of black window screening. The side of the shaded tanks was completely covered with black plastic sheeting.

Leaf elongation rates (cm d^{-1}) for all experimental units were tracked from the time of planting (11 July 2006; time period 1), until 25 May 2007 (time period 23). Elongation was measured bimonthly using the leaf punching technique (Dennison 1990).

A treatment to test germination (in this case emergence of either the cotyledon or foliage leaves; Churchill 1992) success in sediments from each site was also initiated immediately after whole plant experimental units (12 July) were placed in the mesocosms. Seeds were collected from

Picnic Cove (see Selting et al., Chapter 6) and placed in test tubes at a burial depth of 4 cm. Five individual seeds were planted in sediments from the three sites in separate test tubes that were randomly placed into a test tube holder. Germination was recorded when either the cotyledon or a foliage leaf was observed within a test tube. At the end of the experiment, all test tubes in which no germination was observed were checked and if seeds or immature seedlings were found the developmental stage was recorded. If intact seeds were found these were tested for viability using the vital red stain Tetrazolium chloride (Conacher et al. 1994; Wyllie-Echeverria et al. 2003b).

Results

There were distinctly different elongation patterns between the ambient light and the shaded tanks. Experimental units in the shaded tank outperformed those in the ambient tank until November, but suffered a decline in elongation rates from mid September until January, by which point all of the units in the shaded tank had died. Experimental units in the ambient tank declined from the time of their planting until January and then began to increase elongation rates until the end of the monitoring in May. When the experiment was terminated eight of the original fifteen experimental units were still growing; four in Westcott Bay sediment; two in Mosquito Pass sediment and two in Picnic Cove sediment. Elongation curves for all units in the shaded and ambient tanks are displayed in Figure 1.

Within the ambient tank, experimental units in each treatment were monitored and the leaf elongation curves are shown in Figure 2. Experimental units in the Westcott Bay sediment shifted from declining elongation rates to increasing elongation rates slightly earlier than the other two treatments, and increased at a higher rate. Figure 3 shows the elongation curves for the shaded tank, showing no significant difference in the performance of each of the treatments.

Germination (see definition in Methods section) was also significantly different between the shaded tank and ambient tank. Only four seeds developed foliage leaves in the shaded tank, and all during the summer of 2006; of these, three were growing in Westcott Bay sediments. Four intact seeds were found in the shaded tank sediments, three of these were not viable. There was also a very high rate of missing seeds in the shaded tank (47%) compared to the ambient light tank (13%). Seven seedlings germinated in the ambient tank, (4 in Picnic Cove sediments, 2 in Westcott Bay sediments and 1 in Mosquito Pass sediments). Germination data for both submarine light environments are displayed in Table 1.

Avg growth per day (cm)

Figure 1.

Ambient Light Growth Rates

Figure 2.

Shaded growth rates
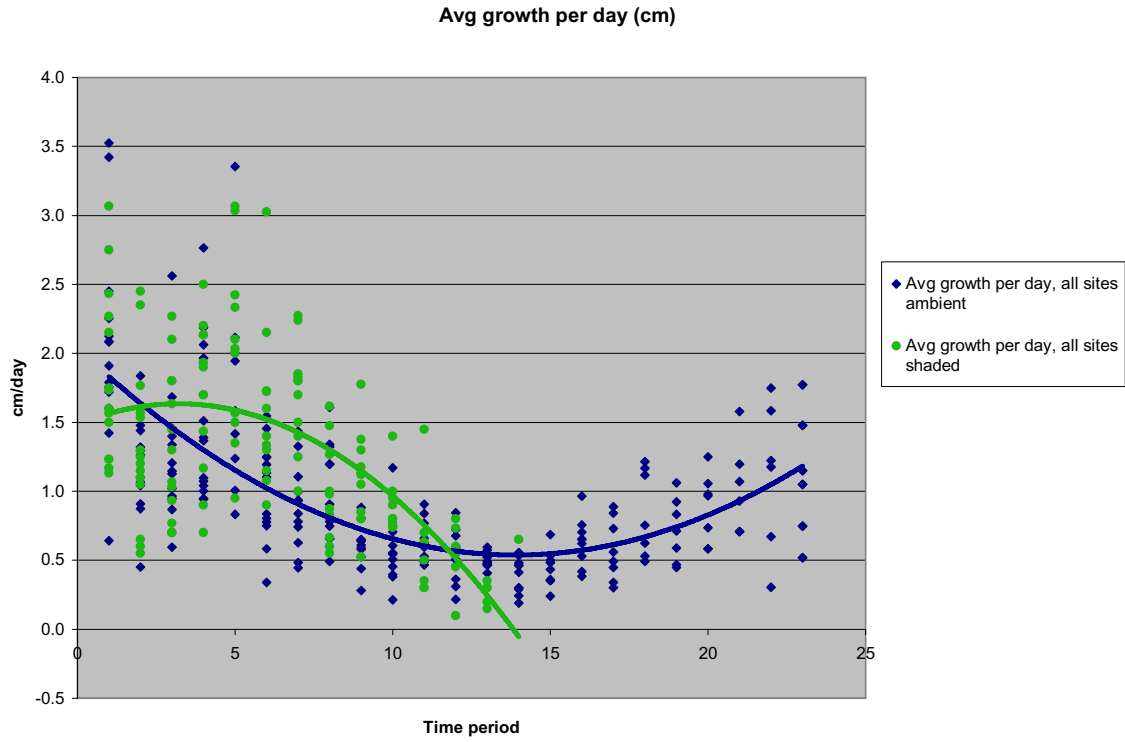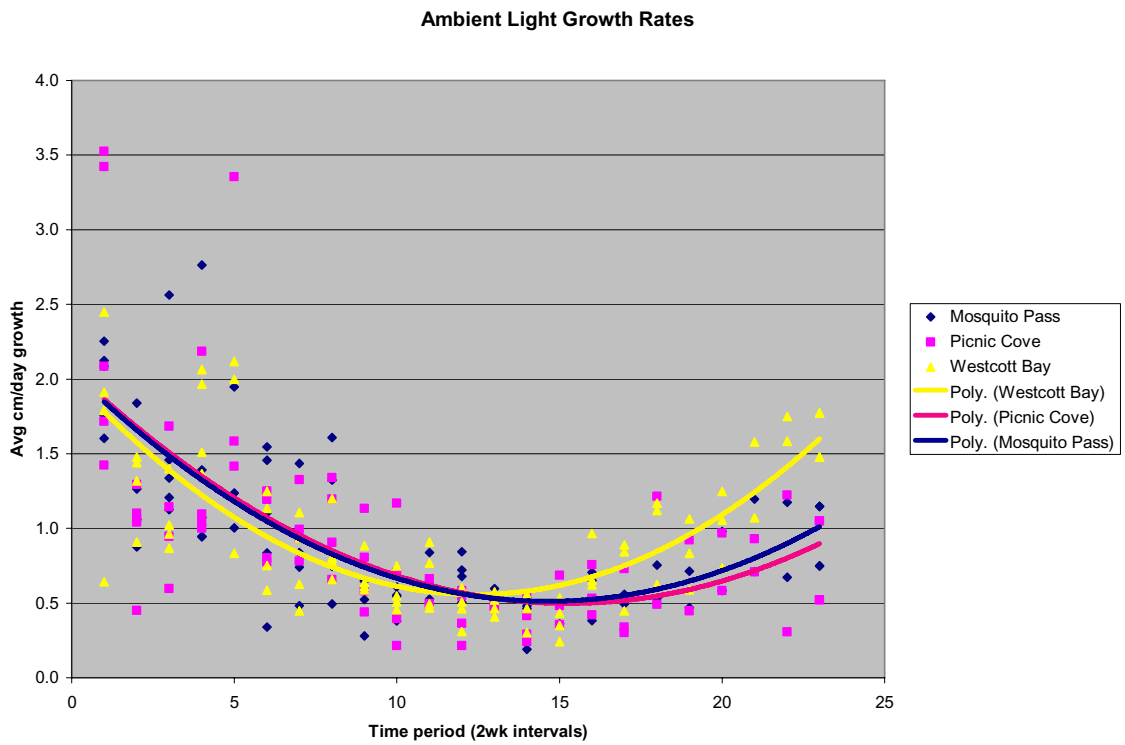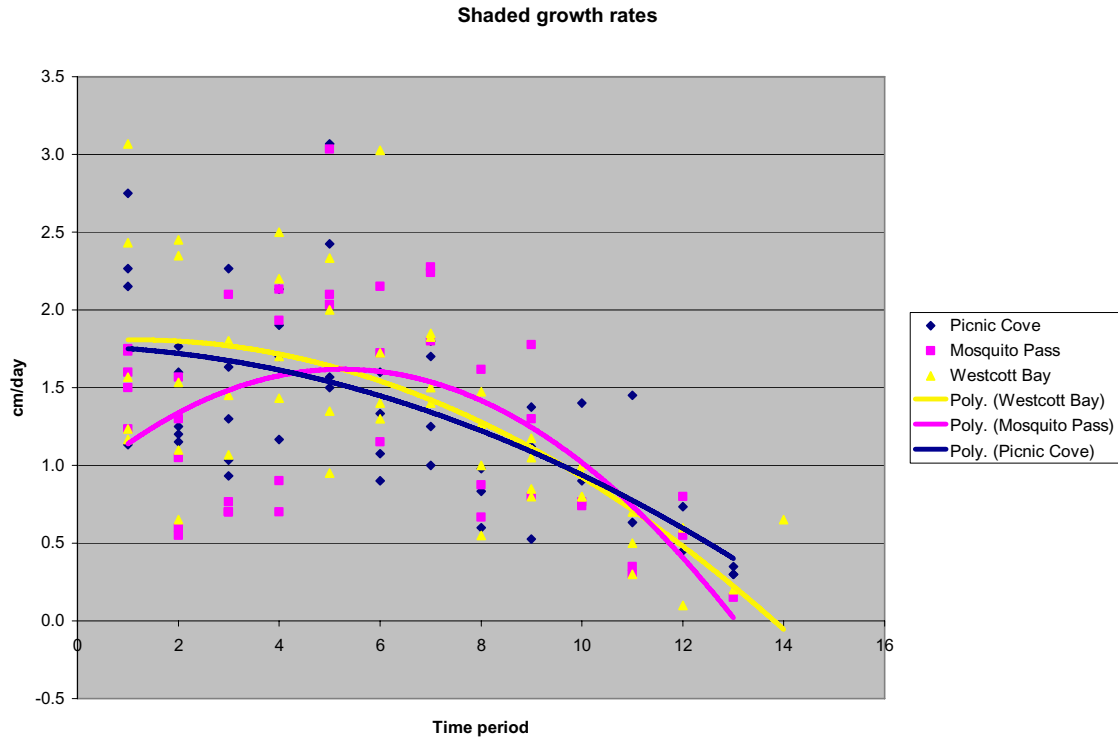
Figure 3.

Shaded	Sprout Date	Seed Development	Viable	**Ambient**	Sprout Date	Seed Development	Viable
PC1	N/A	2	N	PC1	16-Nov-06	6	
PC2	N/A	ND		PC2	29-May-07	6	
PC3	N/A	2	N	PC3	14-Mar-07	6	
PC4	N/A	ND		PC4	N/A	ND	
PC5	N/A	ND		PC5	14-Mar-07	6	
MP1	N/A	ND		MP1	N/A	2	Y
MP2	N/A	ND		MP2	4-Oct-06	6	
MP3	N/A	ND		MP3	N/A	4	
MP4	19-Aug-06	6		MP4	N/A	1	
MP5	N/A	2	N	MP5	N/A	1	
WB1	13-Jul-06	6		WB1	14-Mar-07	6	
WB2	11-Jul-06	6		WB2	14-Mar-07	6	
WB3	N/A	ND		WB3	N/A	4	
WB4	N/A	2	Y	WB4	N/A	ND	
WB5	11-Jul-06	6		WB5	N/A	1	
Seed development categories:	1 = Seed coat only			5 = ≥ 5cm extension			
	2 = Intact seed coat			6 = Foliage leaves			
	3 = Embryonic failure			ND = No data, seed not found			
	4 = ≤ 5cm extension						

Table 1.

Discussion

Unexpectedly, the experimental units in the shaded tank outperformed those in the ambient tank during certain light conditions. It was observed that there were no epiphytes in the shaded tank, while the ambient tank had to be cleaned often of epiphytes and macroalgae. Likely, there is a threshold of light conditions in the San Juan Archipelago that is detrimental to algae and epiphytes but provides sufficient light for *Z. marina* to survive (e.g., Mazzella and Alberte 1986). However, as the amount of available light continued to decline, *Z. marina* also began to suffer until the point that light was reduced and none of the experimental units were able to survive. Figure 4 describes a scale of possible light conditions affecting *Z. marina* in this region.

Enough Light for epiphytes and Z. marina to thrive	Enough light for epiphytes to thrive, epiphytes limit light availability for Z. marina	Not enough light for epiphytes, Z. marina not as limited	Not enough light for epiphytes or Z. marina to live
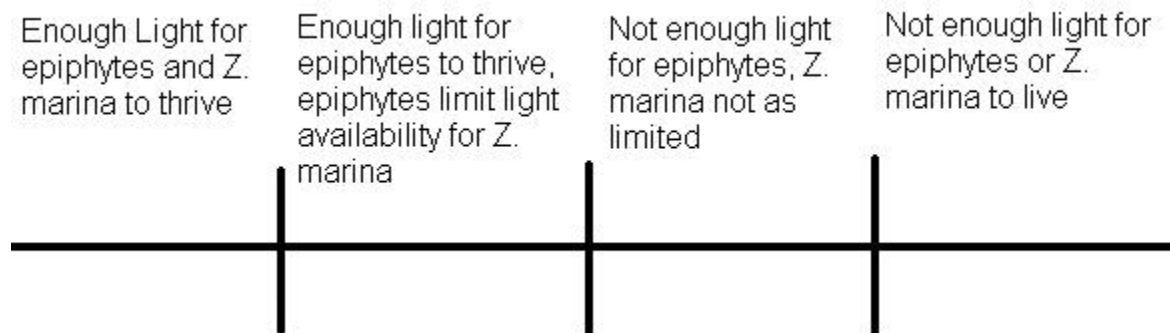
Figure 4.

Our germination experiment suggests that there may be a relationship between light availability and the breaking of dormancy in the San Juan Archipelago. Germination in the shaded tank occurred at the beginning of the experiment, when light availability was at its highest; however in the ambient tank germination took place in fall and late winter, both of which have similar light regimes. These data and other studies (reviewed in Orth et al. 2000) indicate that there could be a relationship between light availability and the timing of seed germination. Because the reduction of submarine light in winter and early spring related to predicted increases in rainfall during these seasons (Snover et al. 2003) may retard the breaking of dormancy, which, in turn could lead to a negative effect on recruitment success, we encourage further investigation of the environmental factors that break the dormancy of *Z. marina* seeds.

Also important to note is the relationship between Westcott Bay sediments and leaf growth. Our experiment demonstrates that Westcott Bay sediment could possibly support *Z. marina* as LER was comparable to the other sediment treatments and four of the five experimental units remained alive in the ambient treatment at the end of the experiment. However these results should be viewed with caution for two reasons. First, sediment in our treatments was modified (removed in small (approx. 1 kg portions) and placed in garden pots that were positioned in the respective light treatments) before planting. Secondly, although we did not compare the submarine light environment in our ambient treatment and submarine light available in the head of Westcott Bay, it is quite likely that our experimental units were receiving more photosynthetically active radiation (PAR) than they would have in the bay. Therefore, we suggest that before a large-scale transplant is undertaken more analysis of the submarine light environment and the geochemical properties of the sediment are required.

Literature Cited

Brun, F.G., J.J. Vergara, G. Peralta, M. P. Garcia-Sanchez, I. Hernandez and J.L. Perez-Llorens. 2006. Clonal building, simple growth rules and phylloclimate as key steps to develop functional-structural Seagrass models. *MEPS* **323**:133-148.

Churchill, A.C. 1992. Growth characteristics of *Zostera marina* seedlings under anaerobic conditions. *Aquatic Botany* **43**: 379-392

Conacher, C.A., I.R. Poiner, J. Butler, S. Pun and D.J. Tree. 1994. Germination, storage and viability testing of seeds of *Zostera capricorni* Aschers. from a tropical bay in Australia. *AquaticBotany* **49**:47:58.

Dennison, W.C. 1990 Leaf Production. Pages 77-79. IN: R.C. Phillips and C.P. McRoy (eds) Seagrass Research Methods UNESCO, Paris. 210 pp.

Holmer, M. and E.J. Bondgarrd 2001. Photosynthetic and growth response of eelgrass to low oxygen and high sulfide concentrations during hypoxic events. *Aquatic Botany* **70**: 29-38.

Mazzella, L. and R.S. Alberte. 1986. Light adaptation and the role of autotrophic epiphytes in primary production of the temperate Seagrass *Zostera marina* L. *J. Exp. Mar. Biol and Ecol.* **100**(1-3): 165-180.

Moore, K.A. and R.L.Wetzel. 2000. Seasonal variations in eelgrass (*Zostera marina* L.) responses to nutrient enrichment and reduced light availability in experimental ecosystems *J. Exp. Mar. Biol and Ecol.* **244**:1-28.

Orth, R.J., M.C. Harwell, E.M.Bradley, A. Bartholomew, J.T. Jawad, A.V. Lombana, K.A. Moore, J.M. Rhode and H.E. Woods. 2000. A review of issues in seagrass seed dormancy and germination: Implications for conservation and restoration. *Mar. Ecol. Prog. Ser.* **200**: 277-288.

Snover, A. K., A. F. Hamlet, and D. P. Lettenmaier. 2003. Climate Change scenarios for water planning studies: Pilot applications in thee Pacific Northwest. *Bulletin of the American Meteorological Society* **84**(11):1513-1518.

Wyllie-Echeverria, S., T.F. Mumford, J. Gaydos and S. Buffum. 2003a. *Z. marina* declines in San Juan County, WA: Westcott Bay Taskforce Mini-Workshop. 26 July 2003. SeaDocs Society.

Wyllie-Echeverria, S. P.A. Cox, A.C. Churchill, J.D. Brotherson and T. Wyllie-Echeverria. 2003b. Seed Size variation within *Zostera marina* L. (Zosteraceae). *Bot. J. Linn. Soc.* **142**:281-288.

8 Variation in *Zostera marina* Morphology and Performance: Comparison of Intertidal and Subtidal Habitats at Three Sites in the San Juan Archipelago

Ginger Shoemaker, Sandy Wyllie-Echeverria and Kevin Britton-Simmons
Friday Harbor Laboratories
University of Washington

Zostera marina plant metrics such as shoot density, shoot length and rhizome internode lengths can vary with depth (Backman and Barilotti 1976, Boese et al. 2005). In August 2006, a study was executed in the San Juan Archipelago to sample these metrics in intertidal and subtidal regions at three sites. Our objectives were to (1) compare shoot density (vegetative and reproductive), shoot length and rhizome internode lengths in intertidal and subtidal habitats and (2) compare these same metrics among sites for intertidal and subtidal habitats.

METHODS

Study Sites

Three sites within the Archipelago were selected: Shallow Bay on Sucia Island, Picnic Cove on Shaw Island and Mosquito Pass on San Juan Island (Figure 1). Sites were selected for two reasons: (1) these sites are sampled as part of an ongoing ecological analysis of *Z. marina* condition in the Archipelago and (2) sites were geographically dispersed within the Archipelago. *Zostera marina* meadows extended from the intertidal to the subtidal at each site.
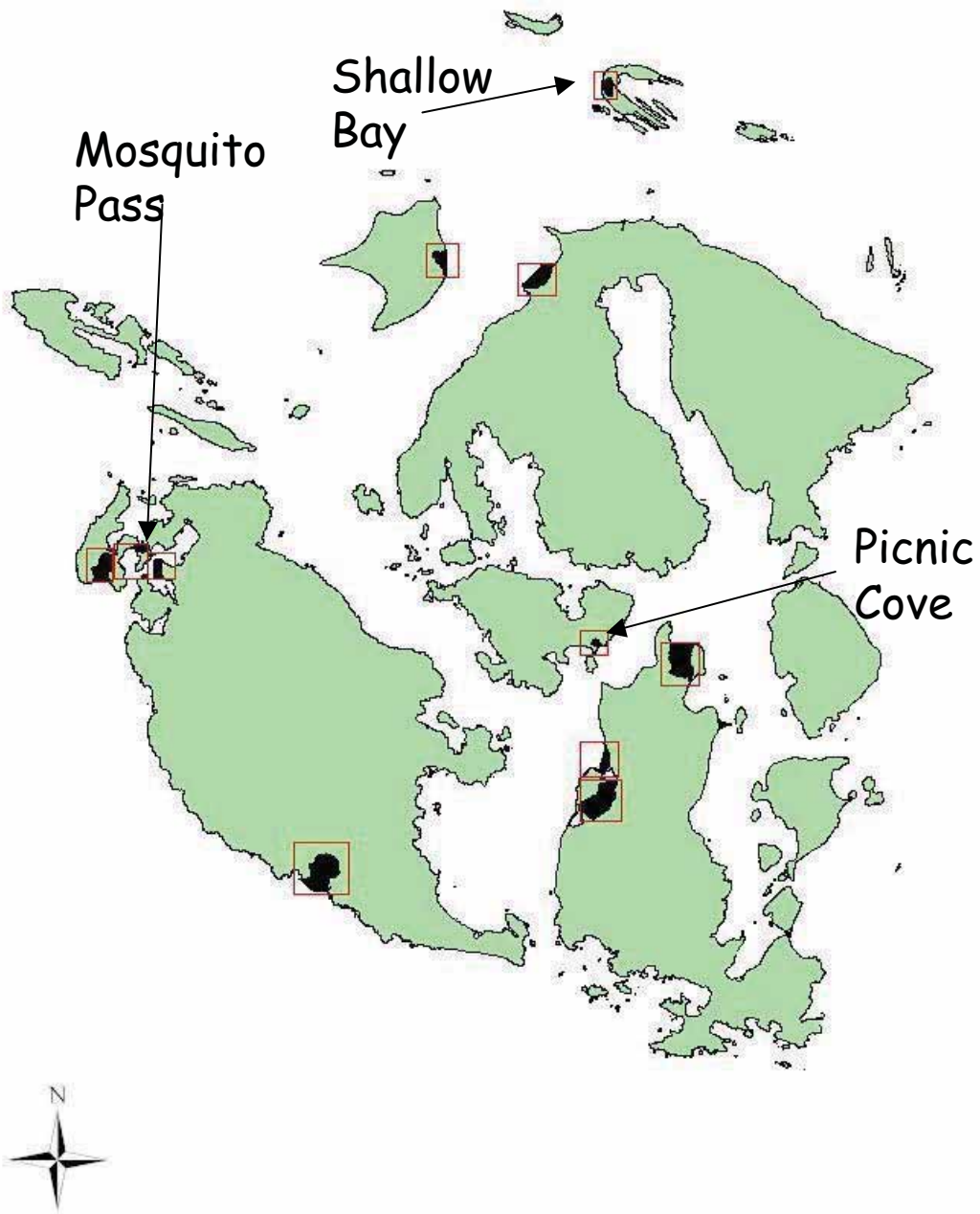
Figure 1. The San Juan Archipelago, Washington, with the three sampling sites marked. The unlabeled sites are the other sites included in the ongoing monitoring study of *Z. marina* in the San Juan Archipelago.

Intertidal Sampling

Intertidal sampling occurred during minus tides from 7-9 August 2006. Ten randomly selected stations were sampled along a 100 m transect laid parallel to the shore at a –1 m mean lower low water (MLLW) tidal elevation. The number of shoots (vegetative and reproductive) were counted within a 0.25 m² quadrat. Shoot density was calculated as the total number of shoots. Tissue samples for the computation of shoot length and rhizome internode length were collected haphazardly by removing one shoot and its attendant rhizome ($\geq$ 7 cm) every ten meters along the same transect. These ten shoots were transported to the lab and the length of the longest leaf in each shoot was measured. Rhizome internode lengths on the same ten shoots were measured using digital calipers.

Subtidal Sampling

Subtidal sampling took place by SCUBA on the 16 and 17 August 2006. A 100 m subtidal transect paralleled the intertidal transect and was placed at approximately one meter from the lower edge of the *Z. marina* meadow at each site. Consequently there was some variation among sites in the depth of the subtidal transects (-3.0 m MLLW at Shallow Bay, -4.0 m MLLW at Mosquito Pass, and –4.3 m MLLW at Picnic Cove). Sampling methodology for shoot density, shoot length and rhizome internode length was identical to that described above for the intertidal habitat.

Statistical Analysis

Statistical analyses were done using NCSS (Number Cruncher Statistical System) software. A mean rhizome internode length was calculated for each shoot prior to statistical analysis. Two-sample t-tests were used to compare differences between tidal elevations and one-way ANOVA was used to test differences between the three sites at each tidal elevation. The data for reproductive shoot densities were not normally distributed due to a large number of zeroes in the dataset. A Mann-Whitney test was used to compare differences within tidal elevations and a Kruskal-Wallis test was used to test differences between sites at each tidal elevation.

RESULTS

Shoot Density

Shoot densities ranged from 0-59 shoots /0.25m^2 along the intertidal transects and from 0-16 shoots/0.25m^2 along the subtidal transects. Intertidal densities were significantly greater than subtidal densities (Figure 2; t = -5.9325, P = 0.0000). At intertidal depths, Picnic Cove *Z. marina* cover was significantly more dense than Shallow Bay and Shallow Bay was significantly more dense than Mosquito Pass (F = 28.14, P = 0.0000). There were no significant differences in density between sites at subtidal depths.

Reproductive Shoot Density

Reproductive shoot density ranged from 0-3 shoots/0.25m^2 along the intertidal transects and from 0-2 shoots/0.25m^2 along the subtidal transects. The reproductive shoot density data were not normal due to a large number of zeroes in the dataset. There were significantly more reproductive shoots in the intertidal habitat than the subtidal habitat

(Figure 3; Mann-Whitney, Z = -2.9024, P = 0.0019). In the intertidal, Picnic Cove had significantly higher reproductive shoot density than Mosquito Pass (Kruskal-Wallis, H = 10.4987, P = 0.0053). There were no significant differences in reproductive shoot density between sites in the subtidal (Kruskal-Wallis, H = 0.7768, P = 0.6782). No reproductive shoots were sampled in the Picnic Cove subtidal.
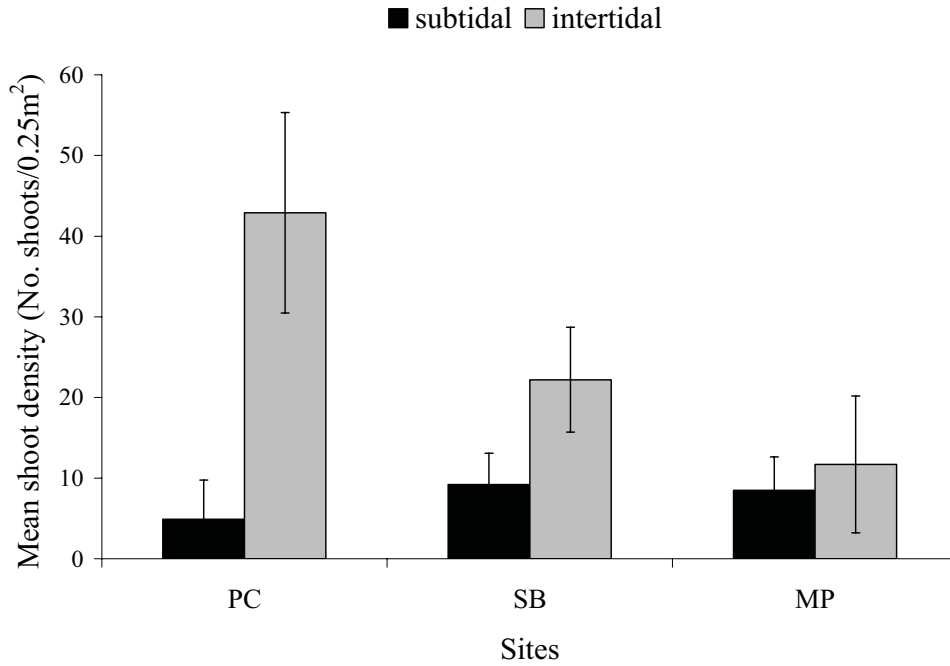
Figure 2. A comparison of mean shoot density along subtidal and intertidal transects. Error bars are ± 1 SD. PC = Picnic Cove, SB = Shallow Bay, MP = Mosquito Pass.
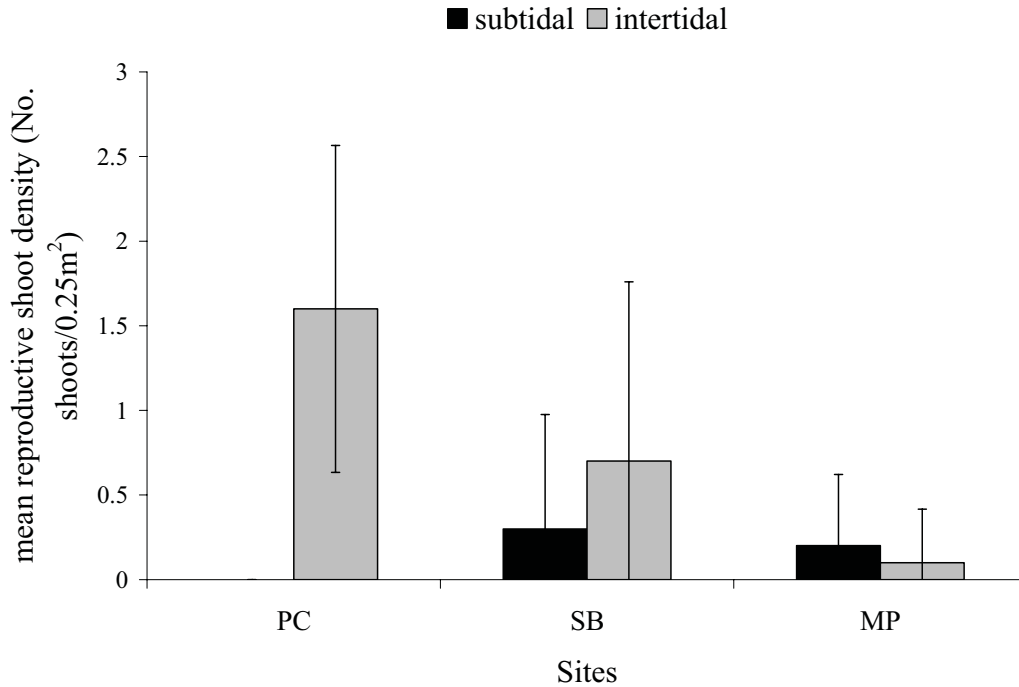
Figure 3. Comparison of reproductive shoot density along subtidal and intertidal transects. Error bars are ± 1 SD. PC = Picnic Cove, SB = Shallow Bay, MP = Mosquito Pass.

Shoot Length
Shoot length ranged from 28.2-136.5 cm along the intertidal transects and from 10.99-221.1 cm along the subtidal transects. The subtidal habitat had significantly longer shoots than the intertidal habitat (Figure 4; $t = 4.5535$, $P = 0.0000$). In the intertidal, Picnic Cove shoots were significantly longer than Mosquito Pass shoots ($F = 5.95$, $P = 0.0072$). There were no significant differences in shoot length between sites in the subtidal.
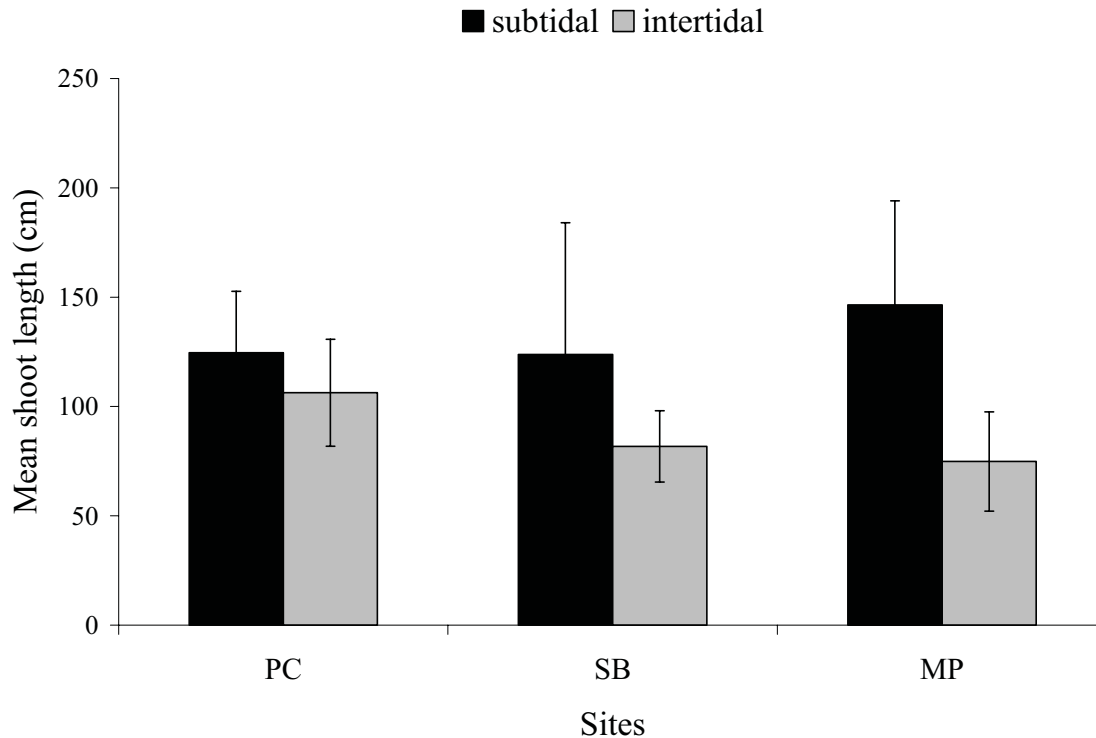
Figure 4. A comparison of mean shoot lengths along subtidal and intertidal transects. Error bars are ± 1 SD. PC = Picnic Cove, SB = Shallow Bay, MP = Mosquito Pass.

Rhizome Internode Lengths
Mean rhizome internode lengths ranged from 7.41-26.49 (± 4.69) mm along the intertidal transects and from 10.14-26.13 (± 4.30) mm along the subtidal transects. There were no significant differences in rhizome internode lengths between tidal elevations (Figure 5; $t = 1.2468$, $P = 0.21758$) or between sites ($F = 0.62$, $P = 0.5468$).

106
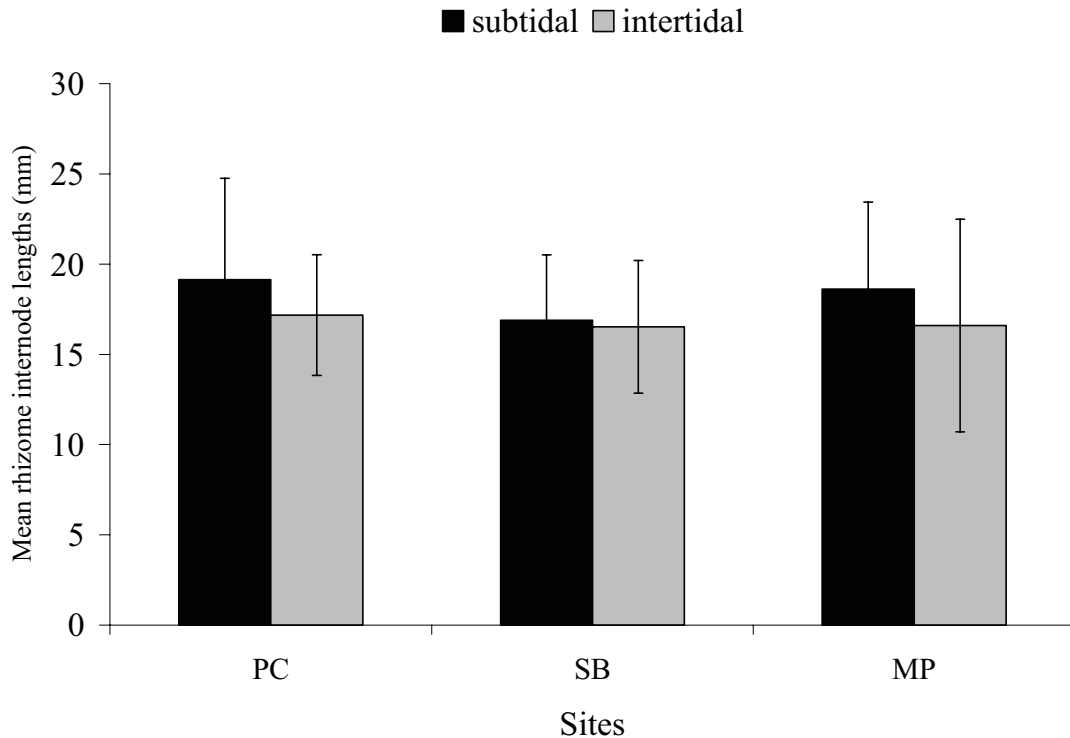
Figure 5. A comparison of mean rhizome internode lengths along subtidal and intertidal transects. Error bars are ± 1 SD. PC = Picnic Cove, SB = Shallow Bay, MP = Mosquito Pass.

SUMMARY

Zostera marina plants within the same meadow displayed shoot density and morphological differences based on tidal elevation. Subtidal eelgrass plants had longer shoots, lower shoot density, fewer reproductive shoots and less between-site variance than intertidal eelgrass plants. These results suggest that light limitation of subtidal *Z. marina* is less of a factor in the San Juan Archipelago than desiccation stress on intertidal *Z. marina* and may help explain the decline of intertidal *Z. marina* in several bays on San Juan Island.

LITERATURE CITED

Backman, T.W., and D.C. Barilotti. 1976. Irradiance reduction: effects on standing crops of the eelgrass *Zostera marina* in a coastal lagoon. *Marine Biology* 34: 33-40.

Boese, B.L., B.D. Robbins, and G. Thursby. 2005. Desiccation is a limiting factor for eelgrass (*Zostera marina* L.) distribution in the intertidal zone of a northeastern Pacific (USA) estuary. *Botanica Marina* 48: 274-283.

9   Differences in water chemistry and light availability within the San Juan Islands

Kristy Kull and Sandy Wyllie-Echeverria
Friday Harbor Laboratories, University of Washington

Jill Coyle and Miles Logsdon
Spatial Analysis Lab
School of Ocean & Fisheries Sciences, University of Washington

Chuck Schietinger
Luxel Corporation

Introduction

Nearshore currents help shape ecological communities, often via bottom-up control of phytoplankton, algae, and angiosperm diversity and abundance. The nutrient demands of these primary producers must be met to establish a base on which a food web can flourish. In addition, oceanographic conditions such as temperature, salinity, pH, dissolved oxygen, and flow speed must be within tolerable ranges. These conditions usually vary widely between open-coast habitats and protected coasts or bays, shaping the intertidal communities found in each (Lewis 1964).

The strong tidal currents that funnel through the Strait of Juan de Fuca and bathe the San Juan Archipelago create a well-mixed, relatively protected, unique ecological region that differs from the more stratified waters of Puget Sound and the Strait of Georgia (Thomson 1994). The unequal semi-diurnal tides of the eastern Pacific are further complicated by the time and routes required for tidal waves to funnel through the Strait, past the Islands, and eventually down into Puget Sound. Current speeds in the San Juan Islands range from more than 1.6 m·sec^{-1} at maximum ebb, to nearly stagnant at peak neap tides (Queisser 2004).

These variable current speeds can result in homogenization of waters, or can create patches of different conditions that affect primary producers differently in areas of close proximity (Alcaraz et al. 2002). Even within *sites* in the San Juan Channel, stratification

of water can range from strong to non-existent, and the influence of fresh water and nutrient input from the Fraser River to the north causes more variety in water conditions toward the top of the Channel (Riordan 2004). The Washington Department of Ecology (1995) found that the nutrient-rich, upwelled waters funneled through the Strait often exhibit dissolved oxygen levels below the "biological ideal" of 7 mg·l^{-1}, but then become so thoroughly mixed that nutrient levels generally do not deplete, and phytoplankton blooms do not have an opportunity to accumulate in specific areas within the Channel.

As the next ecological step in the food web, primary and secondary consumers such as suspension feeders are directly affected by nutrient supply and phytoplankton biomass. Menge et al. (1997) found that differences in intertidal communities may reflect differences in nearshore pelagic productivity, and individual growth rates of suspension feeders can be used as a proxy for availability of planktonic food. Plankton delivery via currents to intertidal communities is therefore an essential link in the chain of events that leads to the growth of suspension feeders such as barnacles, mussels, and anemones. Engie and Klinger (2007) found that intertidal species in the San Juan Archipelago typically produce larvae with short dispersal distances and low site variance, making them likely to recruit well locally, but not contribute significantly to the larval pool reaching other areas. Menge et al. (2002) showed that food concentration can impact the fitness of organisms, either by shaping functional cellular processes, or through determination of growth rates. However, Sanford and Menge (2001) found that phytoplankton abundance by itself did not fully explain variations in newly-settled barnacle growth in the field, and suggest that zooplankton abundance and water temperature may also affect growth.

Klinger et al. (2004) postulated specifically that sites on northern San Juan Island are more likely to encounter water coming from the Strait of Georgia, whereas areas south of Point Caution are more likely to encounter waters that enter the San Juan Channel from the Strait of Juan de Fuca. Freshwater from the Fraser River flows primarily southward through the straits and islands, and enters the San Juan Archipelago largely through President Channel. Flood tides bring oceanic waters into the Archipelago from Haro Strait, via Spieden Channel (Washburne, 2007). This study was conducted in late spring 2007, and looks at water conditions, chlorophyll content, and light transmission at seven sites within the San Juan Islands at ebb and flood tides, in an attempt to gauge the extent to

which fresh, sediment-laden waters from the Fraser reach the Islands. While these measurements were solely observational, demonstration of estuarine conditions in the Archipelago could be a precursor for extensive ecological impacts, especially on planktonic primary producers and intertidal flora such as *Zostera marina* (eelgrass).

Methods

Water and potential growth conditions around San Juan Island were assessed by collecting measurements and samples from several different vessels. A skiff was used for initial site appraisal and testing, and later water column profiling was done from a 40' trawler. Observation of a freshwater influence from the Fraser River was targeted by selection of three *areas* north of San Juan Island: President Channel, east of Flattop Island, and Spieden Channel. In President Channel two additional *sites*, notable for eelgrass growth, were assessed, creating a 3-site transect across the Channel. These five northern sites were compared to a location in the middle of San Juan Channel, and a spot just north of Cattle Pass at the southern tip of San Juan Island, making a total of seven assessed sites (Figure 1, Table 1).

Each site was sampled on five dates in late spring 2007 at varying tidal exchanges including both flood and ebb, and surface measurements of temperature, dissolved oxygen, salinity and pH were taken using YSI instrumentation. Quality assurance of temperature and salinity measurements made by the YSI was achieved by additional measurements with a temperature probe and refractometer. PAR was measured using a LICOR meter to 10 m depth at each station, which was later graphed by depth, linearized, and the negative slope of the graph taken as the light attenuation coefficient for each site. On-the-water PAR measurements were also coordinated with overhead satellite passes, which allowed calibration of resulting satellite imagery with field measurements. A Seabird CTD-19 was deployed on two dates to record temperature, dissolved oxygen, salinity and fluorescence at half-meter increments to 100 m where topography allowed. The upper 3 m of fluorescence data was average for each site before graphing, because these readings are highly variable on small spatial scales.

A preliminary satellite image of reflectance intensity of the Fraser River plume on May 10 was provided by Miles Logsdon of the University of Washington's School of

110

Ocean and Fishery Sciences. Subsequent images from May 29 were obtained from the MODIS Aqua satellite and prepared at 250 m resolution by Jill Coyle at the School's Spatial Analysis Lab, under the guidance of Miles Logsdon. These images were processed to display the relationship between the infrared and red light absorption of the water, offering a "terrestrial signature" concentration as means of identifying the plume.

Surface water samples were collected by bucket and stored in clean bottles that had been triple-rinsed with sample water before filling, for later analysis of transmission. At the time of this report, water transmission from each site had been analyzed from the first three sampling dates, using a Varian 500i spectrophotometer and a 10 mm sample path length.

A multivariate Global R test (Primer 6 software) was performed on the six water parameters tested on 18 May (flood tide) and 29 May (ebb tide), because water chemistry results from those two dates were very different from each other. The Global R test examined the covariance of the parameters (temperature, dissolved oxygen, salinity, pH, light attenuation, and fluorescence) across the five *areas* studied (Mail Bay and West Beach were not included).

Results and Discussion

A thorough analysis of the many physical factors at play in the San Juan Archipelago at any given time and the resulting effects on ecosystems and organisms would require an intensive sampling regime, but the snapshot provided here should provide a jumping-off point for future projects. Because observational water data was not taken on replicate days, statistics were not run; however, graphing surface data from all seven stations on differing tides and north-south gradients revealed distinct patterns.

Surface temperature measurements compared by station and tidal series revealed elevated temperatures on the May 29 ebb tide at Mail Bay, President Channel, West Beach, Flattop Island, and San Juan Channel (Figure 2). Interestingly, Spieden Channel had a surface temperature more similar to Cattle Pass on that date, but six of seven stations showed temperatures higher than those measured on any other date. The last two sampling dates, June 10 and 22, both exhibited higher temperatures than a previous ebb tide sampling, and had nearly-parallel across-station profiles. Large fluctuations in temperature

across fairly large (~30 km) spatial scales, tidal regimes, and dates suggest a variable, relatively warm freshwater presence in the San Juan Islands.

Dissolved oxygen concentrations in surface waters, again graphed by station and tidal series (Figure 3), was highest on May 29 at the northernmost sites -- Mail Bay and West Beach. The comparatively normal dissolved oxygen reading in President Channel on that date was surprising, and together with the Mail Bay and West Beach readings, it may be indicative of an algal bloom that flourished in the quieter "side pockets" of the Channel, that had not yet invaded further into the Archipelago. A later die-off of that theoretical bloom may have caused the lower oxygen values measured across most sites during both June sampling dates.

Ebb and flood tide series were graphed together in different colors, in the hope that patterns due to tidal state would be revealed; however, very few parameters seem to be consistent across the same tidal state. This may be a function of constantly-varying freshwater influence, via changes in river input and monthly tidal cycles.

While performing exploratory measurements on the vessel after the ebb tide had turned on May 29, the upper 1-2 m of surface water were actually found to be flowing *against* the tide, while equipment cast further below the surface was drifting strongly with the expected tidal current. Wind was insignificant at the time, and there was little chop on the water surface – this phenomenon was clearly a function of conflicting water masses: presumably a freshwater lens atop the saltwater, being continuously fed by flood waters and pushed toward the Strait of Juan de Fuca, even against (or over the top of) a robust tidal flood. The waters of Mail Bay, President Channel, West Beach, Flattop Island, and San Juan Channel also differed visually from the other sites on that date: the water was greener and had an abundance of what looked to be plant material floating in it.

Acidity, or pH, measurements revealed a notable reversal in station profiles on May 18 and 29 on opposing tides, with a change in the northern sites to more basic conditions during that time frame, probably a signature of alkaline River water (Figure 4). This freshwater influx likely carried different chemical loads and buffering capabilities, and station profiles on June 10 and 22 appear to have normalized somewhat throughout the Islands.

Salinity levels showed a clear freshwater intrusion from the north on May 29, with lower values at sites high in the Archipelago, and salinity was apparently tempered in Spieden Channel during this event by oceanic water from the Strait (Figure 5).

The temperature gradients revealed within the Islands on an ebb tide were surprisingly different from flood temperatures, 5°C higher at some stations. Mail Bay, President Channel, West Bay, Flattop Island, and San Juan Channel all shared temperatures near 14°C on May 29, and these three stations also shared low salinities, high attenuation coefficients, and elevated fluorescence readings during this estuarine event. These four factors together paint a clear picture of a Fraser River plume reaching the San Juan Archipelago. Whether the plume is currently spreading or not is unknown, but a large snow pack in the British Columbia interior coupled with a warm spring have led to record flooding, last seen 35 years ago. Spieden Channel was expected to share findings with President Channel and Flattop Island, as they are the three northernmost areas surveyed, but the >1.6 m·sec^{-1} tidal input of oceanic water from Haro Strait seen with certain tide regimes clearly overrides any Fraser input.

Regardless of the tidal state during sampling, the five dates graphed across these parameters appear to demonstrate a sudden influx of Fraser River water on May 29, followed by a partial return to "normal" parameters and another, smaller, influx of fresh water on June 22. Especially visible in the temperature and salinity graphs, May 18 and 19 measurements appear normal, but May 29 showed a spike in temperature and a drop in salinity across many sites. June 10 measurements appeared to be trending back toward "normal," with a slight regression visible again on June 22.

Graphing of the light attenuation coefficients obtained from PAR profiles further defines the differences between sampling dates, with turbidity generally increasing with time due to increased sediment loads in the water (Figure 6). A light attenuation coefficient is a measure of the amount of light absorbed per unit depth of water, which can be related to the photosynthetic potential of that water (Brower et al., 1998). Gaps in the data presented in Figure 6 are due to adverse sampling conditions encountered at some sites and dates, mostly due to large tidal fluxes.

Coordinating attenuation coefficients with satellite data yielded a preliminary image of reflectance intensity in the straits on May 10, wherein the Fraser River plume is

visible as an aqua/white region north of the San Juan Archipelago, picked up by the satellite due to the plume water's unique reflective characteristics (Figure 7).

Examination of water fluorescence as a proxy for chlorophyll allows an approximation of primary productivity in an area. Figure 8 shows much higher fluorescence on May 29, particularly in the areas that seem to funnel Fraser River water through the islands: President Channel, Flattop Island, and San Juan Channel. The comparatively high light attenuation and fluorescence readings measured on May 29 versus previous samplings prompted further tracking of the Fraser River plume via satellite images which targeted specific reflectance signatures that identified the plume, and may be used to track it in the future.

Data captured by the MODIS Aqua satellite on May 29 resulted in maps of the infrared and red wavelength reflectance. Infrared light is absorbed in the upper 15 cm of normal seawater, and the white areas in Figure 9 represent waters of reflection in this wavelength, suggesting water heavily laden with sediment in the upper 15 cm which caused a change in the reflectance signature of the water. A dense signature of the surface sediment is visible right at the River mouth, and also in the northeast San Juan Islands, such as in President Channel. This additional patch appears to be disconnected from the mouth plume, and could be the result of a large pulse of water from the Fraser that was subsequently pushed south by tidal or longshore currents.

Visible red light is absorbed in the upper few meters of normal seawater; white areas in Figure 10 suggest water carrying sediment *below* the top 15 cm, presumably in the process of settling out of the water column. The plume of deeper sediment-laden waters at the Fraser's mouth is larger than the upper-15 cm plume – presumably the result of slower water and increased sediment settlement farther from the River mouth.

The relative difference between the two wavelength bands mentioned above allowed identification of rough "terrestrial signature" areas based on the concentration of surface sediment determined via reflectance. Figure 11 shows the Fraser River plume in red at its densest, green where it is moderate, and blue where the plume is not detectable by satellite.

Spectrophotometric analysis of light transmission through the water was used to help ground-truth the satellite imagery, because light transmission is inversely related to

114

particle load in the water. Figure 12 is a broad wavelength scale demonstrating an entire transmission profile from May 18, the telling area of which is between 350 and 750 nm. An enlargement of this region can be seen in Figure 13, where each station is discernible, and a sharp curve drop-off at 400 nm is probably indicative of higher salinity, such as at Cattle Pass. Spieden Channel, San Juan Channel, and Cattle Pass had the highest overall transmissions, indicating clearer water and low River influence on May 18. Broad-scale curves from May 19 and 29 retained the same overall shape, especially in the higher wavelengths; thus only 350 to 750 nm is shown for each. Figure 14, the curve for sites sampled on May 19, shows Flattop Island, Mail Bay, and West Beach with the highest transmission percentages, but the overall range of transmission is lower for this date than it was on May 18. Mail Bay and Cattle Pass had the highest transmissions on May 29 (Figure 15), and the range of curves on this date was lower than either May 18 or 19, indicating more turbid waters overall.

A multivariate analysis was performed on normalized data of all six parameters graphed above (temperature, dissolved oxygen, pH, salinity, light attenuation, and fluorescence), on 18 May (flood tide) and 29 May (ebb tide), at each of the five *areas* sampled. Closer points in Figure 16 indicate greater similarity of all the physical parameters. Ebb and flood points, collectively, are significantly separated (Global R test, p = 0.008). This analysis of the water column data revealed patterns across all six parameters, with equal weight given to each. The results support those indicated by other graphs *when only these dates are considered*, such as flood readings being consistently dissimilar to ebb readings at the same sites. The two Cattle Pass tidal samples were closer to each other than any other site on opposing tides, strengthening the indication that Cattle Pass' location at the south end of the San Juan Channel keeps it largely "oceanic" and/or requires extra time for a flood plume to affect water parameters there. Points consistently plotted close together, such as President Channel and Flattop Island, have greater similarity to each other than to other points. This visual method of interpreting results is also useful for seeing overall trends: northern sites (like President Channel) experienced very different water masses on ebb vs. flood tides, whereas southern sites (like Cattle Pass) consistently encountered oceanic waters from the Strait.

Future monitoring of local oceanography coupled with assessment of intertidal communities could reveal yet-unknown facets of physical-biological interactions. Investigation into the effects of dissolved nutrients and salinity on the growth of intertidal invertebrates and other organisms, such as seagrasses, would also be interesting areas of future study, with the possibility of divulging the River's influence across multiple ecosystems and regions. While the findings presented here were solely observational, they demonstrate the presence of large volumes of fresh, turbid water in the San Juan Islands.

Acknowledgements

Literature cited

Alcaraz, M., Marrase, C., Peters, F., Arin, L., and A. Malits. 2002. Effects of turbulence conditions on the balance between production and respiration in marine planktonic communities. Marine Ecology Progress Series 242: 63-71.

Brower, J.E., Zar, J.H., and C.N. von Ende. Field and Laboratory Methods for General Ecology. McGraw-Hill, San Francisco, 1998.

Engie, K., and T. Klinger. 2007. Modeling passive dispersal through a large estuarine system to evaluate marine reserve network connections. Estuaries and Coasts 30: 201-213.

Klinger, T., Wonham, M., Kappel, C., Copello, S., Dean, N., Evans, K., Guarderas, A.P., Haderlie, L., Northern, J., Outlaw, R., Pajuelo, M., Ribeiro, S., Papiez, C., and H. Weiskel. 2004. A comparison of multiple biological metrics between the Point Caution research reserve and neighboring public access sites. Friday Harbor Laboratories Marine Conservation Biology: Summer Term B.

Lewis, J.R. The Ecology of Rocky Shores. English University Press, London, 1964.

Menge, B.A., Daley, B.A., Wheeler, P.A., and P.T. Strub. 1997. Rocky intertidal oceanography: an association between community structure and nearshore phytoplankton concentration. Limnology and Oceanography 42: 57-66.

Menge, B.A., Olson, A.M., and E.P. Dahlhoff. 2002. Environmental stress, bottom-up effects, and community dynamics: integrating molecular-physiological and ecological approaches. Integrative and Comparative Biology 42: 892-908.

Queisser, M.R. 2004. The effects of currents on biomass and productivity in the San Juan Islands. Friday Harbor Laboratories Pelagic Ecosystems Apprenticeship: August.

Riordan, E.C. 2004. Effects of turbulent water mixing on phytoplankton morphology and species composition in the San Juan Channel, WA. Friday Harbor Laboratories Pelagic Ecosystems Apprenticeship: August.

Sanford, E. and B.A. Menge. 2001. Spatial and temporal variation in barnacle growth in a coastal upwelling system. Marine Ecology Progress Series 209: 143-157.

Thomson, R.E., edited by Wilson, R., Beamish, R., Aitkens, F., and J. Bell. 1994. Physical oceanography of the Strait of Georgia - Puget Sound - Juan de Fuca Strait system. Canadian Technical Report of Fisheries and Aquatic Sciences 1948: 36-100.

Washburne, R. Washburne's Table 2007 for use with Current Atlas Juan de Fuca Strait to Strait of Georgia. Canadian Hydrographic Service.

Washington Department of Ecology. 1995. Watershed Briefing Paper for the San Juan islands. Washington State Department of Ecology Ambient Monitoring Marine: 5-10.

Appendix
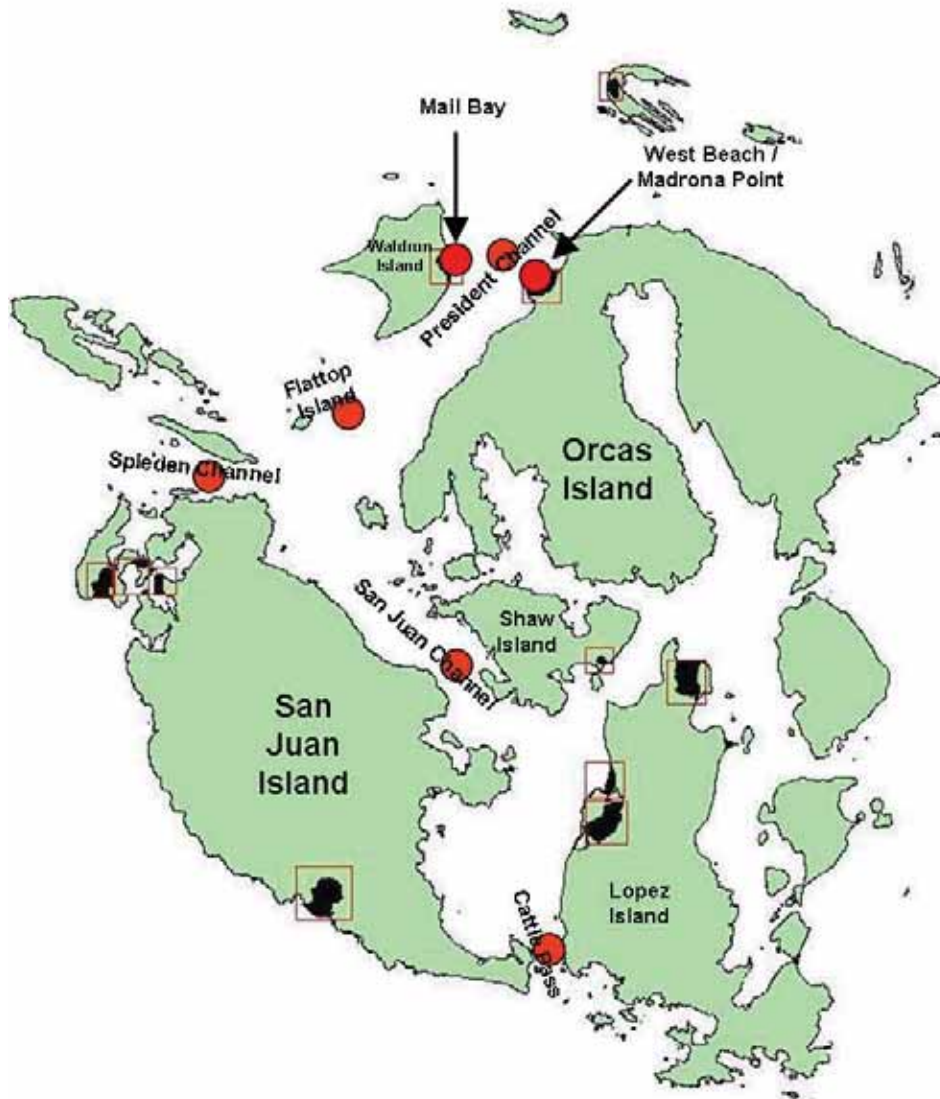
Figure 1: Seven study sites assessing differences in water parameters within the San Juan Archipelago.

Table 1: Water sampling sites listed generally north-to-south, with coordinates.

SITE NAME	LATITUDE	LONGITUDE
Mail Bay	48 42.120 N	123 00.299 W
President Channel	48 41.768 N	122 58.916 W
West Beach / Madrona Point	48 41.541 N	122 57.835 W
Flattop Island	48 38.710 N	123 03.631 W
Spieden Channel	48 37.634 N	123 07.265 W
San Juan Channel	48 33.518 N	122 59.966 W
Cattle Pass	48 28.293 N	122 57.119 W
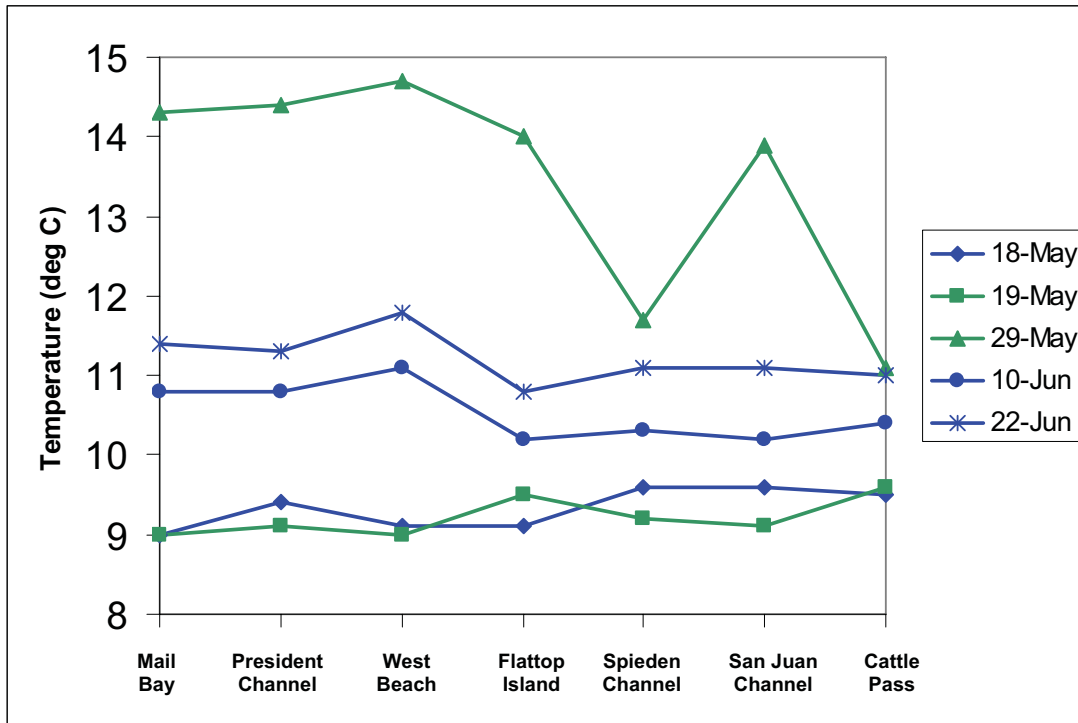
Figure 2: Surface temperatures, by station and date in late spring 2007. Ebb and low tide sample series are green, flood and high tide series are blue.
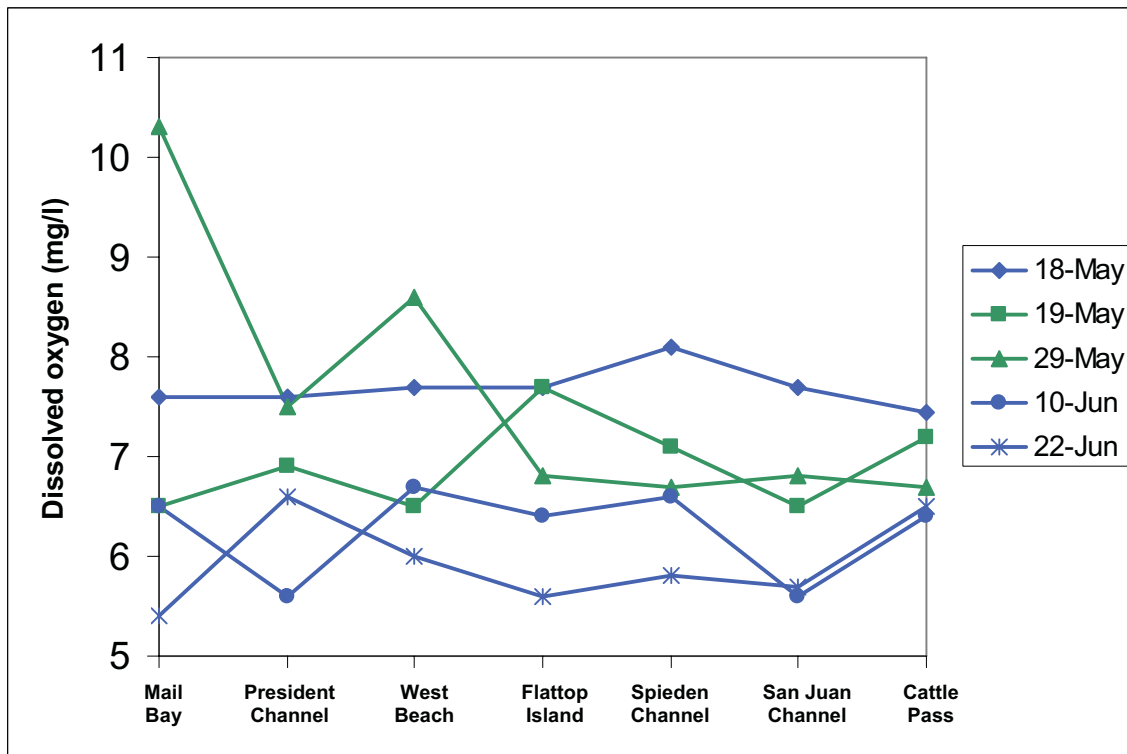
Figure 3: Surface dissolved oxygen concentrations, by station and date in late spring 2007. Ebb and low tide sample series are green, flood and high tide series are blue.
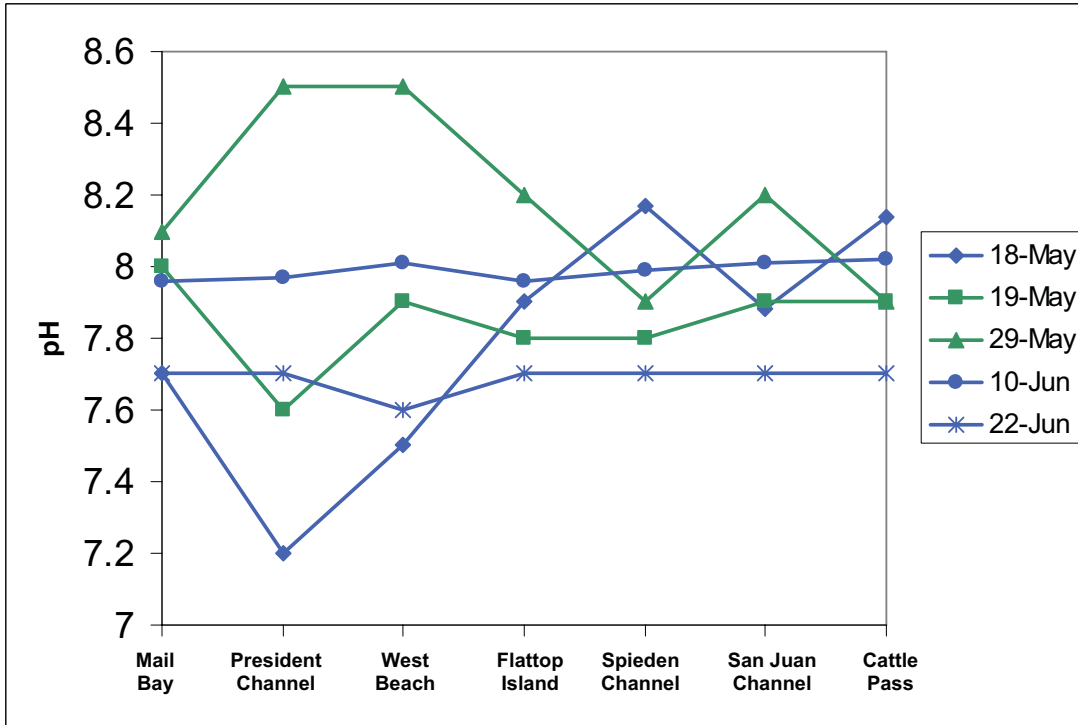
Figure 4: Surface pH, by station and date in late spring 2007. Ebb and low tide sample series are green, flood and high tide series are blue.
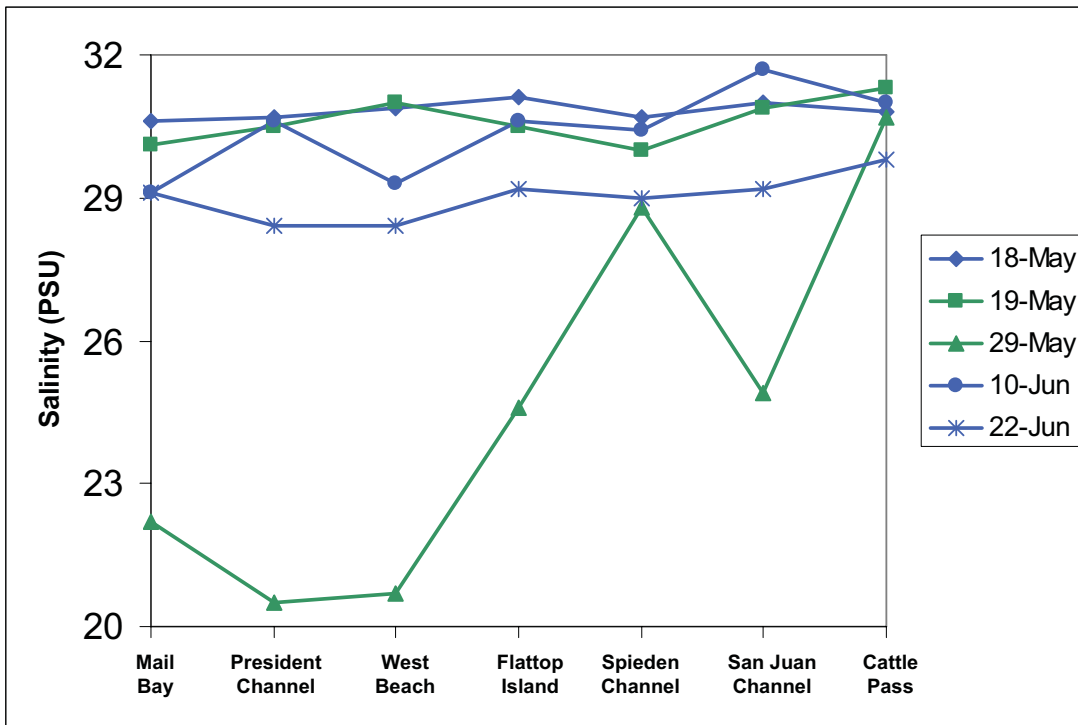
Figure 5: Surface salinities, by station and date in late spring 2007. Ebb and low tide sample series are green, flood and high tide series are blue.
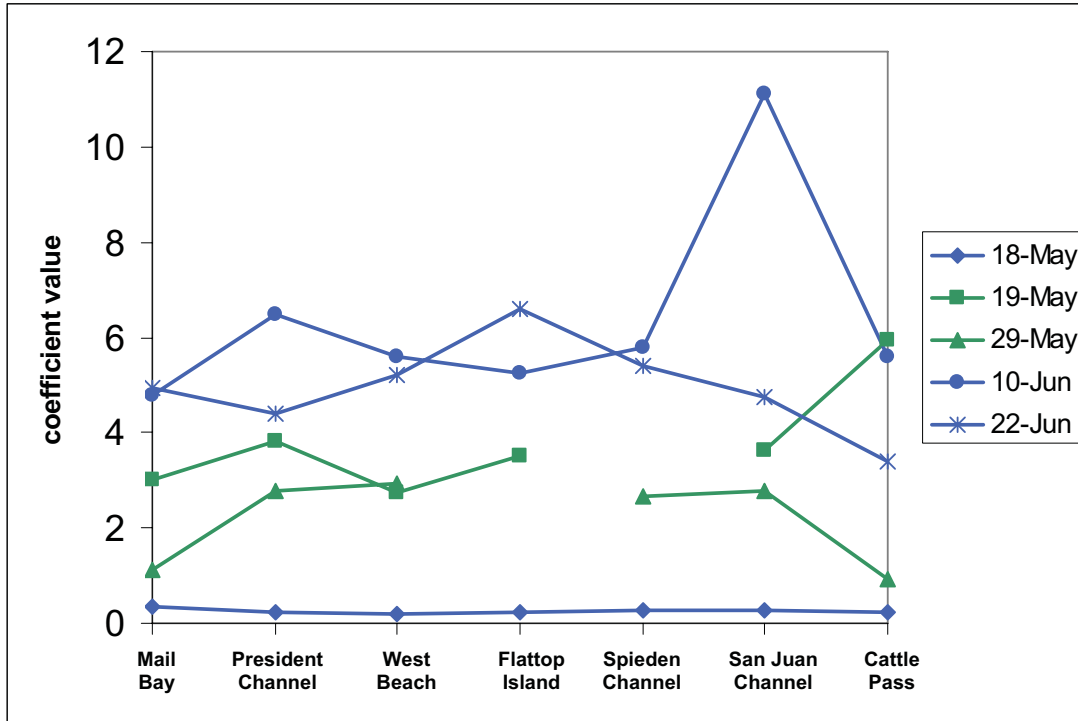
Figure 6: Light attenuation with depth, by station and date in late spring 2007. Ebb and low tide sample series are green, flood and high tide series are blue.
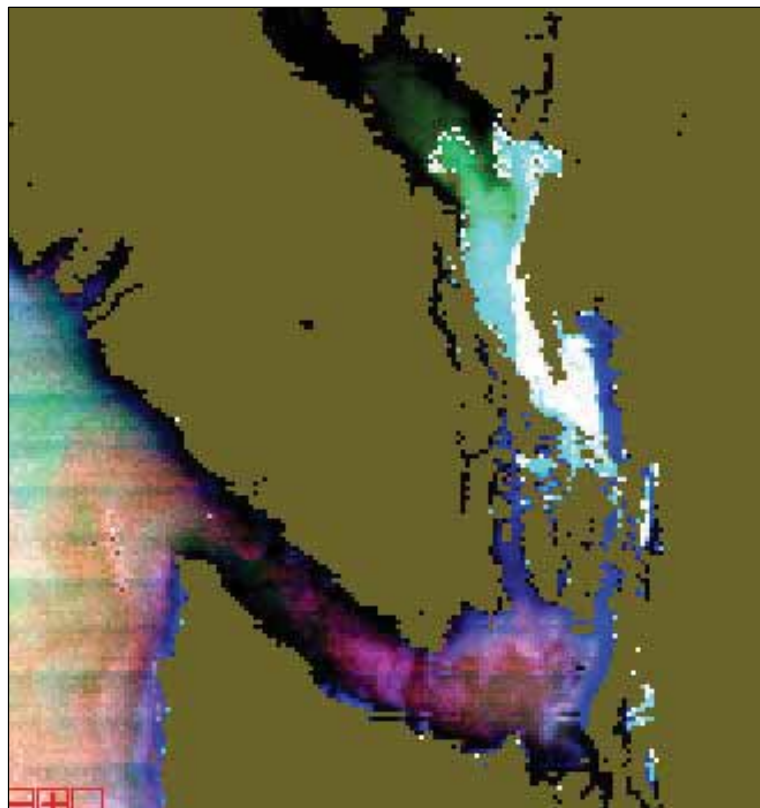
Figure 7: May 10 satellite image of reflectance intensity, revealing Fraser River waters in aqua and white. (Courtesy of Miles Logdson, University of Washington Oceanography)
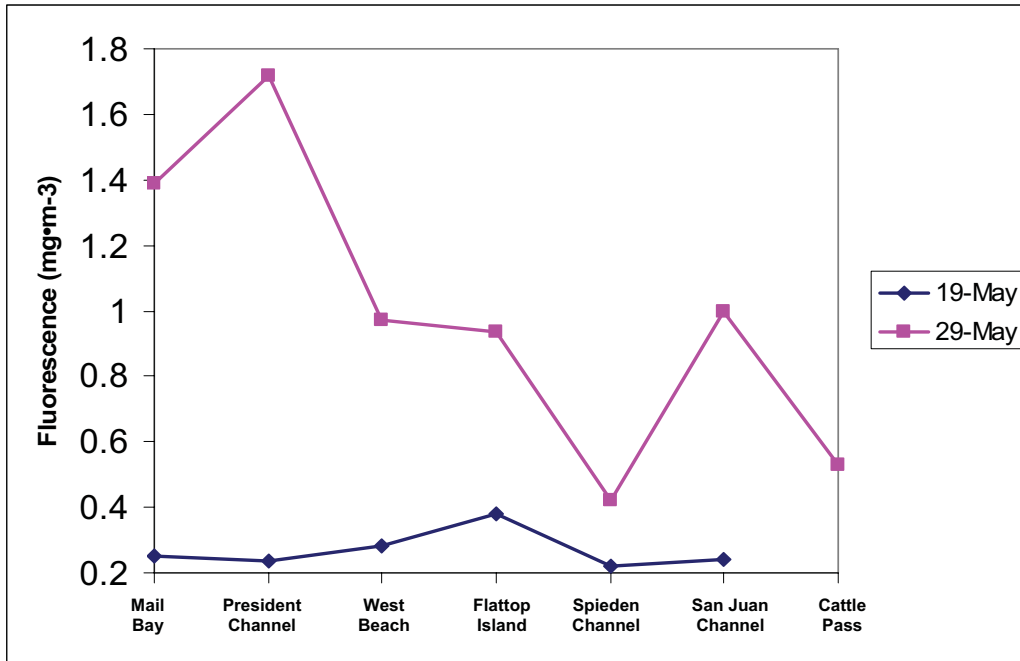
Figure 8: Chlorophyll concentration on the surface, by station and tidal series in late May 2007. Both May 19 and 29 were sampled on ebb tides. Only one fluorescence measurement was taken at Cattle Pass.
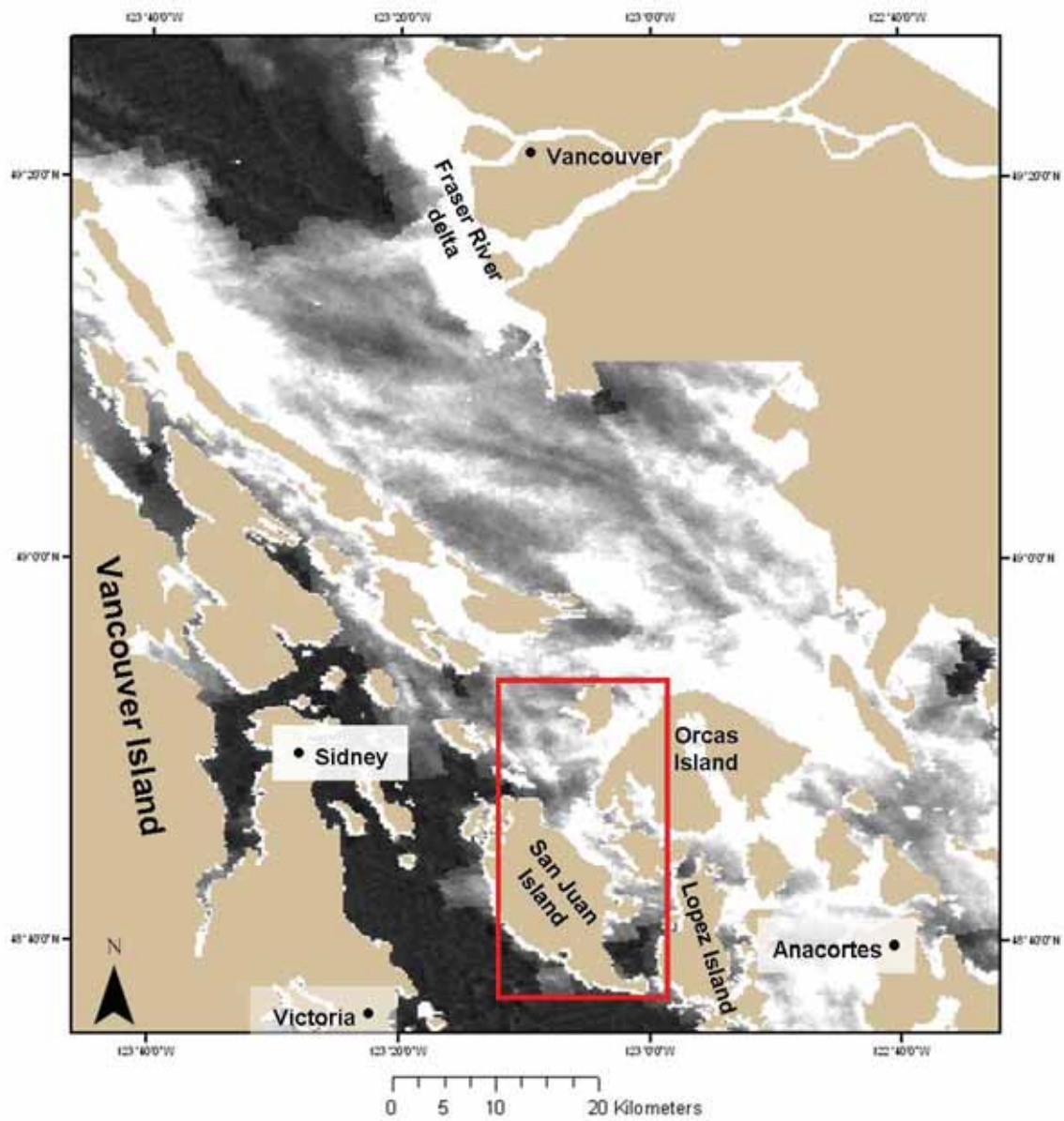
Figure 9: Map of <u>infrared</u> wavelength reflectance of Fraser River plume at 250 m resolution, with higher reflectance in white, lower in black. Ground sampling area boxed in red. Satellite data acquired for 29 May 2007 by MODIS Aqua satellite, image prepared by University of Washington Spatial Analysis Lab.
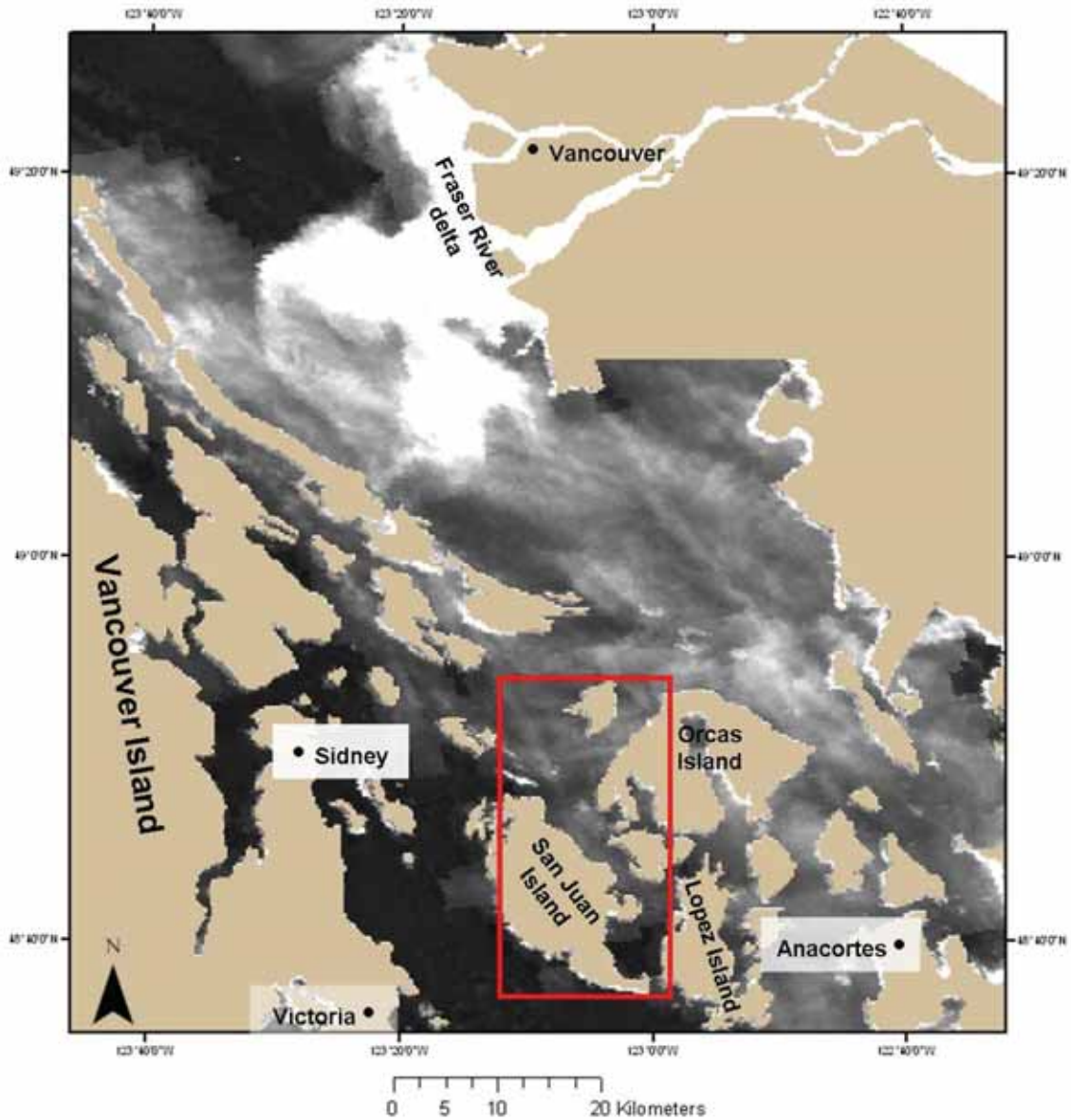
Figure 10: Map of <u>red</u> wavelength reflectance of Fraser River plume at 250 m resolution, with higher reflectance in white, lower in black. Ground sampling area boxed in red. Satellite data acquired for 29 May 2007 by MODIS Aqua satellite, image prepared by University of Washington Spatial Analysis Lab.
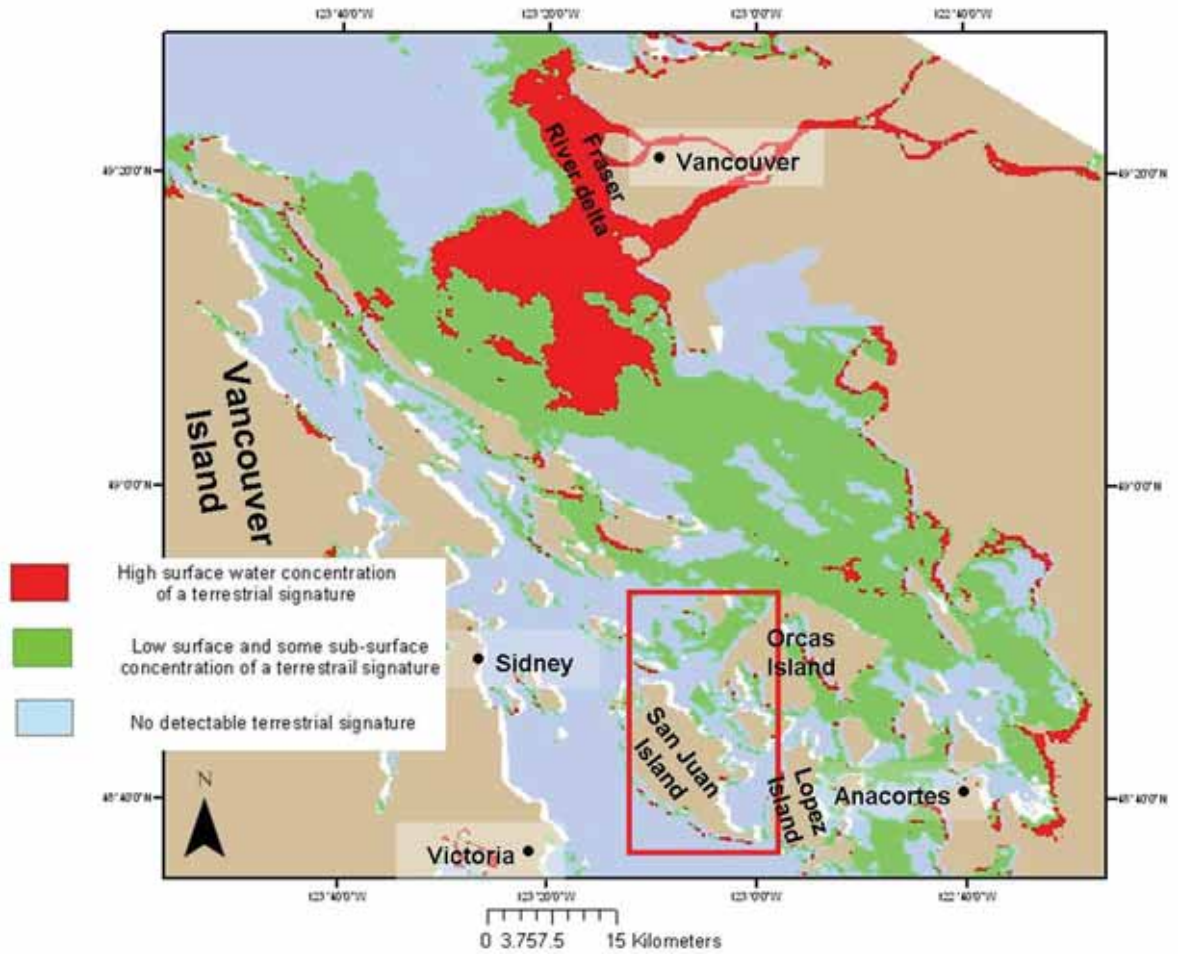
Figure 11: Map of terrestrial signature of Fraser River plume at 250 m resolution. Ground sampling area boxed in red. Satellite data acquired for 29 May 2007 by MODIS Aqua satellite, image prepared by University of Washington Spatial Analysis Lab.
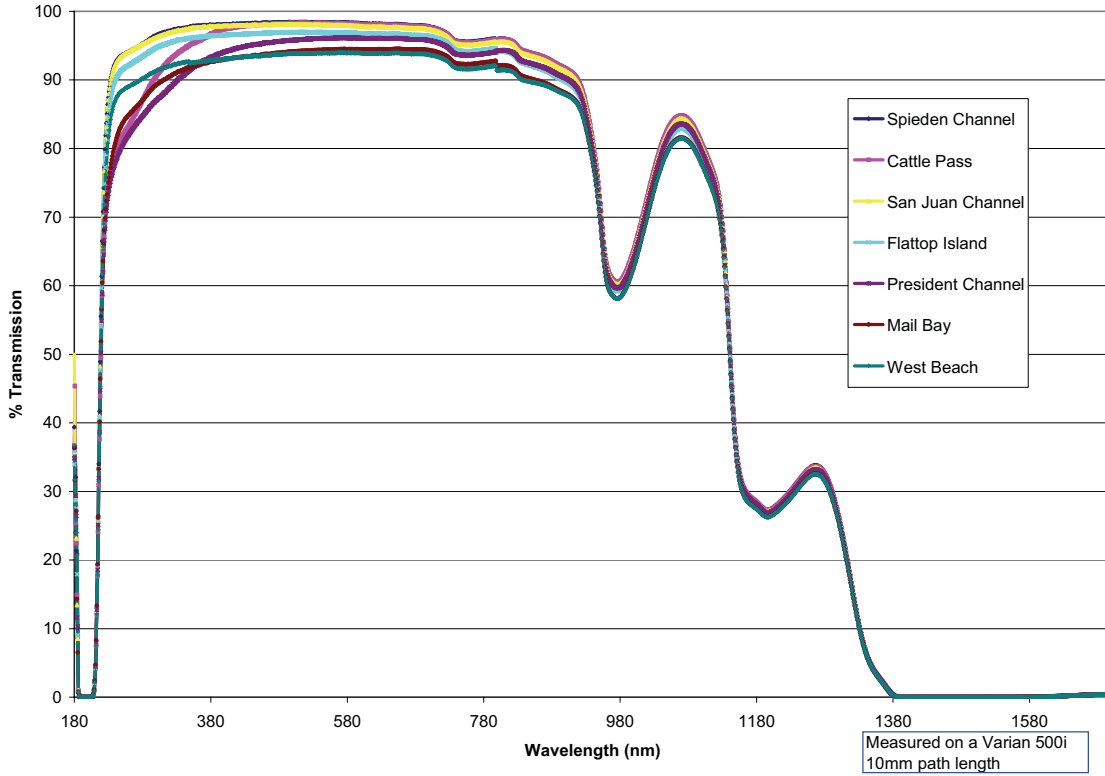
Figure 12: Broad-scale transmission profile of surface water from seven study sites on 18 May.
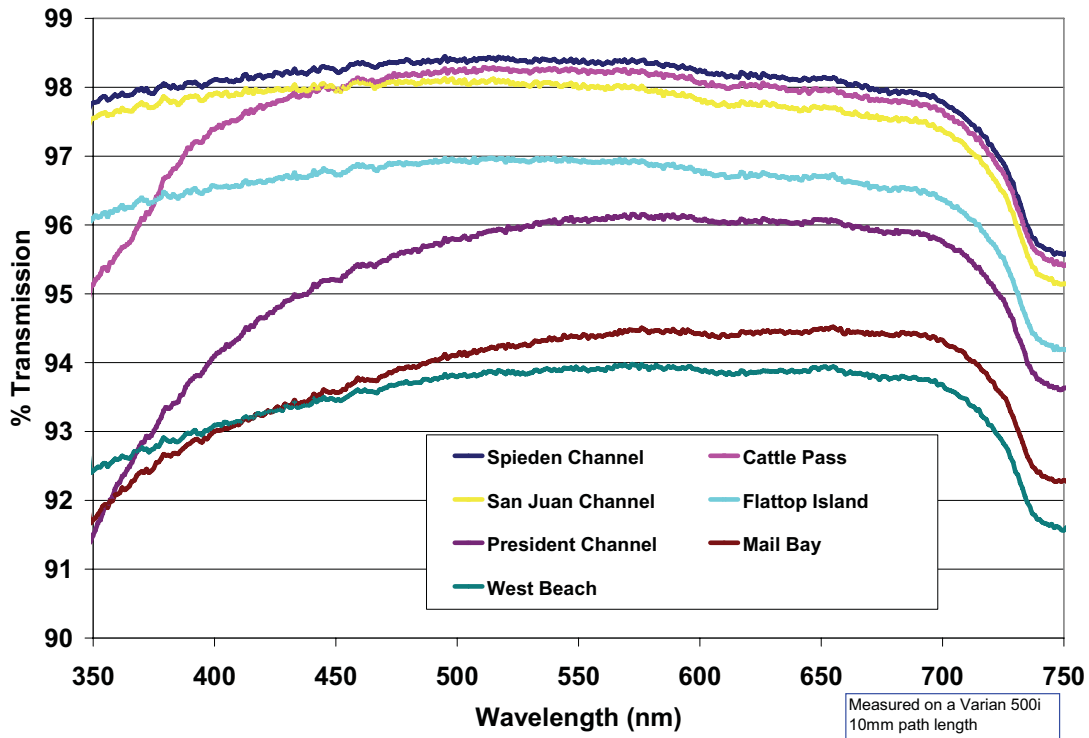
Figure 13: Transmission of surface water collected from study sites on <u>May 18</u>.
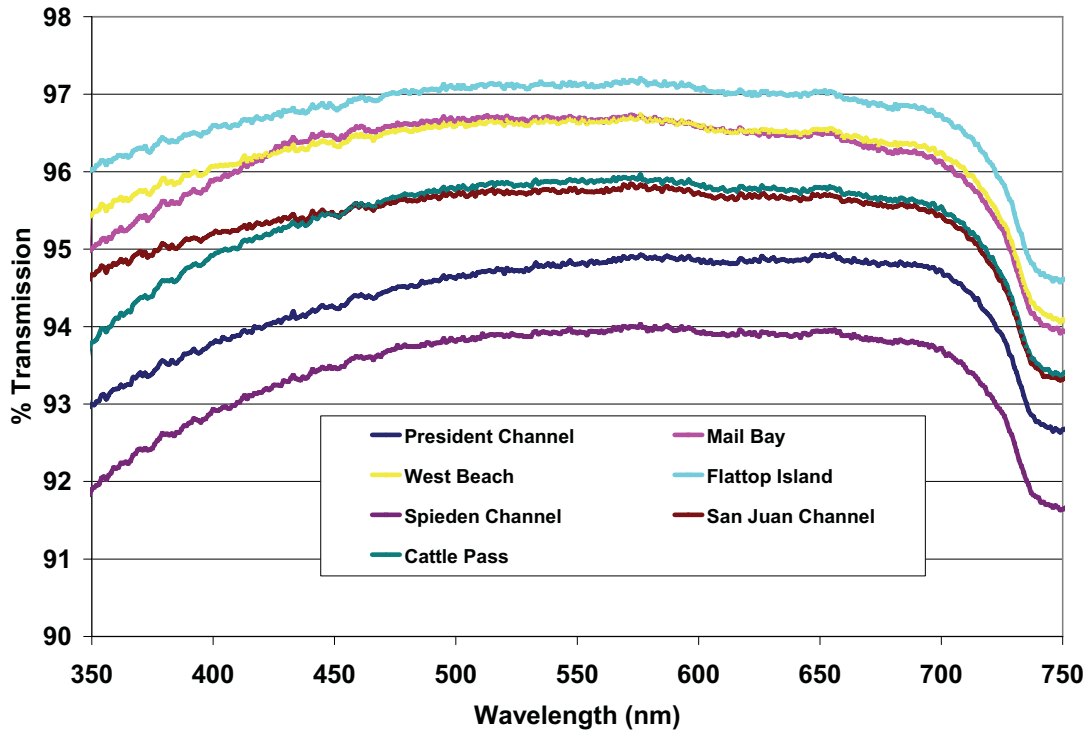
Figure 14: Transmission of surface water collected from study sites on <u>May 19</u>.

Measured on a Varian 500i
10mm path length
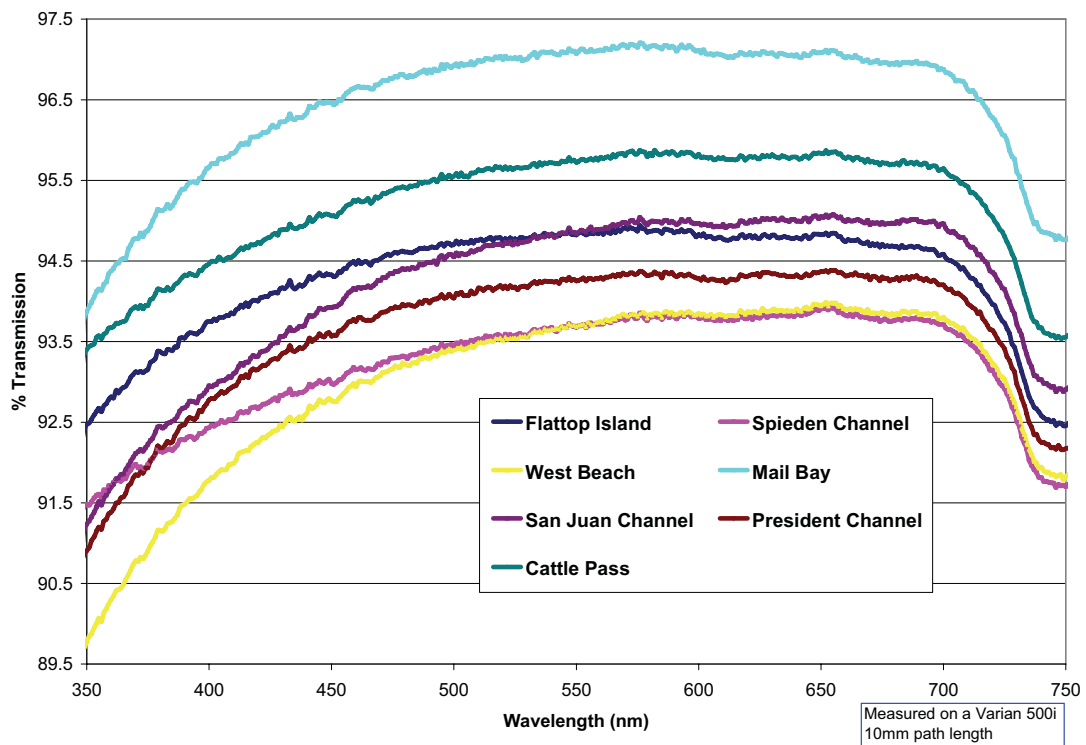
Figure 15: Transmission of surface water collected from study sites on <u>May 29</u>.
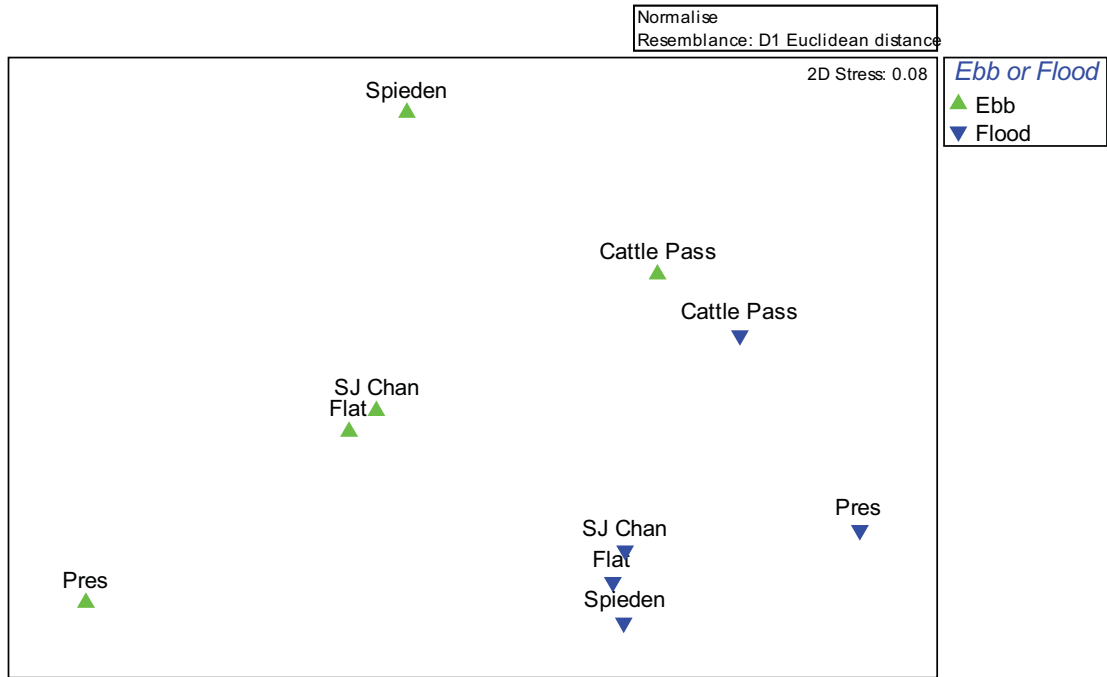
Figure 16: Non-metric multidimensional scaling graph of the 6 physical water column parameters measured at 5 sites on 18 May (flood tide) and 29 May (ebb tide). Closer points indicate greater similarity of all the physical parameters. Ebb and Flood points are significantly separated (Global R test, p = 0.008).

10 Genetic Structure and Diversity of *Zostera marina* in the San Juan Archipalago and Hood Canal, Puget Sound, Washington

Jolene Rearick and Sandra Talbot
Alaska Science Center
U.S. Geological Survey

Sandy Wyllie-Echeverria
Friday Harbor Laboratories
University of Washington

Pete Dowty
Washington State Department of Natural Resources

Executive Summary

We examined genetic characteristics of eelgrass in eight populations in the San Juan Archipelago (SJA), and six populations in Hood Canal (HC), of Puget Sound, Washington, using eight variable nuclear microsatellite loci. Puget Sound populations included Bell Point, Wescott Bay, (BPWB), Mosquito Pass, Wescott Bay (MPWB), Fisherman's Bay, Inner (FBI), Fisherman's Bay, Outer (FBO), Shoal Bay (SHB), Shallow Bay (SB), False Bay (FAL), and Picnic Cove (W) in San Juan Archipelago, and core004 (CORE), hdc2344 (A2344), hdc2359 (B2359), hdc2386 (C2386), hdc2465 (D2465), and hdc2468 (E2468) in Hood Canal. The genetic data were evaluated to address the following questions: 1) Are there differences in the level of genetic diversity, and clonality, in populations characterizing the two regions (SJA and HC)? 2) Is the level and type of variation similar to levels found in other populations along the North Pacific Coast? 3) What is the connectivity between populations in the SJA, and those in HC? 4) Is there population substructuring within the two regions? Aside from providing baseline information useful for assessing the genetic characteristics and health of eelgrass populations in Puget Sound, these data will help elucidate patterns and mechanisms of dispersal among eelgrass populations in the Sound and elsewhere along the north Pacific coast of North America.

Such data are valuable when considering source populations in efforts to re-establish eelgrass beds in areas where they have declined or been decimated, and when attempting to predict the impact of global change.

Genetic Diversity and Clonality

We assessed both levels of genetic diversity and levels of clonality in each of the 14 populations. Levels of genetic diversity are based on analyses of genets (genetic individuals) only, whereas levels of clonality are assayed using all samples. It is possible that populations with high levels of clonality can also have high levels of genetic diversity among the genets representing the population.

Levels of genetic diversity. Levels of genetic diversity were estimated using three standard measures: 1) average number of alleles (A) at each locus, across loci; 2) expected heterozygosity (H_E, which in populations in Hardy-Weinberg equilibrium is not significantly different from observed heterozygosity, H_O); and 3) percent polymorphism (the percentage of polymorphic loci in the suite of loci examined). Values for A increase as sample sizes increase. Therefore, because the populations were represented by different numbers of genets, we substitute the value allelic richness (AR) for A. Allelic richness represents the same diversity measure as A, while also accounting for sample size disparities between populations.

Overall, SJA and HC showed similar levels of genetic diversity measured in terms of average allelic richness (2.74 and 2.73, respectively), and in terms of expected heterozygosity (0.43 for both populations). Average polymorphism, however, was lower overall in SJA. Among populations, genetic diversity was highly variable. The average number of alleles was highest in SJA, and both the lowest and the highest allelic richness values were found within different SJA populations (BPWB and SB), respectively). However, although overall expected heterozygosity values were the same between the regions, the highest heterozygosity value among populations was observed within a population in HC (E2468). The highest percent polymorphism (1.0) was also observed within five of the six of the HC populations, but none of the SJA populations were polymorphic at all loci.

130

The three measures of genetic diversity (number of alleles or allelic richness, heterozygosity and polymorphism) are correlated, but can show contradictory patterns, in many cases due to differences in recent demographic dynamics characterizing the populations. In particular, recent deviations from equilibrium can affect different genetic diversity values disparately. For example, in cases where populations are experiencing a rapid expansion, numbers of alleles exceeds numbers expected under mutation-drift equilibrium, relative to heterozygosity values. On the other hand, in populations experiencing a rapid decrease in population size, expected heterozygosity will exceed values expected under mutation-drift equilibrium, given the numbers of alleles present. However, polymorphism may not be seriously impacted by demographic fluctuations except in extreme and prolonged bottlenecks. Since each population behaves independently within regions, comparing genetic diversity at the regional level only may conceal population-level dynamics. Thus, levels of genetic diversity at both the populational and regional level should be examined to understand trends in the target populations.

We used these concepts to examine genetic signatures of demographic fluctuations. With three exceptions (two populations in SJA and one in HC, each demonstrating a signature consistent with recent population expansion), the populations appeared to be demographically stable. We note that extremely recent demographic fluctuations (e.g., those that occurred within the current and last generation) cannot be detected using these genetic methods.

Levels of clonality. Levels of clonality were estimated using match statistics and the value *genotypic richness* (R). Populations composed solely of genets have genotypic richness values of 1.0 (and 0.0% clonality). Lower genotypic richness values indicate higher levels of clonality.

Based on match statistics, two hundred and forty-seven of the 365 samples collected in San Juan Archipelago shared identical genotypes with at least one other sample and are presumed to be clones. Similarly, in HC, 27 individuals among the 180 samples collected shared identical genotypes with at least one other sample. Lower genotypic richness values in SJA populations sampled in 2006 demonstrate higher levels

of clonality in these populations than in Picnic Cove (SJA, sampled in 2000) and HC populations. We uncovered no instances of interpopulational clonality. Lower probability-of-identity values indicate higher confidence in our ability to identify clones within a population. Average probability of identity values estimated for these populations are reasonably low across Puget Sound, though values were higher in some populations. Therefore, we may be overestimating the level of clonality within those populations. These populations include Bell Point, Wescott Bay and Picnic Cove.

The differences in estimated levels of clonality between the two regions may in part be due to differences in sample collection interval. In 2006, samples from the SJA were collected at 2m intervals. However, samples collected in HC in 2006, and in Picnic Cove (SJA) in 2000, were sampled at 3 – 4 m intervals. Since sampling at closer intervals increases the likelihood of sampling ramets, it is possible that the lower levels of clonality estimated for the HC and Picnic Cove populations can be attributed in part due to sampling bias. This was tested using sample interval simulations within these populations.

Genotypic richness values (clonality) between the two areas were directly compared by simulating genetic identity of samples as if they were based on the same sampling interval. The simulation was done by selecting samples collected every 10 and 18m, and calculating genotypic richness values using only those samples. Based on these simulations, genotypic richness values overall were still lower (and thus clonality was estimated to be higher) in SJA. However, in this simulation, two populations within SJA (SB and FAL), contain genotypic richness (clonality) levels that became more similar to those in HC populations. This supports the hypothesis that differences in sample interval affects estimates of clonality levels in these populations, but nevertheless shows that San Juan Archipelago populations generally contain lower genotypic richness, and therefore higher levels of clonality.

Levels of genetic diversity in populations of eelgrass in Puget Sound are, in general, similar to levels observed within populations in California (Crown Beach, San Francisco Bay), Oregon (Yaquina Bay), and Alaska (Alexander Archipelago in Southeastern Alaska, and Izembek Lagoon, on the Alaska Peninsula). The three measures of genetic diversity are midrange in Puget Sound relative to other North Pacific

132

populations. This research demonstrates that earlier findings of relatively low overall levels of genetic variation at neutral nuclear microsatellite markers in Puget Sound are representative of the North Pacific as a whole.

Levels of Differentiation and Substructuring[1]

We found significant genetic differentiation, among most populations between SJA and HC. This suggests substantial genetic substructuring (and restriction of homogenizing gene flow) among Puget Sound eelgrass populations. Genetic differentiation was measured using allelic goodness of fit tests of distribution of alleles, and F-statistics (variance in allele frequencies, the F_{ST}). Neighbor-joining analyses based on Cavalli-Sforza's genetic distances, also suggest substantial differences between San Juan Archipelago and Hood Canal. Although substructuring was observed within each of the two regions, SJA populations demonstrated greater levels of substructuring than HC populations. Comparison of R_{ST} and R_{ST} analyses suggest that processes associated with migration and drift are playing a role in the differentiation of populations within each region. However, within SJA, as well as between the two regions, these processes have been occurring for a time period sufficiently long that mutation is beginning to play a role in population and regional differentiation.

---

[1] substructuring here refers to a phenomenon whereby a region, or a population (by definition considered to be comprised of a single population of randomly interbreeding individuals), is actually comprised of two or more smaller "subpopulations" that are distinct.

Abstract

      We investigated the levels of genetic variation within and among, eelgrass

populations sampled from eight locales in the San Juan Archipelago, and six locales in

Hood Canal, Puget Sound, using data from eight autosomal microsatellite loci.

Populations within San Juan Archipelago had both the highest and lowest allelic richness,

ranging from a low of 2.31 in Bell Point, Wescott Bay, to a high of 3.05 in Shallow Bay.

Overall expected heterozygosity was similar between the two regions, 0.42 in San Juan

Archipelago and 0.43 in Hood Canal. However, expected heterozygosity (H_E) was lowest

in a San Juan Archipelago population (Bell Point, Wescott Bay, 0.31), and highest in a

Hood Canal population (hdc2468, 0.49). Two hundred and forty-seven samples collected

in San Juan Archipelago shared identical genotypes with at least one other sample and are

presumed to be clones; similarly, in Hood Canal, 27 individuals shared identical genotypes

with at least one other sample. Genotypic diversity (R) ranged from 0.08 in Fisherman's

Bay, Inner, San Juan Archipelago to 0.93 in hdc2468, Hood Canal. Between the two

regions, Hood Canal was found to have more than two times greater genotypic diversity

among all populations than San Juan Archipelago (0.85 Hood Canal, 0.32 San Juan

Archipelago). We uncovered no instances of interpopulational clonality. Although

average estimated probability of identity values estimated for populations comprised of

closely-related individuals ($P_{(ID)sib}$) is reasonably low across Puget Sound populations, the

values were higher in some populations (> 0.02). Therefore, we may be overestimating the

level of clonality within some populations. We found significant genetic differentiation,

measured using allelic goodness of fit tests of distribution of alleles, and f-statistics

(variance in allele frequencies, the F_{ST}), among most populations within and between the

134

two areas (San Juan Archipelago and Hood Canal); this suggests substantial genetic

substructuring within Puget Sound eelgrass populations. Neighbor-joining analyses based

on Cavalli-Sforza's genetic distances, also suggest substantial differences between San

Juan Archipelago and Hood Canal. Levels of genetic diversity in populations of eelgrass

in Puget Sound are, in general, similar to levels observed within populations in California,

Oregon, and Alaska.

Introduction

Seagrass beds form one of the most widespread and productive coastal habitat

types in the world. They stabilize and enrich sediments and provide critical food resources

and habitat for a variety of waterbirds and marine organisms. Eelgrass (*Zostera marina* L.)

is a seagrass adapted to the cold waters of the North Atlantic and North Pacific. In the last

30 years, there has been a dramatic decline in seagrasses worldwide (Short and Wyllie-

Echeverria 1996). Losses have been especially severe in temperate waters where eelgrass

is the dominant seagrass species (den Hartog and Polderman 1975, Orth and Moore 1983,

Valiela and Costa 1988).

Along the Pacific coastline of Washington eelgrass meadows occur within shallow

bay habitats, to some extent, in all of the larger bays and estuaries, including the San Juan

Archipelago and Hood Canal. These areas have been greatly impacted by increasing

human development. While the subsistence of healthy eelgrass beds is critical for

maintaining an ecological equilibrium in coastal environments, there are no studies

characterizing the population genetic substructuring of *Z. marina* meadows in Puget

Sound, and studies of other North Pacific Coast populations are not yet published (Talbot

et al. unpublished data). However, studies characterizing more southerly North Pacific populations as well as Atlantic coast populations, using the same suite of autosomal DNA microsatellite loci, suggest eelgrass populations demonstrate a wide range of genotypic diversity, with levels of diversity ranging from complete monoclonality to maximal diversity (Reusch *et al.* 1999, Reusch *et al.* 2000, Muñiz *et al.* 2005, 2006).

These disparate results from these other populations are counter to expectation for a sessile marine organism, such as eelgrass, that disperses seeds in water over only short (1-10m) distances, even in high-current environments. Nevertheless, results from Atlantic coast populations (Reusch *et al.* 1999, Olsen *et al.* 2004), and results from 19 Pacific Coast populations (Muñiz-Salazar *et al.* 2005, 2006; Talbot *et al.* in prep.), using 9-10 autosomal microsatellite loci, indicate many or most perennial eelgrass populations examined display pronounced subdivision, even within lagoons. This suggests perennial populations along the eastern and western Atlantic coast and along the Pacific Coast of North America have evolved into locally-adapted subpopulations. This is expected, given the perennial habit of *Z. marina* along most of the north Pacific coast of North America, and the observation that movement of dislodged vegetative material is the only adaptation the fruits have for dispersal (den Hartog 1970, cited in Haynes 2000). The apparent lack of adaptation of eelgrass for dispersal, supported by the finding of pronounced subdivision of populations along the Pacific coast of North America, from Alaska to Baja California, has implications when assessing the impact of catastrophic anthropogenic or natural perturbations, or more long-term changes expected due to global change, in local *Z. marina* populations on the Pacific. The assessment of fine-scaled population differentiation also provides critical data

needed to design appropriate restoration programs along the Pacific coast, including Puget Sound.

DNA microsatellite loci have been used successfully to evaluate within- and among-genetic differences in annual and perennial populations of marine seagrasses (Procaccini *et al.* 2001), including *Z. marina* in Europe (Reusch *et al.* 1999, Reusch *et al.* 2000, Olsen *et al.* 2004), and the southern Pacific coast of North America (Muñiz-Salazar *et al.* 2005, 2006; Talbot *et al.*, in prep.). The objectives of this study are to use microsatellite data to: 1) compare levels of genetic variability (including levels of clonality) of eelgrass within and among populations representing two geographically separated areas within Puget Sound (the San Juan Archipelago, and Hood Canal); 2) determine the extent of population substructuring and relationships within and among these populations, and 3) seek genetic signatures of demographic change within these populations. Aside from providing baseline information useful for assessing the genetic characteristics and health of eelgrass populations in Puget Sound, these data will help elucidate patterns and mechanisms of dispersal among eelgrass populations in the Sound and elsewhere along the north Pacific coast of North America. Such data are valuable when considering source populations in efforts to re-establish eelgrass beds in areas where they have declined or been decimated, and when attempting to predict the impact of global change.

Materials and Methods

<u>Study Sites</u>

Eelgrass from beds occupying seven sites (hereafter called "populations") in the San Juan Archipelago (SJA), and six populations in Hood Canal (HC), Puget Sound, Washington were collected in the summer of 2006 (Figure 1; see Table 1 for population identifiers). One population in the SJA, W, was collected in the summer of 2000. Eelgrass samples were collected along a linear transect within each population. A sample was collected from a single individual at 30 – 50 sites along each transect, except in the case of W, where only 18 samples were collected. Samples were taken every two (SJA) or three (HC and W) meters, and GPS coordinates were recorded for all sites. Individual plants were selected haphazardly, and the healthiest shoot on the individual plant was collected. One leaf shoot was collected from each selected individual and a 5-cm fragment cut off and stored in 1.7mL microcentrifuge tubes containing powdered silica gel. Samples were sent to the Molecular Ecology Laboratory at the Alaska Science Center, USGS, Anchorage, Alaska, for genetic processing. Plants were prepared for DNA extraction immediately upon arrival.

<u>DNA Extraction and Microsatellite Genotyping</u>

Genomic DNA was extracted from approximately 0.02 to 0.04 g (dry weight) of leaf tissue using the CTAB/PVP (hexadecyltrimethylammonium bromide/polyvinylpyrrolidone) protocol described by Muñiz-Salazar *et al.* (2005). DNA samples were genotyped using eight microsatellite loci described by Reusch (2000) and Reusch *et al.* (1999, 2000). Loci used included Zmar (GA1, GA2, GA3, GA5, CT3,

CT17, CT19, and CT20). These loci are known to be polymorphic within other Pacific Coast populations (Muniz-Salazar *et al.* 2005, 2006; Talbot *et al.* in prep.), including Puget Sound. Microsatellite data were amplified and visualized as described by Muniz-Salazar *et al.* (2005), with protocols modified to allow for multiplexing of loci. For Quality Control and Quality Assurance purposes, we reamplified and reprocessed a minimum of 10% of individuals from each of the populations.

Verification of Species

Subtle morphological characteristics differentiate *Z. marina* and *Z. japonica*, which both occur along the coast of Washington, Oregon, and California (Haynes 2000, Susan McBride, California SeaGrant, pers. comm.). Preliminary data suggest only four (ZmarCT3, GA2, GA5 and CT 20) of the 12 microsatellite primer sets used in genetic studies of North American Pacific Coast *Z. marina* amplify a product *in Z. japonica* obtained from Boundary Bay, British Columbia, and Humboldt Bay, California (Talbot *et al.*, unpublished data). However, the extent of polymorphism at all eight loci used in this study has not been tested across North American populations of *Z. japonica*. Thus, using a quick fragment-based species screen developed in the Molecular Ecology Laboratory (Talbot, Rearick and Sage, unpublished data) we compared fragments for 2 individuals randomly selected from each locale in SJA and HC. Sizes of fragments were compared against fragments generated from a specimen of *Z. marina* vouchered at UAM and a specimen of *Z. japonica* from Boundary Bay (see Talbot *et al.* 2006).

Genetic Variability and Clonality

Probability of Identity. The probability of sampling identical genotypes in unrelated individuals was calculated based on theoretical equations which generally assume associations between alleles within and among loci based on random mating. Due to population substructuring (Muñiz-Salazar *et al.* 2005, Talbot *et al.* in prep.), and given the perennial mating system of eelgrass in most populations in the North Pacific, this is probably not a realistic assumption. Thus, it is important to select and use a suite of markers sufficiently variable to distinguish ramets (clones) from genets (individuals) with some level of confidence. To gain a more realistic assessment of the resolution of the markers used in this study, we assessed not only the probability of identity for a randomly-breeding population ($P_{(ID)}$), but also the probability of identity calculated under the assumption that the target population is comprised of first-order relatives ($P_{(ID)sib}$), for each of the populations. $P_{(ID)}$ is the probability that another individual with the same genotype would be observed, given the sample frequency of the alleles observed across loci, within a randomly breeding target population. $P_{(IDsib)}$ is the probability at which another individual with the same genotype would be observed, given the sample frequency of the alleles observed across loci, within a target population comprised entirely of first-order relatives. These values, particularly the $P_{(ID)sib}$, provide conservative bounds for the probability of observing identical multilocus genotypes between two (or more, for clones) individuals sampled from a population. General guidelines for identifying individuals using microsatellite loci suggest using a suite of markers that achieve a reasonably low $P_{(ID)}$ (bounded between 0.01 and 0.0001, Waits *et al.* 2001), will allow assessment of

confidence in estimating the number of clones in our sample. Tests of all loci for linkage

disequilibrium and conformation to Hardy-Weinberg equilibrium (HWE) expectations

were conducted before $P_{(ID)}$ was assessed (see below).

Clonality. After ascertaining the suite of eight loci used had sufficient

power to determine individuals, we assessed clonality by examining match statistics for

multilocus genotypes among samples, using Microsatellite Toolkit (Park 2000) and

GenClone ver. 1.0 (Arnaud-Haond and Belkir 2006). Here, a multilocus genotype (MLG)

is defined as any sample with a unique eight locus genotype, and is treated as equivalent to

a genet. Clonality is presumed between two or more samples, when each sample is

identical at all of the eight loci compared, and when the number of loci compared is > 6

(and includes the most polymorphic locus, CT-17; see results). Genotypic richness (R),

another measure of clonality, was also evaluated for each population in Genclone

(Appendix I). Genotypic richness was calculated as in Dorken and Eckert (2001).

Populations with a genotypic richness value of 1.0 are composed solely of genets, and have

0.0% clonality. Lower genotypic richness values indicate higher levels of clonality.

Multilocus genotypes were mapped along transects for each population in HC, and

for seven in SJA, using GenClone. Picnic Cove (W), SJA, is excluded from this analysis

due to lack of specific UTM readings for individual samples. Samples within populations

sharing the same MLG are represented graphically by a number assigned to the MLG by

Genclone. MLG numbers assigned to one population are not transferable to other

populations. For example, an MLG assigned as "2" in one population does not have the

same mulitlocus genotype as an MLG assigned as "2" in another population. For ease of

interpretation, prior to mapping the spatial distribution of MLGs, samples were pooled and

grouped by site, region, and overall, and the lowest northings and eastings were subtracted from the northings and eastings of all samples.

All but one of any set of samples that matched at all eight loci (presumably clones), were eliminated from any subsequent population-level analyses following clonality analyses.

Hardy-Weinberg Equilibrium and Linkage Disequilibrium. Microsatellite loci were tested for gametic phase genotypic disequilibrium (for all two-locus comparisons) and for deviations from Hardy-Weinberg Equilibrium (HWE) (for each locus and for each population overall), using the Fisher's Exact Test in GENEPOP 3.2a (Raymond and Rousset 1995). All *p*-values were adjusted for number of statistical tests (Sokal and Rohlf 1997), and we set an *a priori* condition that any loci found to be significantly linked across populations would be excluded from subsequent population-level analyses requiring adherence to HWE expectations.

Genetic Diversity. We estimated observed (H_O) and expected (H_E) heterozygosity (unbiased, Nei 1987), mean number of alleles per locus (A) and allele size variance, using Microsatellite Toolkit (Park 2000). For comparative purposes, we also estimated allelic richness, AR, which corrects A for disparity in sample sizes (El Mousadik and Petit 1996), using the program FSTAT Ver. 2.9.3.2 (Goudet 2002). Estimates of H_O and H_E were used to generate inbreeding coefficients (F = 1 - [H_O / H_E]) combined across loci for each and tested for significance as described in Li and Horovitz (1953). To determine the resolution of the markers for assessment of clonality we estimated $P_{(ID)}$ and $P_{(ID)sib}$ (see above, Waits *et al.* 2001) using GIMLET (Valière 2002).

Population Substructuring and Relationships

Gene frequencies were estimated for each microsatellite locus. Levels of population structuring were assessed using two standard indices of population differentiation: allelic goodness-of-fit, and F-statistics (in this case, the F_{ST}) F_{ST} estimators (including analogs) and allelic goodness of fit tests are more powerful than genotypic goodness-of-fit tests, and, when sample sizes are unequal, allelic goodness-of-fit tests are the most powerful (Goudet *et al.* 1996).

Allelic Goodness-of-fit Tests of Population Differentiation. Significance of heterogeneity in the distribution of alleles was assessed using GENEPOP Ver. 3.3, using 5000 replicates, as described in Raymond and Rousset (1995). Replications were based on a Markov chain adaptation of row-by-column contingency tables, as generated by GENEPOP. Multiple test significance was judged using Fisher's exact test method and/or by applying sequential Bonferroni procedures (Rice 1989).

F-statistics tests of Population Differentiation. Significance of spatial variation in frequency of alleles was assessed using F-statistics (Weir and Cockerham 1984). These measures can be viewed simply as variance components, and they describe the apportionment of allelic variance among individuals within populations (F_{IS}) and among populations (F_{ST}). Values of F_{ST} are summary statistics describing the extent of spatial variation among populations or population groupings, and range from 0.0 to 1.0. A value of 1.0 at a specific locus would imply that all populations are "fixed" for different alleles (i.e., the total variance at that locus is segregating among populations). On the other extreme, a value of 0.0 implies all populations share the same alleles in equal frequency. Global multilocus estimates of F_{ST}, θ, were obtained using the program FSTAT (Ver.

2.9.3.2, Goudet 2002), with significance assessed using confidence intervals. Estimates of

interpopulational variance (θ_{ST}) were derived using the program ARLEQUIN 3.1.

(Schneider et al. 1997). Significance of θ_{ST} values were based on permutation tests (n =

1000), whereby alleles were randomly permuted between the two populations compared.

A significant θ_{ST} value implies that a significant portion of the total genomic variation of

the specific locus is partitioned among the populations.

      F_{ST} values assume adherence to the infinite allele model (IAM) of mutational

change (Maruyama and Fuerst 1985). We also calculated R_{ST} (ρ) an analogue of F_{ST}

(Michalakis and Excoffier 1996) which assumes a stepwise mutation model (SMM) that is

derived from variances in mean allele size and frequency in relation to sample size, and is

seen as a more conservative distance measure relative to F_{ST} (Slatkin 1995). Statistical

significance of ρ was tested in the same manner as θ, described above. For both tests, p-

values were adjusted using Bonferroni corrections (Sokal and Rohlf 1997).

      Hierarchical Analysis of Variance. We also used analysis of molecular

variance (AMOVA; Excoffier *et al.* 1992) to further test for significance of geographic

partitioning among SJA and HC populations. AMOVA is a hierarchical analysis of

variance analogous to an analysis of variance (ANOVA) in which correlations among

genotype distances at various levels are used as *F*-statistic analogues (θ-statistics for

microsatellite loci). We estimated partitioning of allele frequencies within and across

populations and regions using both hierarchical F-statistics (Weir 1996) and R-statistics,

using the program ARLEQUIN. Significance of partitioning of genetic variance within

individuals (*F*), among individuals within populations (*f*), among populations (θ_s or ρ_s) and

between regions (θ_p or ρ_p), was evaluated based on 95% confidence intervals determined

144

by bootstrapping across loci. Nominal alpha levels were adjusted for multiple comparisons (Manly 1985). Estimates were made with AMOVA, weighting the allele frequencies using molecular information under the infinite alleles model of evolution (IAM; Maruyama and Fuerst 1985, for calculation of θ) and the stepwise mutation model (SMM; Ohta and Kimura 1973, Freimer and Slatkin 1996; Jarne and Lagoda 1996, for calculation of ρ), or based with ANOVA, based on frequencies alone.

Estimation of Gene Flow. To evaluate gene flow between populations, we obtained indirect theoretical gene flow estimates (number of effective migrants per generation, Nm), based on microsatellite data, using the private allele model (Barton and Slatkin 1986) for all population pairs. Values were obtained using GenePop 3.3 (Raymond and Rousset 1995).

Genetic Distance and Relationships Between Populations. Genetic distances among populations were estimated with Cavalli-Sforza and Edwards (1967) distance (D$_{CE}$). A graphical representation of the distance matrix illustrating relationships among the populations, was constructed with the neighbor-joining (Saitou and Nei 1987) algorithm using a program written by J. Cornuet (INRA, Laboratoire de Neurobiologie Comparee des Invertebres, Bures-sur Yvette, France). Statistical confidence for topology was assessed by bootstrapping (2000 repetitions).

We carried out a principle component analysis (PCA) using PCA-GEN Version 1.2.1 (Goudet 1999) to describe the geographic clustering of populations. This analysis uses allele frequencies to define new variables (components) that summarize the variance among populations. Significance of each component was tested using permutation tests (5000 randomizations).

Population Demography

Populations that experience a recent reduction of effective population size, such as during a founder event, are expected to show a reduction in both number of alleles and levels of heterozygosity at polymorphic loci (Watterson 1984). However, allelic diversity is reduced much more rapidly than levels of heterozygosity (Nei *et al.* 1975, Denniston 1978, Maruyama and Fuerst 1985), observed heterozygosity being larger than expected if the population was at mutation-drift equilibrium. The converse is also true; for populations that have expanded due to an influx of new alleles from another population, allelic diversity is increased more rapidly than levels of heterozgyosity (Luikart and Cornuet 1998). We used two statistical tests, the sign test and the Wilcoxon test, to detect an excess or deficit of heterozygosity (relative to number of alleles) for polymorphic microsatellite loci as an indicator of recent bottlenecks or expansions in each population (Cornuet and Luikart 1996). The sign test determines if the proportion of loci with heterozygosity excess is significantly larger or smaller than expected at equilibrium, and the Wilcoxon test determines if the average of standardized differences between observed and expected heterozygosity is significantly different from zero. These two statistical tests detect recent bottlenecks or expansions using heterozygosity and allele frequency data for each of several loci, and require no data on historical population sizes or levels of genetic variation.

Tests were conducted using the program BOTTLENECK (Cornuet and Luikart 1996, Luikart and Cornuet 1998), under three models thought to represent the range of possible mutation modes generating polymorphism at microsatellite loci. These include

the IAM, the SMM, and the two-phase model (TPM, see DiRienzo *et al.* 1994) of

microsatellite mutation. Parameters for the TPM were set at 88% single step mutations,

with a variance of 9 (Piry *et al.* 1999, Garza and Williamson 2001). One thousand

simulations were performed for each population.

Results

Microsatellite Analyses

We extracted genomic DNA and collected microsatellite fragment data from eight

loci in 30 to 50 individual samples representing each population within HC and seven

populations within SJA (Appendix I). One SJA population, W, is represented by 17

samples. In all, a total of 545 individual samples were genotyped at each of the eight loci

(Appendix I). We obtained eight-locus genotypes for 544 of the 545 individuals; one

individual is characterized by seven loci. One sample from SHB, a SJA population, was

removed from analyses due to the presence of multiple banding patterns at one of the

microsatellite loci.

Verification of Species

All SJA and HC samples characterized using the 5.8S rRNA/ITS-1 and ITS-2 gene

screen were consistent with *Z. marina* sampled from southeastern and Wide Bay, Alaska,

and Yaquina Bay, Oregon, and inconsistent with fragment sizes generated using *Z.*

japonica samples obtained from Boundary Bay (data not shown).

<u>Statistical Analyses</u>

Estimation of Clonality and Mapping of Clones

Probability of Identity. The eight-locus genotype has sufficient variation
that it can distinguish a single individual from among over 160,000 individuals (observed
probability of identity ($P_{ID)}$ = 5.94E-06) in the pooled SJA and HC populations (Table 2).
The lowest $P_{(ID)}$ value occurred in SHB, allowing individual identification from among
over 6 million individuals (observed unbiased P_{ID} = 1.60E-07). The highest $P_{(ID)}$ value
occurred in the BPWB population, allowing individual identification from among almost
4,000 individuals (observed unbiased P_{ID} = 2.54E-04). Thus, given random breeding in
these populations, these eight markers alone provide sufficient variation to distinguish
among individuals and should have high power to identify clones.

Overall, $P_{(IDsib)}$ was approximately 0.0136 (Table 2). Therefore, our ability to
resolve clones within populations of eelgrass comprised of many closely related
individuals (a reasonable expectation, given the clonal and perennial nature of the species)
is reasonably high. However, among some populations, $P_{(IDsib)}$ was substantially higher.
For example, in BPWB, a specific eight-locus suite of loci is expected to be found in 1/14
individuals, given the population is comprised mostly of first-order relatives ($P_{(IDsib)}$ =
0.0723; Table 2). Thus, we caution that in some populations, we may be overestimating
the level of clonality using these markers. Inclusion of clones further increases $P_{(ID)}$ and
$P_{(IDsib)}$ values, decreasing the estimated resolution of these loci (See Appendix II).

Clonality. Table 3 displays the number of samples assumed to represent
clones. These samples were identified based on MLG assignment by GenClone analyses
and match statistics, employing our criterion whereby we identified clones as samples that

share all alleles at all loci compared, when the number of loci compared is > 6 (and includes the most polymorphic locus, CT-17).

Over 69% of samples from 2006 SJA populations were clones. W, the 2000 SJA population, differed in sample collection protocols from other SJA populations in both distance between samples (3m in W, 2m in all others), and collection year (2000 in W, 2006 in all others). Clones comprised only 29% of W, and 15% of HC. Overall genotypic richness was 0.30 in 2006 SJA populations, 0.69 in W, and 0.85 in HC populations. Genotypic richness ranged from 0.08 to 0.51 in 2006 SJA populations, and 0.76 to 0.93 in HC populations.

All but one representative of each MLG was removed from the dataset for population-level analyses (see below). Of 545 samples genotyped, 274 were removed (Table 3A). Two hundred forty-seven samples from SJA and 27 samples from HC were removed, with the final dataset for population genetics analyses (see below, and Table 3), comprising 271 MLGs.

Mapping of Clones. MLGs (and ramets) mapped along transects within each population are displayed as Appendix III. No clones were found to cross between populations or regions; thus, numbers on transects assigned to unique MLGs within one population do not refer to the same MLG in another population (Appendix III).

Samples sharing the same multilocus genotype (clones) were frequently adjacent within the sampling transect, as observed in the clone maps (Appendix III). Distances between samples differed in SJA and HC due to differences in sample collection. Obvious blank spaces between samples represent interruptions in collection due to areas lacking *Z.*

marina (D2465 and E2468, see Appendix III, L and M), or sample omission due to

multiple banding patterns (most likely, sample contamination) within a locus (SHB).

We generated clones maps for seven SJA populations (Appendix III A to G). Five

or fewer MLGs represented more than half the samples collected in five of these

populations. In many cases, a single MLG was represented in more than a quarter of the

samples in SJA populations. Shallow Bay (SB, Appendix III, F) and False Bay (FAL,

Appendix III, G), the exceptions, had the highest genotypic richness values in 2006 SJA

populations (0.46 and 0.51, respectively; see Appendix I). Though clones often occurred

adjacent on SJA transects, they also occurred varying distances from other samples

analyzed sharing the same MLG.

Clone maps were generated for all HC populations (Appendix III, H to M). No

single MLG in HC appeared more than four times within any transect, or represented more

than 15% of the overall population. In HC, the majority of clones occurred within

approximately 25m of one another. However, in population C2386 (Appendix III, K),

MLG 18 occurs only twice, more than 80m apart. Interrupted transects, D2465 and E2468

(Appendix III, L and M, respectively) were found to share no clones between the isolated

transect ends.

Tests of Linkage Disequilibrium and Deviation from Hardy-Weinberg Equilibrium

Hardy-Weinberg Equilibrium and Linkage Disequilibrium. The global test

for deviation from Hardy-Weinberg equilibrium (HWE) across populations and loci

revealed no significant departure from equilibrium overall. No deviation was observed

within any population after application of multiple-test (Bonferroni) adjustments ($\chi^2 =$

150.0, df = 116, $P = 0.019$; α = 0.00045; data not shown). F_{IS}, which detects heterozygote deficit within populations, showed no significant departure from zero in any population ($F_{IS} = -0.146 – 0.238$, $P > 0.0063$), suggesting a general lack of inbreeding.

The exact test for linkage disequilibrium for each population rejected the null hypothesis of independence in 18 of 282 (6.4%) possible locus-by-locus comparisons, slightly above the numbers expected spuriously (14.1 of 282). Populations demonstrating pairs of loci in disequilibrium included SHB, W, C2386 and E2468 (n = 1 comparison each), B2359 (n = 2 comparisons), and FBO, SB, and D2465 (n = 3 comparisons each). Fisher's exact test for each locus pair across all populations revealed no statistically significant overall association between loci (P > 0.00045). Since we observed no significant association of alleles within or between loci, all eight loci were retained for the following population genetics analyses.

Estimation of Genetic Diversity

Genetic diversity metrics are based on analyses using multilocus genotypes only to represent a population (Table 3). For comparative purposes, we performed the same diversity analyses with all samples, including clones (Appendix I).

All eight loci were polymorphic within Puget Sound, and all displayed low to moderate levels of genetic variability within all populations studied (Table 3, 4), except for CT17, which was characterized by high levels of polymorphism ($H_O = 0.78$ to 1.00; Table 4). Whereas in HC most populations exhibited 100% polymorphism across loci, all populations in SJA were monomorphic (fixed for only one allele) at one to four loci (Table 3, 4). Total number of alleles per locus ranged from 1 to 45 (data not shown); average

number of alleles was 13.38 (Table 3A). Mean number of alleles per population, A, across

all eight loci, ranged from 2.5 in FBI to 5.5 in B2359 (Table 3B). Allelic richness, AR,

which corrects for disparate sample sizes (Petit *et al.* 1998), suggests that SB is the richest

population examined, while BPWB had the lowest level of allelic richness (Table 3B).

Overall H_E was identical in the HC and SJA populations (Table 3A), although H_O was

higher in HC. Levels of heterozygosity (H_E) ranged from 0.31 in BPWB to 0.53 in E2468

(Table 3B). However, overall number of alleles (A) was higher in SJA than in HC. The

total number of alleles detected within a population per locus ranged from 1 to 19 (data not

shown). Overall, the SJA region possessed more private alleles (PA) than the HC region

(Table 3B). However, among populations, B2359 had the highest number of private

alleles (PA = 6; Table 3B).

Population Substructuring and Relationships

Allelic Goodness-of-fit Tests of Population Differentiation. Fisher's

combined test of independence across all loci showed significant differences in the

distribution of alleles across all populations (χ^2=infinity; df =16, *P* < 0.0001) and between

all populations across loci (χ^2 = 28.145 – infinity; df = 16, *P* < 0.0006), with the exception

of FBI and SHB (χ^2 = 25.34 –, *P* < 0.0314). Similarly, significant differences in the

distribution of genotypes across all populations (χ^2=infinity; df=16, *P* < 0.0001) was

observed. Pairwise population comparisons uncovered significant differences in the

distribution of alleles in 59% (54/91) of comparisons (Table 5). The majority of non-

significant comparisons (70%) involved within-area comparisons (HC, 10 comparisons;

SJA, 16 comparisons; Table 5). When clones are included in analyses, the number of

significant comparisons increases to over 91%; exceptions involve within-HC comparisons

(Appendix IV).

      F-statistics tests of Population Differentiation. Multilocus estimates of F_{ST}

(θ) and R_{ST} (ρ) showed large and highly significant genetic differentiation across

populations (0.128 and 0.380, respectively). Population pairwise comparisons uncovered

significant differences in the variance in allele frequency (θ_{ST}) between most (80/91: 88%)

of populations (Table 5). All non-significant comparisons involved comparisons among

populations within the two regions (HC, 6 comparisons; SJA, 5 comparisons; Table 5).

Pairwise calculations of ρ among populations uncovered fewer (51/91; 56%) significant

pairwise differences than for θ (Table 5). The highest θ_{ST} value was between FAL, SJA,

and D2465, HC, ($\theta_{ST} = 0.2674$, $P < 0.0001$, Table 5). The highest ρ value was between W,

SJA, and E2468, HC, ($\rho_{ST} = 0.7946$, $P < 0.0001$, Table 5). Values of ρ_{ST} were higher than

θ_{ST} values in all but twenty-seven pairwise comparisons (10 among populations within

SJA; 11 among populations within HC; six between populations between the two areas,

Table 5).

      Hierarchical Analysis of Variance. Results of hierarchical analysis of

molecular variance (AMOVA) of multilocus microsatellite data describe statistically

significant genetic structure at the regional level ($\theta_p = 0.131$, $P < 0.0001$), and among-

population level ($\theta_s = 0.061$, $P < 0.0001$), but not at the within-population level ($f = -$

0.03102, $P = 0.968$). Thus, most (13.1%) of the variance in allele frequency is partitioned

between SJA and HC, and a small portion (5.3%) is partitioned among populations within

the two regions. AMOVA based on ρ also found most of the variance partitioned at the

regional level ($\rho_c = 0.441$, $P < 0.0001$), but at much higher percentage (44.1%); significant

variance was also partitioned among populations within groups ($\theta_s = 0.097$, $P < 0.0001$).

Variance was not significantly partitioned among individuals within populations ($f = -$

0.023, $P = 0.665$). ANOVA analysis based on frequencies only were congruent with

AMOVA analyses, but fixation indices were lower ($F_{CT} = 0.002$, $P < 0.002$; $F_{SC} = 0.007$, P

< 0.0001, $F_{IS} = -0.0103$, $P = 0.955$),

   Estimation of Gene Flow. Pairwise population gene flow estimates, based

on the private alleles model of Barton and Slatkin (1986), were highest among populations

within HC (1.89 – 4.54 migrants per generation , average $N_m = 4.17$; Table 5). Overall

highest average gene flow occurred between A2344 and B2359 (4.54). Average number of

migrants per generation is estimated at 2.49 among SJA populations and 4.17 among HC

populations. Gene flow between SJA and HC populations ranged from 0.35 to 1.82

estimated migrants per generation, and is estimated at < 1 individual per generation in 16

of 48 comparisons (Table 5). We do not suggest the estimated intergenerational dispersal

(gene flow) values reported here are absolute (see Bossert and Prowell, 1998). Rather, we

present them heuristically to illustrate relative differences in estimates of past rates of gene

flow (integrated over several generations) among the populations analyzed.

   Genetic Distance and Relationships Between Populations. The phenogram

generated using neighbor-joining algorithm (Figure 2A) based on D_{CE} illustrates the close

relationship among populations within HC, and among populations within SJA, relative to

between the two regions. Bootstrap values supporting the close relationship within the HC

relative to the SJA are high (91%), although the nodes within this cluster are less well

supported with the exception of B2359 and D2465 (83%), and A2344 and E2468 (53%)

154

within HC, and FAL and W (53%) within SJA. The observed relationships are upheld

when the population input order is changed, although bootstrap values vary (data not

shown). The addition of clones to the analysis increased bootstrap values between the two

regions to 93%, while altering intra-regional groupings with bootstrap support of greater

than 50% (Fig. 2B). HC remains completely partitioned from SJA in both analyses (Fig.

2).

Results of the PCA illustrating the genetic differentiation between SJA and HC

populations are shown in Figure 3A. The first two axes of the PCA accounted for 70.6%

of the total inertia (58.4% and 12.2%, respectively). The first axis explained a significant

portion of the total variance ($P = 0.0001$). The third axis is half that of the 2nd axis (6.7%)

and did not change relationships between SJA and HC (data not shown). Genetic

differentiation between SJA and HC, shown by PCA, mirror the geographic distances

between the regions, displayed in Figure 3B.

Population Demography

We detected no genetic signature of a demographic bottleneck (heterozygote excess

relative to number of alleles) in any of the populations of *Z. marina* examined.

Demographic bottleneck was evaluated using the Wilcoxon test under three models of

mutation which account for variation at microsatellite loci (IAM, TPM, SMM, Table 6).

We detected a signature of expansion, a significant deficit of heterozygotes relative to

number of alleles, in SHB (under the TPM and SMM), and W and E2468 (under the

SMM).

Discussion

This study represents the first analysis of population genetic substructuring and relationships of *Z. marina* in the San Juan Archipelago and Hood Canal, Puget Sound, using eight polymorphic microsatellite loci. Based on 5.8S rRNA and ITS-1 and ITS-2 fragment data, all populations examined were composed of *Z. marina* and not *Z. japonica*; these data were confirmed by microsatellite amplification results.

Assesment of Clonality

We determined, by probability of identity analysis, this eight microsatellite suite provides sufficient resolution to distinguish clones (ramets) and individuals (MLGs,or genets) within Puget Sound eelgrass populations. Probability of identity values were, in general, within ranges recommended to ensure confidence in individual identification given breeding occurs among individuals not related at the first order level. However, high levels of clonality in some populations may violate the assumption of non-random breeding made during probability of identity analyses, leading to over-estimations of clonality. Confidence in individual identification estimates may be increased by reducing clones sampled, and increasing the number of individuals available for population level diversity analyses.

High levels of clonality were evident in San Juan Archipelago populations collected in 2006, requiring more than half the samples to be removed for population genetics analyses. Population genetics analyses require that unrelated individuals be used to describe the target population. In some San Juan Archipelago populations, though 50 samples were collected, population genetics analyses were performed on 10 or fewer

individuals. The high levels of clonality observed may be due, in part, to distance between sample collections. Other eelgrass populations sampled for population genetic and phylogeography studies have maintained minimum distances of 10m between sample collections, five times the distance between San Juan Archipelago samples collected in 2006. Hood Canal and Picnic Cove (San Juan Archipelago) had greater distances between samples, and lower levels of clonality than 2006 San Juan Archipelago populations, but still contained higher clonality levels than those observed in other North American Pacific eelgrass populations, for which samples were typically taken 20m apart (Muñiz-Salazar *et al.* 2005, 2006; Talbot *et al.* in prep.).

Without a *priori* information about the levels of clonality within a target population, it is difficult to devise a sampling strategy that will provide sufficient resolution to assess clonality and map clones, while at the same time providing an adequate sample size of genets (i.e., n = 30) to use in comparative population-level analyses. In the former case, the geographic distribution of clones needs to be mapped at a fine scale; therefore, multiple sampling of ramets is desired. In the latter case, sampling of clones needs to be reduced to near zero. Information at both the microgeographic and macrogeographic level is necessary to understand the genetic characteristics of the target population.

We used the information presented herein and the clone maps shown in Appendix III to determine the level of sampling that would likely yield a sufficient sample size of genets to perform population genetics analyses (e.g., 30 genets). Sampling at 10m intervals along a transect yielded an average genotypic richness of 0.82 (SD = 0.24), with 6 of the 14 populations showing genotypic richness values of 1.0. Typically, sampling at

10m intervals along the single transects yielded 11 genets per population. Sampling at 18m intervals increased the average genotypic richness to 0.91 (SD = 0.10), with 11 of the 14 populations showing genotypic richness values of 1.0. Sampling at 18m intervals along the single transects yielded 4-6 genets per population. Thus, transect length must be increased or sampling on parallel or perpendicular transects at appropriate intervals will be needed to collect an adequate number of genets to represent each population in this area. However, for two San Juan Archipelago populations, Fisherman's Bay, Inner and Shoal Bay, diversity is so low that it is unclear whether a sufficient number of genets could be sampled to reach the target sample size of 30 genets. Nevertheless, for most populations in this area, sampling at a minimum of 18ms should yield a sufficient number of genets for population genetics analyses. We recommend sampling at least 35 individuals at 20m intervals to ensure adequate population-level characterization. However, studies assessing the clonal movement across landscapes should sample in a grid, with short distances between sample collections (i.e. as here, <10m). Obviously, larger sampling intervals of 20ms can be incorporated into sampling schemes examining more microgeographic questions. We also recommend that sampling occurs at consistent intervals, to guarantee comparability across populations, localities, and regions. For this study sampling was conducted along transects, allowing mapping of multilocus genotypes along only those transects, a small slice of the populations. However, results from this study show potential applicability of multilocus genotype mapping of ramets and genets to determine the extent of clones within eelgrass populations in this area.

Mapping of multilocus genotypes showed varying distributions of clones along transects. For example, interrupted transects were found to share no clones between ends,

single MLGs were found in spans of clones, and clones were found more than 80m apart. Distribution of MLGs within populations may depend on many factors, among them being microscale fluctuations in salinity, depth, temperature, turbidity, tidal zone, and disturbance. Further sampling to determine the relation of multilocus genotypes to these factors may provide information for making management and conservation decisions. Large-scale clonality analyses could show patterns of distribution and allow the identification of centers of diversity, or genetic corridors of high conservation interest within and between eelgrass populations.

Genetic Diversity

Microsatellite-based analyses of heterozygosity, number of alleles, allelic richness, and clonal diversity reveal low to moderate levels of genetic variability in Puget Sound eelgrass populations. We found the lowest allelic richness and heterozygosity (H_E) in Bell Point, Wescott Bay, a San Juan Archipelago population, and the lowest number of alleles and highest levels of clonality in Fisherman's Bay, Inner, also a San Juan Archipelago population. Overall intrapopulation heterozygosity (H_E) for each locus in San Juan Archipelago and Hood Canal populations are generally similar to those reported in studies of other eelgrass populations along the Pacific Coast of North America. Expected heterozygosity, H_E, ranges from 0.31 to 0.53 in San Juan Archipelago and Hood Canal populations, and from 0.23 to 0.54 in other eelgrass populations ranging from San Francisco Bay to the Alaska Peninsula (Appendix V). Numbers of alleles are moderately lower in San Juan Archipelago and Hood Canal populations when compared to other populations, ranging from 2.5 to 5.5 in Puget Sound, and from 4.38 to 7.13 among other

populations along the Pacific Coast of America (Appendix V). However, allelic richness values in Puget Sound fall within the range observed in other eelgrass populations along the Pacific Coast of North America (1.84 to 2.68, Appendix V). Since allelic richness, unlike number of alleles, accounts for disparities in sample size, the aforementioned differences in number of alleles are apparently due to differences in sample sizes.

Z. *marina* reproduces in two ways: sexually by means of monoecius flowers, and asexually via extensive vegetative propagation (Laushman 1993). While both perennial and annual beds of *Z. marina* inhabit coastal regions along the southernmost portion of the species' range, in Puget Sound, eelgrass populations are generally characterized by perennial life history, reproducing sexually during the shorter summer months, but also growing actively through clonal reproduction. As would be expected in populations characterized by high clonality (Les 1988), the majority of allelic variation characterizing perennial eelgrass beds in the Puget Sound populations ($F_{ST} = 0.128$) is distributed between populations, and not within populations. Unlike more southern populations (Talbot *et al.* 2004), however, we found no instances of inter-populational clonality in Puget Sound.

Different populations of *Z. marina* demonstrate a remarkable level of morphological and physiological variability, with leaf width and length often correlating with habitat (McMillan 1982, Dennison and Alberte 1986, Haynes 2000). We have not yet assessed differentiation among individuals occupying different locations within eelgrass beds, and recommend this be done at least for some of the of the differentiated populations within the two areas. In general, within North Pacific populations, we have found little to no genetic differentiation among "populations" assayed from the same site, but

representing different locations within the tidal zone. For example, at some sites within

Izembek Lagoon, in western Alaska, samples collected within the high intertidal zone were

found to be identical, based on a 10-locus suite of markers, to samples (presumed to be

clones) collected from the low intertidal zone (Talbot *et al*, unpublished data). Multilocus

genotype distribution in relation to landscape features, such tidal zones, was not

investigated in this study.

Spatial genetic differentiation was evident between regions (θ_p=0.131, p<0.0001),

and among all populations studied [except for eleven pairwise comparisons, all within

region (five pairwise comparisons within San Juan Archipelago, and six within Hood

Canal)], as demonstrated by the analyses of variance in allele frequencies using traditional

F-statistics. This suggests that populations within the San Juan Archipelago and Hood

Canal are isolated to such an extent that the forces of drift, migration (gene flow) and

perhaps mutation, are shaping the characteristics of neutral genetic markers in these

populations. As such, we are likely to be able to use genetic mixed stock analysis for

assessment of source populations for newly-colonized eelgrass beds, given sufficient

baseline data (e.g., Pearce *et al.* 2000).

We can use the comparison of F_{ST} (θ) and R_{ST} (ρ) analyses to gain insight into the

forces shaping population subdivision among the various populations of eelgrass

examined. Traditional F-statistic analysis of genetic diversity under an IAM assumes each

mutation is to a completely new state, erasing any memory of the prior state. Therefore,

genetic similarity between populations is attributable to migration or recent divergence

from a common ancestor. However, mutational processes at microsatellite loci do not

erase all information about the ancestral allelic state, since mutations tend to at least

approximately proceed under a SMM. When analyzing microsatellite loci, this tends to bias F_{ST} values by overestimating coalescence times. Slatkin (1995) used SMM to calculate R_{ST} values and showed they generally provided a less-biased estimate for demographic parameters than did F_{ST}, given sufficient coalescence times. However, with recently diverged populations, the performance of F_{ST} improves because genetic drift is the dominant process creating local differentiation, and mutational events are of less importance. If R_{ST} values are somewhat lower than F_{ST}, this may suggest that these populations are of relatively recent evolutionary origin, and that drift and migration have predominated over mutation in shaping the pattern of genetic differentiation. The opposite pattern suggests that mutation is beginning to play a role in differentiation between populations.

For this study, overall R_{ST} (ρ) values are larger than overall F_{ST} (θ) values for 70.3% (64/91) of all θ and ρ comparisons within Puget Sound. Between the San Juan Archipelago and Hood Canal regions within the Puget Sound, overall R_{ST} (ρ) values are larger than overall F_{ST} (θ) in 87.5% (42/48) of all θ and ρ comparisons. In population comparisons within regions, overall R_{ST} (ρ) values were higher than overall F_{ST} (θ) values in 64.3% (18/28) of comparisons within San Juan Archipelago, and 26.7% (4/15) of comparisons within Hood Canal. These comparisons indicate drift and migration is the primary factor shaping genetic differentiation within the Hood Canal. However, within the San Juan Archipelago, mutation is beginning to play a role, though drift and migration are also driving genetic differentiation. Between the regions overall R_{ST} (ρ) values are larger than overall F_{ST} (θ) values this suggests that separation between the regions has existed for

a period long enough to allow mutation to augment the forces of drift and migration in differentiation of populations between the regions.

Despite the low levels of genetic variability observed within the Puget Sound eelgrass populations in general, we detected no signatures of genetic bottleneck within any of the populations assayed. However, one population, Shoal Bay, may have experienced a recent expansion, or influx of alleles from another population, under two of the three models of mutation (the TPM and the SMM). Two other populations, Picnic Cove, and hdc2468, show a signature of expansion or influx of new alleles only under the SMM.

The ability of microsatellite data to track recent expansions and contractions of populations is dependent upon the rate and level of expansion or severity of bottleneck; Luikart and Cornuet (1998) suggest that the temporal framework within which severe bottlenecks or rapid expansions are detectable, using the ratio of heterozygosity excess or deficit, is during the past 2 to 20 generations. Differences in population fluctuations among models (IAM, TPM, and SMM) may be because of underlying assumptions of mutation models, such that IAM does not allow for homoplasy (i.e. each mutation results in a new allele) and SMM allows for mutations to existing allelic states (homoplasy). The TPM is intermediate between the other two models. When mutation rate is held constant, IAM will have more distinct allelic states and a higher expected heterozygosity under mutation drift equilibrium, and therefore may be better able to detect population declines. Simulation data indicate that IAM may better detect weak population bottlenecks than SMM (Cornuet and Luikart 1996), and empirical data suggest SMM may not be as able to detect recent population declines (Cornuet and Luikart 1996). Therefore, differences in detectability of population fluctuations between mutation models may reflect differences in

population size over evolutionary time, with IAM detecting recent population fluctuations, and SMM detecting long-term population growth.

Under this scenario, because evidence for expansion in these three populations (Shoal Bay, Picnic Cove and hdc2468, for which heterozygosity deficit relative to numbers of alleles was observed) was detected under the more conservative models explaining microsatellite mutation (the TPM and/or the SMM), we suggest this population expansion or admixture may have occurred more historically, rather than more recently, farther back in time along the 2 to 20 generation time span appropriate for this analysis. Studies employing microsatellite analyses in populations elsewhere (San Francisco Bay; Talbot *et al.*, 2004; San Quintin Bay; Muñiz-Salazar *et al.* 2006) have also detected genetic signatures of expansions in populations or components of what may be larger metapopulations of eelgrass demonstrating fluctuating patch dynamics. For example, Muñiz-Salazar *et al.* (2006) observed a signature of expansion in "populations" of eelgrass occupying the mouth of San Quintin Bay, Baja California, Mexico, although eelgrass population in the Bay has recently seen a 14% decline in cover.

Generation-time for a plant that reproduces both vegetatively and sexually is difficult to determine (Ruckelhaus 1994). Ruckelhaus (1996) suggested eelgrass clones can live 20-50 years, and Setchell (1929) suggests sexual reproduction can begin as early as the second year. Given these values, our microsatellite data suggest no bottleneck has occurred in these populations within the past century. However, since this method is not sensitive to recent demographic fluctuations (e.g., within the past generation), these values are conservative, and may not reflect the current demography of eelgrass populations within Puget Sound.

164

Acknowledgements

Literature Cited

Arnaud-Haond, S., and K. Belkhir. 2006. GENCLONE: a computer program to analyse genotypic data, test for clonality and describe spatial clonal organization. Molecular Ecology Notes. 7: 15-17.

Barton, N. H. and M. Slatkin. 1986. A quasi-equilibrium theory of the distribution of rare alleles in a subdivided population. Heredity 56:406-441.

Bossart, J. L. and D. P. Prowell. 1998. Genetic estimates of population structure and gene flow: limitations, lessons and new directions. Trends Evol. Ecol. 13: 202-206.

Cavalli-Sforza, L. L. and A. W. F. Edwards. 1967. Phylogenetic analysis: models and estimation procedures. Evolution 21:550-570.

Cornuet, J-M., and G. Luikart. 1996. Description and power analysis of two tests for detecting recent population bottlenecks from allele frequency data. Genetics 144: 2001-2014.

den Hartog, C., and P. G. Polderman. 1975. Changes in the seagrass populations of the Dutch Wadden Zee. Aquatic Botany 1:141-147.

Denniston, C. 1978. Small population size and genetic diversity: implications for endangered species. Pp. 281-289 In: S.A. Temple (ed.). Endangered Birds: Management Techniques for Preserving Threatened Species. Univ. Wisc. Press, Madison.

Dennison, W .C., and R. S. Alberte. 1986. Photoadaptation and growth of *Zostera marina* L. (eelgrass) transplants along a depth gradient. Journal of Experimental Marine Biology and Ecology 98: 265-282.

DiRienzo, A., A. C. Peterson, J. C. Garza, A. M. Valdes, M. Slatkin and N. B. Freimer. 1994. Mutational processes of simple-sequence repeat loci in human populations. Proc. Natl. Acad. Sci. USA 91: 3166-3170.

Dorken, M. E., and C.G. Eckert. 2001. Severly reduced sexual reproduction in northern populations of a clonal plant, *Decodon verticillatus* (Lythraceae). Journal Ecology 89: 339-350.

El Mousadik, A. and R. J. Petit. 1996. High level of genetic differentiation for allelic richness among populations of the argan tree [*Argania spinosa* (L.) Skeels] endemic of Morocco. Theor. App. Gen 92: 832-839.

Excoffier L, PE Smouse and JM Quattro. 1992. Analysis of molecular variance inferred from metric distances among DNA haplotypes: Application to human mitochondrial DNA restriction data. Genetics **131**:479-491.

Freimer, N. B., and M. Slatkin. 1996. Microsatellites: evolution and mutational processes. Ciba Found. Symp. 197: 51-72.

Garza, J.C. and E. G. Williamson. 2001. Detection of reduction in population size when using data from microsatellite loci. Molecular Ecology 10:305-318.

Goudet, J. 1999. PCA-GEN (version 1.2). Lausanne, Switzerland. Available online at: www.unil.ch/izea/softwares/pcagen.html on 15 December 2005.

Goudet, J. 2002. FSTAT, a program to estimate and test gene diversities and fixation indices (version 2.9.3.2). Available from http://www.unil.ch/izea/softwares/fstat.html.

Goudet, J., M. Raymond, T. de Meeüs and F. Rousset. 1996. Testing differentiation in diploid populations. Genetics 144: 1933-1946.

Haynes, R. R. 2000. Zosteraceae Dumortier: Eel-grass Family. Pp. 90-93 In: Flora of North America Editorial Committee (eds.) Flora of North America North of Mexico, Volume 22: Magnoliophyta: Alismatidae, Arecidae, Commelinidae (in part), and Zingiberidae. New York: Oxford University Press.

Jarne, P., and P. Lagoda. 1996. Microsatellites, from molecules to populations and back. Trends in Ecol. Evol. 11: 424-429.

Laushman, R. H. 1993. Population genetics of hydrophilous angiosperms. Aquatic Botany 442: 147-158.

Les, D. H. 1988. Breeding systems, population structure and evolution in hydrophilous angiosperms. Annals of the Missouri Botanical Garden 75: 819-835.

Li, C. C. and D. G. Horovitz. 1953. Some methods for estimating the inbreeding coefficient. Amer. J. Hum. Gen. 5:107-117.

Luikart, G. and J-M. Cornuet. 1998. Empirical evaluation of a test for identifying recently bottlenecked populations from allele frequency data. Cons. Biol. 12:228-237.

Manly B. F. J. 1985. *The Statistics of Natural Selection*. Chapman Hall, London.

Maruyama, T. and P. A Fuerst. 1985. Population bottlenecks and non-equilibrium

    models in population genetics. II. Number of alleles in a small population that

    was formed by a recent bottleneck. Genetics 111: 675-689.

McMillan, C. 1982. Isozymes in seagrasses. Aquatic Botany 14: 231-243.

Michalakis, Y., and L. Excoffier. 1996. A genetic estimation of population subdivision

    using distances between alleles with special reference for microsatellite loci.

    Genetics 142:1061-1064.

Muñiz-Salazar, R., S. L. Talbot, G. K. Sage, D. H. Ward, and A. Cabello-Pasini. 2005.

    Population genetic structure of annual and perennial populations of *Zostera marina*

    L. along the Pacific coast of Baja California Peninsula and the Gulf of California.

    Molecular Ecology 14: 711-722.

Muñiz-Salazar, R., Talbot, S. L., Sage G. K., Ward D. H., and A. Cabello-Pasini. 2006.

    Genetic structure of eelgrass *Zostera marina* meadows in and embayment with

    restricted water flow. Marine Ecology Progress Series 309: 107-116.

Nei, M. 1987. Molecular Evolutionary Genetics. New York: Columbia University Press.

Nei, M., T. Maruyama and R. Chakraborty. 1975. The bottleneck effect and genetic

    variability in populations. Evolution 29: 1-10.

Ohta T. and K. Kimura. 1973. The model of mutation appropriate to estimate the number

    of electrophoretically detectable alleles in a genetic population. Genetical

    Research 22: 201-204.

Olsen, J.L., Stam,W.T., Coyer, J.A., Reusch, T.B., Billingham, M., Bostrom, C., Calvert,

    E., Christie, H., Granger, S., Lumiere, R.L., Milchakova, N., Oudot-Le Secq, M.P.,

    Procaccini, G., Sanjabi, B., Serrao, E., Veldsink, J., Widdicombe, S., Wyllie-

Echeverria, S., 2004. North Atlantic phylogeography and large-scale population differentiation of the seagrass *Zostera marina* L. Mol. Ecol. 13: 1923–1941.

Orth, R. J. and K. A. Moore. 1983. Chesapeake Bay: an unprecedented decline in submerged aquatic vegetation. Science 222: 51-52.

Park, S. 2000. User's Manual, Microsatellite ToolKit for MS Excel 97 or 2000 (PC). Available from Stephen Park, Molecular Population Genetics Lab, Smurfit Institute of Genetics, Trinity College, Dublin, Ireland.

Pearce, J. M., B. J. Pierson, S. L. Talbot, D. V. Derksen, and D. Kraege. 2000. A genetic evaluation of morphology used to identify harvested Canada geese. J. Wildlife Mgt. 64: 863-874.

Petit, R., A. El Mousadik and O. Pons. 1998. Identifying populations for conservation on the basis of genetic markers. Conservation Biology 12, 844-855.

Piry, S., G. Luikart, and J-M. Cornuet. 1999. BOTTLENECK: A computer program for detecting recent reductions in the effective population size using allele frequency data. J. Hered: 90: 502-503

Procaccini, G., L. Orsini, M. V. Ruggiero and M. Scardi. 2001. Spatial patterns of genetic diversity in *Posidonia oceanica*, an endemic Mediterranean sea grass. Molecular Ecology 10: 1613-1622.

Raymond, M. and F. Rousset. 1995. GENEPOP (Ver. 1.2): population genetics software for exact test and ecumenicism. J. Hered. 86: 248-249.

Reusch, T. B. H. 2000. Five microsatellite loci in eelgrass *Zostera marina* and a test of cross-species amplification in *Z. noltii* and *Z. japonica*. Molecular Ecology 9: 365-378.

Reusch, T. B. H., W. T. Stam and J. L. Olsen. 1999. Microsatellite loci in eelgrass *Zostera marina* reveal marked polymorphism within and among populations. Molecular Ecology 8: 317-322.

Reusch, T. B. H., W. T Stam, and J. L. Olsen. 2000. A microsatellite based estimation of clonal diversity and population subdivision in *Zostera marina*, a marine flowering plant. Molecular Ecology 9: 127-140.

Rice, W. R. 1989. Analyzing tables of statistical tests. Evolution 43: 223-225.

Ruckelhaus, M. 1994. Ecological and genetic factors affecting population structure in the marine angiosperm *Zostera marina.* Ph.D. Dissertation, University of Washington, Seattle.

Ruckelhaus, M. 1996. Estimation of genetic neighborhood parameters from pollen and seed dispersal in the marine angiosperm *Zostera marina* L. Evolution 50: 856-864.

Saitou, N., and M. Nei. 1987. The neighbour-joining method: a new method for reconstructing phylogenetic trees. Mol. Biol. Evol. 4: 406-425.

Setchell, W. A. 1929. Morphological and phenological notes on *Zostera marina* L. Univ. Calif. Pub. Bot. 14:389-452.

Schneider, S., J.-M. Kueffer, D. Roessli, and L. Excoffier. 1997. ARLEQUIN: an exploratory population genetics software environment. Available: http://anthropologie.unige.ch/arlequin.

Short, F. T. and S. Wyllie-Echeverria. 1996. A review of natural and human-induced disturbance of seagrasses worldwide. Environ. Conserv. 23: 17-27.

Slatkin, M. 1995. A measure of population subdivision based on microsatellite allele frequencies. Genetics 139:457-462.

Sokal, R. R. and F. J. Rohlf. 1997. Biometry: the principles and practice of statistics in biological research. 3rd Edition. W. H. Freeman and Co., New York.

Talbot, S.L., G. K. Sage, J.R. Rearick , and R. Muñiz-Salazar,. 2004. Genetic structure of *Zostera marina* in San Francisco Bay: preliminary results of microsatellite analyses. U. S. Geological Survey unpublished report submitted to Merkel & Associates, Inc., 7 March, 2004.

Talbot, S.L., Wyllie-Echeverria, S., Ward, D.H., Rearick, J.R., Sage, G.K., Chesney, and R.C. Phillips. 2006. Genetic characterization of *Zostera asiatica* on the Pacific Coast of North America. Aquatic Botany 85: 169-176.

Talbot, S. L., G. K. Sage, R. Muñiz-Salazar, J. R. Rearick, D. H. Ward and A. Cabello-Pasini. Population genetic structure of *Zostera marina* L. along the Pacific and Bering coasts of Alaska. In prep.

Valière, N. 2002. GIMLET: a computer program for analysing genetic individual identification data. Molecular Ecology Notes 2: 377-379.

Valiela, I. and J. Costa. 1988. Eutrophication of Buttermilk Bay, a Cape Cod coastal embayment: concentrations of nutrients and watershed nutrient budgets. Environmental Management 12:539-551.

Waits, L. P., G. Luikart and P. Taberlet. 2001. Estimating the probability of identity among genotypes in natural populations: cautions and guidelines. Molecular Ecology, **10**, 249-256.

Watterson, G. A. 1984. Allele frequencies after a bottleneck. Theoretical Population Biology 26: 387-407.

Weir, B. S., 1996 Genetic Data Analysis II: Methods for Discrete Population Genetic Data. Sinauer Assoc., Inc., Sunderland, MA, USA.

Weir, B. S. and C. C. Cockerham. 1984. Estimating F-statistics for the analysis of population structure. Evolution 38: 1358-1370.

Wright, S. 1951. The genetical structure of populations. Ann. Eugen. 15: 323-354.

Figure Legends

Figure 1. (A) Aerial view of *Z. marina* sampling areas in San Juan Archipelago and Hood Canal, Puget Sound, Washington. (B) Sampling locations in San Juan Archipelago. (C) Sampling locations in Hood Canal.

Figure 2. (A) Principal components analysis of *Z. marina* populations in San Juan Archipelgo and Hood Canal. (B) Geographic map of populations generated in Genclone 1.0. Axes represent distance between populations in meters.

Figure 3. Neighbor-joining trees illustrating relationships among all populations in San Juan Archipelago and Hood Canal. (A) Tree based on populations described by MLGs (genets) only. (B) Tree based on dataset including all samples (e.g., weighted by clones). Relationships generated using C_{DE} distances. Bootstrap values (based on 2000 replications) >50% are listed at the node.

Figure 1

A

B

C

174
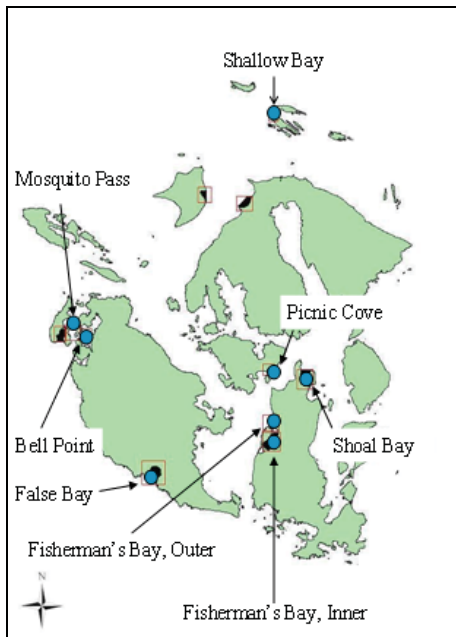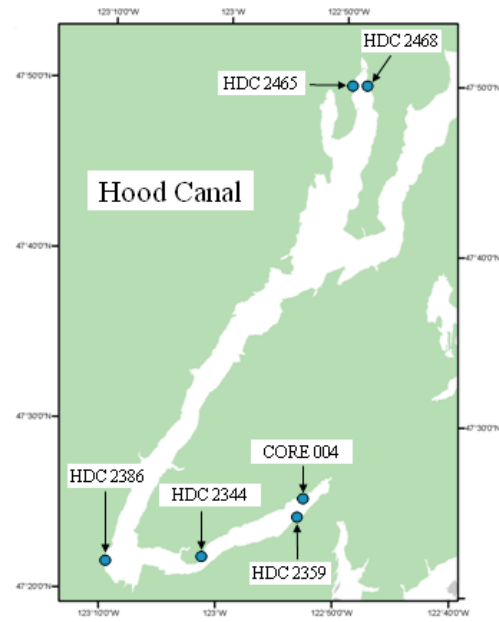
Figure 2

A

B

Figure 3

A

B

176
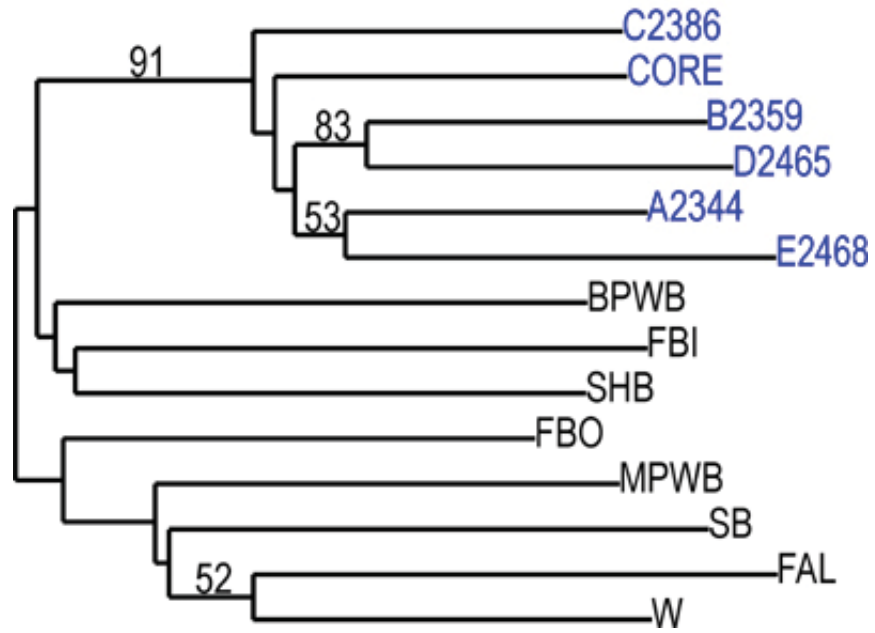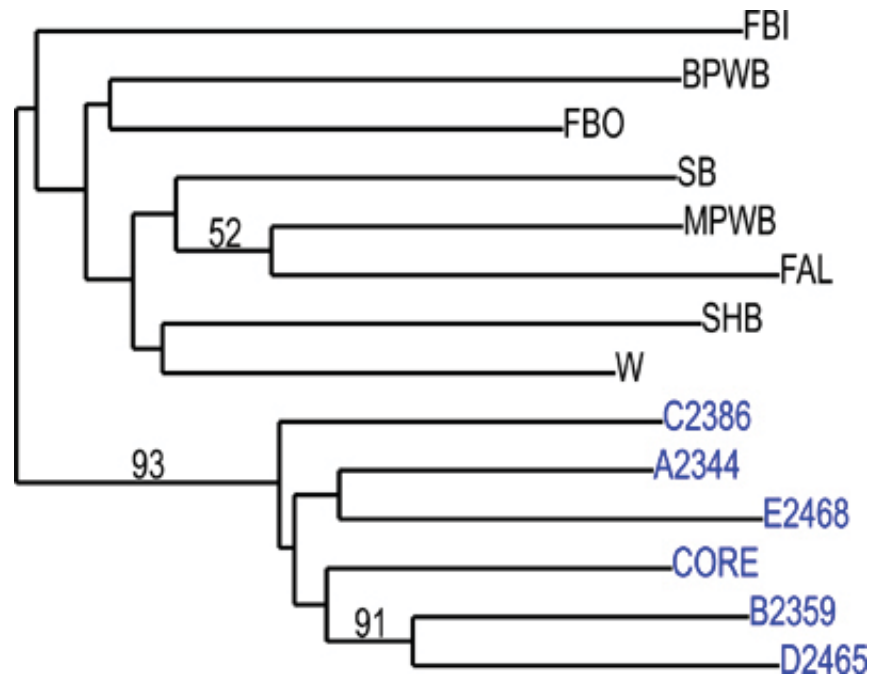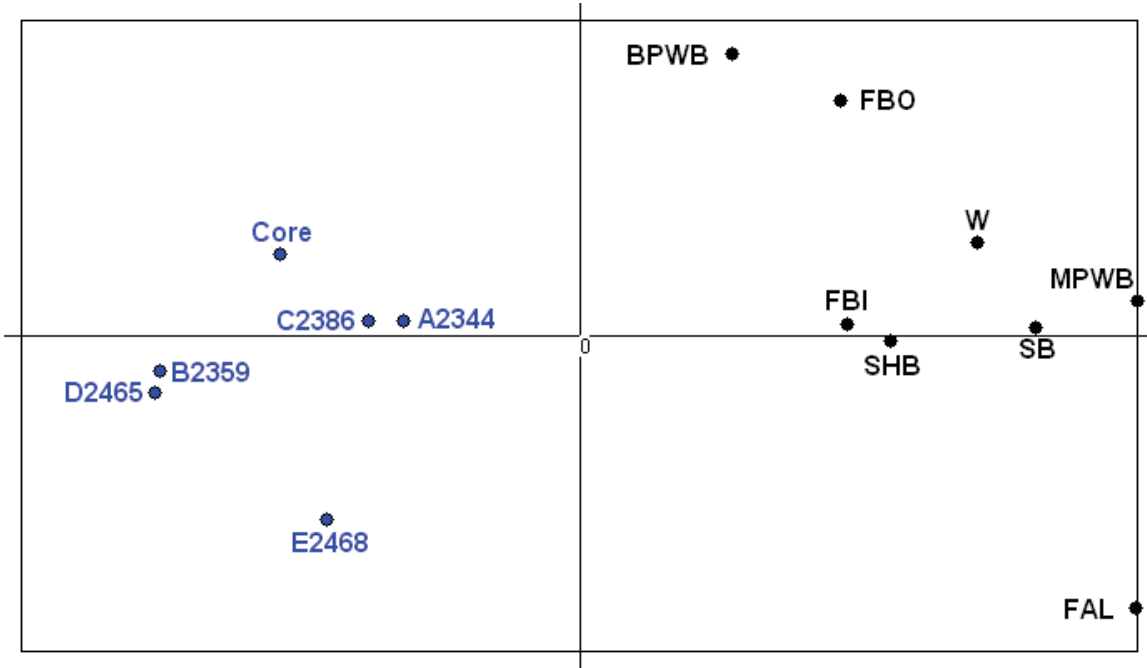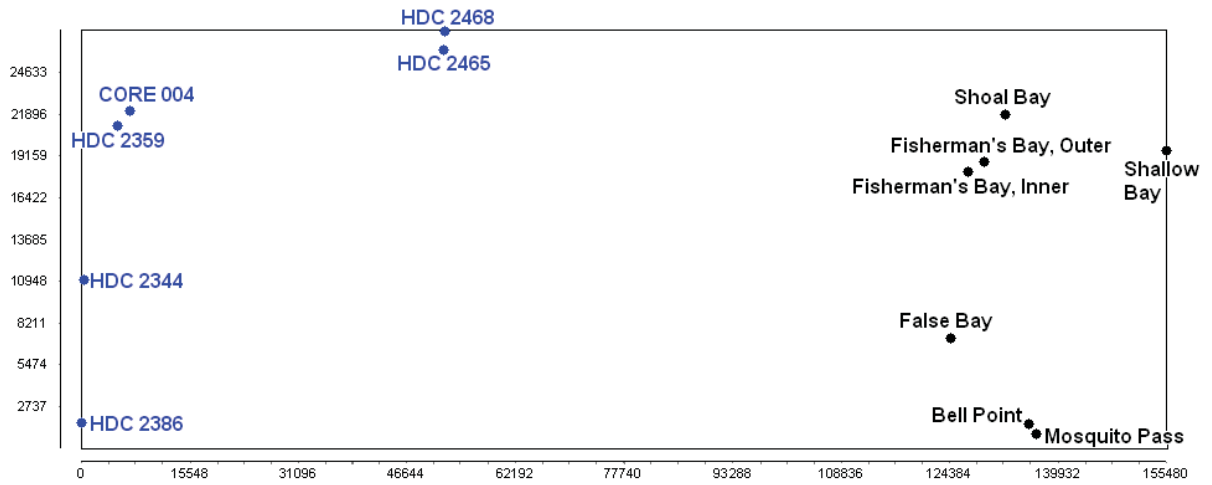
Table 1. Population groupings and acronyms.

San Juan Archipelago	SJA
San Juan Archipelago and Picnic Cove	SJA+W
Hood Canal	HC
San Juan Archipelago, Picnic Cove, and Hood Canal	SJA+W+HC

SJA Sites	
Bell Point, Wescott Bay	BPWB
Mosquito Pass, Wescott Bay	MPWB
Fisherman's Bay, Inner	FBI
Fisherman's Bay, Outer	FBO
Shoal Bay	SHB
Shallow Bay	SB
False Bay	FAL
Picnic Cove	W

HC Sites	
core004	CORE
hdc2344	A2344
hdc2359	B2359
hdc2386	C2386
hdc2465	D2465
hdc2468	E2468

Table 2. Probability of identity ($P_{(ID)}$) and probability of identity between siblings ($P_{(ID)sib}$) computed for each of eight microsatellite loci in 14 populations of *Z. marina* in San Juan Archipelago and Hood Canal, Washington. Values based on multilocus genotypes only.

POPULATION	N	$P_{ID(UNBIASED)}$	$P_{ID(SIBS)}$	$1/_{PID(UNBIASED)}$	$1/_{PID(SIBS)}$
All MLGs Pooled	271	5.94E-06	1.36E-02	168,265	73
San Juan Archipelago (SJA)					
BPWB	10	**2.54E-04**	**7.23E-02**	**3,945**	**14**
MPWB	17	1.51E-06	3.37E-02	664,011	30
FBI	5	2.05E-05	2.59E-02	48,780	39
FBO	18	2.10E-06	3.63E-02	477,099	28
SHB	7	**1.60E-07**	3.10E-02	**6,234,414**	32
SB	23	2.12E-06	1.50E-02	471,320	67
FAL	26	1.19E-05	2.66E-02	83,822	38
W	12	3.21E-05	5.14E-02	31,114	19
Hood Canal (HC)					
CORE	24	9.31E-05	4.62E-02	10,738	22
A2344	23	2.65E-05	2.52E-02	37,807	40
B2359	28	4.21E-05	2.53E-02	23,730	40
C2386	27	3.05E-05	2.38E-02	32,798	42
D2465	23	2.87E-05	1.98E-02	34,880	51
E2468	28	1.95E-05	**1.34E-02**	51,256	**75**

Note: $P_{(ID)sib}$ provides a conservative upper bound on the number of loci necessary for individuals within populations comprised of closely-related indivuals (Waits *et al.* 2001). $P_{(ID)multilocus}$ is the $P_{(ID)}$ given all loci assayed; P_{shadow} is the probability at which another individual with the same genotype will be observed, given the sample frequency of the alleles observed at those loci within the population of interest.

Table 3. Genetic variation of multilocus genotypes only at 8 microsatellite loci (A) overall and (B) within 14 populations of *Z. marina* in San Juan Archipelago and Hood Canal, Washington. Values are based on multilocus genotypes only.

A

Populations	N^1	MLG^2	CR^3	A^4	PA^6	R^7	H_O^8	H_E^9	F^{11}
				Combined Analyses					
SJA&W&HC	545	271	274	13.38	-	1.00	0.42	0.46	0.095
SJA&W	365	118	247	10.38	19	1.00	0.40	0.42	0.056
SJA	348	106	242	9.88	17	1.00	0.40	0.43	0.058
HC	180	153	27	9.75	15	1.00	0.43	0.43	-0.002

B

	N^1	MLG^2	CR^3	A^4	AR^5	PA^6	R^7	H_O^8	H_E^9	P^{10}	F^{11}
				Population Analyses							
				San Juan Archipelago (SJA)							
BPWB	50	10	40	3.00	**2.31**	2	1.00	**0.29**	**0.31**	0.88	0.062
MPWB	50	17	33	4.75	2.89	2	1.00	0.40	0.37	0.88	-0.066
FBI	50	**5**	**45**	**2.50**	2.50	1	1.00	0.35	0.45	0.75	**0.217**
FBO	50	18	32	4.88	2.80	4	1.00	0.35	0.36	0.88	0.032
SHB	49	7	42	3.50	2.98	1	1.00	0.41	0.40	0.75	-0.027
SB	49	23	26	4.88	**3.05**	4	1.00	0.51	0.46	0.88	-0.105
FAL	50	26	24	4.63	2.85	3	1.00	0.39	0.38	**0.63**	-0.025
W	17	12	5	3.75	2.58	2	1.00	0.34	0.34	0.88	-0.024
				Hood Canal (HC)							
CORE	30	24	6	4.38	2.48	2	1.00	0.39	0.34	0.75	**-0.143**
A2344	30	23	7	4.50	2.70	2	1.00	0.42	0.41	**1.00**	-0.013
B2359	30	**28**	**2**	**5.50**	2.72	6	1.00	0.40	0.41	**1.00**	0.025
C2386	30	27	3	5.25	2.81	**0**	1.00	0.43	0.41	**1.00**	-0.041
D2465	30	23	7	4.38	2.77	**0**	1.00	0.42	0.44	**1.00**	0.055
E2468	30	**28**	**2**	5.00	2.89	**5**	1.00	**0.53**	**0.49**	**1.00**	-0.093

[1] number of samples used in analyses
[2] number of multilocus genotypes
[3] number of clones removed for population genetics analyses, based on multilocus genotyping
[4] average number of alleles at eight microsatellite loci
[5] allelic richness (El Mousadik and Petit 1996)
[6] number of private alleles
[7] genotypic richness
[8] observed heterozygosity
[9] unbiased expected heterozygosity (Nei 1987; eq. 7.39, pg. 164)
[10] percent polymorphism
[11] inbreeding coefficient (Wright 1951)

Table 4. Expected and observed heterozygosities for all populations by locus. Populations are described by multilocus genotypes.

Multilocus Genotypes Only, Expected Heterozygosities

Locus	BPWB	MPWB	FBI	FBO	SHB	SB	FAL	W	CORE	A2344	B2359	C2386	D2465	E2468
CT3	0.44	0.63	0.73	0.55	0.86	0.72	0.82	0.61	0.57	0.62	0.59	0.70	0.69	0.64
CT17	**0.85**	**0.95**	**0.89**	**0.92**	**0.87**	**0.94**	**0.91**	**0.88**	**0.92**	**0.91**	**0.90**	**0.89**	**0.86**	**0.84**
CT19	0.10	**0.00**	**0.00**	**0.00**	**0.00**	**0.00**	**0.00**	**0.00**	0.48	0.43	0.50	0.49	0.53	0.50
CT20	0.51	0.21	0.53	0.67	0.47	0.52	0.29	0.51	0.34	0.45	0.42	0.41	0.29	0.39
GA1	0.10	0.21	0.69	0.30	0.00	0.32	**0.00**	0.00	**0.00**	0.12	0.26	0.14	0.43	**0.14**
GA2	0.10	0.40	**0.00**	0.16	0.14	0.43	0.55	0.37	**0.00**	0.32	0.17	**0.07**	0.24	0.51
GA3	0.35	0.06	0.20	0.16	0.47	0.26	**0.00**	0.08	0.30	0.41	0.43	0.14	0.38	0.44
GA5	**0.00**	0.51	0.53	0.16	0.38	0.51	0.50	0.23	0.12	**0.04**	**0.04**	0.47	**0.13**	0.43

Multilocus Genotypes Only, Observed Heterozygosities

Locus	BPWB	MPWB	FBI	FBO	SHB	SB	FAL	W	CORE	A2344	B2359	C2386	D2465	E2468
CT3	0.40	0.65	0.60	0.50	**1.00**	0.83	0.88	0.83	0.75	0.74	0.57	**0.89**	0.48	0.71
CT17	**0.80**	**0.94**	**1.00**	**0.82**	**1.00**	**1.00**	**0.96**	**1.00**	**0.92**	**0.91**	**0.82**	0.78	**0.87**	**0.89**
CT19	0.10	**0.00**	**0.00**	**0.00**	**0.00**	**0.00**	**0.00**	**0.00**	0.67	0.43	0.50	0.52	0.57	0.61
CT20	0.40	0.24	**0.00**	0.72	0.29	0.61	0.19	0.33	0.33	0.48	0.43	0.33	0.17	0.50
GA1	0.10	0.24	1.00	0.33	**0.00**	0.30	**0.00**	**0.00**	**0.00**	0.13	0.25	0.15	0.43	**0.14**
GA2	0.10	0.41	**0.00**	0.17	0.14	0.39	0.54	0.25	**0.00**	0.22	0.18	**0.07**	0.26	0.54
GA3	0.40	0.06	0.20	0.11	0.43	0.30	**0.00**	0.08	0.33	0.39	0.43	0.15	0.43	0.36
GA5	**0.00**	0.65	**0.00**	0.17	0.43	0.65	0.58	0.25	0.13	**0.04**	**0.04**	0.56	**0.13**	0.50

Table 5. Pairwise measures of microsatellite differentiation based on analysis of multilocus genotypes only. θ_{ST} (Weir and Cockerham 1984) across all loci; ρ_{ST} (Slatkin 1995) across all loci; χ^2 (Raymond and Rousset 1995) across all loci. Pairwise N*m* values were calculated using the private alleles method of Barton and Slatkin (1989), implemented in GenePop 3.3. (Raymond and Rousset 1995). Values significantly different from zero in bold face ($P < 0.005$; values adjusted by a sequential Bonferroni correction).

Populations	θ_{ST}	ρ_{ST}	χ^2	N$_m$	Populations	θ_{ST}	ρ_{ST}	χ^2	N$_m$
BPWB & FBI	**0.2046**	**0.3688**	**Infinity**	0.6785	**FBO & SB**	**0.0602**	**0.0600**	**Infinity**	2.1294
BPWB & SHB	**0.1260**	0.0374	**Infinity**	1.1886	**FBO & FAL**	**0.1575**	0.1186	**Infinity**	1.5129
BPWB & MPWB	**0.1303**	0.1591	56.2800	1.4363	**FBO & W**	**0.0572**	0.0004	47.7200	1.8524
BPWB & FBO	**0.0558**	0.0715	**Infinity**	1.6102	**FBO & CORE**	**0.1379**	**0.3685**	**Infinity**	1.6073
BPWB & SB	**0.1059**	-0.0013	63.5600	1.1409	**FBO & A2344**	**0.0875**	**0.3810**	**Infinity**	1.8191
BPWB & FAL	**0.2006**	0.0850	**Infinity**	0.9788	**FBO & B2359**	**0.1818**	**0.3964**	**Infinity**	1.4150
BPWB & W	**0.1013**	**0.1461**	53.8400	1.3105	**FBO & C2386**	**0.1182**	**0.3765**	**Infinity**	1.6717
BPWB & CORE	**0.1193**	**0.2949**	**Infinity**	1.1379	**FBO & D2465**	**0.1842**	**0.4535**	**Infinity**	1.3528
BPWB & A2344	**0.0792**	**0.3137**	**Infinity**	1.0683	**FBO & E2468**	**0.1471**	**0.5679**	**Infinity**	1.3462
BPWB & B2359	**0.1709**	**0.3231**	**Infinity**	1.4090	**SB & FAL**	**0.0789**	0.0622	**Infinity**	1.2088
BPWB & C2386	**0.1134**	**0.2878**	**Infinity**	1.3149	**SB & W**	**0.0591**	0.0834	**Infinity**	1.0850
BPWB & D2465	**0.1696**	**0.4039**	**Infinity**	0.8115	**SB & CORE**	**0.1933**	**0.3573**	**Infinity**	0.9210
BPWB & E2468	**0.1452**	**0.5883**	**Infinity**	0.9689	**SB & A2344**	**0.1278**	**0.3712**	**Infinity**	1.0571
FBI & SHB	0.0866	0.3028	**25.3400**	1.3230	**SB & B2359**	**0.2098**	**0.3818**	**Infinity**	1.1100
FBI & MPWB	**0.0962**	**0.5775**	40.7300	1.5343	**SB & C2386**	**0.1475**	**0.3535**	**Infinity**	1.4075
FBI & FBO	**0.1380**	**0.3723**	43.1600	1.7345	**SB & D2465**	**0.2033**	**0.4572**	**Infinity**	1.0432
FBI & SB	0.0660	**0.4200**	42.6000	0.9853	**SB & E2468**	**0.1516**	**0.5925**	**Infinity**	1.1837
FBI & FAL	**0.1744**	**0.6641**	**Infinity**	0.5990	**FAL & W**	**0.0918**	0.1412	**Infinity**	1.8472
FBI & W	**0.1657**	**0.6864**	51.6400	0.9033	**FAL & CORE**	**0.2587**	**0.5600**	**Infinity**	0.7360
FBI & CORE	**0.2086**	0.0576	68.1600	0.7861	**FAL & A2344**	**0.1881**	**0.5726**	**Infinity**	0.8475

Populations	θ_{ST}	ρ_{ST}	χ^2	N_m	Populations	θ_{ST}	ρ_{ST}	χ^2	N_m
FBI & A2344	**0.1510**	**0.0236**	Infinity	0.7879	**FAL & B2359**	**0.2673**	**0.5692**	**Infinity**	0.6511
FBI & B2359	**0.2038**	**0.0258**	65.2300	1.1195	**FAL & C2386**	**0.2053**	**0.5413**	**Infinity**	0.8618
FBI & C2386	**0.1321**	**0.0118**	45.6600	1.5531	**FAL & D2465**	**0.2674**	**0.6376**	**Infinity**	0.6512
FBI & D2465	**0.1805**	**0.0096**	62.7200	0.8108	**FAL & E2468**	**0.1935**	**0.7569**	**Infinity**	0.6688
FBI & E2468	**0.1563**	**0.0936**	57.6500	1.0428	**W & CORE**	**0.1862**	**0.5709**	**Infinity**	1.1780
SHB & MPWB	**0.0590**	**0.2069**	37.1000	1.7270	**W & A2344**	**0.1196**	**0.5826**	**Infinity**	1.0360
SHB & FBO	**0.0799**	**0.0649**	43.4000	1.6532	**W & B2359**	**0.2182**	**0.5762**	**Infinity**	0.8583
SHB & SB	0.0417	0.0475	38.5500	1.6306	**W & C2386**	**0.1515**	**0.5520**	**Infinity**	1.2142
SHB & FAL	**0.0869**	**0.2972**	61.1500	0.8289	**W & D2465**	**0.2207**	**0.6560**	**Infinity**	**0.6136**
SHB & W	0.0515	0.2269	28.1500	1.8236	**W & E2468**	**0.1683**	**0.7946**	**Infinity**	0.9976
SHB & CORE	**0.1547**	0.1934	64.5000	1.0857	**CORE & A2344**	0.0128	-0.0140	34.2000	2.5406
SHB & A2344	**0.0859**	0.2110	49.5900	1.4532	**CORE & B2359**	0.0245	-0.0109	37.2000	4.1552
SHB & B2359	**0.1591**	**0.2210**	71.2200	1.2896	**CORE & C2386**	0.0122	-0.0160	34.2800	2.8122
SHB & C2386	**0.1169**	0.1950	66.8400	1.2495	**CORE & D2465**	**0.0429**	0.0268	53.5900	1.8872
SHB & D2465	**0.1738**	**0.3324**	73.5900	0.8575	**CORE & E2468**	**0.0565**	**0.1226**	Infinity	2.3773
SHB & E2468	**0.1276**	**0.5420**	74.3100	1.0943	**A2344 & B2359**	**0.0338**	-0.0113	42.3700	**4.5436**
MPWB & FBO	**0.0825**	0.0058	59.3600	2.0117	**A2344 & C2386**	0.0258	-0.0170	49.3700	2.5198
MPWB & SB	0.0209	0.1103	43.4100	2.2364	**A2344 & D2465**	**0.0443**	0.0120	49.0500	2.4857
MPWB & FAL	**0.0725**	**0.1394**	Infinity	1.7095	**A2344 & E2468**	0.0189	0.0828	34.5900	4.3440
MPWB & W	**0.0559**	-0.0263	47.8300	1.4864	**B2359 & C2386**	**0.0424**	-0.0138	Infinity	3.2161
MPWB & CORE	**0.2334**	**0.5412**	Infinity	1.1877	**B2359 & D2465**	0.0095	0.0026	35.5500	3.9541
MPWB & A2344	**0.1624**	**0.5518**	Infinity	1.3955	**B2359 & E2468**	**0.0556**	0.0777	Infinity	4.3332
MPWB & B2359	**0.2492**	**0.5569**	Infinity	1.3729	**C2386 & D2465**	**0.0470**	0.0060	Infinity	2.2410
MPWB & C2386	**0.1797**	**0.5364**	Infinity	1.5217	**C2386 & E2468**	**0.0492**	0.0780	Infinity	3.7885
MPWB & D2465	**0.2509**	**0.6172**	Infinity	1.2644	**D2465 & E2468**	**0.0530**	0.0209	68.4700	3.2112
MPWB & E2468	**0.1970**	**0.7298**	Infinity	1.3835					

Table 6. Wilcoxon tests for heterozygosity in 14 populations of eelgrass (*Z. marina*) from San Juan Archipelago and Hood Canal, Washington. Values for heterozygote excess are based on 5 or more microsatellite loci for all populations. Populations are composed of multilocus genotypes only. Values in bold are significant at *P* < 0.05 (Bonferroni correction applied).

Population	NA[1]	WILCOXON TEST					
		IAM[3]		TPM[3]		SMM[3]	
		H[2] excess	H deficit	H excess	H deficit	H excess	H deficit
BPWB	20	0.8515	0.1875	0.9453	0.1484	0.9883	0.0195
MPWB	34	0.8516	0.1875	0.9805	0.0270	0.9883	0.0195
FBI	10	0.0234	0.9844	0.0781	0.9453	0.0781	0.9453
FBO	34	0.9609	0.0547	0.9883	0.0195	0.9961	0.0078
SHB	14	0.9766	0.0391	1.0000	**0.0078**	1.0000	**0.0078**
SB	46	0.9922	0.0117	0.5313	0.5313	0.7109	0.3438
FAL	52	0.0156	1.0000	0.6875	0.4063	0.8906	0.3125
W	24	0.9453	0.0781	0.9922	0.0156	1.0000	**0.0078**
CORE	48	0.5000	0.5781	0.7813	0.2813	0.9219	0.2188
A2344	46	0.3203	0.7266	0.8750	0.1563	0.9629	0.0977
B2359	56	0.7695	0.2734	0.9805	0.0273	0.9902	0.0137
C2386	54	0.8438	0.1914	0.9902	0.0137	0.9902	0.0137
D2465	46	0.4219	0.6289	0.8750	0.1563	0.9023	0.1250
E2468	56	0.5273	0.5273	0.9941	0.0098	0.9981	**0.0039**

[1]Number of alleles compared

[2]Ratio of heterozygote excess or deficit (Cornuet and Luikart 1996)

[3]IAM, TPM, SMM = infinite alleles, two-phase and stepwise mutational models of microsatellite evolution, respectively (see text)

183

Appendix I. Genetic variation of all samples at eight microsatellite loci within 14 populations of *Z. marina* in San Juan Archipelago and Hood Canal, Washington. All samples (including clones) are included in analyses.

A — **Combined Analyses**

Populations	N^1	A^2	PA^3	R^4	$H_O{}^5$	$H_E{}^6$	F^7
SJA&W&HC	545	13.38	-	0.50	0.39	0.45	0.130
SJA&W	365	10.38	19	0.32	0.37	0.41	0.101
SJA	348	9.88	17	0.30	0.37	0.42	0.103
HC	180	9.75	15	0.85	0.43	0.43	-0.008

B — **Population Analyses**

	N^1	A^2	AR^3	PA^4	R^5	$H_O{}^6$	$H_E{}^7$	P^8	F^9
San Juan Archipelago (SJA)									
BPWB	50	3.00	2.54	2	0.18	**0.26**	**0.27**	0.88	**0.062**
MPWB	50	4.75	3.79	2	0.33	0.41	0.37	0.88	-0.108
FBI	50	**2.50**	**2.30**	1	**0.08**	0.35	0.32	0.75	-0.094
FBO	50	4.88	3.87	4	0.35	0.35	0.34	0.88	-0.036
SHB	49	3.50	3.15	1	0.13	0.45	0.36	0.75	**-0.260**
SB	49	4.88	4.10	4	0.46	0.45	0.42	0.88	-0.070
FAL	50	4.63	3.89	3	0.51	0.36	0.37	**0.63**	0.030
W	17	3.75	3.75	2	0.69	0.33	0.30	0.88	-0.089
Hood Canal (HC)									
CORE	30	4.38	3.72	2	0.79	0.41	0.35	0.75	-0.165
A2344	30	4.50	3.92	2	0.76	0.45	0.42	**1.00**	-0.062
B2359	30	**5.50**	4.40	**6**	0.93	0.39	0.41	**1.00**	0.038
C2386	30	5.25	**4.45**	**0**	0.90	0.42	0.41	**1.00**	-0.026
D2465	30	4.38	3.81	**0**	0.76	0.40	0.42	**1.00**	0.039
E2468	30	5.00	4.29	5	**0.93**	**0.53**	**0.48**	**1.00**	-0.089

[1] number of samples used in analyses

[2] average number of alleles at eight microsatellite loci

[3] allelic richness (El Mousadik and Petit 1996)

[4] number of private alleles

[5] genotypic richness

[6] observed heterozygosity

[7] unbiased expected heterozygosity (Nei 1987; eq. 7.39, pg. 164)

[8] percent polymorphism

[9] inbreeding coefficient (Wright 1951)

184

Appendix II. Probability of identity (P$_{(ID)}$) and probability of identity between siblings (P$_{(ID)sib}$) computed for each of eight microsatellite loci in 14 populations of *Z. marina* in San Juan Archipelago and Hood Canal, Washington. Values based on all samples, including clones.

POPULATION	N	P$_{ID(UNBIASED)}$	P$_{ID(SIBS)}$	1/$_{PID(UNBIASED)}$	1/$_{PID(SIBS)}$
All Samples Pooled	545	5.22E-06	1.44E-02	191,571	69
San Juan Archipelago (SJA)					
BPWB	50	**3.46E-03**	**8.85E-02**	**289**	**11**
MPWB	50	1.33E-04	3.50E-02	7,541	29
FBI	50	1.85E-03	5.83E-02	541	17
FBO	50	2.28E-04	4.36E-02	4,394	23
SHB	49	3.04E-04	3.84E-02	3,285	26
SB	49	2.47E-05	2.09E-02	40,519	48
FAL	50	4.53E-05	3.01E-02	22,099	33
W	17	2.74E-04	6.72E-02	3,651	15
Hood Canal (HC)					
CORE	30	1.29E-04	4.16E-02	7,764	24
A2344	30	3.77E-05	2.33E-02	26,560	43
B2359	30	5.25E-05	2.64E-02	19,055	38
C2386	30	3.57E-05	2.43E-02	27,988	41
D2465	30	8.07E-05	2.39E-02	12,390	42
E2468	30	**2.18E-05**	**1.38E-02**	**45,809**	**72**

Note: P$_{(ID)sib}$ provides a conservative upper bound on the number of loci necessary for individuals within populations comprised of closely-related indivuals (Waits *et al.* 2001). P$_{(ID)multilocus}$ is the P$_{(ID)}$ given all loci assayed; P$_{shadow}$ is the probability at which another individual with the same genotype will be observed, given the sample frequency of the alleles observed at those loci within the population of interest.

Appendix III. Maps of multilocus genotypes and clones generated in GenClone 1.0. Axes represent distance between populations in meters. Maps are included for (A) BPWB, (B) MPWB, (C) FBI, (D) FBO, (E) SHB, (F) SB, (G) FAL, (H) core004, (I) hdc2344, (J) hdc2359, (K) hdc2386, (L) hdc2465, and (M) hdc2468.

A
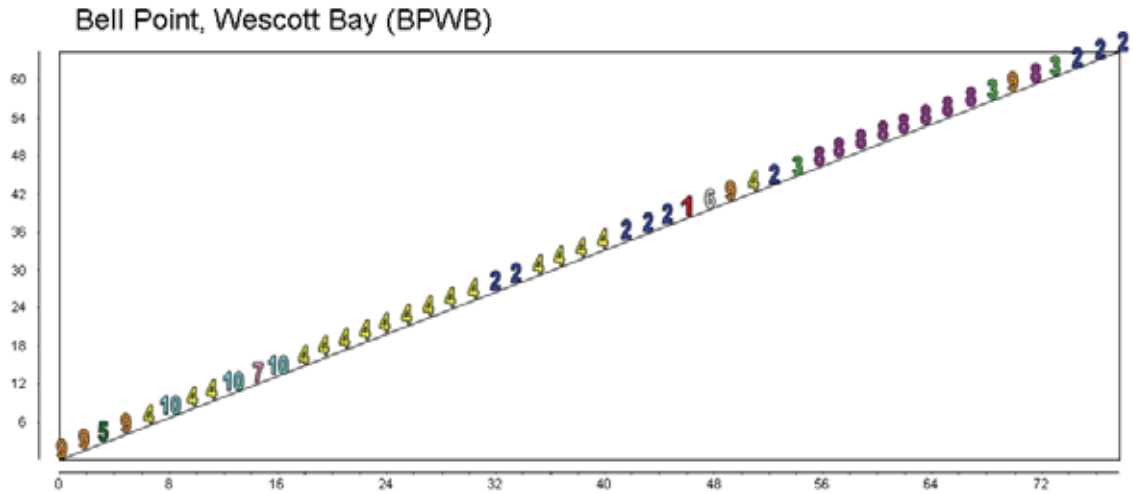
B
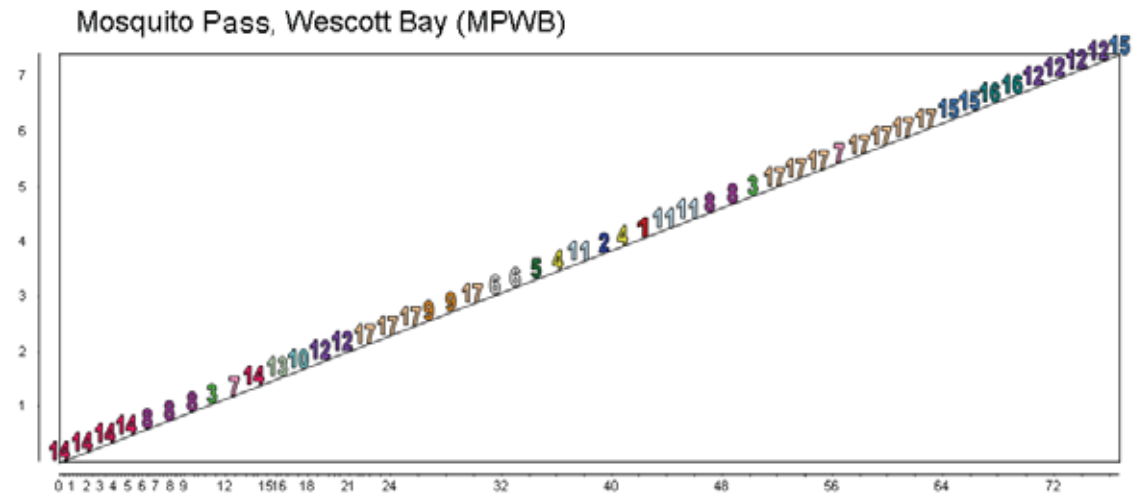
C

Fisherman's Bay Inner (FBI)

D

Fisherman's Bay Outer (FBO)

E

Shoal Bay (SHB)

187

F

Shallow Bay (SB)

G

False Bay (FAL)

H

core004

I

hdc2344

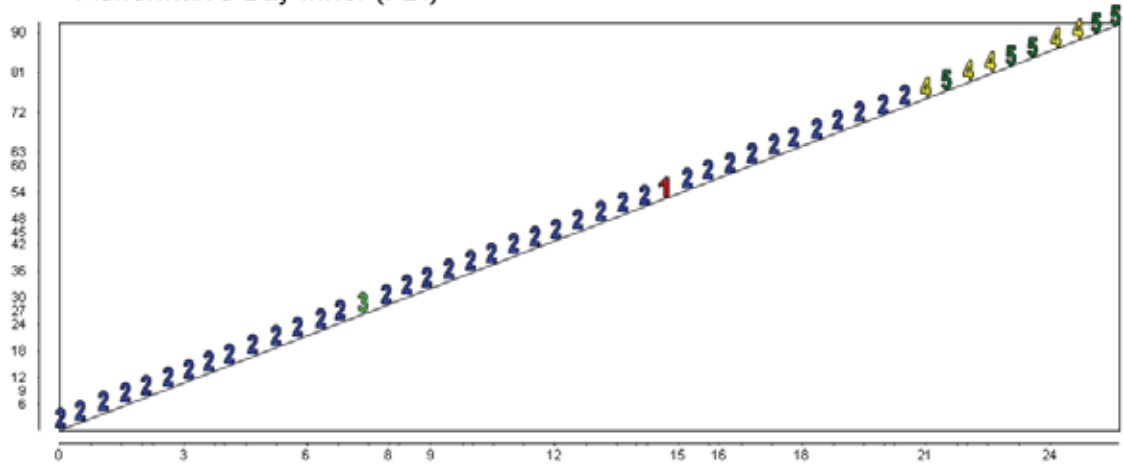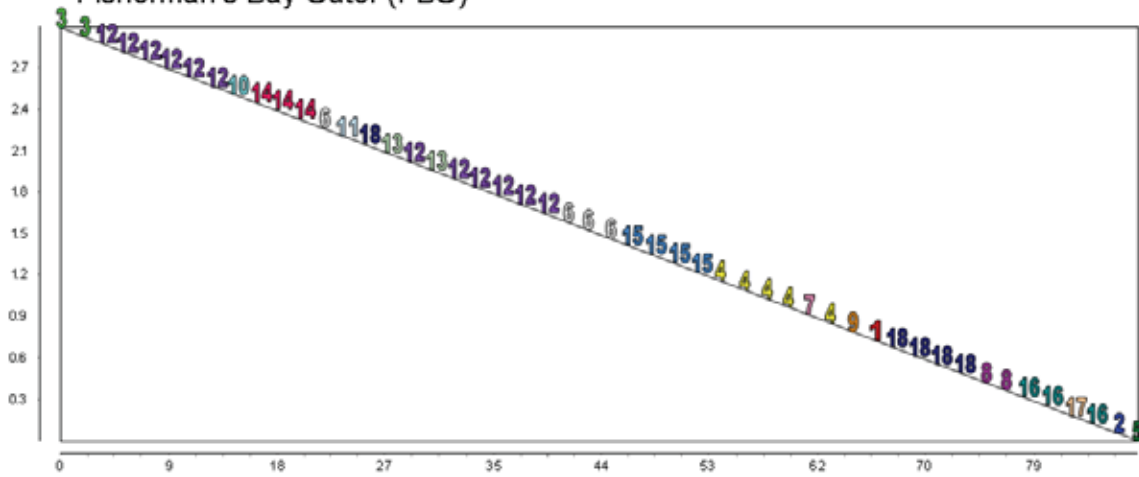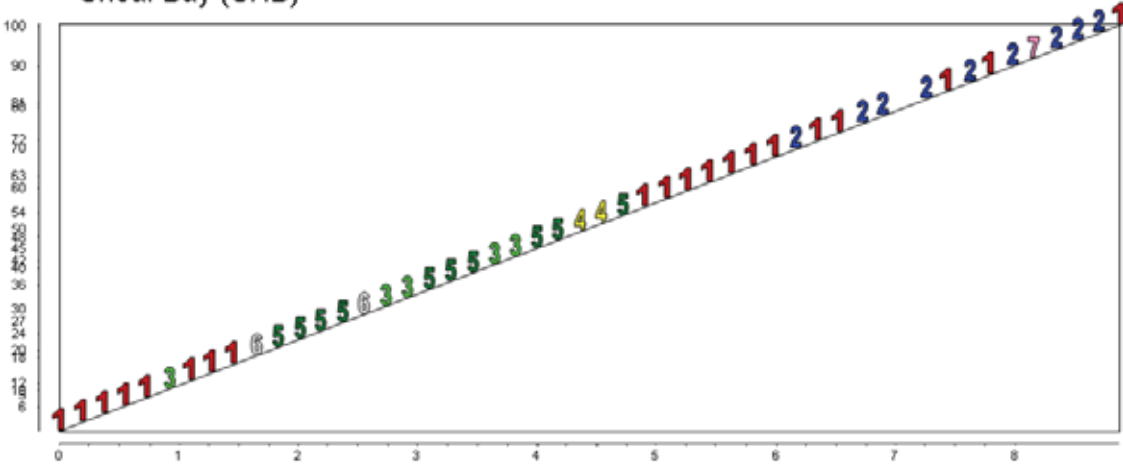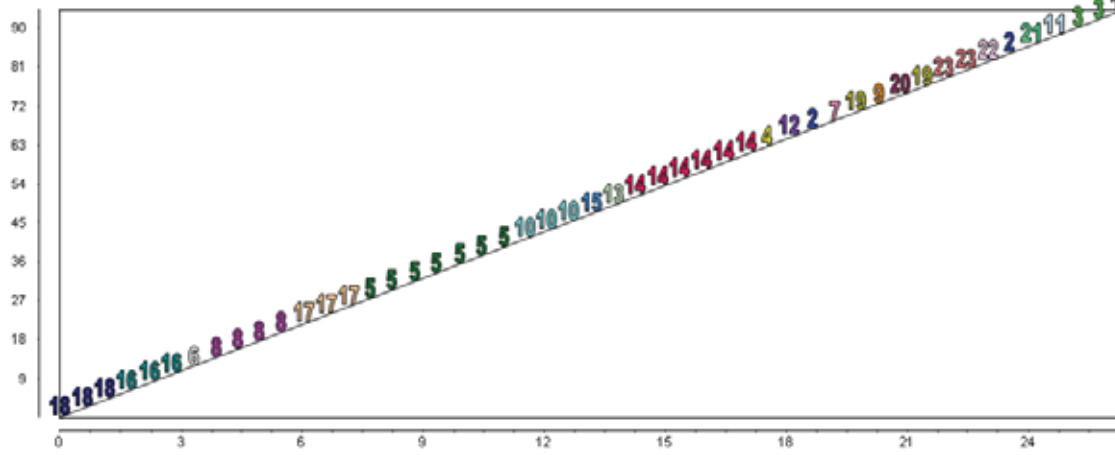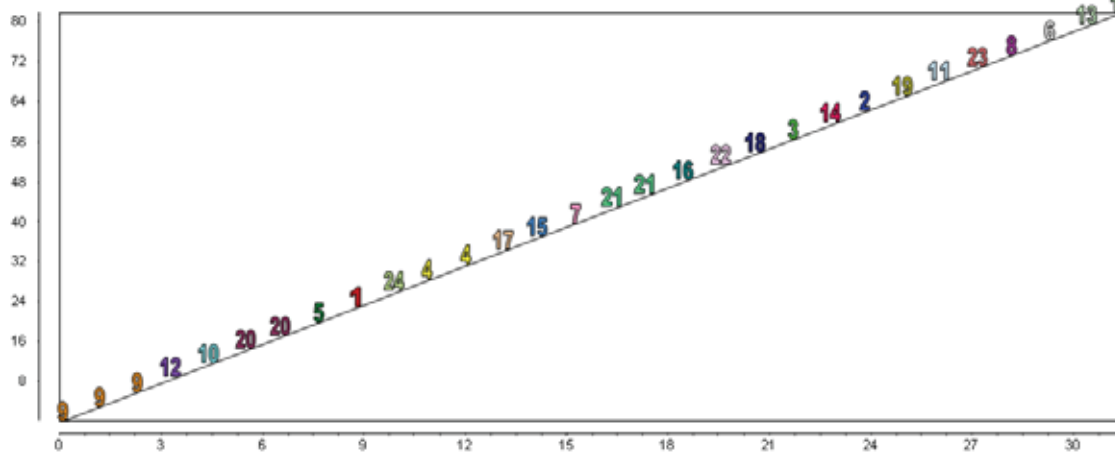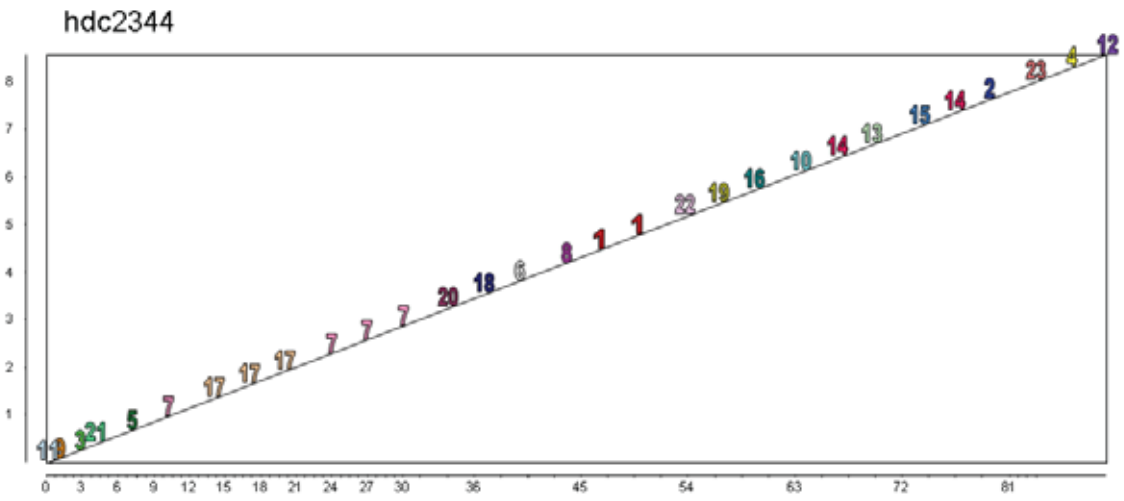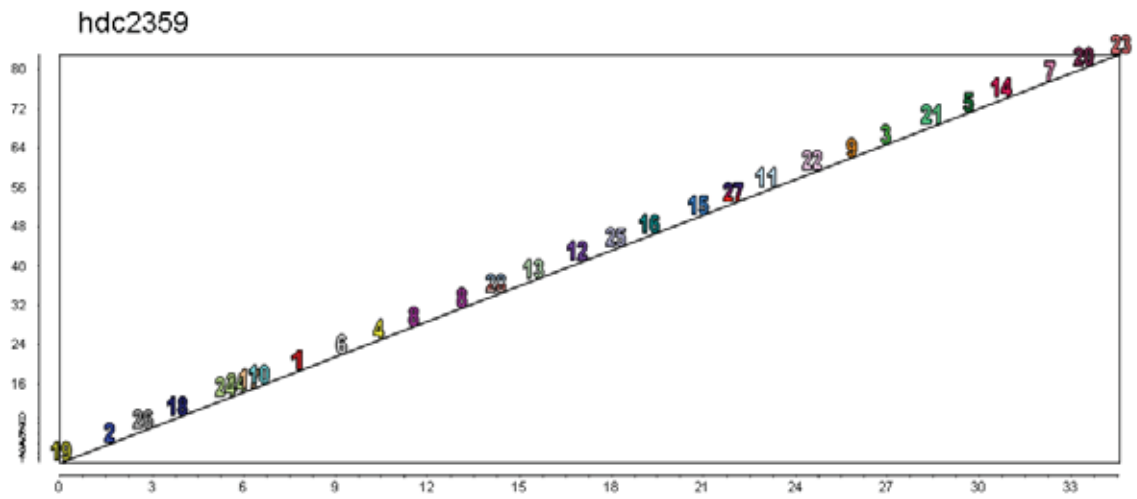*J*

hdc2359

K

hdc2386

189
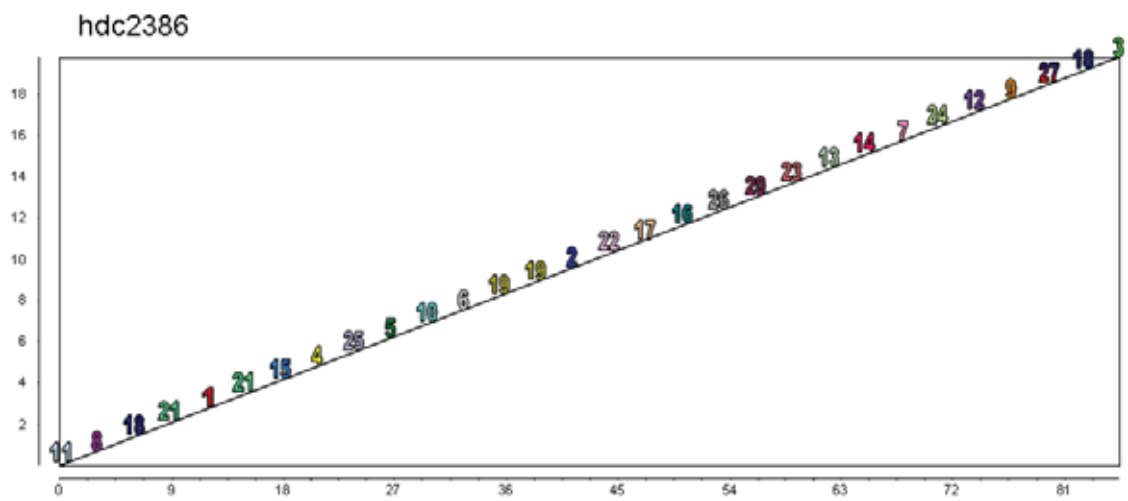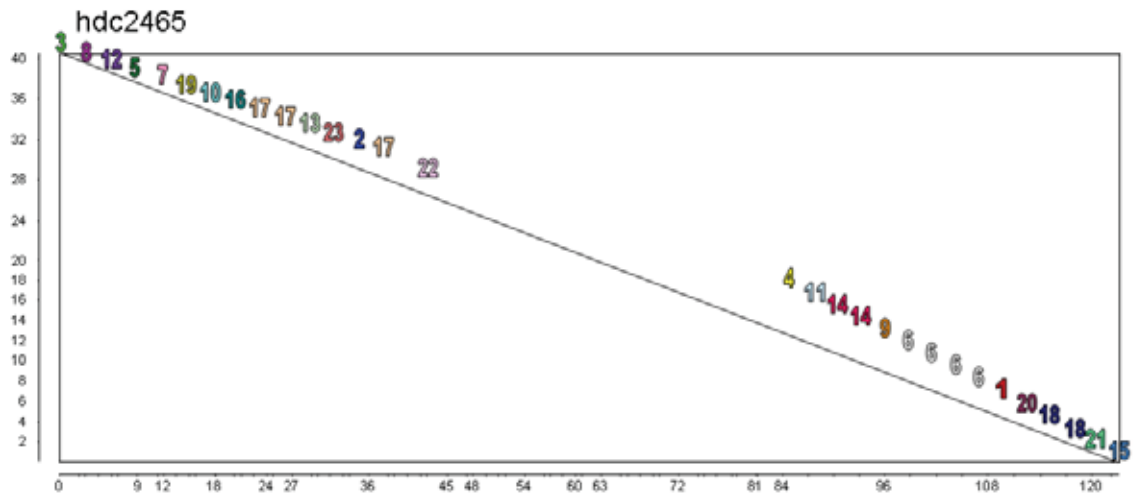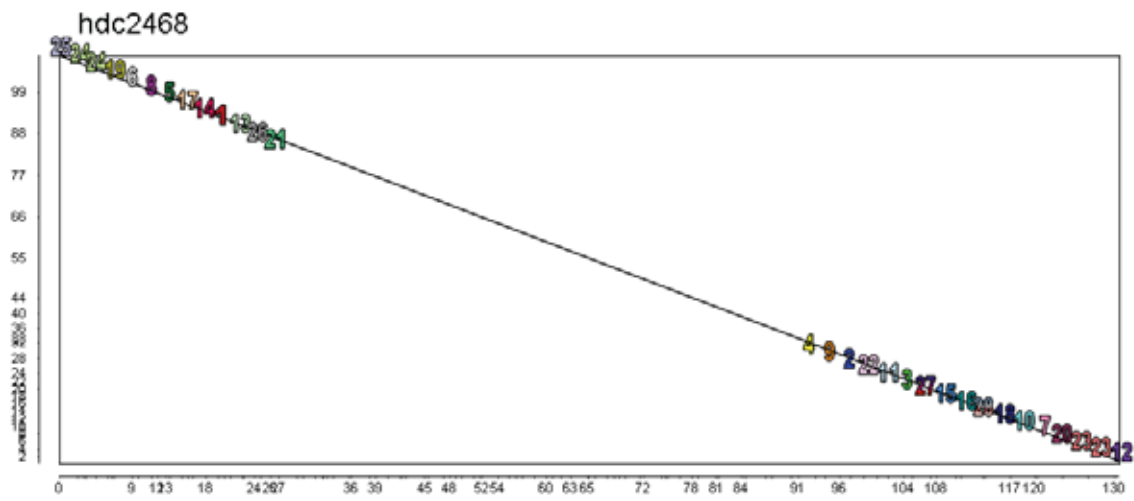
L

hdc2465

M

hdc2468

190
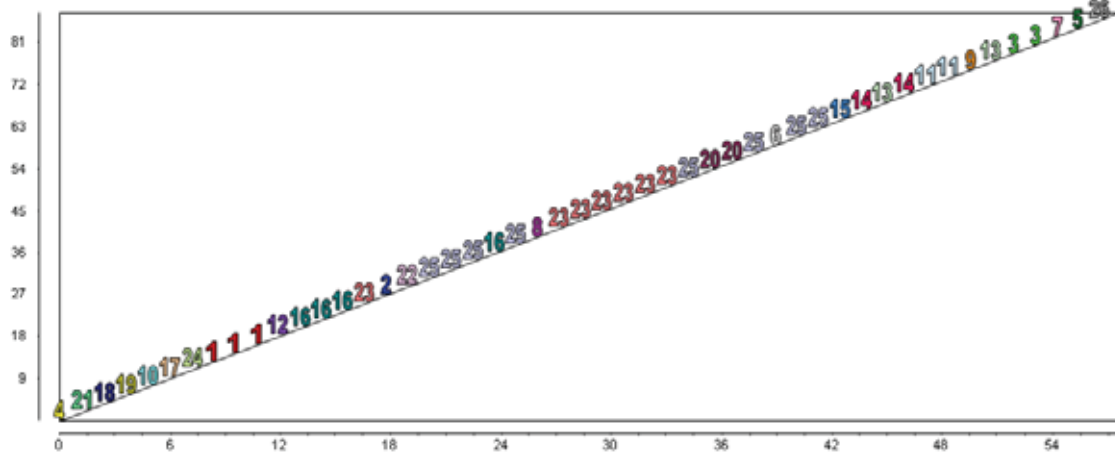
Appendix IV. Pairwise measures of microsatellite differentiation based on analysis of all samples, including clones. θ_{ST} (Weir and Cockerham 1984) across all loci; ρ_{ST} (Slatkin 1995) across all loci, χ^2 (Raymond and Rousset 1995) across all loci. Values significantly different from zero in bold face ($P < 0.005$; values adjusted by a sequential Bonferroni correction).

Populations	θ_{ST}	ρ_{ST}	χ^2	Populations	θ_{ST}	ρ_{ST}	χ^2
BPWB & FBI	0.38693	0.52485	Infinity	FBO & SB	0.10362	0.09270	Infinity
BPWB & SHB	0.18679	0.14187	Infinity	FBO & FAL	0.20610	0.15699	Infinity
BPWB & MPWB	0.17594	0.20203	Infinity	FBO & W	0.10508	0.00707	Infinity
BPWB & FBO	0.10436	0.20770	Infinity	FBO & CORE	0.13869	0.43774	Infinity
BPWB & SB	0.13708	0.06927	Infinity	FBO & A2344	0.11009	0.42620	Infinity
BPWB & FAL	0.25442	0.13959	Infinity	FBO & B2359	0.20482	0.43378	Infinity
BPWB & W	0.14506	0.19943	Infinity	FBO & C2386	0.13708	0.43942	Infinity
BPWB & CORE	0.17970	0.28635	Infinity	FBO & D2465	0.21379	0.48614	Infinity
BPWB & A2344	0.15187	0.26683	Infinity	FBO & E2468	0.16258	0.54789	Infinity
BPWB & B2359	0.24901	0.28464	Infinity	SB & FAL	0.10062	0.08984	Infinity
BPWB & C2386	0.19089	0.27805	Infinity	SB & W	0.19094	0.04047	Infinity
BPWB & D2465	0.26189	0.35933	Infinity	SB & CORE	0.14299	0.42384	Infinity
BPWB & E2468	0.22242	0.47173	Infinity	SB & A2344	0.22979	0.40111	Infinity
FBI & SHB	0.27376	0.62094	Infinity	SB & B2359	0.16715	0.41540	Infinity
FBI & MPWB	0.20856	0.68521	Infinity	SB & C2386	0.24685	0.41623	Infinity
FBI & FBO	0.32551	0.60621	Infinity	SB & D2465	0.16922	0.48948	Infinity
FBI & SB	0.21844	0.62369	Infinity	SB & E2468	0.07755	0.58538	Infinity
FBI & FAL	0.28620	0.72749	Infinity	FAL & W	0.27192	0.17401	Infinity
FBI & W	0.32499	0.80634	Infinity	FAL & CORE	0.21076	0.56087	Infinity
FBI & CORE	0.34757	0.23016	Infinity	FAL & A2344	0.29650	0.53915	Infinity
FBI & A2344	0.30684	0.20415	Infinity	FAL & B2359	0.23426	0.55092	Infinity
FBI & B2359	0.35260	0.21395	Infinity	FAL & C2386	0.31197	0.54193	Infinity
FBI & C2386	0.29411	0.16883	Infinity	FAL & D2465	0.21224	0.61064	Infinity
FBI & D2465	0.35189	0.18368	Infinity	FAL & E2468	0.12892	0.70246	Infinity
FBI & E2468	0.30420	0.19650	Infinity	W & CORE	0.20300	0.59329	Infinity
SHB & MPWB	0.12635	0.18976	Infinity	W & A2344	0.14786	0.56073	Infinity
SHB & FBO	0.13322	0.16128	Infinity	W & B2359	0.02494	0.56982	Infinity

191

Populations	θ_{ST}	ρ_{ST}	χ^2	Populations	θ_{ST}	ρ_{ST}	χ^2
SHB & SB	0.08557	0.10013	Infinity	W & C2386	0.18440	0.56899	Infinity
SHB & FAL	0.14699	0.31971	Infinity	W & D2465	0.26951	0.65307	Infinity
SHB & W	0.09449	0.17299	Infinity	W & E2468	0.19519	0.77764	Infinity
SHB & CORE	0.20479	0.37103	Infinity	CORE & A2344	0.01374	0.01244	47.05
SHB & A2344	0.16095	0.34772	Infinity	CORE & B2359	0.02787	0.01239	55.61
SHB & B2359	0.24259	0.36299	Infinity	CORE & C2386	0.02009	0.01256	52.44
SHB & C2386	0.18387	0.37588	Infinity	CORE & D2465	0.05330	0.00959	Infinity
SHB & D2465	0.27217	0.45834	Infinity	CORE & E2468	0.05124	0.08016	Infinity
SHB & E2468	0.20387	0.56305	Infinity	A2344 & B2359	0.02930	0.00927	49.29
MPWB & FBO	0.15657	0.01261	Infinity	A2344 & C2386	0.02740	0.01067	68.16
MPWB & SB	0.04765	0.05596	Infinity	A2344 & D2465	0.04529	0.01397	66.28
MPWB & FAL	0.08957	0.12435	Infinity	A2344 & E2468	0.02003	0.07698	48.94
MPWB & W	0.10784	0.00936	Infinity	B2359 & C2386	0.04872	0.00962	Infinity
MPWB & CORE	0.24728	0.51870	Infinity	B2359 & D2465	0.01539	0.00331	Infinity
MPWB & A2344	0.19594	0.50178	Infinity	B2359 & E2468	0.05319	0.07788	44.40
MPWB & B2359	0.28506	0.51080	Infinity	C2386 & D2465	0.05807	0.00251	Infinity
MPWB & C2386	0.21318	0.51346	Infinity	C2386 & E2468	0.04807	0.05254	Infinity
MPWB & D2465	0.29284	0.56992	Infinity	D2465 & E2468	0.06206	0.02787	Infinity
MPWB & E2468	0.22024	0.64459	Infinity				

Appendix V. Measures of genetic diversity for populations of eelgrass in Puget Sound, Crown Beach, San Francisco Bay (CRNLE), Yaquina Bay, Oregon (YAB), three sites in Alexander Archipelago, Alaska (FUN, CRAB, NAK), and Izembek Lagoon, Alaska (IZ). Values are based on multilocus genotypes only.

North America Eelgrass Population Analyses

	MLG[1]	A[2]	AR[3]	PA[4]	H_O[5]	H_E[6]
BPWB	7	2.75	1.99	2	0.32	0.33
MPWB	8	3.38	2.26	1	0.39	0.38
FBI	**3**	**2.25**	2.25	1	**0.29**	0.42
FBO	9	3.75	2.32	1	0.38	0.39
SHB	6	3.38	2.42	1	0.42	0.41
SB	10	4.13	2.49	**0**	0.49	0.48
FAL	11	3.75	2.29	1	0.40	0.38
W	6	3.00	2.05	**0**	0.33	0.31
CORE	11	3.38	2.04	1	0.40	0.34
A2344	10	3.75	2.34	1	0.45	0.44
B2359	11	3.75	2.27	**0**	0.40	0.42
C2386	11	4.00	2.27	**0**	0.39	0.40
D2465	11	3.25	2.09	**0**	0.34	0.38
E2468	11	3.75	2.44	**0**	**0.58**	0.50
CRNLE	30	4.38	2.23	**9**	0.36	0.38
YAB	24	6.38	**2.68**	1	0.55	**0.54**
FUN	29	4.75	2.05	7	0.35	0.33
CRAB	28	5.38	**1.84**	3	0.22	**0.23**
NAK	30	6.00	2.04	3	0.31	0.31
IZ	**51**	**7.13**	2.11	8	0.32	0.33

194

Appendix VI. Wilcoxon tests for heterozygosity in 14 populations of eelgrass (*Z. marina*) from San Juan Archipelago and Hood Canal, Washington. Values for heterozygote excess are based on 5 or more microsatellite loci for all populations. Samples identified as clones by multilocus genotype were included in this analysis. Values in bold are significant at *P* < 0.05 (Bonferroni correction applied).

| | | **WILCOXON TEST** | | | | | |
| | | IAM[3] | | TPM[3] | | SMM[3] | |
Population	NA[1]	H[2] *excess*	H *deficit*	H *excess*	H *deficit*	H *excess*	H *deficit*
BPWB	100	0.5313	0.5313	0.9453	0.1484	0.9609	0.0547
MPWB	100	0.0547	0.9609	0.9223	0.0195	0.9883	0.0195
FBI	100	0.0547	0.9609	0.2188	0.9219	0.3438	0.7188
FBO	98	0.8125	0.2344	0.9883	0.0195	0.9961	0.0078
SHB	98	0.0391	0.9766	0.7813	0.2813	0.9453	0.0781
SB	98	**0.0039**	1.0000	0.7109	0.3438	0.9727	0.0391
FAL	100	0.0156	1.0000	0.8906	0.3125	0.9688	0.0469
W	34	0.9766	0.0391	1.0000	**0.0078**	1.0000	**0.0078**
core004	60	0.3438	0.7188	0.7813	0.2813	0.7813	0.2813
hdc2344	60	0.1914	0.8438	0.7266	0.3203	0.8438	0.1914
hdc2359	60	0.7695	0.2734	0.9805	0.0273	0.9902	0.0137
hdc2386	60	0.7266	0.3203	0.9902	0.0137	0.9941	0.0098
hdc2465	60	0.4727	0.5781	0.8750	0.1563	0.9629	0.0977
hdc2468	60	0.4727	0.5781	0.9941	0.0098	0.9981	0.0039

[1]Number of alleles compared

[2]Ratio of heterozygote excess or deficit (Cornuet and Luikart 1996)

[3]IAM, TPM, SMM = infinite alleles, two-phase and stepwise mutational models of microsatellite evolution, respectively (see text)

Appendix VII. Expected and observed heterozygosities for all populations by locus. Populations are composed of all samples, including clones.

Expected Heterozygosities

Locus	BPWB	MPWB	FBI	FBO	SHB	SB	FAL	W	CORE	A2344	B2359	C2386	D2465	E2468
CT3	0.36	0.68	0.65	0.53	**0.76**	0.67	0.81	0.61	0.55	0.64	0.59	0.71	0.66	0.65
CT17	**0.76**	**0.87**	**0.68**	**0.88**	0.75	**0.91**	**0.89**	**0.83**	**0.92**	**0.90**	**0.89**	**0.88**	**0.85**	**0.84**
CT19	0.02	**0.00**	**0.00**	**0.00**	**0.00**	**0.00**	**0.00**	**0.00**	0.48	0.45	0.49	0.47	0.52	0.49
CT20	0.50	0.20	0.32	0.67	0.48	0.40	0.21	0.39	0.40	0.47	0.41	0.41	0.26	0.41
GA1	0.17	0.21	0.59	0.24	**0.00**	0.22	**0.00**	**0.00**	**0.00**	0.18	0.24	0.16	0.44	**0.13**
GA2	0.02	0.43	**0.00**	0.13	0.10	0.39	0.55	0.32	**0.00**	0.28	0.16	**0.07**	0.19	0.50
GA3	0.37	0.02	0.02	0.11	0.28	0.28	0.00	0.11	0.33	0.40	0.43	0.13	0.35	0.43
GA5	**0.00**	0.51	0.32	0.13	0.47	0.51	0.48	0.17	0.16	**0.03**	**0.03**	0.45	**0.10**	0.41

Observed Heterozygosities

Locus	BPWB	MPWB	FBI	FBO	SHB	SB	FAL	W	CORE	A2344	B2359	C2386	D2465	E2468
CT3	0.36	0.72	0.80	0.46	**1.00**	0.82	**0.94**	0.88	0.73	0.80	0.53	**0.90**	0.40	0.70
CT17	**0.72**	**0.78**	**1.00**	**0.90**	**1.00**	**1.00**	**0.94**	**1.00**	**0.93**	**0.93**	**0.80**	0.77	**0.90**	**0.90**
CT19	0.02	**0.00**	**0.00**	**0.00**	**0.00**	**0.00**	**0.00**	**0.00**	0.70	0.53	0.50	0.50	0.63	0.60
CT20	0.32	0.22	**0.00**	0.80	0.59	0.45	0.16	0.24	0.40	0.47	0.43	0.30	0.17	0.53
GA1	0.18	0.24	**1.00**	0.26	**0.00**	0.20	**0.00**	**0.00**	**0.00**	0.20	0.23	0.17	0.43	**0.13**
GA2	0.02	0.50	**0.00**	0.14	0.10	0.27	0.36	0.24	**0.00**	0.20	0.17	**0.07**	0.20	0.50
GA3	0.44	0.02	0.02	0.10	0.29	0.33	**0.00**	0.12	0.37	0.40	0.43	0.13	0.40	0.37
GA5	**0.00**	0.76	**0.00**	0.14	0.61	0.55	0.46	0.18	0.17	**0.03**	**0.03**	0.53	**0.10**	0.47

196

Appendix VII. Neighbor-joining tree illustrating relationships among all populations in San Juan Archipelago. (A) Populations described by samples including multilocus genotypes only; W not included. (B) Populations described by samples including clones; W not included. (C) Populations described by samples including multilocus genotypes only; W included. (D) Populations described by samples including clones; W included. Relationships generated using C_{DE} distances. Bootstrap values (2000 replications) >50% are listed at the node.
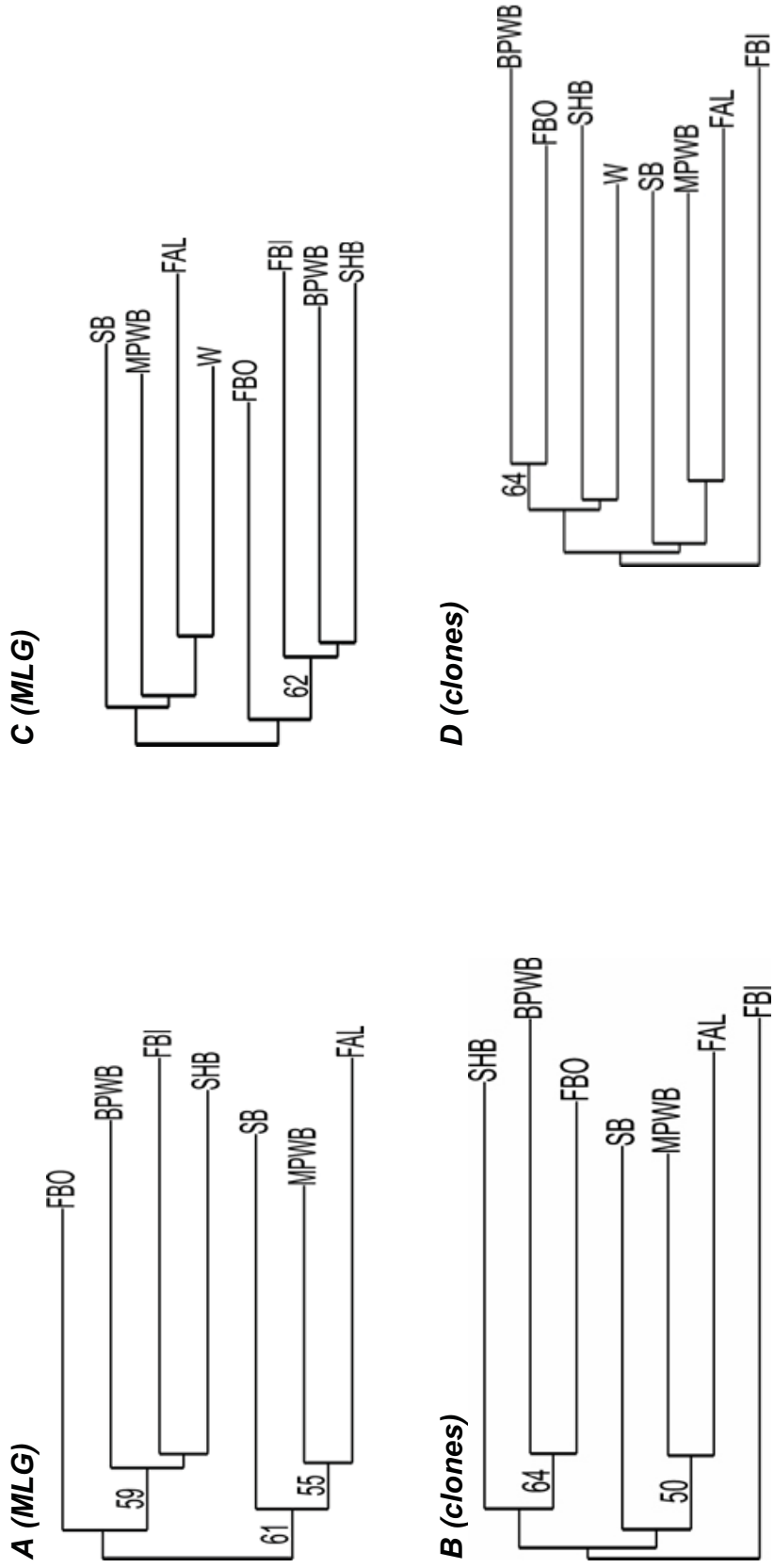
Appendix VII. Neighbor-joining tree illustrating relationships among all populations in Hood Canal. (A) Populations described by samples including multilocus genotypes only; (B) Populations described by samples including clones. Relationships generated using C_{DE} distances. Bootstrap values (2000 replications) >50% are listed at the node.

A

B

197
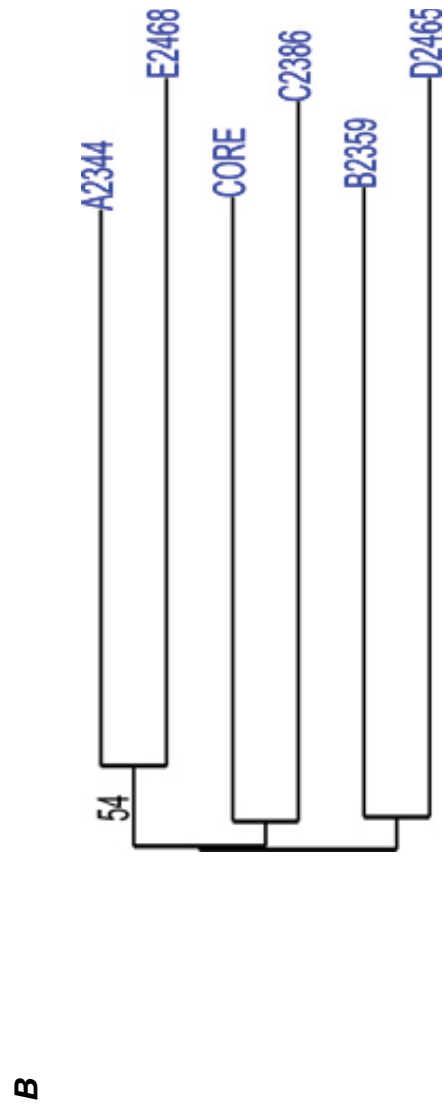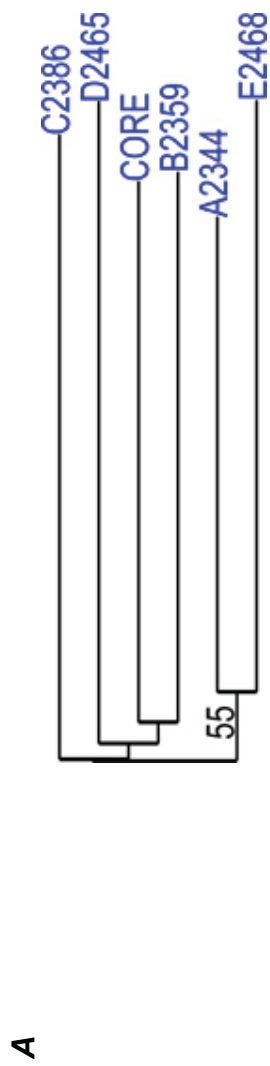
11 Discussion of First Biennium Results

The Eelgrass Stressor-Response Project benefits from a clearly defined primary objective – to identify the causes of observed *Z. marina* losses. This chapter discusses the key results from previous chapters in light of this objective. The goal is to reassess the conceptual framework presented in Chapter 2 and to identify areas in need of refinement or further development to help prioritize future work.

The overall lesson is that there is no simple and easily identifiable stressor that is responsible for *Z. marina* losses. In both the San Juan Island and Hood Canal cases that have been the focus of the first biennium, the observed *Z. marina* losses appear to be only one manifestation of change in complex ecosystems.

11.1 Hood Canal

The conceptual model presented for Hood Canal in Chapter 2 focuses primarily on the role of nutrients and macroalgal growth as well as the underlying role of genetic diversity. With respect to nutrient effects, stable isotope techniques are very useful because of their ability to reveal patterns of ecosystem-scale elemental cycling (Fourqurean et al. 1997). The stable nitrogen isotope ^{15}N in particular is useful in detecting anthropogenic perturbations to nitrogen cycling.

At first glance, there is nothing unusual about the *Z. marina* stable isotopic composition reported in Chapter 3. When the results from all Hood Canal sites and all sampling times are considered together, the overall ranges in $\delta^{13}C$ (-13.7 to -6.7‰) and $\delta^{15}N$ (3.8 to 9.6‰) are consistent with other seagrass values reported in the literature – especially those specific to *Zostera* species (Figure 11-1).

11.1.1 Stable Isotopes – Temporal Variation

However, the magnitude of the temporal variation in $\delta^{13}C$ appears to be unusually high – both relative to the variation in $\delta^{15}N$ and relative to levels reported in the literature. For example, while the mean seasonal variation in $\delta^{15}N$ (1.8‰) is comparable to that found in *Thallassia testudinum* in Florida Bay, the mean seasonal variation in $\delta^{13}C$ found in Hood Canal (4.6‰) is more than two times greater than reported for Florida Bay (1.9‰) (Figure 11-2, Fourqurean et al. 2005). Furthermore, the seasonal variation in $\delta^{13}C$ is also greater than that reported for *Z. marina* in California (~0.5‰; Fourqurean et al. 1978), in North Carolina (~1‰; Thayer et al. 1978), and for *Posidonia oceanica* in Sicily (~2‰, Vizini et al. 2003). The large variation observed in Hood Canal is unusual but not completely unprecedented – a seasonal variation of ~4‰ has been reported for *Z. marina* in South Korea (Min-Sub et al. 2006).

While the magnitude of the seasonal variation in $\delta^{13}C$ is relatively large, the temporal pattern (^{13}C enrichment in spring and summer, depletion in winter) follows the pattern that
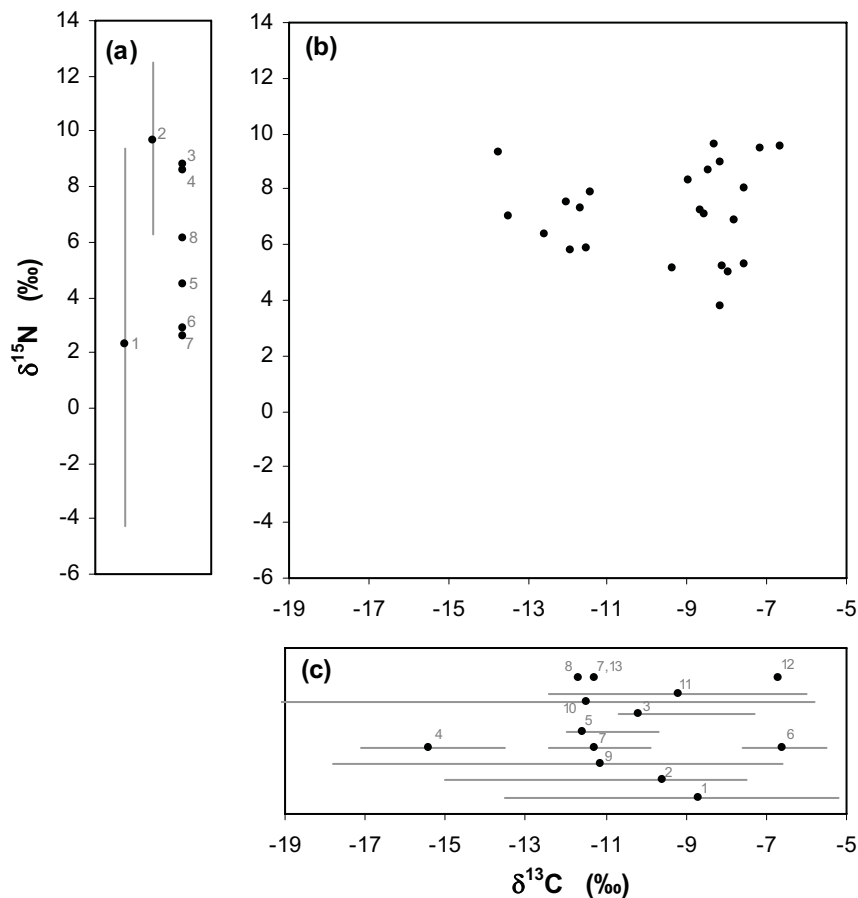
Figure 11-1. Comparison of Hood Canal *Z. marina* leaf carbon and nitrogen isotopic composition to previous seagrass isotope results reported in the literature: (a) literature ^{15}N results; (b) Hood Canal ^{15}N and ^{13}C results from Chapter 3; (c) literature ^{13}C results. The literature results are mean values (points) and overall ranges (bars) when reported.

(1) Fourqurean et al. 2005, *Thallassia testudinum*; (2) Fourqurean et al. 1997, *Zostera marina*; Grice et al. 1996: (3) *Z. capricorni*, (4) *Halophila spinulosa*, (5) *Cymodocia serrulata*, (6) *Syringodium isoetifolium*, (7) *Halodule uninervis*; (8) Guest et al. 2004, *Z. capricorni*; (9) Boyce et al 2001, *Ruppia megacarpa*; Hemminga and Mateo 1996 (10) survey of 48 species in 32 studies, (11) survey of four *Z. marina* studies; (12) Kharlamenko et al. 2001, *Z. marina*; (13) Smit et al. 2006, *Posidonia sinuosa*.

The Boyce et al. (2001) results reflect the combined isotopic signature of leaf, rhizome and root while all the other studies are leaf signatures only. The minimum overall $\delta^{13}C$ value reported by Hemminga and Mateo (1996) is below the scale shown (-20.8‰).

has been consistently reported in other seagrass studies from diverse environments (Fourqurean et al. 2005, Min-Sub et al. 2006, Vizini et al. 2003, Thayer et al. 1978). This pattern has also been observed in other macrophytes, including kelp (Fredriksen 2003). As discussed by Wheat (Chapter 3, p.29), this pattern is thought to be caused by the variation in seasonal growth rates (Fourqurean et al. 2005). This is well supported by experimental mesocosm work (Grice et al. 1996).

To interpret the large magnitude in $\delta^{13}C$ variation, we must consider the mechanism causing seasonal variation. As mentioned by Wheat (Chapter 3, p.29), it is generally thought that there is a reduction in discrimination against the heavier ^{13}C due to the high carbon demand during high productivity (Fourqurean et al. 2005). There could also be a shift in source carbon from isotopically light dissolved CO_2 (e.g. $\delta^{13}C \sim$ -9‰ in open
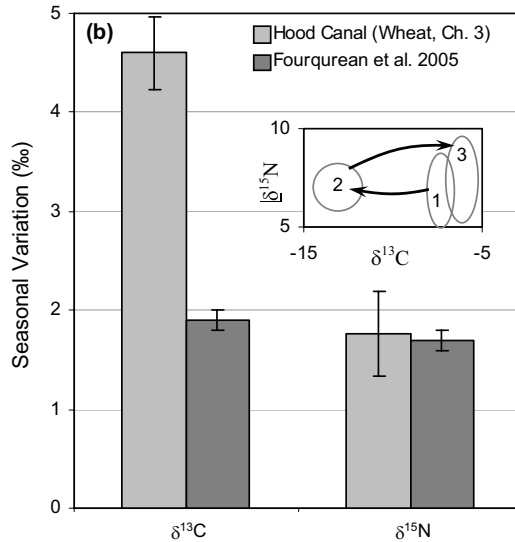
199

Figure 11-2. Seasonal variation in *Z. marina* δ^{13}C and δ^{15}N in Hood Canal. The annual range in isotopic signatures, averaged across sites (±SE) (Wheat, Chapter 3), is shown with comparable results from *Thallassia testudinum* in Florida Bay (Fourqurean et al. 2005). The inset graph shows the shift in Hood Canal seasonal signatures from Aug 2006 (1) to Nov 2006 (2) to Apr 2007 (3). Each ellipse was determined by overall mean values (centroid) and the standard deviations of the mean values (semimajor and semiminor axes) for each sampling period.

marine waters) as it becomes less available (through photosynthetic uptake or seasonal availability associated with water temperature and solubility) to the isotopically heavier and more energetically costly HCO_3^- (e.g. δ^{13}C ~ 0‰ in open marine waters) (Hemminga and Mateo 1996). Given these hypothesized mechanisms, the relatively high magnitude of seasonal variation in *Z. marina* δ^{13}C could possibly be explained by either a relatively large magnitude in seasonal temperature shifts in Hood Canal or a large range in seasonal productivity of *Z. marina* in Hood Canal. Either of these possibilities would suggest unique physiologic adaptations in *Z. marina* in Hood Canal that could explain a unique response to changing stressors with the greater Puget Sound region.

A possible alternative hypothesis explaining the δ^{13}C temporal pattern is the seasonal shifts in the relative importance of marine and riverine carbon sources in Hood Canal. This hypothesis is frequently cited to explain spatial patterns in δ^{13}C (see next section) and the spatial pattern could be considered here as a proxy for site-level temporal pattern. This alternative hypothesis can be dismissed because the temporal pattern in δ^{13}C in Hood Canal *Z. marina* does not correspond well with streamflow patterns in the basin (e.g. the Skokomish River) and previous reports of this pattern encompass environments with very different seasonal rainfall patterns and therefore contrasting patterns of relative marine/riverine influence (Fourqurean et al. 2005 – Florida Bay; Min-Sub et al. 2006 – South Korea; Vizini et al. 2003 – western Sicily; Thayer et al. 1978 – North Carolina).

Although there was temporal variation in δ^{15}N in Hood Canal *Z. marina*, the differences between mean seasonal signatures were small (Aug.→Nov., +0.2‰; Nov. →Apr., +0.3‰). The amplitude of seasonal variation in δ^{15}N was larger at individual sites (mean site range

= 1.8‰; Figure 11-2) but there was little coherence across sites in comparison to the temporal patterns of $\delta^{13}C$ (Figure 11-3). This result suggests that the primary controls on *Z. marina* $\delta^{15}N$ in Hood Canal do not operate at the basin scale, but rather at smaller spatial scales.
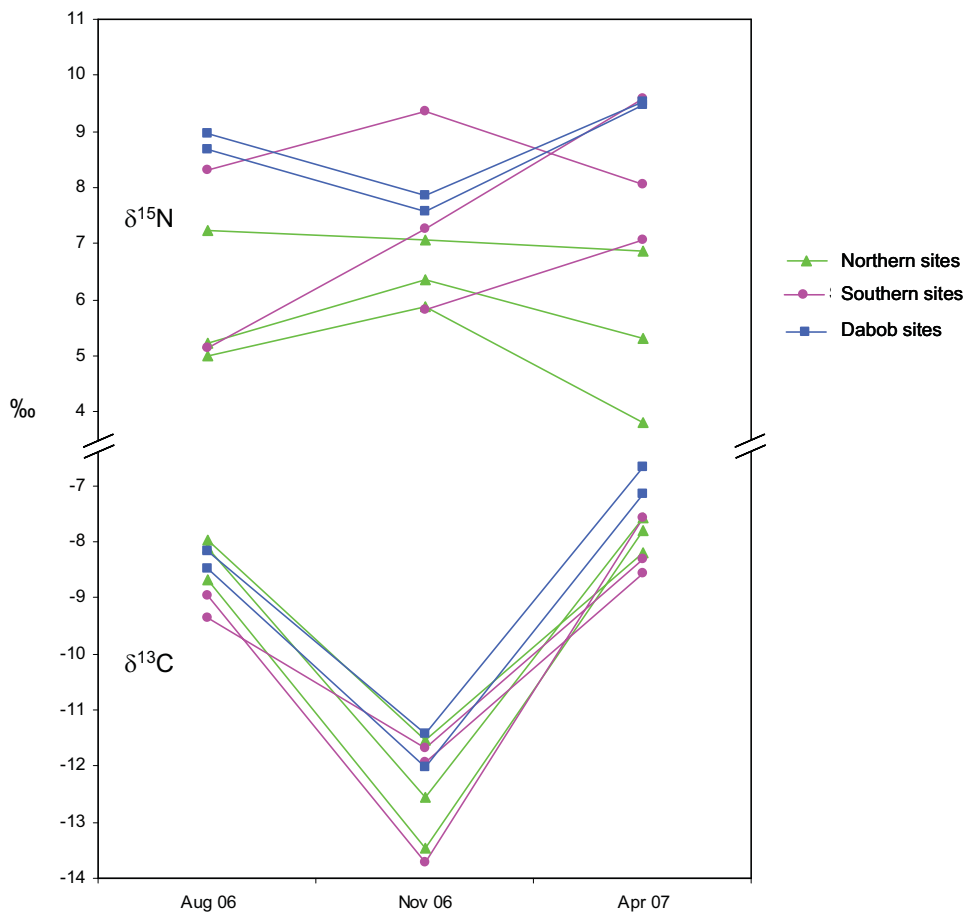

Figure 11-3. Site level temporal patterns in mean $\delta^{13}C$ and $\delta^{15}N$ in Hood Canal *Z. marina* leaves (redrawn from Figure 3-7).

11.1.2   Stable Isotopes – Spatial Variation

There were no regional differences in *Z. marina* $\delta^{13}C$ (Figure 3-7, p.27; see Figure 3-1, p.20, for a map of Hood Canal sites and the northern, southern and Dabob Bay groupings). The factors driving the temporal variation in $\delta^{13}C$ apparently do not vary at the spatial scale of the regions within Hood Canal. Surprisingly, this also suggests that the relative differences in riverine and marine influence, in terms of supplying source carbon to *Z. marina*, are not significant across the Hood Canal regions. This contrasts with other studies of $\delta^{13}C$ patterns which found greater depletion as riverine influence increased – in *Z. marina* (Fourqurean et al. 1997; +2‰ over 20km in Tomales Bay) as well as clams (Fry 1999; +6‰ over 46km transect in San Francisco Bay). This has been attributed to riverine sources having isotopically light dissolved inorganic carbon (e.g. Stribling and Cornwell 1997) and to greater availability of carbon in the form of dissolved CO_2 (isotopically light) due to microbial respiration during decomposition of riverine organic carbon (Fourqurean et al. 1997).

In contrast to the *Z. marina* results, the oyster $\delta^{13}C$ signatures did show differences between regions with the southern sites being relatively depleted by about 1-2‰ (Figure 3-6, p.26). This is consistent with the observations of Fry (1999) and Fourqurean et al. (1997). The discrepancy between the *Z. marina* and oyster results suggests that freshwater influence is indeed greater in southern Hood Canal but that perhaps the isotopic signatures vary between the components of riverine carbon inputs – in particular the dissolved inorganic component (utilized by *Z. marina*) and the particulate organic components (utilized by oysters).

Wheat (Chapter 3) observed clear differences between regions in $\delta^{15}N$ for both the *Z. marina* and oysters. In general, the ^{15}N levels in marine biota increase as the local inputs of wastewater increase (Carmichael et al. 2004, McClelland and Valiela 1998, Carruthers et al. 2005, Fourqurean et al. 2005, Fry 1999, Grice et al. 1996). Steffy and Kilham (2004) showed a clear relationship between enrichment of ^{15}N in aquatic food webs and upland density of septic systems over spatial scales < 10km. Wheat (Chapter 3) concludes that the relatively depleted values of $\delta^{15}N$ at the northern sites in both *Z. marina* (Figure 3-7, p.27) and oysters (Figure 3-6, p.26) indicate a relatively low influence of anthropogenic nitrogen. The $\delta^{15}N$ signatures suggest anthropogenic influence on nitrogen cycling in both Dabob Bay and southern sites.

This result is also seen in the seasonal data at individual sites (Figure 11-3, p.201). Results from the Dabob Bay and southern sites generally reflect enrichment in ^{15}N in April which could be explained by the period of higher rainfall and presumably greater leaching of anthropogenic nitrogen that preceded the April sampling. In contrast, the northern sites show no enrichment in ^{15}N in April. An important exception to this interpretation is the April depletion in ^{15}N seen at hdc2359 – a southern site at Sunset Beach near Lynch Cove that has had consistent observations of declining *Z. marina* (Appendix B). This anomalous result deserves further exploration. This exploration would hopefully lead to either rejection of the explanation given here to explain ^{15}N patterns or to the discovery of important local processes that deviate from the broader regional patterns and perhaps critical to understanding decline at this site.

Given that DNR's monitoring project, SVMP, has found significant *Z. marina* decline at *both* southern and northern sites with their contrasting ^{15}N signatures (see Appendix B, p.222), it is unlikely that nitrogen inputs from septic systems are directly responsible for these declines. This conclusion needs to be subject to further scrutiny especially since the total concentration of nitrogen has not been considered, only the relative contribution of anthropogenic nitrogen inferred from $\delta^{15}N$ signatures. The indirect effects of nitrogen on macroalgal blooms also have not been considered.

It is important to note that anthropogenic perturbations to the nearshore nitrogen cycling may occur on a very localized scale. Localized groundwater inputs enriched in ^{15}N have been shown to enrich *Z. marina* and macroalgae on scales of tens of meters and produce local eutrophication effects normally associated with enclosed bays (Maier and Pregnall 1990).

11.1.3   Genetic Analysis
The genetic analysis of selected Hood Canal *Z. marina* populations (Chapter 10) addresses a key element of the conceptual framework presented in Chapter 2. This work represents the first analysis comparing genetic patterns in *Z. marina* in Hood Canal and the San Juan Archipelago.

The basic premise that motivated this work is that some *Z. marina* populations may be more vulnerable to decline under a given set of stressors due to genetic isolation. This would result in a loss of gene flow into the population, loss of genetic variation and reduced adaptive potential (Hedrick 1996). In reality, the genetic assessment of a population is multi-dimensional in nature and rests on a number of potentially conflicting genetic parameters.

The analysis presented in Chapter 10 focused on eight microsatellite loci found in *Z. marina* chromosomes. An individual locus is simply a physical location of a gene along a chromosome (Hartl and Jones 2000). In cases where a particular gene is found to vary within a population, this is called polymorphism and the alternate forms of the gene are called alleles. The study utilized a type of polymorphism that consists of repeating DNA sequences and is useful for assessing the degree of genetic relatedness between individuals. Loci where genes exhibit this type of polymorphism in a population are called microsatellites. Polymorphism represents a form of genetic diversity.

In each individual, there are two copies of each chromosome. If the two genes at a particular locus are indistinguishable, the individual is said to be homozygous. If a locus has two different alleles the individual is said to be heterozygous. The level of heterozygosity in a population is another measure of genetic diversity.

The main results presented in Chapter 10 fall into three categories:
- Assessment of clonality
- Assessment of genetic diversity
- Assessment of population substructuring

Clonality is a measure of the membership of individual genetic samples to larger clones. Greater membership of samples in clones reduces the number of unique genotypes at a site. The numbers of unique multi-locus genotypes (either individual plants or clones) that were identified by Rearick et al. (Chapter 10) are shown graphically in Figure 11-4 together with the genotypic richness which normalizes the number of genotypes by sample size. Overall, Hood Canal had greater genotypic richness (range: 0.76 – 0.93; mean: 0.85) than the San Juan Archipelago (range: 0.08 – 0.51; mean: 0.30).
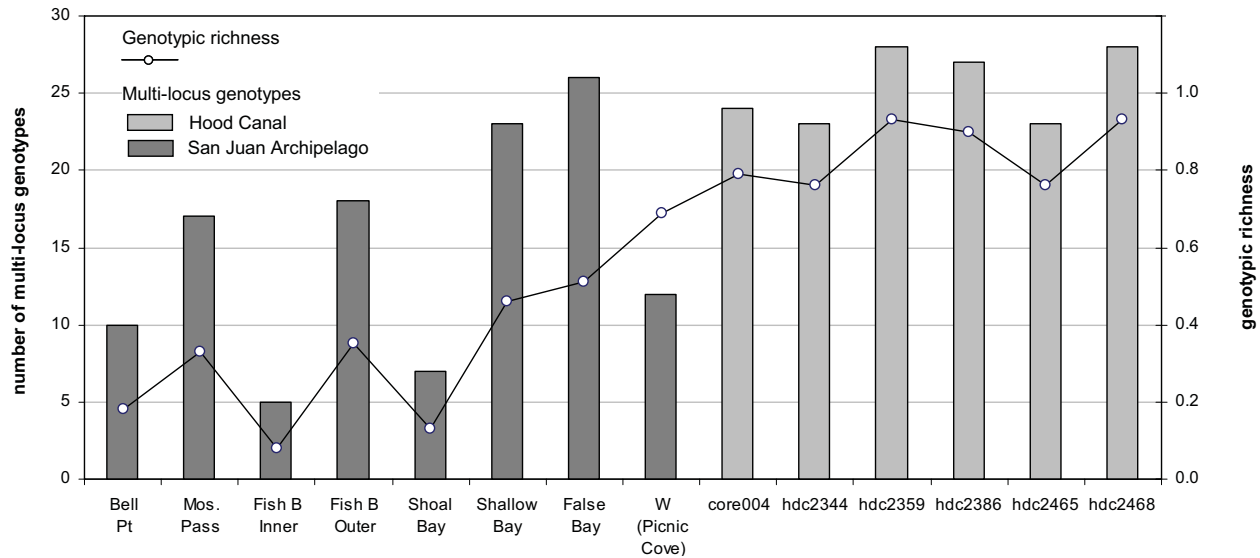
Figure 11-4. Measures of clonality of *Z. marina* at six Hood Canal sites and eight San Juan Archipelago sites. The presence of more extensive clones leads to lower numbers of unique multi-locus genotypes and lower genotypic richness. Data from Table 3 in Chapter 10. Mos. Pass = Mosquito Pass; Fish B = Fisherman's Bay; W is used to distinguish results from Picnic Cove collected earlier (2000) with somewhat different protocols.

Genetic diversity was assessed using parameters that included the three shown in Figure 11-5: allelic richness, expected heterozygosity and percent polymorphism across the eight microsatellites. Hood Canal displayed greater genetic diversity than the San Juan Archipelago in terms of percent polymorphism but the results were similar between the two regions for average allelic richness and expected heterozygosity. In general these results were also similar to *Z. marina* genetic diversity observed in California, Oregon and Alaska (Appendix V of Chapter 10, p.195).

The most striking result in the Hood Canal populations is the fact that core004 (Lynch Cove) has markedly lower measures of genetic diversity for all three parameters. This site has by far the greatest abundance of *Z. marina* within Hood Canal (Figure 2, Appendix B) with no evidence of decline (Table 1, Figure 1, Appendix B). Anecdotal field observations suggest that the *Z. marina* at this site is very productive and not stressed. In contrast, hdc2344 and hdc2359 are sites with clear signs of *Z. marina* decline but with higher levels of genetic diversity.

The assessment of population substructuring found significant substructuring in the Hood Canal populations but less so than in the San Juan Archipelago populations. This suggests that while the Hood Canal populations have evolved into locally-adapted subpopulations, there is greater gene flow and regional genetic homogenization relative to populations in the San Juan Archipelago. No genetic signature was detected that would suggest demographic bottleneck in any of the populations studied.
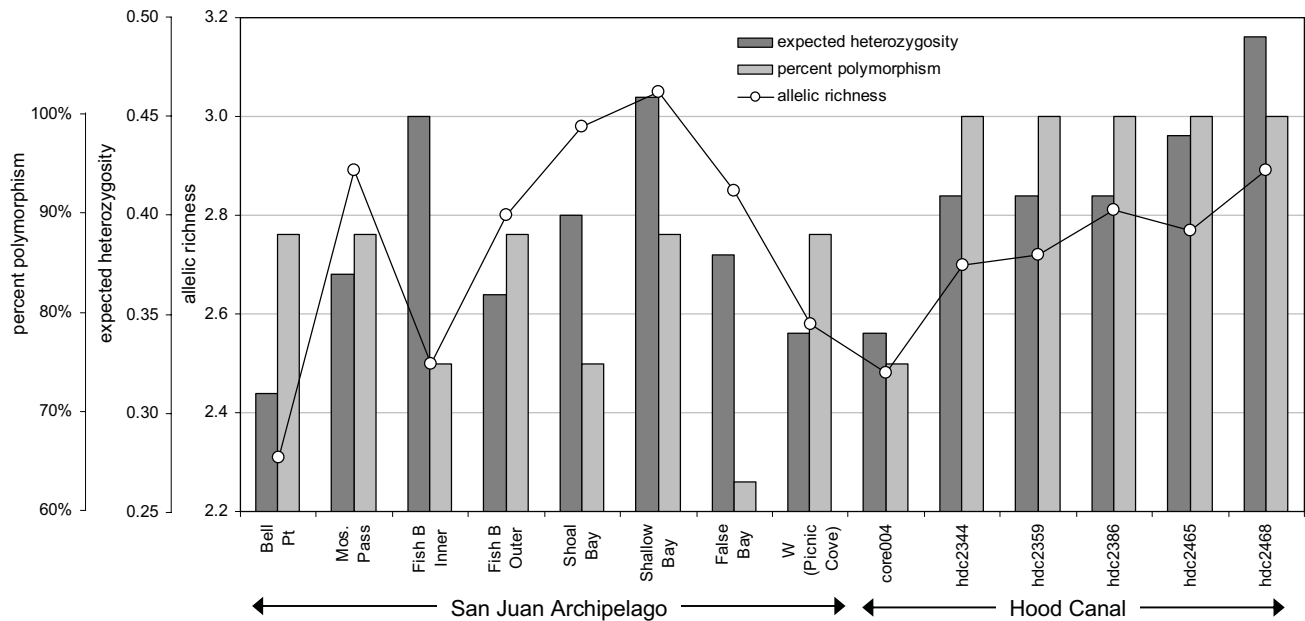
Figure 11-5. Genetic diversity of *Z. marina* at six Hood Canal sites and eight San Juan Archipelago sites as measured by allelic richness, expected heterozygosity and percent polymorphism. Data from Table 3 in Chapter 10. Mos. Pass = Mosquito Pass; Fish B = Fisherman's Bay; W is used to distinguish results from Picnic Cove collected earlier (2000) with somewhat different protocols.

11.2   Westcott Bay

Based on initial field observations and discussions, high levels of turbidity emerged as a central hypothesized stressor causing *Z. marina* decline at the head of Westcott Bay (Chapter 2). The continuing analysis of field data collected in the 2007 season will hopefully contribute to the critical evaluation of this hypothesis. The results of those analyses will be presented in a later report.

The main work completed in 2006-2007 that relates to *Z. marina* in Westcott Bay includes the analysis of genetic patterns, leaf physiology, growth rates in contrasting sediments and effects of the Fraser River. Detailed studies of substrate, bathymetry and circulation in the Westcott Bay area, as well as plant morphology provide important baseline data to support future comparative studies as well as critical input data needed to support future modeling work.

11.2.1   Genetic Analysis

The primary basis for evaluating the genetic characteristics of *Z. marina* populations in the Westcott Bay area, and more broadly in the San Juan Archipelago, is comparison with Hood Canal populations. In this comparison, the populations in the San Juan Archipelago populations overall have lower genotypic richness, lower genetic diversity in terms of frequency of polymorphism, and greater population substructuring.

Most importantly, the Bell Point population had the lowest genetic diversity of any population examined by Rearick et al. (Chapter 10, Figure 11-5). This population also had

relatively low genotypic richness. This is notable because this population is the last remaining population when moving from the mouth of the bay at Mosquito Pass toward the head of Westcott and this population is thought to be in decline. Beyond Bell Point (toward the head of Westcott) there has been complete loss of *Z. marina*. This suggests the possibility of population substructuring within the Westcott Bay complex with a loss of diversity relative to populations outside the bay. This would be consistent with a pattern of within-embayment substructuring reported by Muñiz-Salazar et al. (2006) within an embayment with restricted water flow in northern Mexico.

A comparison of genetic and geographic distances (particularly as measured by the Principal Components Analysis; Figure 3, Chapter 10) also suggests some level of genetic isolation of the Bell Point populations. It is widely accepted that the loss of genetic diversity has a negative effect on population viability (Hedrick 1996). However this is a general relationship that may not hold in any specific example since a multitude of factors play a role in population viability.

11.2.2   Leaf Physiology
The overall objective of the leaf physiological measurements (Chapter 6) was to assess whether there were detectable differences in leaf physiology in *Z. marina* populations in the San Juan Archipalago, including Bell Point within the Westcott Bay complex. This information is important to assess two relevant hypotheses: (1) the genotypes present at sites of decline have inherently lower rates of net photosynthesis and are therefore less resilient under conditions of increased stress; (2) the populations in decline would typically resemble surrounding populations in terms of rates of net photosynthesis but under conditions of increased stress net photosynthesis declines and overall plant performance is reduced.

The study of Selting et al. (Chapter 6) was not designed to distinguish between these two hypotheses but to produce results for evaluation of these hypotheses together – whether they merit further consideration or they are unlikely to be true. The key result from the perspective of the Eelgrass Stressor – Response Project is that Bell Point appears to have reduced rates of light-saturated net photosynthesis (P_{max}) and greater rates of dark respiration (R_d) relative to Picnic Cove and Mosquito Pass. This is suggested by inspection of both P_{max} and R_d data as shown in Figure 11-6 even though statistical significance was only found in the case of R_d. For P_{max}, Picnic Cove was found to have significantly higher values but Mosquito Pass and Bell Point could not be distinguished. Inspection of Figure 11-6 suggests the possibility that Bell Point does have reduced rates of P_{max} but this was not detected because of limited statistical power.

These results indicate there is a reasonable likelihood that physiological performance is reduced at Bell Point. There are a number of possible explanations for this. This may be an inherent characteristic of the *Z. marina* genotypes represented at Bell Point. The genetic uniqueness of the Bell Point population that emerged from the genetic analysis is consistent with this explanation. Environmental conditions in-situ may further limit limiting physiological performance.
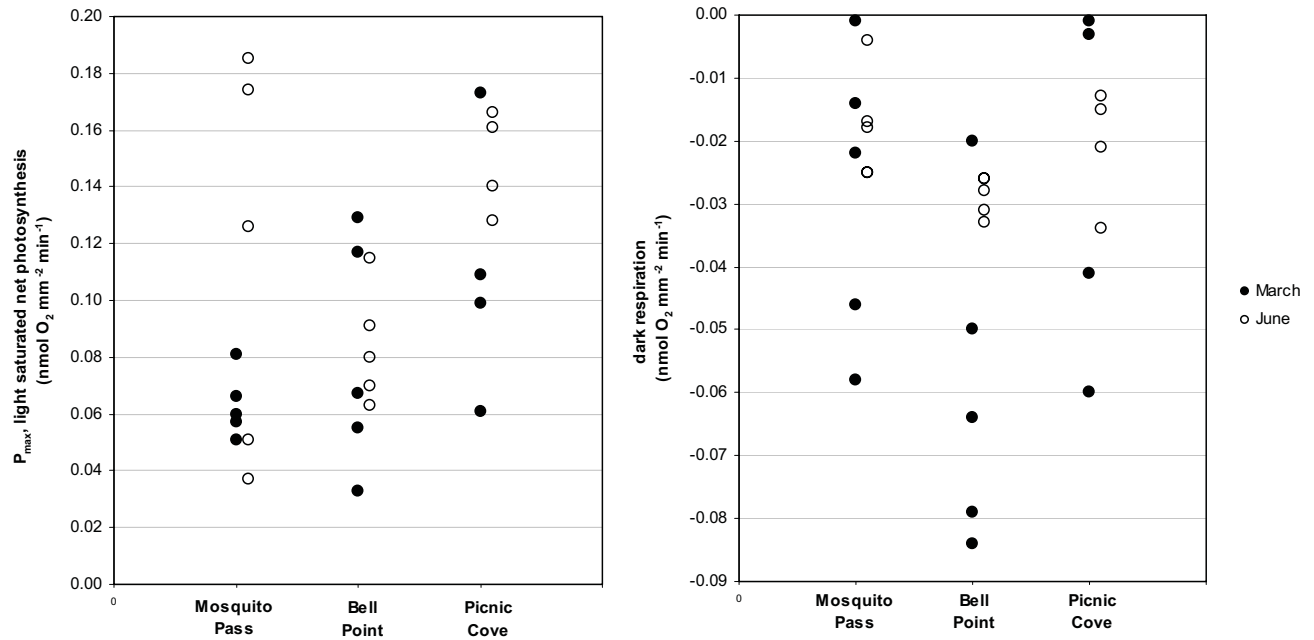
Figure 11-6. Leaf physiology results from Bell Point, Mosquito Pass and Picnic Cove. Data from Selting et al. (Appendix 1 of Chapter 5).

Such environmental conditions could include gradients in total dissolved inorganic carbon (DIC), which has been shown in the Baltic to explain a 38% drop in net photosynthesis (Hellblom and Björk 1999). The concentration of DIC has been shown to be an important factor limiting of seagrass photosynthesis (Invers et al. 2001). Gradients in pH could also play a role in patterns of photosynthesis through its control on the relative availability of DIC in the form of HCO_3^- or dissolved CO_2. Gradients in temperature have also been shown to directly affect photosynthesis (Masini and Manning 1997).

11.2.3   Sediment Composition Effects

The mesocosm experiment described in Chapter 7 addressed the hypothesis that the current absence of *Z. marina* at the head of Westcott Bay is associated with sediment characteristics – particularly sediment texture and organic matter content. Using plants harvested from Picnic Cove, growth rates were measured for individuals planted in sediment from the head of Westcott Bay, Mosquito Pass and Picnic Cove. The results showed no discernable difference in growth rates. This supports rejecting the hypothesis that sediment texture and organic matter content have an effect on plant performance at the head of Westcott Bay.

As noted by Hughes and Wyllie-Echeverria (Chapter 7), it is important to acknowledge limitations on the scope of the experiment. Most importantly, the sediment was significantly disturbed in setting up the mesocosm experiment thereby perturbing the *in-situ* porewater geochemistry. Any stressors related to sediment porewater geochemistry were therefore outside the scope of this experiment (e.g. sulfide accumulation, anerobic conditions).

11.2.4   Fraser River Influence

Chapter 9 examines water quality data on five dates in the late spring of 2007 and MODIS imagery on one of these dates to characterize the nature of Fraser River influence in the San Juan Archipelago in this time period. This work provides an opportunity to assess the likelihood that the Fraser River provides a major stressor within the Westcott Bay complex – either directly through elevated turbidity or lowered salinity or possibly through some unidentified indirect effects.

The results provided clear evidence of Fraser River influence within the San Juan Archipelago with a discrete intrusion event captured in the data series. However, there was no evidence that the plume reached the west side of San Juan Island and the Westcott Bay complex in particular. In fact, on May 29, 2007 while the plume signal in the water quality data was strong in President's Channel and San Juan Channel, the water characteristics in Spieden Channel, the first point on the route to the Westcott Bay area, retained ambient characteristics – the Fraser plume was not detected. This pattern is clear in the temperature (Figure 2, Chapter 9), salinity (Figure 5, Chapter 9) and chlorophyll concentration data (Figure 8, Chapter 9). The May 29 MODIS imagery also does not provide any evidence for Fraser River influence in the Westcott Bay area. Spieden Channel to the north of San Juan Island and Haro Strait to the west have low reflectance values (Figure 9, Chapter 9) indicating an absence of the Fraser River plume in a broad zone around the Westcott Bay area.

The limited scope of this study does not support rejection of the hypothesis of Fraser River influence but the evidence of a plume in some areas but not in the Westcott Bay area certainly does not support the hypothesis either. The study of Feely and Lamb (1979) provides another examination of the extent of Fraser River plumes in the San Juan Archipelago using satellite imagery and this study also does not reveal clear support for the hypothesis of Fraser River influence.

References

Boyce, M.C., P. Lavery, I.J. Bennett and P. Horwitz. 2001. Spatial variation in the δ^{13}C signature of *Ruppia megacarpa* (Mason) in coastal lagoons of southwestern Australia and its implication for isotopic studies. **Aquatic Botany**, 71:83-92.

Carmichael, R.H., B. Annett and I. Valeila. 2004. Nitrogen loading to Pleasant Bay, Cape Cod: application of models and stable isotopes to detect incipient nutrient enrichment of estuaries. **Marine Pollution Bulletin**. 48:137-143.

Carruthers, TJB; van Tussenbroek, BI; Dennison, WC. 2005. Influence of submarine springs and wastewater on nutrient dynamics of Caribbean seagrass meadows. **Estuarine, Coastal and Shelf Science**. 64(2-3):191-199.

Feely, R.A. and M. F. Lamb, 1979, A Study of the Dispersal of Suspended Sediment from the Fraser and Skagit River into Northern Puget Sound Using Landsat Imagery, Report

from the NOAA Pacific Marine Environmental Laboratory to the EPA MESA Project, EPA-600/7-79-165, 46pp.

Fourqurean, J.W., S.P. Escorcia, W.T.Anderson and J.C. Zieman. 2005. Spatial and Seasonal Variability in Elemental Content, δ^{13}C, and δ^{15}N of *Thalassia testudinum* from south Florida and its Implications for Ecosystem Studies. **Estuaries**. 3:447-461.

Fourqurean, J.W., T.O. Moore, B. Fry and J.T. Hollibaugh. 1997. Spatial and temporal variation in C:N:P ratios, δ^{15}N, and δ^{13}C of eelgrass *Zostera marina* as indicators of ecosystem processes, Tomales Bay, California, USA. **Marine Ecology Progress Series**. 157:147-157.

Fredriksen, S. 2003. Food web studies in a Norwegian kelp forest based on stable isotope (δ^{13}C and δ^{15}N) analysis. **Marine Ecology Progress Series**. 260:71-81.

Fry, B. 1999. Using stable isotopes to monitor watershed influences on aquatic trophodynamics. **Canadian Journal of Fisheries and Aquatic Sciences**. 56:2167-2171.

Grice, A.M., N.R. Loneragan and W.C. Dennison. 1996. Light intensity and the interactions between physiology, morphology and stable isotope ratios in five species of seagrass. **J Exp Mar Biol and Ecology**. 195:91-110.

Guest, M.A., R.M. Connolly and N.R. Loneragan, 2004, Within and among-site variability in d13C and d15N for three estuarine producers, Sporobolus virginicus, Zostera capricorni, and epiphytes of Z. Capricornia, **Aquatic Botany**. 79:87-94.

Hartl, D.L. and E.W. Jones. 2000. **Genetics: Analysis of Genes and Genomes**. Jones and Bartlett Pulishers, Sudbury, Massachusetts, 858pp.

Hedrick, P.W. 1996. Conservation Genetics and Molecular Technuqies: A Perspective, In: **Molecular Genetic Approaches in Conservation**. Oxford University Press, New York , pp.459-477.

Hellblom, F. and M. Björk. 1999. Photosynthetic responses in *Zostera marina* to decreasing salinity, inorganic carbon content and osmolality. **Aquatic Botany**. 65:97-104.

Hemminga, M.A. and M.A. Mateo. 1996. Stable carbon isotopes in seagrasses: variability in ratios and use in ecological studies. **Marine Ecology Progress Series**. 140:285-298.

Hemminga, M.A., F.J. Slim, J. Kazungu, G.M. Ganssen, J. Nieuwenhuize and N.M. Kruyt. 1994. Carbon outwelling from a mangrove forest with adjacent beds and coral reefs (Gazi Bay, Kenya). **Marine Ecology Progress Series**. 106:291-301.

Invers, O., R.C. Zimmerman, R.S. Alberte, M. Pérez and J. Romero. 2001. Inorganic carbon sources for seagrass photosynthesis: an experimental evaluation of bicarbonate use in species inhabiting temperate waters. **Journal of Experimental Marine Biology and Ecology**. 265:203-217.

Kharlamenko, V.I., S.I. Kiyashko, A.B. Imbs and D.I. Vyshkvartzev. 2001. Identification of food sources of invertebrates from the seagrass *Zostera marina* community using carbon and sulfur stable isotope ratio and fatty acid analyses. **Marine Ecology Progress Series**. 220:103-117.

Kübler J.E., Raven J.A. 1994. Consequences of light limitation for carbon acquisition in three rhodophytes. Marine Ecology Progress Series. 110:203–209

Maier, C.M. and A.M. Pregnall. 1990. Increased macrophyte nitrate reductase activity as a consequence of groundwater input of nitrate through sandy beaches. **Marine Biology**. 107:263-271.

Masini, R.J. and C.R. Manning. 1997. The photosynthetic responses to irradiance and temperature of four meadow-forming seagrasses. **Aquatic Botany**. 58:21-36.

McClelland, J.W. and I. Valiela. 1998. Linking nitrogen in estuarine producers to land-derived sources. **Limnology and Oceanography**. 43(4):577-585.

Min-Sub, K; Lee, S; Shin, K. 2006. 13C, 15N and C:N:P ratio of *Zostera marina* as an eutrophication indicator on the coast of Korea. EOS Transactions. Vol. 87, no. 36, suppl., Sept. 2006.

Muñix-Salazar, R., S.L. Talbot, G.K. Sage, D.H. Ward and A. Cabello-Pasini. 2006. Genetic structure of eelgrass *Zostera marina* meadows in an embayment with restricted water flow. **Marine Ecology Progress Series**. 309:107-116.

Ralph, P.J. and R. Gademann. 2005. Rapid light curves: A powerful tool to assess photosynthetic activity. **Aquatic Botany**. 82:222-237.

Smit, A.J. A. Brearley, G.A. Hyndes, P.S. Lavery and DI. Walker. 2006. $\delta^{15}N$ and $\delta^{13}C$ analysis of a *Posidonia sinuosa* seagrass bed. **Aquatic Botany**. 84:277-282.

Steffy, L and S.S. Kilham. 2004. Elevated $\delta^{15}N$ in Stream Biota in Areas with Septic Tank systems in an Urban Watershed. **Ecological Applications**. 14(3):637-641.

Stribling, J.M. and J.C. Cornwell. 1997. Identification of Important Primary Producers in a Chesapeake Bay Tidal Creek System using Stable isotopes of Carbon and Sulfur. **Estuaries**. 20(1):77-85.

Thayer, G.W., P.L. Parker, M.W. LaCroix and B. Fry. 1978. The Stable Carbon Isotope Ratio of Some Components of an Eelgrass, *Zostera marina*, Bed. **Oecologia**. 35:1-12.

Vizini, S., G. Sarà, M.A. Mateo and A. Mazzola. 2003. $\delta^{13}C$ and $\delta^{15}N$ variability in *Posidonia oceanica* associated with seasonality and platn fraction. **Aquatic Botany**. 76:195-202.

Yamamuro, M., Y. Umezawa and I. Koike. 2004. Internal variations in nutrient concentrations and the C and N stable isotope ratios in leaves of the seagrass *Enhalus acoroides*. **Aquatic Botany**. 79:95-102.

12 Summary and Next Steps

12.1   Summary

The Eelgrass Stressor-Response Project benefits from a clearly defined primary objective – to identify the causes of observed *Z. marina* losses. The project has focused on two regions where losses have been observed – Hood Canal and Westcott Bay in the San Juan Archipelago. The initial work has focused on the role of turbidity in limiting light in Westcott Bay and the role of anthropogenic nutrients in stimulating green algal growth in the Hood Canal basin.

Key results from Hood Canal Focus Study include:

1. Stable isotope analysis was used to assess inputs of anthropogenic nitrogen to nearshore habitats, as indicated by enrichment in the ^{15}N isotope in *Z. marina* leaves. Results showed elevated *Z. marina* ^{15}N levels at southern Hood Canal sites and Dabob Bay sites, suggesting a relatively large contribution of anthropogenic nitrogen in these areas. In contrast, levels of anthropogenic nitrogen were substantially lower at sites in the northern portion of the canal. Within this broad nitrogen pattern, differences were evident in anthropogenic nitrogen level over smaller spatial scales and among seasons. This finding is supported by other research which suggests that the delivery of anthropogenic nitrogen to the nearshore through groundwater can be very localized (Chapter 3).

2. Stable isotope analysis of carbon in *Z. marina* showed an unusually high magnitude in the seasonal variation of ^{13}C. This finding may be related to strong seasonal variation in water temperature or an unusually strong variation in seasonal photosynthesis. There were no regional differences in *Z. marina* ^{13}C, which suggests that relative differences in riverine and marine influence are not significant across regions within Hood Canal (Chapter 3).

3. Hood Canal *Z. marina* populations appear to have higher genotypic richness (less clonality) and greater genetic diversity than populations in the San Juan Archipelago. Of the Hood Canal populations studied, core004 (Lynch Cove) had the lowest genetic diversity even though it has a stable *Z. marina* population. This finding argues against a key role for genetic diversity in causing *Z. marina* decline in Hood Canal (Chapter 10).

4. An analysis of impervious surface and land cover in the Hood Canal basin found that the basin has a low level of impervious surface relative to other areas within greater Puget Sound. Change analysis showed greater increases in impervious surface between 1991-1996 than between 1996-2001. The southern and northern areas of the basin have the greatest amount of impervious surface and the greatest increases (Chapter 4).

Key Results from San Juan Archipelago Focus Study include:

7. The remnant *Z. marina* population in inner Westcott Bay at Bell Point has the lowest genetic diversity of all populations analyzed in the San Juan Archipelago and Hood Canal. Genetic isolation of the inner populations in Westcott Bay could affect population viability (Chapter 10).

8. Boat-based sampling of surface waters coupled with remote sensing demonstrated that oceanic water conditions within the San Juan Archipelago vary greatly over space and time. This work provided an opportunity to assess the likelihood that Fraser River outflow stresses habitat conditions within the Westcott Bay complex. It documented complex patterns in temperature, salinity, pH, dissolved oxygen, light attenuation, and fluorescence that are linked to outflow from the Fraser River, strong currents, and basin topography. However, there was no evidence that the river plume reached the west side of San Juan Island and Westcott Bay. In addition to providing insight into one hypothesis of *Z. marina* loss in Westcott Bay, these findings underscore the importance of intensive, local monitoring of water characteristics (Chapter 9).

9. High resolution mapping of nearshore bathymetry, substrate type, and circulation patterns was employed to characterize conditions in Westcott Bay. These results will help us to address the hypothesis that *Z. marina* loss is related to changes in turbidity associated with sedimentation or biological productivity. Nearshore mapping data can be used in future efforts to develop models of sediment transport and habitat conditions that explore environmental variability and possible thresholds of stress to *Z. marina* growth and recovery (Chapter 5).

10. A census of intertidal and subtidal *Z. marina* plant morphology at three sites characterized how plant metrics such as shoot density, shoot length, reproductive shoot density, and rhizome internode length vary with depth and with location. These results provide preliminary information on the variation of plant metrics within the San Juan Archipelago (Chapter 8).

11. A mesocosm experiment explored *Z. marina* plant growth rates and seed germination rates in sediments from sites with healthy and stressed *Z. marina* populations. Results suggest that differences in leaf elongation rates and germination rates were more closely related to shading than to sediment source (Chapter 7).

12. Physiological performance of *Z. marina* in response to stress was measured at three sites by observing respiration and maximum photosynthesis rates in response to changes in applied irradiance. Results suggest that physiological performance is reduced at Bell Point, the site of a remnant *Z. marina* bed in Westcott Bay (Chapter 6).

Next Steps
The Eelgrass Stressor – Response Project is currently completing analysis of *Z. marina* transplant and water quality data collected in Westcott Bay and Hood Canal in 2007. Results of this research will be integrated with results of studies summarized in this report

to refine hypotheses for *Z. marina* decline in Westcott Bay and Hood Canal and to develop field work priorities for the 2008 season.

In Hood Canal, research priorities focus on exploring plant performance and the nature of nutrient delivery to the nearshore:

- Review conceptual model of stressors in Hood Canal and consider expanding model to include potential stressors beyond anthropogenic nitrogen.
- Conduct field studies to assess plant performance in response to hypothesized stressors such as anthropogenic nitrogen, algal blooms.
- Deploy additional water monitoring systems to assess conditions in nearshore areas.
- Integrate findings from other research efforts on nutrient delivery into Hood Canal, including work by the Hood Canal Dissolved Oxygen Program and the USGS Washington Water Science Center.
- Integrate laboratory results into overall results as they become available.

Appendix A. Summary of *Z. marina* Monitoring Results in the San Juan Archipelago

Table 1 – Inventory of DNR site-level data (1=sampled; 0=not sampled) and results of tests for change and trend in *Z. marina* area utilizing all available data. When only two years of data were available for a site, a two-tailed test of significant (non-zero) relative change was applied to the two years of data ("Change" test). When three or more years were available, a test for significant linear regression slope was applied to the data ("Trend" test). Results are mapped in Figure 1. The TYPE field indicates the sampling stratum for each site: cor=core; fl=flats; frw=wide fringe; fr=narrow fringe.

Site	TYPE	2000	2001	2002	2003	2004	2005	2006	Total No.Yrs	Latest *Z. marina* area estimate (ha) (95% CI)	Test	Two-Tailed Test Result based on DNR data only	notes
core002	cor	1	1	1	1	1	1	1	7	2.8 ± 0.5	Trend	Not sig. (p>0.05)	
flats51	fl	0	0	0	0	1	0	0	1	11.2 ± 1.7			
flats52	fl	0	0	0	0	1	0	0	1	14.9 ± 1.7			
flats53	fl	1	1	0	0	0	0	0	2	0	Change	Not sig. (p>0.05)	WDFW herring spawn survey showed *Z. marina* to be virtually absent by 2003; Confirmed by Friends of San Juans 2005 survey.
flats55	fl	0	0	0	0	1	0	0	1	3.5 ± 1.1			
flats56	fl	0	0	0	0	1	0	0	1	6.9 ± 2.0			
flats58	fl	0	0	0	0	1	0	0	1	7.4 ± 0.8			
flats60	fl	1	1	1	0	0	0	0	3	2.3 ± 0.5	Trend	Not sig. (p>0.05)	
flats61	fl	0	0	0	0	1	0	0	1	6.3 ± 0.8			
flats62	fl	1	1	1	1	1	0	0	5	9.4 ± 2.8	Trend	Not sig. (p>0.05)	
flats63	fl	0	0	0	0	1	0	0	1	5.5 ± 2.2			
flats64	fl	0	0	0	0	0	1	1	1	1.4 ± 2.3			
flats67	fl	0	0	0	0	1	1	1	3	4.7 ± 2.6	Trend	Not sig. (p>0.05)	
flats73	fl	0	0	0	0	0	0	0	0	163.9 ± 41.2			Estimate based on 2003 data provided by Friends of the San Juans.
sjs0002	fr	0	0	0	0	1	0	0	1	5.4 ± 0.7			
sjs0005	frw	0	1	1	1	0	0	0	3	0	No *Z. marina*		
sjs0081	fr	1	1	1	1	1	1	0	6	1.2 ± 0.4	Trend	Not sig. (p>0.05)	Overall site trend marginally significant (p=0.074). Examination of spatial pattern reveals clear sub area in decline within site. Regression slope: -0.1 ha/year (-9%/year).
sjs0115	fr	0	0	0	0	1	0	0	1	15.7 ± 1.5			
sjs0118	fr	0	0	0	0	0	0	1	1	24.1 ± 3.3			
sjs0138	fr	0	0	0	0	1	0	0	1	1.5 ± 0.8			
sjs0140	fr	0	0	0	0	1	0	0	1	2.2 ± 0.3			
sjs0153	fr	0	0	0	0	1	0	0	1	0	No *Z. marina*		
sjs0154	fr	0	0	0	0	1	0	0	1	0.2 ± 0.0			
sjs0182	fr	0	0	0	0	1	0	0	1	0.3 ± 0.0			
sjs0192	fr	0	0	0	0	1	0	0	1	0.5 ± 0.2			
sjs0205	fr	0	0	0	0	1	0	1	2	12.6 ± 1.0	Change	Not sig. (p>0.05)	
sjs0311	fr	1	1	1	1	1	0	0	5	1.9 ± 0.4	Trend	Not sig. (p>0.05)	
sjs0335	fr	1	1	0	0	0	0	0	2	0.7 ± 0.3	Change	Not sig. (p>0.05)	
sjs0345	fr	0	0	0	0	1	0	0	1	0	No *Z. marina*		
sjs0346	fr	0	0	0	0	1	0	0	1	3.4 ± 0.5			
sjs0351	frw	1	1	1	1	0	0	0	4	24.6 ± 0.9	Trend	Not sig. (p>0.05)	
sjs0359	fr	0	0	0	1	0	0	0	1	0.2 ± 0.1			

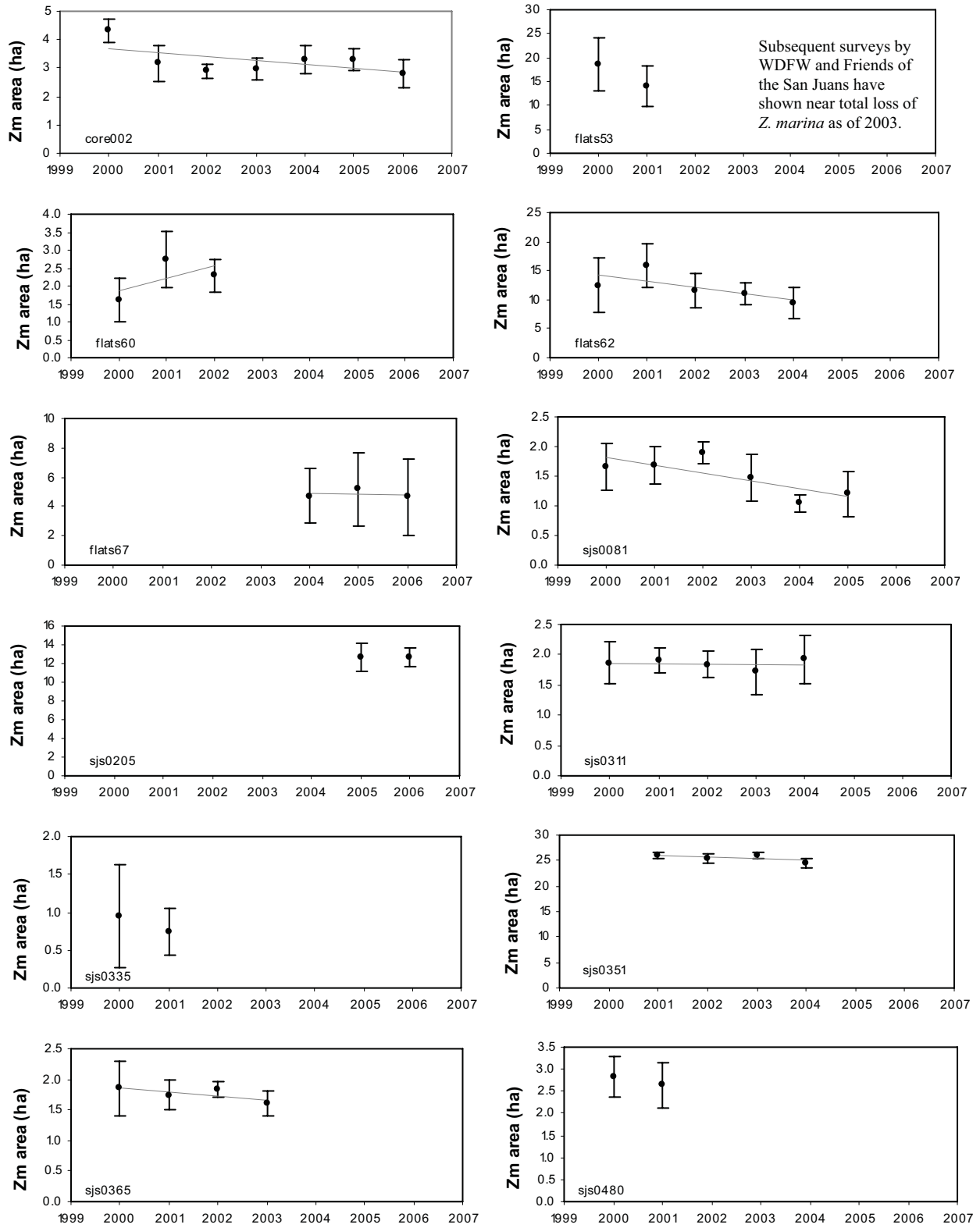| Site	TYPE	2000	2001	2002	2003	2004	2005	2006	Total No.Yrs	Latest Z. marina area estimate (ha) (95% CI)	Test	Two-Tailed Test Result based on DNR data only	notes
sjs0365	fr	1	1	1	1	0	0	0	4	1.6 ± 0.2	Trend	Not sig. (p>0.05)	
sjs0392	fr	0	0	0	0	1	0	0	1	0.3 ± 0.1			
sjs0400	fr	0	0	0	0	1	0	0	1	0	No Z. marina		
sjs0434	fr	0	0	0	0	1	0	0	1	4.0 ± 0.7			
sjs0437	fr	0	0	0	0	1	0	0	1	0.7 ± 0.1			
sjs0448	fr	0	0	0	0	0	0	1	1	5.3 ± 1.0			
sjs0452	fr	0	0	0	0	0	0	1	1	13.6 ± 1.9			
sjs0453	fr	0	0	0	0	1	0	0	1	3.8 ± 0.6			
sjs0480	fr	1	1	0	0	0	0	0	2	2.6 ± 0.5	Change	Not sig. (p>0.05)	
sjs0488	fr	0	0	0	0	0	0	1	1	0	No Z. marina		
sjs0499	fr	0	0	0	0	1	0	0	1	2.1 ± 0.4			
sjs0557	fr	0	0	0	0	1	0	0	1	4.5 ± 0.9			
sjs0600	fr	0	0	0	0	0	0	1	1	2.9 ± 3.4			
sjs0617	fr	0	0	1	1	1	1	1	5	2.4 ± 0.7	Trend	**Significant (p<0.05)**	Increasing trend. Regression slope: +.2 ha/year (+11%/year) Inspection of transects reveals no obvious bed expansion.
sjs0622	fr	1	1	0	0	0	0	0	2	0.1 ± 0.1	Change	Not sig. (p>0.05)	
sjs0635	fr	0	0	0	1	1	1	1	4	1.5 ± 0.4	Trend	**Significant (p<0.05)**	Decreasing trend. Regression slope: -0.6 ha/year (-27%/year). Inspection of transects indicates loss from shallow edge in southern bed.
sjs0637	fr	1	1	1	0	0	0	0	3	3.0 ± 0.9	Trend	Not sig. (p>0.05)	
sjs0639	fr	0	0	0	0	0	1	1	2	0	No Z. marina		
sjs0649	fr	0	0	1	1	1	1	1	5	0	Trend		
sjs0683	fr	0	0	0	1	1	1	1	4	0.8 ± 0.3	Trend	Not sig. (p>0.05)	
sjs0695	fr	1	1	1	1	1	1	0	6	0	No Z. marina		
sjs0736	fr	1	1	1	0	0	0	0	3	0	No Z. marina		

Figure 1. Site data for sites with at least two years of data. Linear regression lines are shown for sites with at least three years of data. Error bars are 95% confidence intervals.
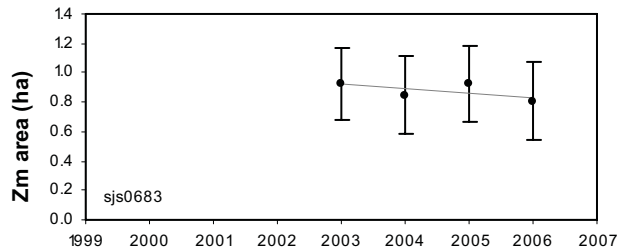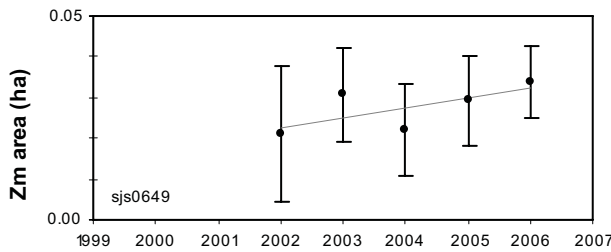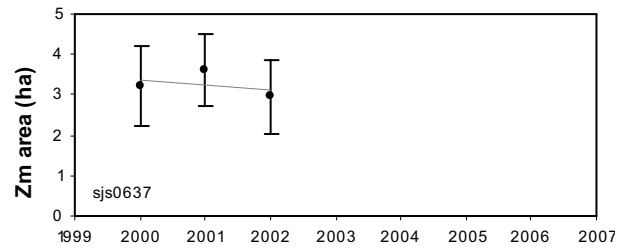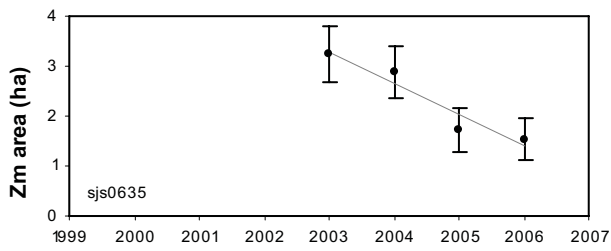
The text box in the flats53 panel reads: "Subsequent surveys by WDFW and Friends of the San Juans have shown near total loss of *Z. marina* as of 2003."
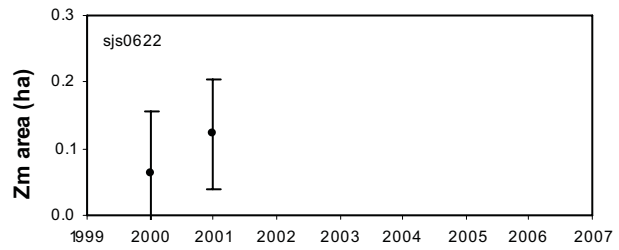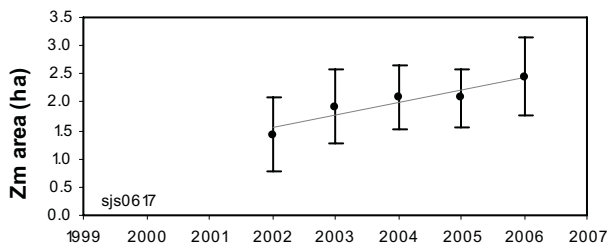
Figure 1 (continued).
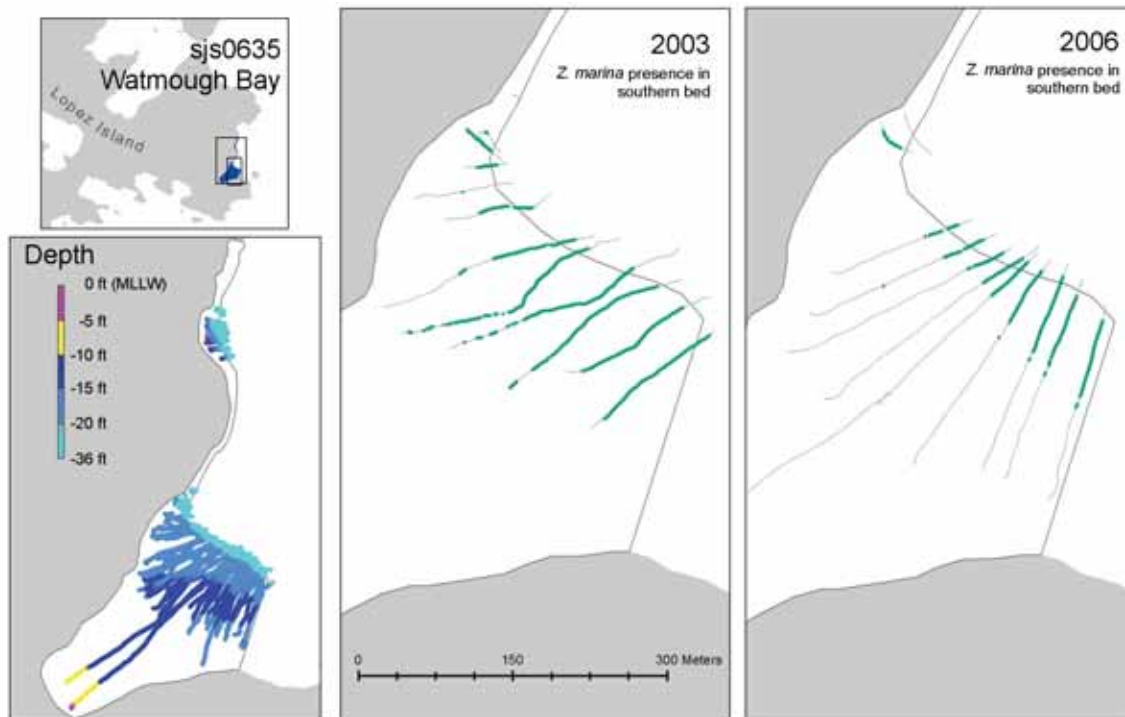
Figure 2. Loss at Watmough Bay (sjs0635) is from the shallow edge even though this is a deep bed overall.
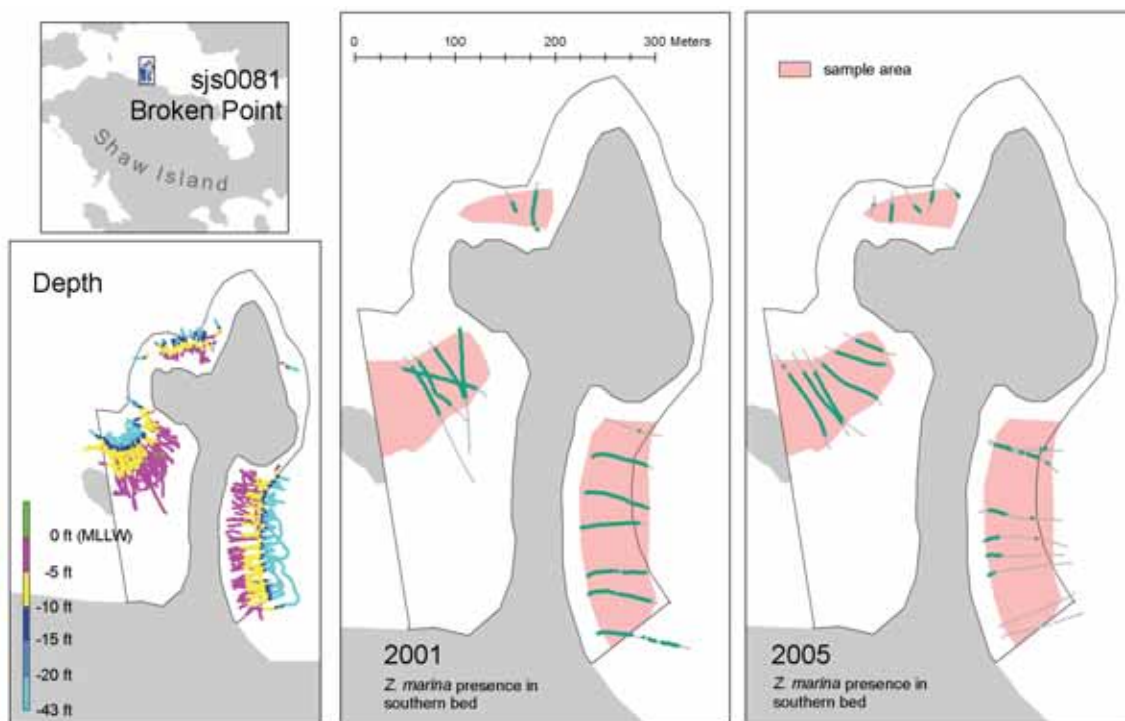

Figure 3. Loss in eastern bed at Broken Point (sjs0081) is from the deep edge.
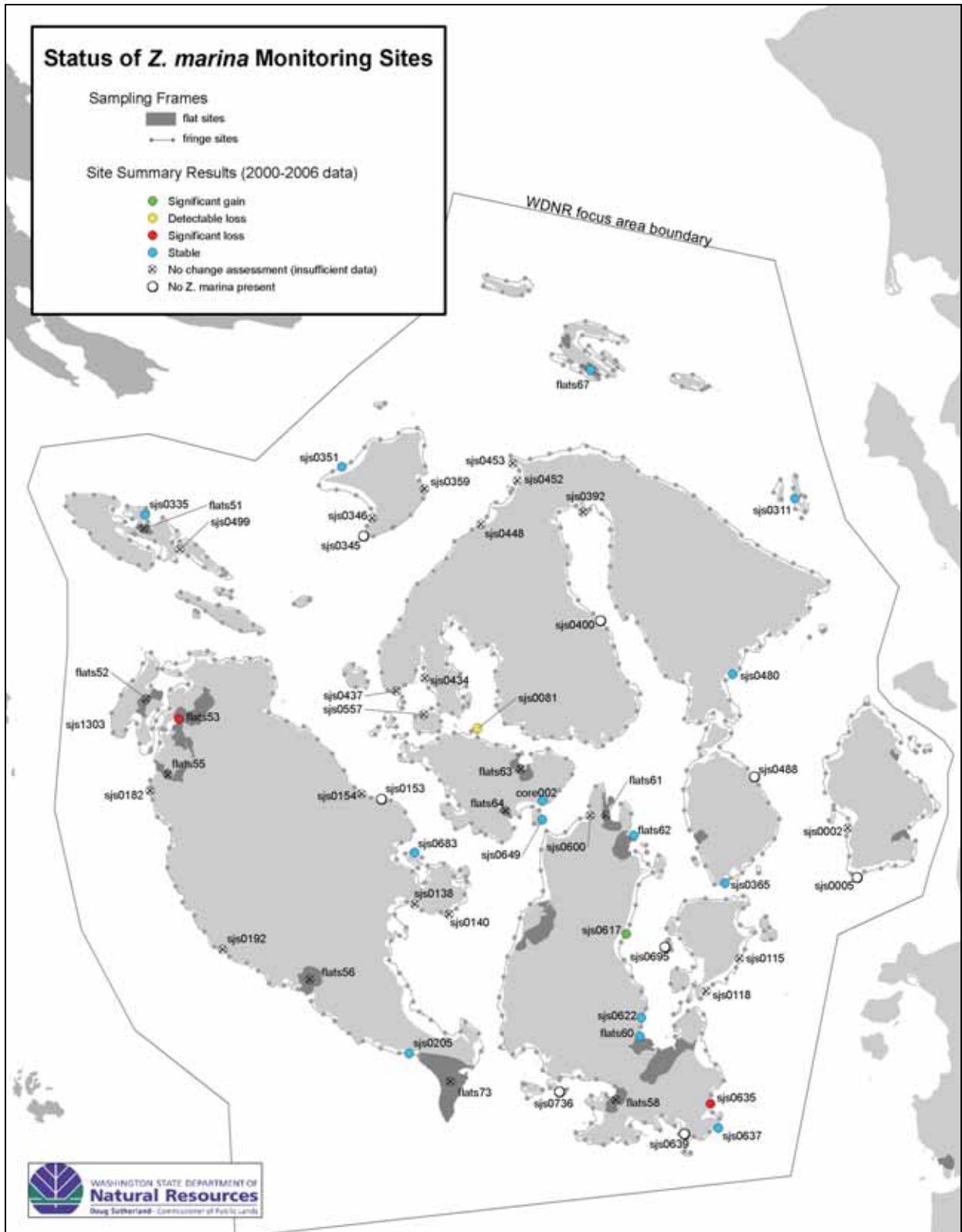
Figure 4. Assessments of *Z. marina* based on available WDNR data. The data record is not consistent across sites (see Table 1). The assessment for Westcott Bay (flats53) relies on supplementary data sources (see Table 1).
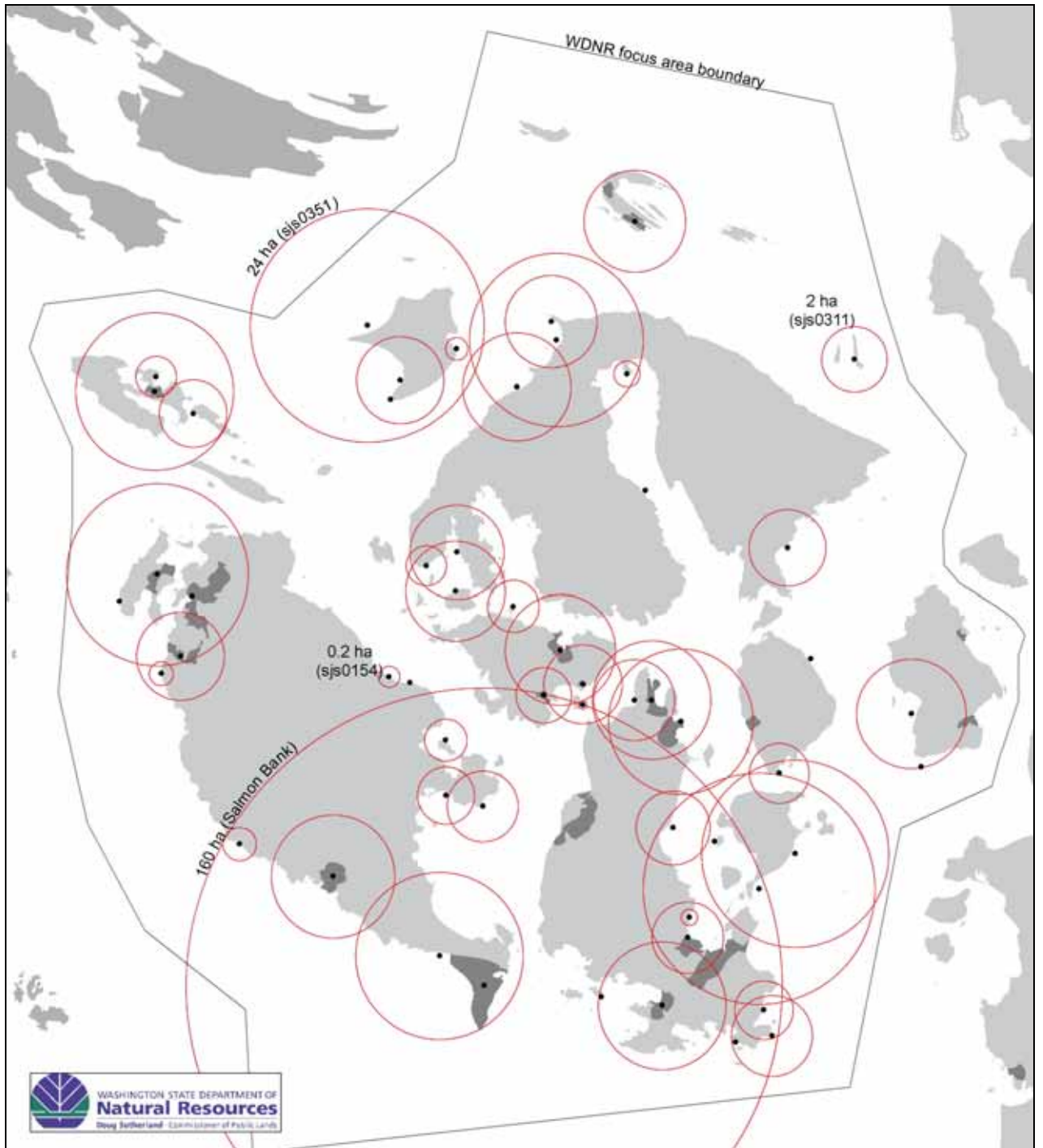
220

Figure 5. Abundance of *Z. marina* at all sites sampled. The diameter of the circles varies with the latest available *Z. marina* area estimate for each site. The circles are centered on dots which indicate the exact site location. Salmon Bank (flats73) has not been sampled by WDNR – the estimate here is based on data from 2003 provided by Friends of the San Juans. Sites without circles have no *Z. marina* present.

Appendix B.   Summary of *Z. marina* Monitoring Results in Hood Canal

Table 1 – Inventory of DNR site-level data (1=sampled; 0=not sampled) and results of tests for change or trend in *Z. marina* based on 2000-2006 data. When only two years of data were available for a site, a two-tailed test of significant (non-zero) relative change was applied to the two years of data ("change" test). When three or more years were available, a test for significant linear regression slope was applied to the data ("trend" test). The result field is red for the four cases with statistically significant (p<0.05) measures of decline. The result field is yellow for the three additional cases where inspection of the data suggests decline even though the initial test results were not significant (see notes field). Confidence intervals, where specified, are 95% confidence intervals. There were no significant or marginally significant gains in *Z. marina* area using these tests. Results are mapped in Figure 1. The TYPE field indicates the sampling stratum for each site: cor=core; fl=flats; frw=wide fringe; fr=narrow fringe.

Site	TYPE	2000	2001	2002	2003	2004	2005	2006	Total No.Yrs	Latest *Z. marina* area estimate (ha) (95% CI)	Test	Two-Tailed Test Result	notes
core004	cor	1	1	1	1	1	1	1	7	132 ± 39 ha	Trend	Not sig. (p>0.05)	
flats41	fl	0	0	0	0	1	1	1	3	92 ± 16 ha	Trend	Not sig. (p>0.05)	
flats42	fl	0	0	0	0	0	1	1	2	92 ± 11 ha	Change	Not sig. (p>0.05)	
flats43	fl	1	1	1	1	1	1	0	6	12 ± 3 ha	Trend	Not sig. (p>0.05)	Marginal significance (p=0.083). Significant decline under one-tailed test (p<0.05). Regression slope: -5%/year.
flats44	fl	0	0	0	0	0	1	0	1	19 ± 6 ha			
flats45	fl	0	0	0	0	0	1	0	1	7.0 ± 2.1 ha			
hdc2239	frw	0	0	1	1	1	1	1	5	6.9 ± 1.0 ha	Trend	Significant (p<0.05)	Declining trend. Regression slope: -13%/year.
hdc2240	frw	0	1	0	0	0	1	0	2	10 ± 1 ha	Change	Significant (p<0.05)	Decline of –27 ± 15%.
hdc2253	frw	0	0	0	0	0	1	0	1	18 ± 1 ha			
hdc2262	fr	0	0	0	0	0	1	0	1	1.7 ± 0.8 ha			
hdc2277	fr	0	0	0	0	0	1	0	1	1.2 ± 0.6 ha			
hdc2283	frw	0	0	0	0	0	0	1	1	12 ± 2 ha			
hdc2284	fw	0	0	0	0	1	1	1	2	7.1 ± 1.2 ha	Change	Not sig. (p>0.05)	
hdc2308	fr	0	0	0	0	1	1	0	1	13 ± 3 ha			
hdc2310	fr	1	1	1	0	0	0	0	3	2.5 ± 0.3 ha	Trend	Not sig. (p>0.05)	
hdc2314	frw	0	0	0	0	1	1	0	1	0.22 ± 0.16 ha			
hdc2323	fr	0	0	0	0	1	1	0	1	0.07 ± 0.11 ha			
hdc2331	fr	0	0	0	0	1	1	0	1	0.60 ± 0.37 ha			
hdc2338	fr	1	1	1	1	1	1	0	6	1.0 ± 0.2 ha	Trend	Significant (p<0.05)	Declining trend. Regression slope: -11%/year.
hdc2344	fr	0	0	0	1	1	1	1	4	0.7 ± 0.3 ha	Trend	Not sig. (p>0.05)	Marginal significance (p=0.095), but sig. annual declines (see Table 2). Significant decline under one-tailed test (p<0.05). Regression slope: -43%/year.
hdc2345	fr	1	1	0	0	0	0	0	2	0.6 ± 0.3 ha	Change	Not sig. (p>0.05)	Results of annual monitoring show no change but special survey in March 2007 showed total loss.
hdc2353	fr	0	0	0	0	1	1	0	1	1.5 ± 0.7 ha			
hdc2355	frw	0	0	0	0	1	1	0	1	2.9 ± 1.1 ha			
hdc2356	frw	0	0	0	0	1	1	0	1	7.3 ± 1.6 ha			
hdc2359	fr	1	1	1	1	1	1	0	6	9.0 ± 0.6 ha	Trend	Significant (p<0.05)	Declining trend. Regression slope: -5%/year.
hdc2364	fr	0	0	0	0	0	1	0	1	1.2 ± 0.6 ha			

Site	TYPE	2000	2001	2002	2003	2004	2005	2006	Total No.Yrs	Latest *Z. marina* area estimate (ha) (95% CI)	Test	Two-Tailed Test Result	notes
hdc2365	fr	0	0	0	0	0	1	0	1	1.9 ± 0.9 ha			
hdc2380	frw	0	0	0	0	0	1	0	1	32 ± 5 ha			
hdc2381	frw	0	0	0	0	0	1	0	1	26 ± 2 ha			
hdc2383	frw	0	0	0	0	1	1	1	3	2.9 ± 1.3 ha	Trend	Not sig. (p>0.05)	
hdc2386	frw	0	0	0	0	0	1	0	1	9.6 ± 0.8 ha			
hdc2398	fr	0	0	0	0	0	1	0	1	2.0 ± 0.6 ha			
hdc2409	frw	0	0	0	0	0	1	0	1	3.6 ± 1.2 ha			
hdc2418	fr	0	0	0	0	0	1	0	1	1.8 ± 0.3 ha			
hdc2433	fr	1	1	1	0	0	0	0	3	1.9 ± 0.1 ha	Trend	Not sig. (p>0.05)	
hdc2447	fr	0	0	0	0	0	1	0	1	3.1 ± 1.0 ha			
hdc2449	fr	0	0	0	0	0	1	0	1	1.2 ± 0.3 ha			
hdc2450	fr	0	0	0	0	0	1	0	1	0.28 ± 0.31 ha			
hdc2465	fr	0	0	0	0	1	1	1	3	6.4 ± 0.9 ha	Trend	Not sig. (p>0.05)	
hdc2468	fr	0	0	0	0	0	1	0	1	5.1 ± 1.1 ha			
hdc2478	fr	0	0	0	0	0	1	0	1	1.4 ± 0.7 ha			
hdc2479	fr	0	0	0	0	1	1	1	3	7.1 ± 1.0 ha	Trend	Not sig. (p>0.05)	Marginal significance (p=0.07). Significant decline under one-tailed test (p<0.05). Regression slope: -5%/year.
hdc2487	fr	1	1	0	0	0	0	0	2	1.7 ± 0.5 ha	Change	Not sig. (p>0.05)	
hdc2504	fr	1	1	0	0	0	0	0	2	5.0 ± 1.1 ha	Change	Not sig. (p>0.05)	
hdc2507	frw	0	0	0	0	0	1	0	1	12 ± 3 ha			
hdc2518	fr	0	0	0	0	0	1	0	1	5.0 ± 2.6 ha			
hdc2529	fr	1	1	1	1	1	1	0	6	5.4 ± 0.8 ha	Trend	Not sig. (p>0.05)	

Figure 1. Status of DNR *Z. marina* monitoring sites in Hood Canal. See Table 1 for details on site categories.
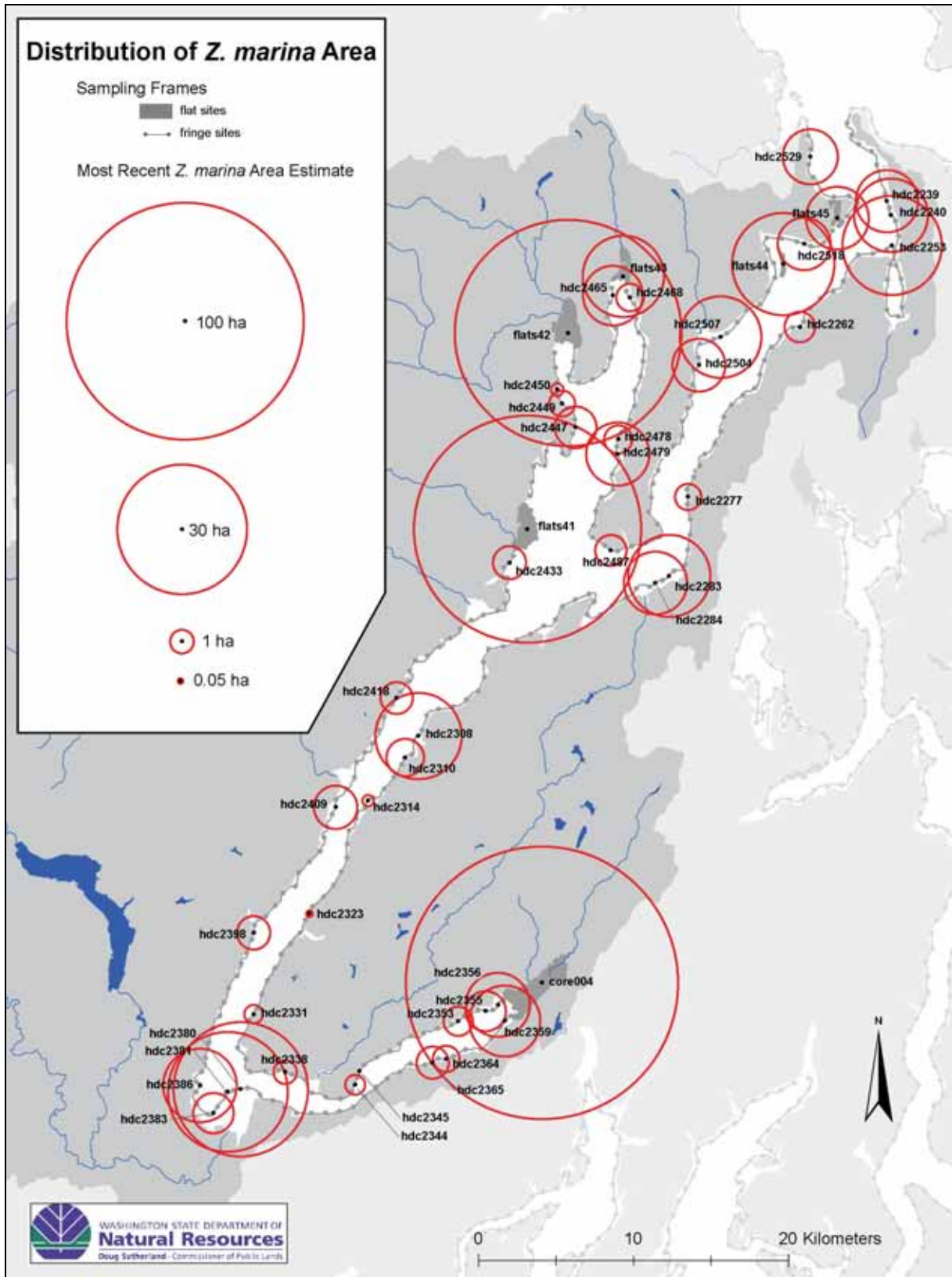
224

Figure 2. Estimated area of *Z. marina* at DNR monitoring sites. For sites sampled in more than one year, the most recent estimate is depicted. Black dots with no associated red circle had no *Z. marina* present in the most recent survey.
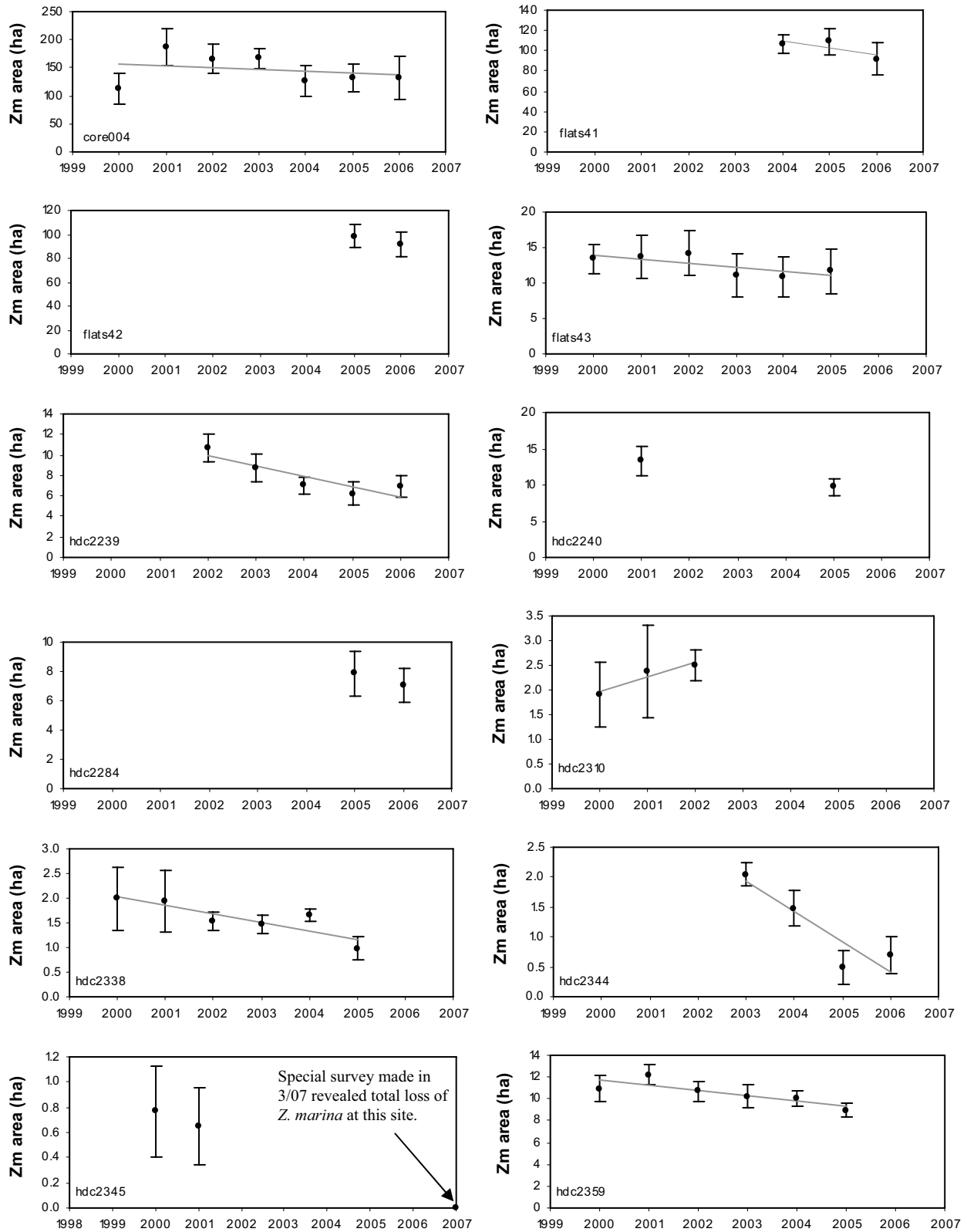
Figure 3. Site data for sites with at least two years of data. Linear regression lines are shown for sites with at least three years of data. Error bars are 95% confidence intervals.
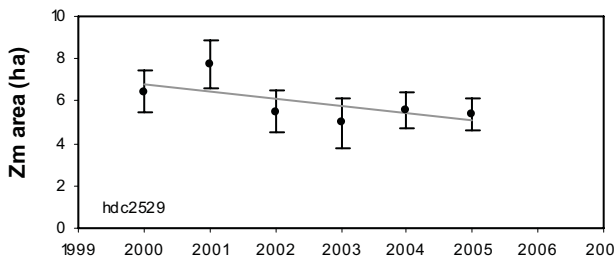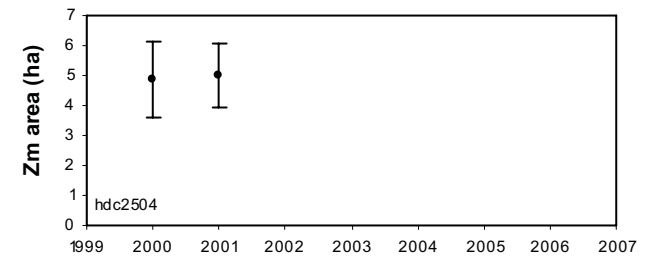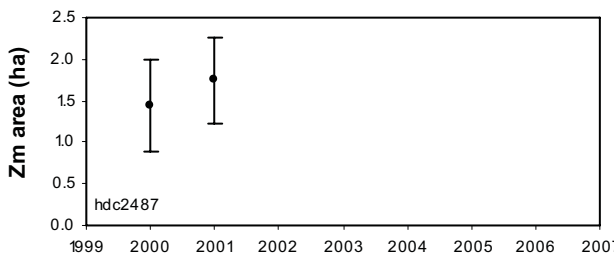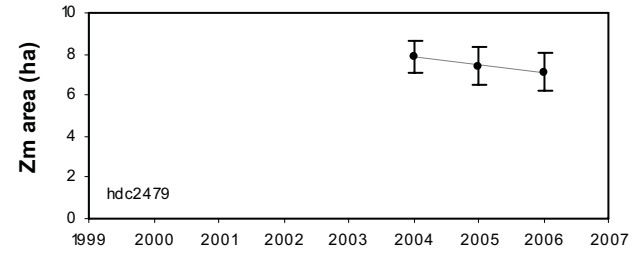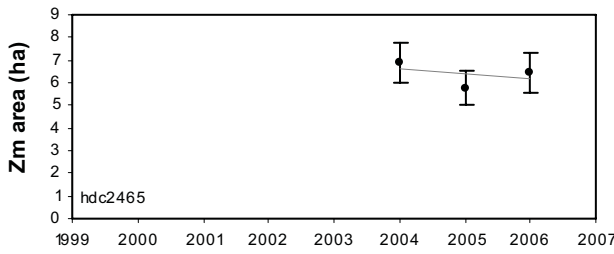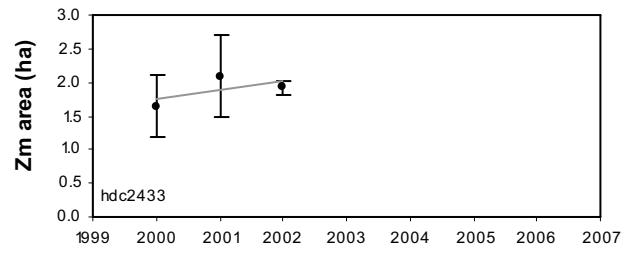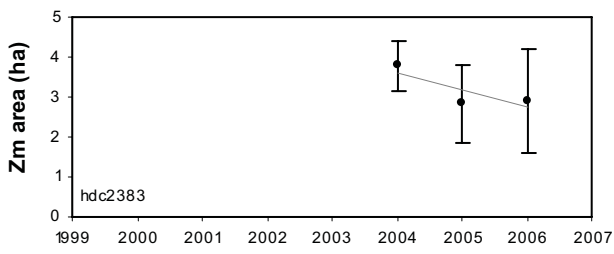
Figure 3 (continued).

Table 2. Summary of estimates of annual relative change in *Z. marina* area for Hood Canal sites. The number of paired sites in each annual interval and their grouping by loss or gain are also shown. (*) indicates statistical significance of $p<0.05$.

	2000-2001	2001-2002	2002-2003	2003-2004	2004-2005	2005-2006
Number of paired sites	10	7	6	7	11	9
Paired sites with an estimated **gain** in *Z. marina* area	core004* flats43 hdc2310 hdc2359 hdc2433 hdc2487 hdc2504 hdc2529	flats43 hdc2310		hdc2338 hdc2529	core004 flats41 flats43	core004 hdc2239 hdc2344 hdc2383 hdc2465
Paired sites with an estimated **loss** in *Z. marina* area	hdc2338 hdc2345	core004 hdc2338 hdc2359* hdc2433 hdc2529*	flats43 hdc2239* hdc2338 hdc2359 hdc2529	core004* flats43 hdc2239* hdc2344* hdc2359	hdc2239 hdc2338* hdc2344* hdc2359* hdc2383 hdc2465* hdc2479 hdc2529	flats41 flats42 hdc2284 hdc2479
Paired sites an estimate of **no change** in *Z. marina* area (<1% change)			core004			